

**Evaluation and Application of Current Methods Used to Estimate Exposure
to Traffic-Related Air Pollutants at High Spatial or Temporal Resolutions.**

By

Chad William Milando

A dissertation submitted in partial fulfillment
of the requirements for the degree of
Doctor of Philosophy
(Environmental Health Sciences)
in the University of Michigan
2018

Doctoral Committee:

Professor Stuart Batterman, Chair
Professor Veronica Berrocal
Professor J. Tim Dvonch
Professor Richard Neitzel

Chad William Milando
cmilando@umich.edu
ORCID iD: 0000-0001-6340-7754

© Chad W. Milando 2018

DEDICATION

This dissertation is dedicated to my family, friends, and to Karin,
for helping me accept and overcome my “brick walls”

ACKNOWLEDGEMENTS

I would like to thank my dissertation chair, Dr. Stuart Batterman, for holding me to high standards, helping improve my writing and critical thinking, and giving me the chance to work on a variety of projects. I would also like to thank my dissertation committee members – Dr. Veronica Berrocal, Dr. Tim Dvonch and Dr. Rick Neitzel – for supporting me in this dissertation and in my professional development.

I am grateful to have received invaluable personal and professional support and advice from Dr. Kendrin Sonneville, Dr. Tom Robins, Kevin Boehnke and Lisa Marchlewicz. Special thanks to Kevin and Lisa for reading countless drafts of my writing in many forms, and for helping me learn how to be the student I wanted to be.

I am very appreciative of the patience and attention afforded to me by Sue Crawford. I would like to thank Katrina Burns for inviting me to participate in the Diversity, Equity and Inclusion efforts in our department; involvement in this work has enriched my life in ways I did not expect.

I would not have survived in my dissertation without the council and friendship of Dr. Sheena Martenies. Thank you for putting up with my antics, for teaching me about log-linear concentration response functions, and for lending your ear when I needed it.

For help with various modeling and data questions, I would like to thank: Dr. Steven Brown at Sonoma Technology Inc. (STI); Chade Saghir, Trevor Brydon, and Jilan Chen at SEMCOG for MOVES and other files; Debbie Sherrod, Susan Kilmer, and Jim Haywood at MDEQ for information on NWS and onsite data; Larry Whiteside and Kevin Krzyemski at MDOT for help with TMIS.

Support for this research was provided by grants from the Health Effects Institute, grant P30ES017885 from the National Institute of Environmental Health Sciences, National Institutes

of Health, and grant T42 OH008455-10 from the National Institute of Occupational Health and Safety.

The final year of candidacy was supported by a Rackham Pre-Doctoral Fellowship, for which I am extraordinarily grateful.

TABLE OF CONTENTS

DEDICATION	ii
ACKNOWLEDGEMENTS	iii
LIST OF TABLES	viii
LIST OF FIGURES	xi
ABSTRACT.....	xiv
Chapter I – Introduction.....	1
I.1 Motivation to study traffic-related air pollution.....	1
I.2 Methods used to estimate exposure to TRAP	3
I.2.1 Dispersion models.....	5
I.2.2 Human exposure models.....	7
I.2.3 Exposure apportionment	8
I.3 Specific Aims.....	9
I.4 Dissertation overview	11
I.5 Tables.....	12
Chapter II – Methods	13
II.1 Aim 1	13
II.1.1 Emissions data	13
II.1.2 Ambient air quality data and treatment.....	13
II.1.3 Receptor modeling	17
II.1.4 Quantifying trends in concentrations and apportionments.....	18
II.2 Aim 2	19
II.2.1 Near-road ambient air quality monitoring data.....	19
II.2.2 Meteorological data.....	20
II.2.3 Point-source modeling	21
II.2.4 Dispersion modeling of mobile sources.....	22
II.2.5 Estimation of background concentrations.....	24
II.2.6 Operational evaluation metrics	25

II.3	Aim 3	26
II.3.1	Meteorological data.....	27
II.3.2	Receptor sets	27
II.3.3	Sensitivity analysis.....	27
II.3.4	Application.....	28
II.4	Aim 4	29
II.4.1	Exposure apportionment	29
II.5	Tables.....	31
II.6	Figures.....	42
Chapter III – Trends in PM _{2.5} emissions, concentrations and apportionments in Detroit and Chicago.....		59
III.1	Summary.....	59
III.2	Results and Discussion	60
III.2.1	Emission inventory trends.....	60
III.2.2	Concentration trends	63
III.2.3	Long term source apportionments.....	67
III.2.4	Source apportionment trends	67
III.2.5	Fractional apportionment trends	68
III.2.6	Vehicle apportionments and comparison to previous work.....	70
III.2.7	Limitations	71
III.3	Tables.....	73
III.4	Figures.....	78
Chapter IV – Operational evaluation of the RLINE dispersion model for studies of traffic-related air pollutants.....		85
IV.1	Summary	85
IV.2	Results.....	85
IV.2.1	Background and un-modeled contribution.....	85
IV.2.2	Performance by site.....	86
IV.2.3	Performance by wind direction	87
IV.2.4	Performance by day-of-week	88
IV.2.5	Performance by season.....	88
IV.3	Discussion.....	89
IV.3.1	Comparison to literature.....	90
IV.3.2	Implications of varying performance	91
IV.3.3	Uncertainty and limitations	94
IV.4	Tables.....	96

IV.5	Figures.....	104
	Appendix A - Expanded tables of Model Performance	106
Chapter V – Sensitivity analysis of the near-road dispersion model RLINE - an evaluation at Detroit, Michigan		
V.1	Summary	114
V.2	Results.....	114
V.2.1	Sensitivity to meteorological inputs.....	115
V.2.2	Emission factors.....	116
V.2.3	Temporal Allocation Factors	116
V.2.4	Exposure estimates.....	117
V.3	Discussion	117
V.3.1	Meteorology	117
V.3.2	Emission factors.....	119
V.3.3	Temporal allocation factors	120
V.3.4	Application.....	121
V.3.5	Comparison to Literature	122
V.3.6	Limitations and Uncertainty.....	122
V.4	Tables.....	124
V.5	Figures.....	133
	Appendix B – Expanded tables of Model Sensitivity	136
Chapter VI – Air pollution exposure apportionment among vulnerable residents of Detroit, MI		
VI.1	Summary	145
VI.2	Results.....	145
VI.3	Discussion	146
VI.3.1	Comparison to literature.....	148
VI.3.2	Limitations and uncertainty	148
VI.4	Tables.....	151
VI.5	Figures.....	154
Chapter VII – Conclusions and Recommendations		
VII.1	Aim 1	158
VII.2	Aim 2	159
VII.3	Aim 3	160
VII.4	Aim 4	160
REFERENCES		162

LIST OF TABLES

Table 1. Summary of datasets used in previous RLINE evaluations.....	12
Table 2. Summary statistics for all Detroit species of speciated PM.....	31
Table 3. Summary statistics for all Chicago species.....	33
Table 4. Parameters for EC and OC artifact correction regression.....	34
Table 5. Starting date (month and year) and percent above detection limit (%>DL) of hourly CO, NO, NO ₂ and NO _x data at Detroit area monitoring sites.	35
Table 6. PM _{2.5} measured at sites in Wayne County, MI.....	36
Table 7. Number of missing met-hours for each NWS data set and hour of the day. There were 1461 hours of data in each hour of the day.....	37
Table 8. Annual emissions (tons, rounded to the nearest integer) of modeled and not-modeled point sources of CO, NO _x and PM _{2.5} in Wayne County and the remaining 6 counties.....	38
Table 9. Hours of traffic count data in each month from 2010 to 2014 separated by NFC class and traffic recorder type (PTR = Permanent Traffic Recorder; SHORT = Short counts).....	38
Table 10. Allocation of commercial and non-commercial traffic.....	39
Table 11. Aggregated Fleet-mix “reality-check” – vehicle fraction by NFC class.	39
Table 12. Matrix for of percentages used in post-processing MOVES emission rate outputs into aggregated HMPS vehicle classes. Generated using Table 2-4 of Decker 1996 [131], MOVES2014 on-road source types table [151], and SEMCOG Fuel type data.....	40
Table 13. Annual modeled emissions (nearest ton) of each pollutant in each year. Major roads have AADT > 10,000.	40
Table 14. Formulas for various performance metrics [55].	41
Table 15. Summary of emissions inventory data in Detroit and Chicago. Expressed as short tons/yr of PM _{2.5} primary (filterable + condensable) and % of total PM _{2.5} . Derived from NEI.....	73
Table 16. Median and 90 th percentile concentrations by year-block and statistical differences between year-block concentrations.....	74
Table 17. Bootstrapped % of species mass at Detroit (200 bootstrapped runs, block size = 220, total samples = 1433).....	76
Table 18. Bootstrapped % of species mass at Chicago (200 bootstrapped runs, block size = 50, total samples = 763).....	77

Table 19. Summary of 2011 Wayne County CO, NO _x and PM _{2.5} emissions from the National Emission Inventory [124] in short tons (rounded to the nearest ton).	96
Table 20. Model performance for daily average NO _x and CO.	97
Table 21. Daily average observed and modeled PM _{2.5} concentrations at the suburban and schools sites (µg/m ³).	98
Table 22. Model performance for daily average NO _x and CO by wind direction type.	99
Table 23. Model performance for daily average NO _x and CO by day type.	100
Table 24. Model performance for daily average NO _x and CO by season.	102
Table 25. Data for Summary of sensitivity analysis for meteorology inputs, showing results of performance evaluation for NO _x and CO for three comparisons.	124
Table 26. Summary of sensitivity analysis for meteorology inputs, showing results of performance evaluation for NO _x and CO for three comparisons.	125
Table 27. Summary of sensitivity analysis for emission factor inputs, comparing results of performance evaluation for nominal (2010) and alternative (2015) emission inventory.	126
Table 28. Matrix of circulation correlation coefficient for wind direction (upper right values) and Pearson correlation coefficients of wind speeds (lower left values) across sites.	127
Table 29. Annual (2011) average NO _x concentrations (µg m ⁻³) predicted at NEXUS and Detroit receptors using KDET and KDTW meteorology.	127
Table 30. Difference in average attributable cases (per 10 ⁻⁴) of various health outcomes predicted using KDET and KDTW meteorology	128
Table 31. Average attributable cases made using KDET and KDTW meteorology at NEXUS and Detroit receptors for various NO _x related health outcomes.	129
Table 32. Percent difference in emission factors between average 2010 and 2015 EF for the 8 Highway Performance Monitoring System (HMPS) classes.	129
Table 33. Checking the impact of the large change in LDDV EF indicated above.	130
Table 34. Ratio between MOVES 2015 emission factors for HDDV to LDGV averaged across months by speed and temperature.	131
Table 35. Aggregated vehicle class fraction by NFC class (i.e., “fleet-mix”).	132
Table 36. Mean hourly exposures (ppb) contributed by source groups in each micro-environment (ME). Exposures < 0.05 ppb have been removed from this table.	151
Table 37. Mean exposure by source and during different seasons; differences between exposures for adults, children and the elderly compared by the KW test.	152
Table 38. Mean exposure by source and during weekday vs weekend; differences between exposures for adults, children and the elderly compared by the KW test.	152

Table 39. Average min/day spent in various micro-environments (ME) for simulated persons in Detroit in 2014.	153
Table 40. Average min/day spent doing various activities for simulated persons in Detroit in 2014.	153
Table A. 1. Model performance metrics for daily average NO _x and various daily subsets.....	106
Table A. 2. Model performance metrics for daily average CO and various daily subsets.	108
Table B. 1. Summary of sensitivity analysis for meteorology inputs, showing results of performance evaluation for NO _x , separated by prevailing wind direction.	136
Table B. 2. Summary of sensitivity analysis for meteorology inputs, showing results of performance evaluation for NO _x , separated by day of week.	137
Table B. 3. Summary of sensitivity analysis for meteorology inputs, showing results of performance evaluation for NO _x , separated by season.	138
Table B. 4. Summary of sensitivity analysis for meteorology inputs, showing results of performance evaluation for CO, separated by prevailing wind direction.	139
Table B. 5. Summary of sensitivity analysis for meteorology inputs, showing results of performance evaluation for CO, separated day of week.	140
Table B. 6. Summary of sensitivity analysis for meteorology inputs, showing results of performance evaluation for NO _x , separated by season.	141
Table B. 7. Summary of sensitivity analysis for emission factor inputs, showing results of performance evaluation for NO _x , separated by prevailing wind direction	142
Table B. 8. Summary of sensitivity analysis for emission factor inputs, showing results of performance evaluation for NO _x , separated by weekday.....	142
Table B. 9. Summary of sensitivity analysis for emission factor inputs, showing results of performance evaluation for NO _x , separated by season.	143
Table B. 10. Summary of sensitivity analysis for emission factor inputs, showing results of performance evaluation for CO, separated by weekday..	143
Table B. 11. Summary of sensitivity analysis for emission factor inputs, showing results of performance evaluation for CO, separated by weekday.	144
Table B. 12. Summary of sensitivity analysis for emission factor inputs, showing results of performance evaluation for CO, separated by weekday.	144

LIST OF FIGURES

Figure 1. Maps showing Allen Park, Detroit (A) and Com Edison, Chicago (B) monitoring sites and nearby point sources emitting more than 25 tons of PM _{2.5} in 2011	42
Figure 2. The modeling domain used in Aim 2, 3 and 4.	43
Figure 3. Wind rose for Detroit City Airport (DET) and Detroit Metro Airport (DTW) stations, for 2012.....	44
Figure 4. Designation of Urban Sources. Sources in Detroit were classified as “urban” with a reference population of 106 and the default surface roughness [127]..	45
Figure 5. Custom mapping algorithm for aligning state roads with existing link-based inventory.	46
Figure 6. For CO, the % of observations below, within a factor of 1, or greater than the detection limit of each monitoring station and analytical method.....	47
Figure 7. For NO _x , the % of observations below, within a factor of 1, or greater than the detection limit of each monitoring station and analytical method.....	48
Figure 8. For PM _{2.5} , the % of observations below, within a factor of 1, or greater than the detection limit of each monitoring station and analytical method.....	49
Figure 9. Boxplots of monthly upwind hourly CO measurements at each monitoring stations method for 2012.....	50
Figure 10. Boxplots of monthly upwind hourly NO _x measurements at each monitoring stations method for 2012.....	50
Figure 11. Boxplots of monthly upwind hourly PM _{2.5} measurements at each monitoring stations method for 2012.....	51
Figure 12. For CO, time-series plots of “leave-one-out” cross validated background values. Each plot is labeled on the top by the AQS Site ID and sampling method (See Table 1).....	52
Figure 13. For NO _x , time-series plots of “leave-one-out” cross validated background values. ...	53
Figure 14. For PM _{2.5} , time-series plots of “leave-one-out” cross validated background values. .	54
Figure 15. Boxplots of background vs monitored CO levels; across monitoring stations, little correlation is seen.	55
Figure 16. Boxplots of background vs monitored NO _x levels; across monitoring stations, the highest correlation is R ² = 0.33.....	56

Figure 17. Boxplots of background vs monitored PM _{2.5} levels; across monitoring stations, very little correlation is seen.	57
Figure 18. The modeling domain, showing, locations of NEXUS receptors, location of Detroit receptors.....	58
Figure 19. Annual and seasonal concentration trends in Detroit from 2001 to 2015.	78
Figure 20. Annual and seasonal concentration trends in Chicago for median and 90th percentile concentrations from 2006 to 2014.	79
Figure 21. Distribution of species by factor in PMF models for Detroit (A) and Chicago (B). Overall percentage contribution to modeled PM _{2.5} is listed for each factor.	80
Figure 22. Annual and seasonal trends of PMF apportionments by source category in Detroit from 2001 to 2014.	81
Figure 23. Annual and seasonal trends of PMF apportionments by source category in Chicago from 2006 to 2014 using an 8-factor model.	82
Figure 24. Annual and seasonal trends of fractional PMF apportionments by source category in Detroit from 2001 to 2014.	83
Figure 25. Annual and seasonal trends of fractional PMF apportionments by source category in Chicago from 2006 to 2014 using an 8-factor model.	84
Figure 26. Observed versus modeled NO _x and CO at the near-road site using the EC9830T and IGpCHEM monitors.....	104
Figure 27. Population rose for Detroit. This shows the % of near-road residents (people within 150m of a road with AADT > 10,000) with a road to any sector (in 5 deg bins).....	105
Figure 28. Scatterplots of NO _x predicted using KDET or KDTW meteorology at NEXUS (n=206) and Detroit receptors (n=543) by days.	133
Figure 29. Investigation of spatial relationship of points on 12/2/11 with large discrepancies in the relationship between KDET and KDTW	134
Figure 30. Histograms of distance between receptors to the nearest major (AADT > 10,000) roads, and the number of nearby large roads.....	135
Figure 31. Hour-of-day average exposures, separated by a) micro-environment and b) source, for 100 simulated individuals in Detroit for 2014, calculated using monitored NO _x	154
Figure 32. Average exposure contributions from background, point sources, non-commercial traffic, and commercial traffic	155
Figure 33. Barplots showing the demographic breakdown of participants in time-activity studies in Consolidated Human Activity Database data from Wayne County, MI	156

Figure A. 1. Comparison of the ratio between predicted and observed concentrations of CO and NO_x at each monitoring site. The x-axis labels describe the AQS Site and the sampling device used. 110

Figure A. 2. Comparison of the ratio between predicted and observed concentrations of CO and NO_x at each monitoring site, differentiated by prevailing wind direction (either downwind or parallel winds). The x-axis labels describe the AQS Site and the sampling device used. 111

Figure A. 3. Comparison of the ratio between predicted and observed concentrations of CO and NO_x at each monitoring site, differentiated by day-of-week. The x-axis labels describe the AQS Site and the sampling device used. 112

Figure A. 4. Comparison of the ratio between predicted and observed concentrations of CO and NO_x at each monitoring site, differentiated by season. The x-axis labels describe the AQS Site and the sampling device used. 113

ABSTRACT

Strategies for reducing exposure to ambient air pollution in urban areas may be less effective as pollutants and their sources have shifted from being dominated by large point sources to more complex mixtures that include a sizeable fraction of traffic-related air pollutants (TRAP). In past decades, urban air pollution management strategies were designed to control pollutant emissions from point sources, while traffic-related emissions primarily were controlled by federal regulations. This approach now may not address the exposures experienced by vulnerable individuals that can result in adverse health impacts and inequities in the distribution of health impacts. New tools and methods are needed to characterize exposures from emission sources including traffic. This dissertation aims to address this need by applying and evaluating several methods to estimate exposures, focusing on TRAP. The specific aims of this dissertation are to describe recent trends of TRAP exposure in two large urban areas (Detroit, MI and Chicago, IL), understand the performance and sensitivity of a recently developed dispersion model used to estimate TRAP exposures through an evaluation using Detroit area data, and describe and apply a novel method for characterizing the contribution from specific sources (e.g., on-road vehicles) to population exposure.

The first aim examines trends in emissions, concentrations and source apportionments of fine particulate matter (PM_{2.5}, particles with a diameter less than 2.5 µm) in two large Midwest U.S. cities, Detroit, Michigan, and Chicago, Illinois. Annual and seasonal trends are assessed for emissions data from the National Emission Inventory (NEI) for 2002 to 2011, speciated ambient PM_{2.5} data from 2001 to 2014, and source apportionments generated using positive matrix factorization (PMF) receptor modeling. Trends in 50th and 90th percentile concentrations and apportionments are evaluated using quantile regression (QR), a technique which distinguishes trends at specific percentiles. The analysis reveals that the fraction of PM_{2.5} due to mobile sources and other local emissions have increased (Detroit) or stayed constant (Chicago), even as total PM_{2.5}

concentrations have decreased in both cities. The methodology demonstrated in this aim could be used to compare trends in the share of PM_{2.5} contributed by vehicles across major cities; many cities have different local regulations and fleet mixes that may affect trends in vehicle-related PM_{2.5}, and the methods in this aim could be used to identify potentially preferred pollution reduction strategies.

The second aim provides an operational evaluation of RLINE, a research-level line-source dispersion model developed by the United States Environmental Protection Agency (EPA) for the near-road environment. Operational evaluations obtain results pertinent to model application, e.g., in regulatory settings. This evaluation compares predictions of oxides of nitrogen (NO_x), carbon monoxide (CO) and PM_{2.5} to observations at air quality monitoring stations located near high traffic roads in Detroit, MI. For CO and NO_x, model performance was best at sites close to major roads, during downwind conditions, during weekdays, and during certain seasons; PM_{2.5} comparisons were uninformative given high background levels and other uncertainties. Implications for regulatory, health impact and epidemiologic applications include the importance of selecting appropriate pollutants, using appropriate monitoring approaches, considering prevailing wind directions during study design, and accounting for uncertainty.

The third aim examines the sensitivity of exposure estimates produced by the RLINE model to the model's meteorological, emission and traffic allocation data. The application focuses on health studies examining near-road exposures to TRAP. Overall, results highlight the need for appropriate model inputs, especially meteorological inputs, in dispersion model applications designed to estimate near-road concentrations and exposures to TRAPs. Systematic biases are identified that might affect analyses using dispersion model predictions as exposure measures, e.g., in air pollution epidemiology and health impact assessment studies.

The fourth aim quantifies source contributions to individual exposures and provides an apportionment of exposures. Using the modeling framework developed in the second aim, point and mobile source contributions and background levels of NO_x are estimated, and a probabilistic human exposure model is used that predicts exposure using simulated population time-activity and estimated pollutant concentrations in various urban micro-environments. Results show that most of the exposure was derived from background levels, although contributions from non-commercial traffic sources provided important contributions during the evening and early morning periods in

the “indoor-at-home” micro-environment. This exposure apportionment complements results from the previous aims pertaining to emissions and concentrations, and it shows the significance of on-road mobile sources to cumulative exposures in Detroit. Using the presented methodology for exposure apportionment, interventions incorporating the temporal and spatial nature of exposure could be applied to potentially lower the exposure of individuals in vulnerable groups.

This dissertation identified results that emphasize the need to target mobile sources of air pollutants in policies and regulations intended to decrease pollutant concentrations in urban areas, and it provides methods to estimate exposures. The modeling evaluations show the importance of using local emission, meteorological, and pollution data when possible, and the importance of characterizing variability and uncertainty in predicting exposure. Predicting exposures of vulnerable and susceptible populations, including low-income and minority individuals living near major roads, may be particularly challenging, but these populations also are likely to suffer a disproportionate share of vehicle-related health impacts. The modeling approaches examined in this dissertation can help to characterize exposures and evaluate strategies that can reduce these adverse impacts.

Chapter I – Introduction

I.1 Motivation to study traffic-related air pollution

Air pollution emissions from on-road motor vehicles, called “traffic-related air pollution” (TRAP), cause serious acute and chronic adverse health impacts and thus represent a major public health issue. TRAP includes a number of components: aerodynamic entrainment of road surface particles, brake and tire wear, which contribute particulate matter (PM) in various size ranges; volatilization of fuels and lubricants, which increases concentrations of volatile organic compounds (VOCs); and incomplete combustion of hydrocarbon fuels, which includes noxious exhaust gases, e.g., carbon monoxide (CO), oxides of nitrogen (NO_x), composed of NO and NO₂), and fine particulate matter (PM_{2.5}). As early as 2002, TRAP was emerging as the dominant source of pollution in many urban areas [1]. Its significance is magnified given that 4% of the US population (11.3 million persons) live within 150 m of a major highway, and this fraction can increase up to 40% in cities [2, 3], where the highest concentrations of TRAP are expected.

Exposure to TRAP has been associated with mortalities in a range of environments. In the US in 2005, the total number of premature deaths related to exposure to vehicle emissions was estimated at 53,000 [4] (compared to an estimated 43,500 vehicle accident-related fatalities among adults below 44 [5]). Outside the US, given the number of megacities with high pollution levels and large populations of at-risk individuals, the number of annual deaths due to vehicle pollution may be an order of magnitude higher, commensurate with the estimate that air pollution as a whole causes 1 in 9 deaths globally [6].

TRAP exposure can cause a wide range of adverse health effects. A comprehensive review completed in 2005 found that the TRAP component of PM_{2.5} is associated with both morbidities and mortalities [7], including worsening existing respiratory and other pre-existing health

conditions and causing disease, particularly among susceptible and vulnerable individuals¹. A 2010 critical review found that exposure to TRAP was causally associated with exacerbation of symptoms of asthma among children with the disease [2]. Exhaust from vehicles using diesel fuel has been causally linked to lung-cancer [8], and truck traffic, the primary emitter of diesel exhaust, has been associated with decreased lung function in children living within 300 m of select roadways in the Netherlands [9]. TRAP exposure has been linked to adverse pregnancy outcomes, e.g., low birth weight and small for gestational age births in Canada from 1998 to 2008 [10]. These conclusions are supported by findings of suggestive but (as of now) insufficient associations between long-term traffic exposure and onset of asthma among children [2], among other conclusions.

Health impacts associated with TRAP exposure disproportionately affect socially and economically disadvantaged populations, including children, the elderly, low socio-economic status, those living in close proximity to high-traffic roads, and individuals with asthma or other respiratory conditions [2]. TRAP exposure has also been associated with differing amounts of sleep disturbance among race/ethnicity and socio-economic status groups in the Boston Area Community Health Survey [11]. Numerous studies have investigated associations between traffic pollution exposure and health effects in the elderly, and associations have been shown with increased heart-rate variability [12], faster progression in disability [13], and degree of coronary atherosclerosis [14].

To mitigate the health effects associated with exposure to TRAP, many countries have enacted policies to reduce emissions and exposures. Several policies have not been successful: a policy restricting car use in Mexico City based on license plate number was found to increase the volume of older, “dirtier” cars on the road [15]. Fortunately, catalytic converters have drastically reduced the amount of NO_x emitted from tail-pipes [16]; and the use of sulfur-free fuel and low-emission zones (e.g., in London and several German cities) lowered concentrations of ultrafine particulate matter (PM_{0.1}), coarse particulate matter (PM₁₀), and NO_x [17–19]. However, these policies may not continue to be as successful, given increasing urbanization in many urban areas. Increases in city population is accompanied by increases in the volume of on-road vehicles, traffic congestion,

¹ Kottow [200] succinctly describes the distinction between susceptible and vulnerable as “... the difference between being intact but fragile – vulnerable – and being injured and predisposed to compound additional harm – susceptible.”

and commuting distances. Concurrently, large roadways become adjacent to residences, schools, and workplaces, micro-environments where a large portion of exposure occurs. These trends in exposure and urbanization, and the large and potentially growing TRAP fraction in many urban areas, motivates the need to better characterize TRAP exposure with the ultimate aim of using this information to inform policies aimed at reducing health impacts.

I.2 Methods used to estimate exposure to TRAP

This section provides an overview of methods used to estimate exposure to TRAP. Exposure estimation is a foundational element of policies that aim to reduce exposures.

There are numerous methods for estimating exposure to TRAP [20]. The most accurate approach for determining exposures, personal measurements, is rarely feasible or cost-effective given the number of subjects required and the cost, burden and other limitations of the sampling equipment. In deference to this method, a number of surrogate methods can be employed. One such method uses concentrations of TRAP measured at an ambient air quality monitoring station nearest to the population of interest. In the U.S., the State and Local Air Monitoring Stations network (SLAMS), the Interagency Monitoring of Protected Visual Environments (IMPROVE) network [21], and the Chemical Speciation Network (CSN) [22] have collected ambient data since the mid-1980s that can facilitate these analyses, as well as ensure compliance with National Ambient Air Quality Standards (NAAQS). As an example, a recent study used fixed site data to show that elemental and organic carbon, which originate primarily from vehicle emissions, were associated with the largest risk for emergency hospitalization of any of the major species of fine particulate matter [23]. Ambient air quality monitoring data can permit a wide range of trend analyses, which can help evaluate the effectiveness of mitigation and control measures, e.g., low emission zones [17], and help to evaluate dispersion and exposure models [24]. Monitoring data also have been widely used to estimate exposures for epidemiology and risk studies investigating and predicting the health consequences of pollutant exposure [25]. Despite these applications, most conventional air quality monitoring networks are spatially too sparse to capture small-scale variation or spatial gradients of TRAP, e.g., the elevated concentrations found near large roadways [26].

Concentrations at fixed sites can also be used to make inferences about relative levels of emissions from contributing sources (e.g., on-road vehicles), analyses known as receptor modeling. Such applications are especially important in areas with susceptible populations and where

concentrations exceed ambient standards, and for those emission sources that are difficult to characterize or that have changed rapidly, e.g., on-road emissions, due to shifts in fuels, emission controls, and fleet mix. In Detroit, for example, receptor model apportionments using positive matrix factorization [27] have identified key $PM_{2.5}$ sources, e.g., secondary sulfate aerosol (SO_4^{2-} , especially in the summer), secondary nitrate (NO_3^-), metal processing, biomass burning, other manufacturing and industrial operations, vehicle-related emissions (including primary and secondary aerosols from tire and brake wear, and entrained dust), and crustal-derived emissions [28–36]. A few recent receptor model apportionments examined long-term trends in vehicle-related contributions – a recent analysis of 2002 to 2013 CSN data in Southern California showed that median $PM_{2.5}$ concentrations attributed to vehicles fell 21 to 24% between the first and last 4 year blocks of the study period (2002 to 2006 and 2008 to 2014, respectively) [37] – although given differences in local emissions and ordinances, these trends are not widely generalizable. Updated analyses in various urban areas are needed to account for changes in city-specific emissions and industrial activity that have occurred over recent decades.

Pollutant concentrations and exposure estimates that vary spatially and temporally, reflecting near-road gradients, are needed for a number of applications, e.g., urban-scale cohort and panel studies [38]. These can be generated by a variety of techniques. Measures that do not directly model the dispersion of pollution through urban areas, such as the proximity to roads and traffic intensity, have been used, but these only indirectly indicate concentrations and have other limitations [39]. Dispersion models use meteorological parameters, e.g., wind speed, wind direction, and measures of atmospheric turbulence, to simulate the concentration of emitted pollutants at pre-defined locations (called “receptors”). Concentrations at receptors placed at relevant locations, e.g., an individual’s residence or workplace, can be predicted to estimate the potential for ambient exposure of that individual. Hourly exposures can also be modeled using probabilistic human exposure models that simulate population-level time-activity in various urban micro-environments. Estimation of hourly exposures to modeled pollutant levels allows for apportionment of exposures and identification of source-activity pairs that contribute the air pollution burden; these pairs could potentially be targeted in interventions aimed at reducing exposures. Dispersion models, exposure models, and exposure apportionment are featured in this dissertation, and are discussed in the following sections.

I.2.1 Dispersion models

Dispersion models have long been used to predict concentrations of emitted pollutants in both rural and urban areas at high spatial and temporal resolutions. Several dispersion models are available and appropriate for TRAP. The current US regulatory dispersion model is the American Meteorological Society (AMS) and U.S. Environmental Protection Agency (EPA) Regulatory Model (AERMOD) [40]. AERMOD uses a complex suite of meteorological parameters to predict pollutant concentrations. While designed to model emissions from stationary industrial point sources, AERMOD incorporates modules to model emissions from line sources (e.g., highways, railroads). The California LINE-source model (CALINE) [41] contains a specifically-tuned interface for processing line-source inputs using a limited set of basic meteorological parameters (e.g., wind speed, wind direction, temperature and atmospheric stability class). Recent literature has suggested replacing CALINE with AERMOD owing to this simplification [42]. The recently developed Research LINE-source dispersion model, RLINE [43], is specifically designed to model near-roadway concentrations, contains updated dispersion algorithms, numerical as well as than analytical solving mechanisms, several beta-tested near-roadway environment specific modules (e.g., barriers and roadway depression) and a novel near-road pollution meander algorithm [43, 44]. A recent model inter-comparisons suggested that RLINE may have some expanded utility compared to CALINE [45]. Performance evaluations of the RLINE model [43–46] show generally comparable results to other line source models that simulate dispersion from on-road traffic emissions [47–50].

Prior performance evaluations of RLINE appropriate to predicting health-relevant exposures (e.g., daily and annual average exposure to TRAP) have limitations. For example, they often lack evaluations of daily (and sometimes annual) average concentrations of TRAP, a commonly used health metric, and they rarely are performed at the urban scale needed for population-level observations of health outcomes. Instead, most evaluations have examined hourly average concentrations, used experimental tracer gases that do not undergo chemical and physical transformations, and examined small ($<1 \text{ km}^2$) and simplified domains that contain few sources [45, 46, 51]. (See Table 1 for datasets used in previous RLINE evaluations.) While providing valuable diagnostic information that can help improve models, these evaluations do not represent the complexity and scale of urban settings, which can span large and diverse areas with many emission sources. The studies that have compared RLINE predictions to observations of TRAP

have other limitations, e.g., the use of short monitoring periods, single pollutants [43, 52], sole examination of annual average concentrations [53], and limited discussions of model performance and study methodology [54]. Further, performance has not been evaluated with respect to exposure-relevant factors (e.g., meteorological and emission variability seen by day-of-week and season) that could alter results and lead to exposure measurement errors and misclassification. Guidance on specific metrics to be used in performance evaluations of air quality models has been published recently, [55, 56] (discussed further in Chapter II).

An additional area requiring evaluation is the sensitivity of RLINE to various input parameters. RLINE, like all dispersion models, requires meteorological data, which fundamentally influence dispersion calculations [57–60]. Ideally, these data use on-site or local observations [60]. However, local meteorological datasets are typically limited, e.g., of the 72 near-road monitoring sites in the USA, only 6 have a National Weather Service (NWS) meteorological station within 5 km, and the average distance to the nearest station is 18.5 km [61]. Previous sensitivity studies using industrial emissions, e.g., mercury and hexavalent chromium, attributed 16 – 25% variability in results to changes in meteorological inputs [62, 63]. However, with regards to TRAPs in urban areas, such sensitivity studies are limited. As a second example, emission data used in dispersion models depend on traffic activity (e.g., number of vehicles, vehicle mix, vehicle speed and acceleration), which in turn depends on commuting and work schedules, construction activity, weather and many other factors [64]. Typically, emission rates are derived using simplified and default allocations to obtain hourly and daily estimates from annual average data. Again, local data regarding traffic volume, mix, and diurnal patterns are recommended, but such inputs are rarely available. While not providing a full measure of model uncertainty, sensitivity analyses reveal the relative amount of uncertainty associated with each model input, the robustness of the model with respect to changes in inputs and parameters, and critical model inputs, i.e., those that are uncertain and that cause large changes in model predictions [57, 65]. Such sensitivity analyses have not been completed for RLINE. Given that RLINE may be incorporated into AERMOD and used in regulatory and health-based applications, it is important to understand the conditions that affect performance and the critical inputs.

1.2.2 Human exposure models

Human exposure models estimate distributions of air pollution exposure in various micro-environments by estimating hourly presence of simulated individuals in various micro-environments (e.g., in residence, in vehicle), and predicting average concentrations in those micro-environments using local or national building penetration rates and other generic transfer coefficients (ambient pollution concentrations are used as inputs in human exposure models). The above described micro-environment approach was introduced in the US in the early 1980s [66–68], and largely remains unchanged in the current EPA model used to estimate human exposures to air pollutants, the Air Pollution EXposures Model (APEX) [69]. This model can simulate populations that match the demographics of the user’s study area. Simulated individuals in APEX are sampled based on Census-block demographic characteristics of the desired study domain from the Consolidated Human Activity Database (CHAD), a national database of time-activity diaries collected from various studies [70].

One limitation of APEX is that CHAD may not accurately characterize activity of individuals in vulnerable groups, e.g., commuters, the elderly, individuals in minority populations and with low socio-economic status (SES). Several studies have compared exposure estimates derived using CHAD with measured exposures in urban populations, and found that intra-person variability in exposures among urban residents may differ by key demographics and contact with various pollutant zones [71]. As examples, urban commuters moved through polluted microenvironments (MEs) more rapidly than did suburban commuters [72], and in-vehicle exposures accounted for up to half of total PM_{2.5} exposure for some commuters [73]. A discrepancy in work travel times recorded in CHAD and those in the American Time Use Study (ATUS) may cause increased errors in exposure estimates among commuters [74]. Among the elderly, exposures modified by changes in behavior related to aging are largely not considered [75], and these modified exposures, especially if they result in increased time indoors or in vehicles, could cause large exposure estimate errors [76]. CHAD also may not reflect time-activity data of minority populations living in urban areas with high pollution levels, so called “hotspots” [77]; recent studies have demonstrated limitations regarding CHAD's representativeness for various sub-populations, including minority or low income [78]. To address these issues, recent work has called for the use of global positioning system (GPS) time-activity data to investigate time-activity patterns among in low SES populations [79] and other populations (e.g., children) with the above noted

discrepancies between actual and diary-recorded time activity patterns [80], and further examination of time-activity among “sentinel” populations (e.g., pregnant women) [81].

I.2.3 Exposure apportionment

Exposure apportionment quantifies contributions from various emission sources or exposure compartments (microenvironments) to an individual’s total exposure. Recent work in personal exposure modeling indicated apportionment of exposures as a tool for the next generation of exposure assessment. Specifically, in 2009, “... if the performance of the emission-based dispersion modeling for a hot spot is improved, a more precise characterization of contributions of different source emission categories (such as point, area, mobile on-road, and mobile non-road) on personal exposure levels to air toxics can be achieved” [82] This approach requires estimates of both total or cumulative exposure, and exposure attributable to the source or compartment of interest. Possibly the only practical approach for obtaining the high spatial and temporal resolution information needed is via modeling, for example, by combining APEX’s capabilities of probabilistic time-activity sampling and compartment modeling with dispersion models of point and mobile sources in an urban area, as can be done with RLINE and AERMOD.

Previous literature has performed exposure apportionment on traffic-related air pollutants, but mostly at lower temporal or spatial-resolutions or over shorter durations. Volatile organic compounds (VOCs) have been subject to numerous studies of “source apportionment of human exposure” [83, 84]. PM_{2.5} exposures were apportioned using combined receptor modeling for a small (n = 30) cohort of hypertensive adults in North Carolina [85], however this analysis took place over the period of a few weeks, and used stationary monitoring to calculate exposures in varying micro-environments: personal, residential indoor, residential outdoor and ambient; notably not near-road or in-vehicle, exposures that might be more relevant in Detroit than other study locations. Previous “source-to-dose” studies of TRAP have also characterized the relative levels of various source groups: outdoor sources of PM_{2.5} were shown to contribute more to exposures than indoor sources during a 2-week pollution episode in Philadelphia, PA [86]. One recent study combined modeled CO, NO_x, and PM₁₀ with activity data in Paris, showing that pollutant-specific health effects may be teased apart [87]; however these modeled pollution concentrations were derived from coarse grid-cell (3km x 3km) chemical model, and all time activity data were collapsed into 3 categories.

Exposure apportionment can provide insights and support actions that existing exposure assessment tools applied to environmental settings generally do not provide. As examples, the approach can identify the source-activity pairs that contribute the majority of the air pollution burden among susceptible populations, the contribution of commuting by personal car or bus, or the sources that contribute significantly to exposures of children. Such analyses can inform state and federal environmental agencies, provide with motivation or justification for validation studies, e.g., projects investigating exposures on certain bus-routes or on certain highways, and lead to targeted interventions to reduce exposure and improve public health. Models of environmental exposure, like other environmental models, cannot be validated [88]. Specific to TRAP apportionment, few sources can be uniquely identified in measured exposures, i.e., they do not have specific and unique source tracers. This fact is pollutant-specific: VOCs can be more easily speciated from single measurements in a way that cannot be done easily for PM_{2.5} (PM_{2.5} speciation requires many instruments and fine-tuning, whereas VOCs can be speciated using mass spectrometry) or NO_x (there are not sufficient tracers to uniquely identify NO_x sources directly from measurements). More generally, dispersion and other models that predict ambient pollution levels contain inherent biases, and often the signal of specific sources does not differentiate from background levels. Still, given the spatial nature of exposure, and common pathways of commuting and working, especially in Detroit which has a large commuting population, exposure apportionment may provide insights into relative contributions that are not observable with only measurements at a few fixed sites, and thus provide output that is useful to policy makers [89].

I.3 Specific Aims

The overall objective of this dissertation is to provide insight into modeling tools used to estimate ambient air pollution exposures, and to develop a method for attributing the total exposures to contributing sources, thus providing an “exposure apportionment”. The research has four specific aims.

Aim 1 examines trends in emissions, concentrations and source apportionments of fine particulate matter (PM_{2.5}, particles with a diameter less than 2.5 microns) in two large Midwest U.S. cities, Detroit, Michigan, and Chicago, Illinois. Annual and seasonal trends in emissions are investigated using data from the National Emission Inventory (NEI) for 2002 to 2011, in concentrations using speciated ambient PM_{2.5} data from 2001 to 2014, and in apportionments using outputs from

positive matrix factorization (PMF) receptor modeling [27]. Trends in 50th and 90th percentile concentrations and apportionments are assessed using quantile regression (QR) [90], a technique which distinguishes trends at specific percentiles, and this aim presents an application of PMF and QR that is novel and relevant to public health.

Aim 2 provides an operational evaluation of a dispersion model designed for near-road environments. Operational evaluations provide context for evaluating model performance under specific conditions. Using a detailed modeling system featuring the Research Line source model (RLINE) and a spatially and temporally resolved mobile source emissions inventory, predictions of NO_x, CO and PM_{2.5} are compared using standard metrics [55, 56] to observations at air quality monitoring stations located near high traffic roads in Detroit, MI. This evaluation differs from previous performance evaluations of RLINE [43–45], which have verified the algorithms of the model using limited test cases. The present application highlights considerations relevant to health impact and epidemiologic applications, including the importance of selecting appropriate pollutants, using appropriate monitoring approaches, considering prevailing wind directions during study design, and accounting for uncertainty.

Aim 3 examines the sensitivity of the exposure predictions to meteorological, emission and traffic allocation inputs. This analysis uses the RLINE model and the Detroit application, and again focuses on applications relevant to health studies examining near-road exposures to TRAP. Daily average modeled and monitored concentrations of NO_x and CO are used to assess the potential for exposure estimate error in cohort and population-based studies. Sensitivity is evaluated using statistical performance metrics [55, 56], nominal and alternative model inputs, and NO_x-attributable health impacts for two sets of meteorology three sets of receptors reflecting different study populations or scenarios. This aim is intended to inform study designs and the use of dispersion modeling in health studies. In particular, as models like RLINE become more widely used, it is critical to understand the potential for biases and other exposure measurement errors.

Aim 4 develops a framework for apportioning exposures, specifically, quantifying contributions from various sources to individual exposures. This work requires high spatial and temporal resolution modeling of TRAP, which in turn requires detailed emission inventories and meteorological datasets. Exposure apportionment is demonstrated through a case study of individuals for a selection of vulnerable groups in Detroit, Michigan. If exposures can be

apportioned, then the source-activity pairs that contribute the majority of the air pollution burden can be targeted for interventions that reduce exposure. This aim also evaluates the representativeness of national time-activity databases for individuals in selected vulnerable subpopulations.

I.4 Dissertation overview

This dissertation is organized into seven chapters. Chapter II provides methods used in subsequent chapters. Chapters III to VI pertain to aims 1 to 4, respectively. Each begins with a brief summary of motivation and methods, continues with results and discussion of each aim, and concludes with limitations of the analysis. Chapter III addresses Aim 1, providing an analysis of trends in apportionments in two large Midwest US cities, emphasizing the vehicle fraction. Chapter IV pertains to Aim 2, providing an operational evaluation of the RLINE dispersion model as it might be used in epidemiological studies. Chapter V covers Aim 3, describing a sensitivity analysis of RLINE in an application pertinent to health-related studies. Chapter VI addresses Aim 4, presenting and evaluating an approach to apportion air pollution exposures using an application in Detroit and focusing on roadway pollution and vulnerable populations. Chapter VII provides a conclusion to the research, summarizes and integrating results in each of the aims and suggesting areas for future research.

Much of this work has been published in the peer reviewed literature. Chapter III was published in 2016 as Milando Chad, Huang Lei, Batterman Stuart (2016) *Trends in PM_{2.5} emissions, concentrations and apportionments in Detroit and Chicago*. Atmospheric Environment 129:197–209 [91]. Chapter IV was published in 2018 as Milando Chad, Batterman Stuart (2018) *Operational evaluation of the RLINE dispersion model for studies of traffic-related air pollutants*. Atmospheric Environment 182:213–224 [92]. Chapter V was published in 2018 as Milando Chad, Batterman Stuart (2018) *Sensitivity analysis of the near-road dispersion model RLINE – An evaluation at Detroit, Michigan*. Atmospheric Environment 181:135–144 [93].

I.5 Tables

Table 1. Summary of datasets used in previous RLINE evaluations.

Evaluation dataset	Pollutant	Sampling location	Sampling period	Sampling resolution	Receptor network
Idaho Falls [94]	SF ₆	Rural	5 days of 3h blocks	15 min	A grid of 58 receptors ranging from 18 to 180m downwind, 2 upwind. Z = 1m
Caltrans [41]	SF ₆	Rural	Several days of 3h blocks	½ hour	9 receptors in a transect
Raleigh near-road [95]	NO	Urban	July and August 2006	20 sec	2 downwind receptors at 7 and 17m
Prairie Grass [96]	SO ₂	Rural	70 releases	10 min	545 samplers placed along arcs of 50, 100, 200, 400, and 800 m from release.
Detroit near-road [97]	CO, NO _x	Urban	Sept 2010 to June 2011	5min	10, 100, 300 m downwind; 1000 m upwind

Chapter II – Methods

II.1 Aim 1

Aim 1 examines trends in emissions, concentrations and source apportionments of PM_{2.5} in Detroit, Michigan, and Chicago, Illinois. Annual and seasonal trends were investigated using National Emission Inventory (NEI) data for 2002 to 2011, speciated ambient PM_{2.5} data from 2001 to 2014, apportionments from positive matrix factorization (PMF) receptor modeling [27], and quantile regression [90].

II.1.1 Emissions data

To inform the source apportionments and to corroborate trends in measured concentrations, emission data were extracted from the 2002, 2005, 2008 and 2011 National Emission Inventories (NEIs) [98] for Wayne and Cook Counties, which include the cities of Detroit and Chicago, respectively. (The NEIs are revised every three years.) This trend analysis considered primary PM_{2.5} (i.e., the sum of filterable and condensable PM_{2.5}) emissions from point, non-point, on-road mobile, and off-road mobile sources. On-road sources, which include exhaust, brake, and tire wear emissions from light and heavy duty diesel and gasoline vehicles, were separated in the analyses. The NEI technical support documents are consulted to explain methodological changes between NEIs.

II.1.2 Ambient air quality data and treatment

To examine trends in concentrations of speciated fine particulate matter (PM_{2.5}, particle diameter < 2.5 µm), monitoring sites in the two cities were chosen based on the PM_{2.5} components measured, the duration and completeness of the monitoring record, and the diversity of nearby sources. The selected sites have speciation records that extend to the early to mid-2000s, and both are part of the Speciation Trends Network (STN), a subset of Chemical Speciation Network (CSN) [22] monitoring sites at which measurements are taken every 3 days [99]. Figure 1 shows the location of these sites and nearby major point sources of PM_{2.5}.

The Allen Park ("Detroit") site in south Detroit (AQS ID: 261630001; lat/long: 42.228611/-83.20833) is a non-source-specific and population-oriented monitoring site that has been used to detect impacts from mobile sources [100]. It has recorded the highest PM₁₀ (particle diameter < 10 µm) levels in the area [101]. The site is located within 200 m of a major interstate highway (I-75). The immediate vicinity is grassy and wooded; a few covered storage tanks are within 100 m; some light industry, trucking firms, suburban areas, etc., are within 1 km; and heavy industry, including refineries, steel production, coke and coal-fired electricity generation are within 15 km. The speciation record began in 2001. Detroit comprises much of Wayne County, which has a population of 1,820,584 (2010) and an area of 1,585 km² [102]. Summary statistics for speciated PM_{2.5} in Detroit are listed in Table 2.

The Com Edison ("Chicago") site is located in an urban neighborhood in south Chicago, IL (AQS ID: 170310063; lat/long: 41.7514/-87.713488) on the grounds of a small facility of the local electrical utility. Nearby emissions sources include rail lines 1 km to the north, and two 6-lane arterials (Routes 50 and 12) located 2 km to the west and south, respectively. Chicago Midway International Airport is 5 km to the northwest. Heavy industry in Calumet and South Chicago, within 20 km, include coal-fired electricity generation, steel mills, and wet corn milling (which emits PM, SO₂ and volatile organic compounds). The speciation record began in 2001, however, instruments were changed in 2005, and so only data after 2005 are considered. Chicago is located within Cook County, which has a population of 5,194,675 (2010) and area of 2,448 km² [102]. Summary statistics for speciated PM_{2.5} in Chicago are listed in Table 3.

The pollutants monitored, as well as monitoring techniques and procedures, have changed over the years, and thus some data screening and treatment were required prior to trend analyses. Both sites measured PM_{2.5} using both federal reference methods (FRMs) and non-FRMs. The CSN has measured PM_{2.5} using MetOne SASS and URG samplers (non-FRMs), which collect PM_{2.5} on Teflon filters that are analyzed gravimetrically. Elements are measured by X-ray fluorescence on Teflon filters, ions by ion chromatography on nylon filters, and elemental (EC) and organic carbon (OC) by thermal optical transmittance (TOT) on quartz filters. Most pollutants are measured every third day [103, 104]. In 2007, to reconcile differences in OC measurements between CSN and IMPROVE samplers (positive artifacts resulted from the absorption of organic vapors to PM [105]), URG 3000N samplers were placed at CSN sites to measure EC and OC. The higher flow

and face velocity of the URG 3000N decreases VOC adsorption and increases OC volatilization, thus lowering OC concentrations [106]. Along with the instrument switch, the preferred analysis method also changed from TOT to thermal optical reflectance (TOR), allowing more direct comparisons between CSN measurements of EC and OC to those in the IMPROVE network (which historically used TOR). To assess long-term trends, EC and OC measured using TOT were used in the present work.

Adjustments made prior to trend analyses included blank correction, censoring of values below detection limits, and artifact correction. CSN speciation data are not blank corrected, and for most CSN species, the median trip and field blank concentration is zero [107]. (Solomon et al. [107] noted that CSN trip and field blanks can be aggregated as was done in this work.) Each measurement was corrected by the median of blanks taken within ± 1 month, as done elsewhere [105, 108, 109]. Any negative blanks were replaced by the median blank for the entire record. Corrected measurements that fell below method detection limits (DLs) or that became negative were replaced with $1/2$ DL and its measurement uncertainty was replaced with the maximum of the reported uncertainty and $5/6$ DL [31]. (Although these are conventional methods, Brown et al. [110] gives guidance and reasoning for not censoring those values.)

The EC/OC instruments and analytical techniques changed midway through the study period. To address the positive sampling artifact in OC measurements using TOT and the MetOne samplers [111], a 2012 EPA memo [105] suggested using monthly median network blanks from passive sampling (i.e., sampling that occurs without pumping of air through the sampling device). However, Solomon et al. [107] noted that passive field blanks may miss artifacts arising during active sampling (i.e., air is pumped through the sampler). Fortunately, both Detroit and Chicago sites include one year of collocated MetOne SASS and URG 3000N measurements. These collocated data were regressed as $OC_{MET} = k OC_{URG} + artifact$, where k is an estimated regression coefficient used to correct OC MetOne measurements prior to the phase-in of URG samplers (April 2009 in both cities). At Detroit, the regression used the period from 4/1/2009 to 3/30/2010 and gave an OC artifact of $0.126 \mu\text{g}/\text{m}^3$ and $R^2 = 0.77$; for EC, $R^2 = 0.59$. At Chicago, the regression used the period from 5/1/2009 to 4/29/2010 and the estimated OC artifact was $0.303 \mu\text{g}/\text{m}^3$ and $R^2 = 0.85$; for EC, $R^2 = 0.69$. (See Table 4 for additional artifact correction details, including the outliers removed in this analysis.) The estimated OC artifacts are similar to those

reported earlier [105, 111]. Future EPA guidance may indicate other methods to harmonize EC and OC data measured using the TOT and TOR methods.

Ambient data used in the PMF apportionments required additional treatment and quality checks. Missing observations for key metal species (e.g., Ni, Cr) were replaced with the median, and the associated measurement uncertainty was set to four times the median [110]. While sometimes the geometric mean is used in place of the median [37], Brown et al. [110] recommends investigating scaled residuals when this imputation is performed. For missing uncertainties, formula 5.1 and 5.2 from the User Manual of EPA PMF 5.0 were used for observations above and below DL values, respectively, with an error fraction of 10% [112]. (Only the URG 3000N sampler did not have recorded uncertainties.) CSN data for Detroit and Chicago did not have missing DLs. To increase the reliability and representativeness of PMF results, a minimum of 50 observations per species per year was required. Species selected for PMF were informed by previous studies: Na^+ and K^+ were used preferentially over Na and K given the higher detection frequencies and relevance for air pollution studies [113], and SO_4^- rather than S was used as the primary tracer of secondary SO_4^- (both have been used) [35, 113].

To improve reliability and increase fit, PMF apportionments used observations from the cleaned datasets for which 'reconstructed' and observed $\text{PM}_{2.5}$ concentrations agreed within $\pm 4 \mu\text{g}/\text{m}^3$. Reconstructed mass was calculated using a simplified stoichiometry and the dominant oxidized forms of measured species (shown in square brackets below) [114]:

$$\text{PM}_{2.5,\text{CM}} = 1.375[\text{SO}_4^-] + 1.29[\text{NO}_3^-] + 3.73[\text{Si}] + 1.63[\text{Ca}] + 2.42[\text{Fe}] + 1.6[\text{OC}] + [\text{EC}]$$

While agreement might be determined using a multiplicative factor, e.g., within 25%, a concentration band may be more appropriate if errors are primarily additive (rather than multiplicative). The $\pm 4 \mu\text{g}/\text{m}^3$ band is reasonably narrow, and fewer than 10% of samples exceeded this criterion. In addition, the holiday periods of 31 December through 2 January and the weekends closest to 4 July were excluded due to the use of fireworks that contain large amounts of potassium nitrate and that can cause deviations from the stoichiometric relationship in eq. (1) [31, 110, 115].

Additional quality checks included comparisons of elemental and ion concentrations (e.g., S to SO_4^- , K to K^+), and comparison of FRM and non-FRM $\text{PM}_{2.5}$ concentrations. After treatment, the

final Detroit dataset had 1422 observations spanning 14 years (2001 to 2014), and the Chicago dataset had 763 observations spanning 9 years (2006 to 2014).

II.1.3 Receptor modeling

Sources were apportioned using Positive Matrix Factorization (PMF 5.0) [112] with PM_{2.5} as the ‘total’ variable (with a designation as ‘weak’). Introduced in 1994 [27], PMF apportions sources using the following equation: $\mathbf{X} = \mathbf{Z} \mathbf{C} + \mathbf{E}$, where $\mathbf{X} = n \times m$ matrix of observed concentrations ($\mu\text{g}/\text{m}^3$) values; n = number of observations; m = number of chemical species), $\mathbf{Z} = n \times p$ matrix of apparent source strengths; p = user-assigned number of factors or source categories; $\mathbf{C} = p \times m$ matrix of derived source compositions; and $\mathbf{E} = n \times m$ matrix of random errors [27, 116]. Error terms are scaled by estimates of observation-level uncertainty, and \mathbf{Z} and \mathbf{C} are constrained to be non-negative. \mathbf{X} is solved to minimize the sum of squares of weighted residuals, $Q = \sum_{i=1}^n \sum_{j=1}^m \mathbf{E}_{ij}^2 / \sigma_{ij}^2$, where σ_{ij} = standard deviation of the random errors, which are assumed known. From the solution, the strength and composition of each of p factors can be viewed. Some PMF factor mass values are allowed to go slightly negative [112], so to maintain the property of each row-normalized PMF sample summing to 1 (critical for assessing factor fractional contribution trends); these slightly negative values were not censored in trend analyses. (At both cities, fewer than 15% of final factors were negative.) PMF 5.0 calculates a signal-to-noise (S/N) ratio for each species, and $S/N < 0.5$ is considered ‘bad’, $0.5 \leq S/N < 1$ ‘weak’, and $S/N \geq 1$ ‘strong’. Weak species are down-weighted in factorization, and bad species are omitted.

A range of “additional modeling uncertainties” (e.g., 0, 5, and 10%) were tested using features in PMF 5.0. Selection of the number of factors and uncertainty additions depends on prior knowledge of potential sources, source-receptor relationships, and the stability of results [116]. The initial models included 6 to 10 factors. A framework for choosing the ‘final’ model used a series of checks examining the distribution of species within each factor: separation of K⁺ and OC; the vehicle factor should contain large fractions of total OC and EC mass and minimal amounts of other species; a crustal factor (Si, Ti, Ca, Al) should emerge; and metals (Ni, Cr, Fe, Mn) should be grouped together. Finally, using PMF 5.0's bootstrapping capability to estimate uncertainties, realized factors should be robust and handle additional model uncertainty.

II.1.4 Quantifying trends in concentrations and apportionments

Trends in species concentrations from 2001 to 2014 at Detroit and from 2006 to 2014 at Chicago were evaluated initially using the non-parametric Kruskal-Wallis (KW) and Mann-Whitney (MW) tests, and subsequently using quantile regression [90]. (These analyses used the `quantreg` [117] and other packages in R.) Trends in the 'major' PM_{2.5} constituents, defined as species constituting an average of at least 1% by mass of PM_{2.5} (including OC, EC, S, NO₃⁻, NH₄⁺, and SO₄⁻) are of primary interest. Trends in PMF factor mass concentrations and percent contributions were evaluated by QR, as described below.

Initially, the study period was broken into year-blocks (2001-2002, 2002-2005, 2006-2009, 2010-2013, 2013-2015) and seasons (Winter = Dec, Jan, Feb; Spring = Mar, Apr, May; Summer = Jun, Jul, Aug; Autumn = Sept, Oct, Nov). Winter trends were analyzed using data from consecutive months (e.g., winter 2002 data included measurements or apportionments from December 2001 through February 2002). As an initial screen, KW (for 3 or more groups) and MW (for 2 groups) tests attaining a p-value of 0.05 or less were used to identify differences in the distributions between valid groups of measurements, where a valid group was defined as having 10 or more observations with fewer than 50% of observations below DLs. (The direction or magnitude of the differences can be investigated using the Dunn and other tests [118]).

Quantile regression (QR) analyses were used to quantify trends of annual median and 90th percentile concentrations, which are exposure measures relevant to chronic and acute health effects, respectively. Trends of peak values may be susceptible to outliers; trends at lower percentiles may be influenced by data censoring. QR also was used to assess trends in relative factor contributions (factor mass divided by total modeled PM_{2.5} mass, also called “abundance”) to reveal the changing sources of PM_{2.5}. Similar to how linear regression coefficients β_i are found by minimizing the sum of squared residuals calculated as $\sum (y_i - (\beta_0 + \beta_1 x_i + \dots))^2$, quantile regression coefficients Γ_i are found by minimizing the sum of absolute residuals applied to the function ρ_τ , $\sum \rho_\tau(\tau, y_i, \xi(x_i, \Gamma))$, where ρ_τ is the “pinball” function at the desired quantile τ , and $\xi(x_i, \Gamma)$ is a linear function of the predictors with Γ_i as coefficients [90]. The function ρ_τ is equal to $\tau * (y_i - \xi(x_i, \Gamma))$ if $y_i > \xi(x_i, \Gamma)$ and $(1 - \tau) * (y_i - \xi(x_i, \Gamma))$ otherwise. Relative (percentage) changes in median and 90th percentile concentrations for calendar years and seasons were quantified by dividing the estimated QR slope by the associated median and 90th percentile

concentrations, respectively. Percent per year changes were deemed significant if the QR slope exceeded twice the bootstrapped QR standard error.

II.2 Aim 2

Aim 2 provides an operational evaluation of RLINE [43] in which predictions of NO_x, CO and PM_{2.5} are compared to observations at air quality monitoring stations located near high traffic roads in Detroit, MI. Daily average concentrations of CO and NO_x predicted using RLINE and a spatially and temporally resolved mobile source emissions inventory are compared to ambient measurements at 5 near-road monitoring sites in Detroit, MI, using standard evaluation metrics.

II.2.1 Near-road ambient air quality monitoring data

The operational evaluation used monitoring data from five Air Quality System (AQS) monitoring stations located near high traffic roads (Figure 2; Table 5). As mentioned in the trend analysis, the “suburban” or Allen Park site (AQS ID 261630001) is 190 m southeast of Interstate 75 (I-75), which has an annual average daily traffic (AADT) volume of 89,800 [119]. This site is shielded on one side by a row of trees, and a power substation and a truck park border the site. The surrounding area is mostly residential with single family homes. The “industrial” or Dearborn site (AQS ID 261631008) is northeast of the Marathon Petroleum refinery in southwest Detroit and 150 m northwest of I-75 (AADT = 105,800). The “schools” or East 7 Mile site (AQS ID 261630019) is in a small park shared by three schools, 390 m east of MI-97 (AADT = 9,500) and 2,000 m south of MI-102 (West 8 Mile Road). Lastly, the “near-road” and “urban” Eliza Howell sites (AQS IDs 261630093 and 261630094, respectively) are 10 and 100 m north of I-96 (AADT = 152,000) with minimal obstructions.

Air quality data for these monitoring stations for 2011 to 2014 were obtained from the US EPA AQS Datamart [120]. Over the study period, several types of monitoring methods/instruments were used that differed in sensitivity and possibly other characteristics although all used federal reference methods (FRM) or equivalent [121]. Hourly concentrations of NO_x were measured at three sites, CO at four, and PM_{2.5} at three. NO_x at the near-road and urban sites was monitored using gas-phase chemiluminescence and Ecotech 9814B monitors (“IGpCHEM”) from October 2011 through December 2013, and using Thermo Environmental Instruments Model 42C instrumental chemiluminescence (“ICHEM”) in 2014. NO_x at the schools site was measured using a Thermo Environmental Instruments Model 42C and by ICHEM. CO was monitored at the near-

road site by instrumental gas filter correlation using an Ecotech 9830 monitor (“EC9830T”) from October through December of 2011, and an Thermo Model 48C monitor using instrumental non-dispersive infrared (“INDiI”) through 2014. CO at the urban site was measured using Thermo Environmental Instruments Model 48C and by INDiI, and at the suburban site using an instrumental gas filter correlation analyzer (“IGFC”). CO at the industrial site was measured using a Teledyne API T300 using IGFC. PM_{2.5} at the schools and suburban sites was monitored as 24-h averages using the FRM and as 1-hr averages at the suburban site using a tapered element oscillating microbalance (TEOM). PM_{2.5} sites and methods are shown in Table 6.

Data processing and quality checks included the following: NO and NO₂ measurements in ppb were converted to NO_x concentrations using the average conversion rate ($1 \mu\text{g m}^{-3} \text{NO}_x = 0.5495 \text{ppb NO}_x$). Only the suburban and schools sites reported PM_{2.5} blanks, thus blank corrections were not used. Negative observations were set to zero. Treatment of measurements below method detection limits (DLs) varied slightly by application. In the operational evaluation and sensitivity analyses, measurements below DL were omitted in most analyses, or set to ½ DL in a sensitivity analysis. Daily averages were calculated from hourly NO_x, CO, and PM_{2.5} measurements. In the exposure apportionment application, measurements below DL were set to ½ DL, and missing sampling hours were approximated using linear interpolation.

II.2.2 Meteorological data

Meteorological data were obtained at the five AQS sites, a local National Weather Service (NWS) (Detroit City Airport or KDET; see Figure 3 for wind rose) [122] and the Pontiac, MI radiosonde site (approximately 45 km north of Detroit) [123]. AQS sites collect only basic parameters, e.g., surface wind speed and direction, temperature, and pressure. In contrast, the NWS data include a range of parameters needed by the AERMET meteorological data preprocessor [40] – sensible heat flux, surface friction velocity, convective velocity, convective stable planetary boundary layer heights, Monin-Obukhov length, surface roughness (back-calculated from AERMET files provided by MDEQ), wind speed, and wind direction – and these parameters are used in AERMET to develop the “surface” (SFC) meteorology files used by the dispersion models in this work (RLINE and AERMOD, described in detail later). Hours missing any required parameter were excluded, and the resulting SFC files were mostly complete, e.g., only 6 to 15% of all hours were missing, with most of the missing hours occurring at night-time (see Table 7).

Each application in this dissertation required slightly different compositions of available meteorological data. For the operational evaluation, KDET data was used due to its central location and presumed representativeness [51].

II.2.3 Point-source modeling

For the operational evaluation, sensitivity analysis, and exposure apportionment work, a point source inventory of CO, NO_x and PM emissions in southeast Michigan (including Lenawee, Livingston, Macomb, Monroe, Oakland, Washtenaw and Wayne counties) was created for the years 2011 to 2014. We consolidated stack-level data in the National Emission Inventory (NEI) [124] with facility and stack-level data in the Michigan Air Emission Reporting System (MAERS) [125]; emission data were available for 564 facilities. Stacks were aggregated to the facility level by assigning emissions to the main stack. A subset of 179 facilities were selected based on the 100 highest emitting facilities for each pollutant). Of these, 58 mostly smaller sources had incomplete information and were excluded. Extensive quality checks, including comparisons between MAERS and the 2011 NEI data, showed good agreement for facility-level emissions for CO and NO_x (e.g., inventories agreed mostly within 5%). PM_{2.5} data showed larger discrepancies, e.g., there were differences in emissions at the same facility between MAERS and NEI at 99 of 121 sources, and MAERS filterable emissions exceeded primary emissions (sum of filterable and condensable PM_{2.5}) at 23 facilities. These discrepancies were resolved following a 3-step procedure [126]: quality checking available data; “trivial” gap filling using available data; and then ranked “best-guess” estimates using, in sequence, data in an NEI year, primary emissions data converted directly using facility-specific SCC conversion factors, the median PM_{2.5} emission estimate generated indirectly, and lastly, the PM_{2.5} estimate created by trivial gap-filling of converted values. The final point source inventory contained 121 sources and represented over 90% of regional point source emissions (Table 8).

Pollutant concentrations from point sources were predicted using the inventory, the AERMOD dispersion model (View v8.1.0; AERMOD.exe v12345) [40], and the preprocessed meteorological data described earlier. Sources in Detroit were classified as “urban” (Figure 4) with a reference population of 10⁶ and the default surface roughness [127].

II.2.4 Dispersion modeling of mobile sources

Concentrations from on-road mobile sources were predicted using a spatially- and temporally-resolved link-based emission inventory and the RLINE model. A road network consisting of 9,701 links and AADT volumes for 2010 [128] was updated using current AADT and commercial AADT (CAADT) volumes reported in the Michigan Trunkline Highway System (which includes interstates, US and state highways) [129] and a custom mapping/linking algorithm that spatially matched Trunkline segments to previously modeled line segments. (A graphical depiction of this algorithm is shown in Figure 5.) Minor manual adjustments were needed to correct 9 misclassified road segments, including the road segment around Allen Park.

Percentage changes in AADT and the CAADT fraction were applied to matched links' 2010 AADT, and the estimated CAADT volumes were subtracted from AADT to derive updated non-commercial volumes by link and year. For unmatched links, 2010 volumes were used, which should not significantly affect results since vehicle miles traveled (VMT) on these roads was modest (below half of the Trunkline roads). The fleet mix on each link was derived using AADT and CAADT estimates, short-term counts (usually 2-3 days of data, excluding ramps and loop measurements), and permanent traffic recorders (PTRs) in the Traffic Monitoring Information System (TMIS; Table 9) [130]. Because count data were sparse, especially on minor roads, fleet mix was estimated by the road's National Function Class (NFC). NFC 12 and 19 links (without traffic count data) were assigned to NFC 14 and 17, respectively [128]. Hourly data using the 13 Federal Highway Administration (FHWA) classes were averaged across days, road direction and stations, and mapped to the 8 Highway Performance Monitoring System (HMPS) classes [131]. The average HMPS-by-NFC volume fractions were allocated to commercial and non-commercial traffic (Table 10), normalized and weighted by average commercial traffic fractions by NFC from the final dataset (Table 11). Hourly commercial and non-commercial volumes for each link were estimated using hour-of-day, day-of-week and monthly temporal allocation factors (TAFs) derived for Detroit area roads [132]. Hourly commercial and non-commercial emission factors for each NFC and speed bin (speeds were assigned to morning and evening rush hours, afternoon and evening periods) were calculated for each pollutant. Finally, link emissions were calculated as the product of link-specific volume with the speed-, month-, temperature- and vehicle type-specific emission factor (described next).

Hourly vehicle volume estimates were derived for each link of the emissions inventory from annual average daily traffic (AADT) estimates by several sets of temporal allocation factors (TAFs) that provide month-of-year, day-of-week and hour-of-day adjustments [128]. Detroit-specific TAFs separate commercial and non-commercial vehicles and are based on 2009 to 2012 data monitored at 13 permanent counting stations in southeast Michigan [132]. Importantly, these “local” TAFs distinguish the morning and afternoon commuting (“rush hour”) volume peaks for passenger vehicles from the mid-day peak for commercial vehicles. Previous work also generated a profile of default US TAFs for a combined commercial and non-commercial fleet [64]. For the sensitivity analysis, the nominal case used the US combined profile, and alternative cases were the commercial and non-commercial Detroit profile, and a profile that merged commercial and non-commercial fleets in Detroit.

Emission factors ($\text{g vehicle}^{-1} \text{ mile}^{-1}$) for the link-based inventory were generated using the Motor Vehicle Emission Simulator (MOVES) version 2014a [133] and 2015 inputs for the Wayne, Macomb and Oakland Counties (the most populated local areas) provided by the Southeast Michigan Council of Governments (SEMCOG). Other MOVES inputs included monthly average local temperatures in 11 bins (0 to 100 °F in 10 degree increments) [128]) and the default barometric pressure, which was similar to local conditions [134]. Following previous work [128], emission factors for running exhaust and running evaporative modes were calculated for CO, NO_x, PM_{2.5} and PM_{2.5} precursors (evaporative hydrocarbon emissions), and for PM_{2.5} tire-wear and brake-wear emissions. Crankcase and other emissions were omitted to reduce computational time; these emissions are small compared to exhaust emissions. Again following previous work [128], emission factors were consolidated within a pollutant type (e.g., tire and brake wear for PM_{2.5}), vehicle types (MOVES sourceTypeIDs) were mapped to the HPMS vehicle classes (Table 12), and averages were calculated weighted by vehicle type counts and VMT fraction on major roads (AADT > 10,000, called “urban restricted” in MOVES) and NFC 11 and 12 in the link network and minor roads (called “urban unrestricted” and NFCs 14, 16, 17 and 19), and the number of weekday and weekend days (5 and 2, respectively). CO, NO_x and PM_{2.5} emission factors were calculated by vehicle type, speed and ambient temperature. The sum of the link-based emissions inventory for Detroit represented 66 and 71% of the CO and NO_x emissions, respectively, of 2011 National Emission Inventory (NEI) on-road emissions for Wayne County (Table 13). Emission factors ($\text{g vehicle}^{-1} \text{ mile}^{-1}$) for 2010 were derived using the Motor Vehicle Emission Simulator

(MOVES) version 2010 [135] and Detroit-specific data. For the operational evaluation and exposure apportionment, 2015 emission factors were used. For the sensitivity analysis, the nominal emission factors were for 2010, and alternative was 2015.

A modified version of RLINE v1.2 was employed in this dissertation. Recent updates to this model include minor changes to the horizontal and vertical dispersion formulae, and major changes to the numerical integration algorithm. We used RLINE's numerical integration method, an iteration limit of 1000, and an error limit of 0.001. The beta modules for roadside barrier and depressed roadway algorithms were not used. Modifications taken to reduce run times and facilitate the large number of hours, links and receptors simulated included omitting calculations for receptor-link distances exceeding 4000 m (these concentrations were very small), using internal loops for multi-hour runs, precomputing emission rates, and a more flexible and efficient input and output scheme.

II.2.5 Estimation of background concentrations

The performance evaluation requires “background” concentrations, defined in this dissertation the sum of local background and contributions from both regional sources (outside the modeled area) and local but unmodeled area and mobile sources. The background sources are not explicitly modeled because they are distant, too numerous or too difficult to simulate [136], or because data are incomplete. Therefore, background at each AQS monitor was estimated using a conditional selection method that subtracted the geometric mean of monthly upwind modeled concentrations due to point and on-road sources from the observed geometric monthly mean concentrations [137]. Missing months were imputed by linear interpolation, and then leave-one-out nearest neighbor linear regressions were performed to obtain a smoothed sequence of monthly background estimates at each monitor.

This method of estimating backing was chosen to reduce potential drawbacks of available methods for calculating urban background. For example, using a large-scale photochemical model (e.g., CMAQ) was not feasible, would produce background estimates also based on measured values (ratios between modeled values with and without local sources are typically used to calculate background from observed values), and normally is not run at high spatial or temporal resolution. Monitored data used to estimate background levels depends on the method detection limit, thus, using a MLE estimator of sub-threshold values [138] would not be appropriate in our study because, for CO, a much (> 80%) of the data were below the MDLs. Our background approach

was adapted from previous work in which upwind $PM_{2.5}$ concentrations represent background amounts [137]. We undertook a number of analyses, some of which are summarized below, that indicate that any potential biases in the method do not significantly affect our results. We highlight five factors.

1. Upwind measurements were removed from the database used to generate daily and sub-daily modeled averages.
2. Second, for all pollutants, the percentage of observations occurring when the monitor is upwind was small ($< 20\%$, Figure 6, Figure 7, Figure 8), thus, removing these values has little effect on the overall representativeness of the observed dataset.
3. Third, the temporal association between background and observations is reduced using the monthly geometric mean of differences between upwind concentrations and modeled values (Figure 9, Figure 10, Figure 11), and further by taking the “leave-one-out” cross-validated time-series value of the geometric means (Figure 12, Figure 13, Figure 14).
4. Finally, calculated background and observed values show only weak correlation (highest $R^2 = 0.33$; Figure 15, Figure 16, Figure 17).
5. A variety of different methods were explored to model the $PM_{2.5}$ background, and all gave similar results (average $B / O + B \sim >80\%$).

II.2.6 Operational evaluation metrics

The operational evaluation, which was guided by previous RLINE evaluations [43–45] and the literature [55, 56], compared observed and predicted concentrations at each monitoring station ($n=5$) using 24-h averages, an averaging period frequently used in epidemiologic and health impact studies. This period also is supported by previous evaluations suggesting that meteorological variability makes comparisons at the hourly level “almost fruitless” [55]. Comparisons were made between observed values and the sum of background and predicted values. (We performed several diagnostic tests to ensure that our results were similar to those obtained when comparing the sum of predicted values to observed minus background values.) Analyses were conducted by pollutant, wind direction, monitoring site, season and day-of-week. Wind directions were defined for wind speeds exceeding 1 m s^{-1} , and monitoring sites were considered to be “downwind” for directions within $\pm 30^\circ$ of perpendicular of the largest nearby road, and “parallel” for directions within $\pm 15^\circ$

of parallel [44]. Daily average downwind or parallel concentrations were calculated for those hours of each (calendar) day that met these conditions if at least 6 h of valid model-observation pairs were available. Periods with fewer than 5 valid days were not considered. Seasons were defined as “winter” (Dec., Jan., Feb.), “spring” (March, April, May), “summer” (June, July, Aug.), and “fall” (Sept., Oct., Nov.).

The statistical evaluation emphasized four metrics recommended in air quality model evaluation guidelines [55, 56]. (Formulas for the metrics are listed in Table 14.) The F2 statistic, the percentage of modeled values within a factor of 2 of observed values, shows over- and under-predictions and provides a measure of overall model performance. The Spearman correlation coefficient (R_{SP}) assesses the similarity between ranked observations and predictions, and may be particularly appropriate for epidemiologic studies since it can indicate whether exposures are correctly ordered. The fractional bias (FB) shows the tendency to over- or under-predict, i.e., the likelihood of false positives (FB_{FP}) or false negatives (FB_{FN}). (Equal weight is given to each.) Lastly, the geometric variance V_G indicates the irreducible (“systematic”) and reducible (“random”) errors. This metric can help identify conditions where performance potentially could be improved, i.e., the percentage of errors that are reducible (% reducible) is the ratio between the natural logarithm of the reducible component of V_G and the total V_G (the product of the systematic and random components). Suggested minimum performance criteria for air quality modeling are $F2 \geq 50\%$, mean bias $\leq 30\%$, and $V_G \leq 1.6$ [55, 56].

II.3 Aim 3

Aim 3 examined the sensitivity of exposure estimates produced by dispersion models, i.e., RLINE and AERMOD, to meteorological, emission and traffic allocation inputs, focusing on applications to health studies examining near-road exposures to TRAP. Daily average modeled and monitored concentrations of NO_x and CO were used to assess the potential for exposure estimate error in cohort and population-based studies. Sensitivity of exposure estimates was assessed by using statistical performance evaluation metrics and three sets of receptors to compare model outputs that used nominal or alternative model inputs.

The sensitivity analysis employed much of the same methodology as Aim 2. The same set of near-road hourly CO and NO_x were used. $PM_{2.5}$ was not considered given the high background and

inability to determine a signal from local roads. The same modeling setup was identical as in Aim 2 (i.e., the link-based inventory was used for RLINE, the point-source inventory for AERMOD).

II.3.1 Meteorological data

In the sensitivity analysis, KDET data is designated as the nominal input. Three sets of alternative meteorological inputs are employed: SFC files using NWS data at the Detroit Metro Airport (KDTW); AQS-site-specific meteorology supplemented with KDET data (on-site/KDET); and site-specific meteorology supplemented with KDTW data (on-site/KDTW). SFC files generated using AERMET and the NWS data are similar to those distributed by the Michigan Department of Environmental Quality (MDEQ) for air quality modeling purposes. Differences between nominal and alternative wind-speed and direction were evaluated using the circular correlation coefficient [128].

II.3.2 Receptor sets

Three sets of receptors are used in the sensitivity analysis. The first placed receptors at the near-road monitoring sites in the study domain (n=5). The second and third sets respectively represent location of a vulnerable school-age population and the general population (Figure 18). The second set used 206 receptors that represented residences of children with asthma participating in the NEXUS study (called “NEXUS” receptors; 6 receptors outside the modeled domain were excluded) [139]. Approximately two-thirds of these children lived within 200 m of roads with AADT > 75,000 (e.g., interstate highways) at the time of enrollment into NEXUS, thus, this set oversamples near-road locations. The third set was designed to be representative of residences in Detroit. This set, called “Detroit,” was created by randomly selecting (with replacement) 1000 of the 2010 Census blocks in Detroit, which resulted in 543 unique blocks. Receptors were placed at the building footprint-centroid of the highest occupancy parcel in each selected block [140, 141]. For the exposure apportionment work, a random sample (n=25) of these 543 receptors were used.

II.3.3 Sensitivity analysis

The sensitivity analyses used metrics from operational evaluation to contrast performance of nominal and alternative nominal model inputs: percent of modeled values within a factor of 2 of observed values (F2); Spearman ranked correlation coefficient (R_{SP}); fractional bias (FB); and geometric variance (V_G). The ratio between the natural logarithm of the reducible component of

V_G and total V_G (the product of the systematic and random components) was used to estimate the percentage of reducible model errors (% Red).

Given the number of comparisons in the analysis (by site, pollutant, input, and metric), several rules were used to identify potentially meaningful differences and produce a summary measure. Each metric was compared to its “best” value (i.e., 1.00 for R_{SP} and V_G , 0.00 for FB and % Red), and symbols were used to show whether an alternative model input improved model performance (●), gave results that were among those that improved results (‘~’), did not conclusively improve model performance (‘ ’), or diminished performance from nominal (○). Only comparisons with at least one $R_{SP} \geq 0.1$ were considered. Only potentially meaningful changes were distinguished; changes in R_{SP} and other metrics had to exceed a chosen threshold of 0.05; this threshold was selected to balance sensitivity and avoid false indications. Comparisons of 2010 (nominal) and 2015 emission factors, and comparisons of the US default TAF (nominal) to the two alternative TAFs (Detroit-specific with commercial and non-commercial traffic separated, and combined) used the above comparison scheme. Comparisons of the four sets meteorological inputs were more complex. We checked whether on-site/KDET meteorology provided the best results (denoted as “on-site/KDET highest?”); whether KDET data provided better results than KDTW data when using NWS data alone or in conjunction with on-site data (“KDET > KDTW?”), and if on-site data generally improved results over NWS data alone (“on-site > NWS?”).

II.3.4 Application

To demonstrate the possible effect of model inputs on health outcomes in an epidemiological study, we estimated NO_x -attributable health impacts for two sets of meteorology and receptor sets 2 (NEXUS) and 3 (Detroit). Daily NO_x concentrations at the NEXUS and residential receptor sets were calculated using KDET and KDTW meteorology for 2011, commercial and non-commercial traffic allocation factors and 2015 emission factors. Every 12th day of the year was analyzed due to the large computation burden of modeling hourly data using 9,701 sources and 543 receptors. Outcomes considered included childhood asthma exacerbations (defined as one or more asthma-related symptoms for children ages 6-14), emergency department (ED) visits for asthma (children ages 0 – 17), and hospitalizations for asthma (ages 0 – 64). Baseline data used in these estimates included current asthma hospitalizations and ED visits in Detroit [142], an incidence rate of 0.412 cases per person-day for asthma exacerbations (6 – 14 years) [143], the prevalence of asthma in

Wayne County [144], and 2010 Census population data [145]. Concentration-response coefficients used log-linear and logistic models [146–149]. Predicted health outcomes for the two sets of meteorological inputs and two sets of receptors were compared using the non-parametric paired Wilcoxon signed rank test and descriptive statistics.

II.4 Aim 4

The exposure apportionment used several previously created and cleaned datasets, including: hourly near-road NO_x data at 3 sites (II.2.1), temperature recorded at KDET (II.2.2), and a random sample (n=25) of the NEXUS receptors (II.3.2). Below detection limit (DL) monitoring data were replaced with ½ DL, and for monitoring data and temperature, hours missing data were filled in using linear interpolations.

II.4.1 Exposure apportionment

To estimate and apportion exposure to TRAP, the Air Pollution Exposures model (APEX) [150] was used. Briefly, APEX, estimates hourly exposures (ppb-hr) in 5 micro-environments (ME) – “indoor-at-home,” “other indoor,” “outdoors,” “near-road,” and “vehicle cabin” – as the product of the ME concentration and the fraction of the hour spent in that micro-environment. The method of calculating ME concentration differs by micro-environment. For each hour in indoor MEs, a mass balance approach is used; the previous hour’s concentration is adjusted by removal rates (e.g., penetration rates), additional source contributions, and estimated room volume. Spatial differences in concentration, e.g., proximity to a large roadway, are accounted for by proximity factors specific to each simulated individual. For this work, default proximity and penetration factors are used. For outdoor MEs, ambient concentrations are used. For near-road, and vehicle cabin MEs, ambient concentrations are modified by roadway-specific concentrations (which the user provides). Census data is used to generate spatial “sectors” for residences and workplaces, and approximates commuting routes and times by the distance between a simulated individual’s residence and workplace.

In this application, APEX was run using modeled NO_x at 25 receptors representing ambient exposure across Detroit (these receptors were randomly selected from the Detroit receptors in Aim 3) and using modeled NO_x at the near-road monitoring side to represent roadway concentrations. Each modeled component – point source contributions, commercial traffic, non-commercial traffic, and background – was labeled as a separate pollutant in APEX, so their effects could be

disaggregated. Each APEX configuration was run for 100 randomly selected simulated persons using national-level databases for health conditions and commuting. The simulated population contained 19 persons with age < 20 (“children”), 68 persons with ages between 20 and 65 (“adults”) and 13 persons with age > 65 (“elderly”).

APEX outputs were presented graphically using plots of the cumulative distribution function and boxplots. Statistical analyses included the use of the Kruskal-Wallis test (for 3 or more groups), as before attaining a p-value of 0.05 or less to identify differences in the distributions between exposures in different time periods between different groups. Sensitivity analysis included comparing APEX outputs with modeled data to outputs using observed NO_x at the three AQS stations that measured NO_x in Detroit (i.e., schools, urban, and near-road).

II.5 Tables

Table 2. Summary statistics for all Detroit species of speciated PM

Species	Coverage		Blank & Detection Limit Correction				Summary Statistics						
	Start	End	# ADL	# BDL	% BDL	Blank Mean	Blank SD	DL Mean	DL SD	10 th	50 th	Mean	90 th
PM _{2.5,FRM} ¹	1/1/00	3/31/15	4455	688	13%	3.28	1.23	2.00	0.00	1.00	7.80	9.62	20.20
PM _{2.5} ²	12/20/00	9/29/14	1580	6	0%	0.87	0.58	0.75	0.06	4.53	10.80	12.56	23.68
Ag ³	12/20/00	4/6/15	38	1612	98%	0.0010	0.0024	0.0136	0.0076	0.0042	0.0065	0.0070	0.0101
Al ³	12/20/00	4/6/15	643	1007	61%	0.0014	0.0043	0.0170	0.0058	0.0065	0.0115	0.0233	0.0517
As ³	12/20/00	4/6/15	470	1180	72%	0.0002	0.0004	0.0018	0.0008	0.0005	0.0013	0.0016	0.0031
Au ³	12/20/00	2/18/09	41	882	96%	0.0006	0.0009	0.0052	0.0029	0.0009	0.0028	0.0027	0.0041
Ba ³	12/20/00	4/6/15	134	1522	92%	0.0052	0.0126	0.0224	0.0234	0.0039	0.0055	0.0136	0.0295
Br ³	12/20/00	4/6/15	1126	524	32%	0.0002	0.0003	0.0017	0.0006	0.0007	0.0027	0.0031	0.0062
Ca ³	12/20/00	4/6/15	1597	53	3%	0.0009	0.0020	0.0060	0.0015	0.0145	0.0396	0.0504	0.0952
Cd ³	12/20/00	4/6/15	52	1598	97%	0.0015	0.0031	0.0144	0.0042	0.0050	0.0080	0.0075	0.0110
Ce ³	12/20/00	4/6/15	41	1609	98%	0.0017	0.0056	0.0293	0.0394	0.0028	0.0041	0.0150	0.0500
Cl ³	12/20/00	4/6/15	760	890	54%	0.0008	0.0033	0.0081	0.0025	0.0039	0.0061	0.0268	0.0540
Co ³	12/20/00	4/6/15	73	1577	96%	0.0002	0.0003	0.0014	0.0003	0.0006	0.0007	0.0008	0.0010
Cr ³	12/20/00	4/6/15	412	1244	75%	0.0006	0.0012	0.0022	0.0003	0.0010	0.0012	0.0027	0.0050
Cs ³	12/20/00	4/6/15	34	1622	98%	0.0010	0.0032	0.0220	0.0162	0.0041	0.0055	0.0113	0.0230
Cu ³	12/20/00	4/6/15	1202	454	27%	0.0006	0.0013	0.0019	0.0004	0.0010	0.0042	0.0074	0.0184
EC _{METSASS} ⁵	12/20/00	3/30/10	976	79	7%	0.0139	0.0381	0.2402	0.0036	0.2800	0.6485	0.7107	1.2500
EC _{URG3k} ⁶	4/1/09	4/9/15	712	1	0%	0.0002	0.0012	0.0020	0.0000	0.1740	0.3660	0.4187	0.7326
Eu ³	12/20/00	2/18/09	84	839	91%	0.0002	0.0005	0.0067	0.0039	0.0019	0.0025	0.0041	0.0085
Fe ³	12/20/00	4/6/15	1641	9	1%	0.0028	0.0052	0.0020	0.0006	0.0371	0.0866	0.1033	0.1848
Ga ³	12/20/00	2/18/09	12	911	99%	0.0002	0.0007	0.0032	0.0017	0.0005	0.0014	0.0016	0.0027
Hf ³	12/20/00	2/18/09	22	901	98%	0.0014	0.0035	0.0148	0.0112	0.0020	0.0042	0.0077	0.0135
Hg ³	12/20/00	2/18/09	61	862	93%	0.0005	0.0010	0.0052	0.0023	0.0017	0.0023	0.0028	0.0047
In ³	12/20/00	4/6/15	63	1587	96%	0.0011	0.0029	0.0170	0.0057	0.0070	0.0080	0.0090	0.0165
Ir ³	12/20/00	2/18/09	34	889	96%	0.0006	0.0014	0.0060	0.0033	0.0012	0.0036	0.0031	0.0044
K ³	12/20/00	4/6/15	1628	22	1%	0.0005	0.0017	0.0069	0.0029	0.0209	0.0472	0.0691	0.0960
K ⁺ ⁴	1/7/01	4/6/15	971	688	41%	0.0019	0.0080	0.0160	0.0059	0.0070	0.0310	0.0586	0.1040
La ³	12/20/00	2/18/09	45	878	95%	0.0025	0.0065	0.0334	0.0344	0.0039	0.0043	0.0174	0.0410
Mg ³	12/20/00	4/6/15	187	1463	89%	0.0009	0.0045	0.0177	0.0112	0.0055	0.0090	0.0129	0.0250
Mn ³	12/20/00	4/6/15	845	805	49%	0.0003	0.0006	0.0020	0.0005	0.0008	0.0019	0.0026	0.0057

Mo	³	12/20/00	2/18/09	13	910	99%	0.0003	0.0007	0.0067	0.0022	0.0015	0.0036	0.0034	0.0045
Na	³	12/20/00	4/6/15	462	1188	72%	0.0073	0.0232	0.0531	0.0400	0.0155	0.0270	0.0486	0.1100
Na ⁺	⁴	1/7/01	4/6/15	1425	227	14%	-	-	0.0243	0.0093	0.0150	0.0600	0.1022	0.2000
Nb	³	12/20/00	2/18/09	18	905	98%	0.0003	0.0007	0.0043	0.0013	0.0014	0.0024	0.0022	0.0031
NH ₄ ⁺	⁴	1/7/01	4/6/15	1636	23	1%	0.0041	0.0288	0.0175	0.0068	0.2588	1.1400	1.5872	3.5920
Ni	³	12/20/00	4/6/15	349	1307	79%	0.0004	0.0007	0.0015	0.0003	0.0006	0.0009	0.0013	0.0024
NO ₃ ⁻	⁴	1/7/01	4/6/15	1645	14	1%	0.0340	0.0376	0.0120	0.0065	0.2965	1.4468	2.3874	5.8763
OC _{METSASS}	⁵	12/20/00	3/30/10	1003	52	5%	1.2664	1.1670	0.2402	0.0036	0.7438	2.4900	2.8370	5.2600
OC _{URG3k}	⁶	4/1/09	4/9/15	707	0	0%	0.1568	0.0665	0.0020	0.0000	0.8878	1.8230	2.0560	3.5092
P	³	12/20/00	4/6/15	46	1610	97%	0.0032	0.0192	0.0104	0.0035	0.0029	0.0050	0.0055	0.0080
Pb	³	12/20/00	4/6/15	551	1099	67%	0.0004	0.0007	0.0041	0.0018	0.0013	0.0029	0.0038	0.0076
Rb	³	12/20/00	4/6/15	43	1613	97%	0.0002	0.0003	0.0020	0.0005	0.0007	0.0010	0.0010	0.0013
S	³	12/20/00	4/6/15	1641	9	1%	0.0019	0.0057	0.0080	0.0030	0.2766	0.7228	0.9865	1.9400
Sb	³	12/20/00	4/6/15	62	1594	96%	0.0025	0.0051	0.0318	0.0105	0.0095	0.0140	0.0170	0.0260
Sc	³	12/20/00	2/18/09	2	921	100%	0.0001	0.0003	0.0113	0.0106	0.0015	0.0050	0.0057	0.0185
Se	³	12/20/00	4/6/15	269	1381	84%	0.0002	0.0003	0.0022	0.0006	0.0007	0.0013	0.0015	0.0030
Si	³	12/20/00	4/6/15	1462	188	11%	0.0026	0.0057	0.0123	0.0039	0.0090	0.0459	0.0625	0.1261
Sm	³	12/20/00	2/18/09	42	881	95%	0.0002	0.0004	0.0061	0.0022	0.0022	0.0025	0.0033	0.0050
Sn	³	12/20/00	4/6/15	64	1586	96%	0.0029	0.0055	0.0222	0.0067	0.0080	0.0100	0.0118	0.0180
SO ₄ ⁼	⁴	1/7/01	4/6/15	1646	7	0%	0.0411	0.0575	0.0099	0.0040	0.7909	2.1488	2.9321	5.8293
Sr	³	12/20/00	4/6/15	176	1474	89%	0.0003	0.0006	0.0024	0.0007	0.0009	0.0012	0.0017	0.0019
Ta	³	12/20/00	2/18/09	59	864	94%	0.0038	0.0078	0.0102	0.0073	0.0019	0.0041	0.0060	0.0145
Tb	³	12/20/00	2/18/09	87	836	91%	0.0001	0.0003	0.0060	0.0027	0.0018	0.0022	0.0037	0.0055
Ti	³	12/20/00	4/6/15	404	1246	76%	0.0005	0.0012	0.0044	0.0008	0.0019	0.0025	0.0037	0.0068
V	³	12/20/00	4/6/15	185	1471	89%	0.0002	0.0003	0.0029	0.0007	0.0010	0.0016	0.0019	0.0025
W	³	12/20/00	2/18/09	28	895	97%	0.0014	0.0030	0.0079	0.0053	0.0012	0.0034	0.0042	0.0105
Y	³	12/20/00	2/18/09	29	894	97%	0.0003	0.0005	0.0029	0.0008	0.0011	0.0014	0.0015	0.0023
Zn	³	12/20/00	4/6/15	1566	84	5%	0.0002	0.0004	0.0023	0.0006	0.0039	0.0126	0.0175	0.0340
Zr	³	12/20/00	4/6/15	106	1550	94%	0.0004	0.0010	0.0052	0.0053	0.0014	0.0021	0.0029	0.0072

¹R & P Model 2025 PM_{2.5} Sequential w/WINS-GRAVIMETRIC (Detroit), Andersen RAAS2.5-300 PM_{2.5} SEQ w/WINS-GRAVIMETRIC (Chicago); ²Met One SASS Teflon-Gravimetric; ³Met One SASS Teflon-Energy Dispersive XRF; ⁴Met One SASS Nylon-Ion Chromatography; ⁵Met One SASS Quartz-STN TOT; ⁶URG 3000N w/Pall Quartz filter and Cyclone Inlet

Table 3. Summary statistics for all Chicago species

Species		Coverage		Blank & Detection Limit Correction						Summary Statistics				
		Start	End	# ADL	# BDL	% BDL	Blank Mean	Blank SD	DL Mean	DL SD	10 th	50 th	Mean	90 th
PM _{2.5,FRM}	1	1/4/06	5/27/15	199	437	69%	14.07	6.01	2.00	0.00	1.00	1.00	3.44	10.10
PM _{2.5}	2	1/2/06	9/29/14	834	5	1%	0.63	0.57	0.75	0.07	4.40	10.00	11.52	20.30
Ag	3	1/2/06	4/6/15	14	883	98%	0.0006	0.0022	0.0148	0.0083	0.0042	0.0065	0.0075	0.0185
Al	3	1/2/06	4/6/15	419	483	54%	0.0010	0.0029	0.0170	0.0055	0.0065	0.0125	0.0255	0.0550
As	3	1/2/06	4/6/15	185	717	79%	0.0001	0.0004	0.0016	0.0006	0.0005	0.0009	0.0011	0.0020
Au	3	1/2/06	2/18/09	7	287	98%	0.0001	0.0002	0.0041	0.0022	0.0009	0.0019	0.0021	0.0040
Ba	3	1/2/06	4/6/15	17	885	98%	0.0004	0.0013	0.0153	0.0152	0.0039	0.0050	0.0084	0.0295
Br	3	1/2/06	4/6/15	702	200	22%	0.0002	0.0003	0.0016	0.0005	0.0007	0.0031	0.0038	0.0070
Ca	3	1/2/06	4/6/15	873	24	3%	0.0001	0.0005	0.0062	0.0014	0.0146	0.0401	0.0480	0.0912
Cd	3	1/2/06	4/6/15	21	876	98%	0.0009	0.0028	0.0155	0.0042	0.0050	0.0085	0.0080	0.0110
Ce	3	1/2/06	4/6/15	1	901	100%	0.0000	0.0001	0.0167	0.0249	0.0028	0.0041	0.0084	0.0430
Cl	3	1/2/06	4/6/15	461	436	49%	0.0003	0.0009	0.0074	0.0020	0.0039	0.0069	0.0342	0.0716
Co	3	1/2/06	4/6/15	45	857	95%	0.0001	0.0002	0.0014	0.0002	0.0006	0.0007	0.0007	0.0010
Cr	3	1/2/06	4/6/15	163	739	82%	0.0003	0.0008	0.0023	0.0002	0.0010	0.0012	0.0027	0.0040
Cs	3	1/2/06	4/6/15	4	893	100%	0.0005	0.0015	0.0188	0.0133	0.0041	0.0055	0.0095	0.0205
Cu	3	1/2/06	4/6/15	457	445	49%	0.0001	0.0003	0.0019	0.0004	0.0008	0.0015	0.0030	0.0053
EC _{METSASS}	5	1/2/06	4/29/10	229	19	8%	0.0093	0.0263	0.2400	0.0000	0.2911	0.6500	0.7202	1.2549
EC _{URG3k}	6	5/3/07	4/6/15	752	5	1%	0.0004	0.0016	0.0020	0.0000	0.1770	0.3720	0.4329	0.7732
Eu	3	1/2/06	2/18/09	8	286	97%	0.0000	0.0003	0.0054	0.0021	0.0019	0.0025	0.0028	0.0055
Fe	3	1/2/06	4/6/15	900	2	0%	0.0012	0.0035	0.0019	0.0005	0.0237	0.0611	0.0800	0.1569
Ga	3	1/2/06	2/18/09	1	293	100%	0.0002	0.0003	0.0024	0.0013	0.0005	0.0013	0.0012	0.0024
Hf	3	1/2/06	2/18/09	1	293	100%	0.0001	0.0004	0.0103	0.0088	0.0020	0.0030	0.0052	0.0135
Hg	3	1/2/06	2/18/09	11	283	96%	0.0001	0.0003	0.0056	0.0027	0.0017	0.0018	0.0029	0.0047
In	3	1/2/06	4/6/15	28	869	97%	0.0013	0.0036	0.0183	0.0060	0.0070	0.0080	0.0096	0.0165
Ir	3	1/2/06	2/18/09	8	286	97%	0.0000	0.0000	0.0049	0.0022	0.0012	0.0021	0.0025	0.0039
K	3	1/2/06	4/6/15	885	17	2%	0.0001	0.0002	0.0069	0.0029	0.0180	0.0446	0.0729	0.0949
K ⁺	4	1/2/06	4/6/15	564	340	38%	0.0003	0.0025	0.0149	0.0058	0.0070	0.0340	0.0626	0.1030
La	3	1/2/06	2/18/09	3	291	99%	0.0001	0.0002	0.0176	0.0223	0.0039	0.0042	0.0089	0.0350
Mg	3	1/2/06	4/6/15	160	742	82%	0.0005	0.0014	0.0144	0.0063	0.0055	0.0090	0.0122	0.0235
Mn	3	1/2/06	4/6/15	389	513	57%	0.0001	0.0002	0.0019	0.0004	0.0008	0.0011	0.0022	0.0046
Mo	3	1/2/06	2/18/09	6	288	98%	0.0001	0.0004	0.0064	0.0027	0.0015	0.0042	0.0033	0.0045
Na	3	1/2/06	4/6/15	339	563	62%	0.0033	0.0158	0.0415	0.0214	0.0155	0.0270	0.0466	0.1061
Na ⁺	4	1/2/06	4/6/15	789	115	13%	-	-	0.0215	0.0102	0.0150	0.0545	0.0768	0.1500
Nb	3	1/2/06	2/18/09	5	289	98%	0.0001	0.0004	0.0039	0.0010	0.0014	0.0017	0.0020	0.0028
NH ₄ ⁺	4	1/2/06	4/6/15	893	6	1%	0.0043	0.0173	0.0162	0.0071	0.2710	1.0200	1.4049	3.1100
Ni	3	1/2/06	4/6/15	160	742	82%	0.0002	0.0005	0.0014	0.0003	0.0006	0.0009	0.0012	0.0020
NO ₃ ⁻	4	1/2/06	4/6/15	897	2	0%	0.0186	0.0287	0.0107	0.0060	0.4015	1.4700	2.4260	6.2220
OC _{METSASS}	5	1/2/06	4/29/10	248	0	0%	1.0083	0.2014	0.2400	0.0000	1.1928	2.5850	2.8347	4.6621
OC _{URG3k}	6	5/3/07	4/6/15	754	3	0%	0.2204	0.1075	0.0020	0.0000	0.9959	2.0255	2.1923	3.6627
P	3	1/2/06	4/6/15	3	894	100%	0.0001	0.0004	0.0114	0.0033	0.0045	0.0050	0.0058	0.0080
Pb	3	1/2/06	4/6/15	272	630	70%	0.0002	0.0005	0.0037	0.0013	0.0013	0.0024	0.0036	0.0073

Rb	3	1/2/06	4/6/15	17	885	98%	0.0001	0.0002	0.0019	0.0004	0.0007	0.0010	0.0010	0.0013
S	3	1/2/06	4/6/15	892	5	1%	0.0002	0.0005	0.0080	0.0018	0.2640	0.6180	0.7985	1.5538
Sb	3	1/2/06	4/6/15	42	860	95%	0.0014	0.0037	0.0358	0.0094	0.0095	0.0195	0.0192	0.0260
Sc	3	1/2/06	2/18/09	1	293	100%	0.0002	0.0004	0.0179	0.0124	0.0015	0.0060	0.0090	0.0185
Se	3	1/2/06	4/6/15	60	842	93%	0.0001	0.0003	0.0021	0.0005	0.0007	0.0013	0.0012	0.0013
Si	3	1/2/06	4/6/15	819	83	9%	0.0004	0.0013	0.0124	0.0036	0.0113	0.0470	0.0601	0.1180
Sm	3	1/2/06	2/18/09	3	291	99%	0.0001	0.0006	0.0054	0.0017	0.0022	0.0025	0.0027	0.0050
Sn	3	1/2/06	4/6/15	30	872	97%	0.0011	0.0039	0.0238	0.0068	0.0080	0.0100	0.0125	0.0180
SO ₄ ⁼	4	1/2/06	4/6/15	896	3	0%	0.0185	0.0183	0.0091	0.0045	0.7190	1.7300	2.2987	4.4941
Sr	3	1/2/06	4/6/15	70	827	92%	0.0001	0.0003	0.0024	0.0006	0.0009	0.0012	0.0018	0.0018
Ta	3	1/2/06	2/18/09	5	289	98%	0.0001	0.0006	0.0073	0.0033	0.0019	0.0039	0.0038	0.0049
Tb	3	1/2/06	2/18/09	8	286	97%	0.0000	0.0001	0.0049	0.0019	0.0018	0.0022	0.0026	0.0050
Ti	3	1/2/06	4/6/15	88	814	90%	0.0002	0.0005	0.0047	0.0005	0.0021	0.0025	0.0029	0.0027
V	3	1/2/06	4/6/15	46	856	95%	0.0001	0.0004	0.0032	0.0005	0.0012	0.0016	0.0018	0.0019
W	3	1/2/06	2/18/09	6	288	98%	0.0001	0.0002	0.0056	0.0026	0.0012	0.0031	0.0029	0.0041
Y	3	1/2/06	2/18/09	5	289	98%	0.0001	0.0003	0.0026	0.0005	0.0011	0.0011	0.0013	0.0019
Zn	3	1/2/06	4/6/15	827	75	8%	0.0001	0.0003	0.0024	0.0006	0.0030	0.0108	0.0170	0.0340
Zr	3	1/2/06	4/6/15	40	862	96%	0.0005	0.0015	0.0058	0.0062	0.0014	0.0017	0.0032	0.0115

¹R & P Model 2025 PM_{2.5} Sequential w/WINS-GRAVIMETRIC (Detroit), Andersen RAAS2.5-300 PM_{2.5} SEQ w/WINS-GRAVIMETRIC (Chicago); ²Met One SASS Teflon-Gravimetric; ³Met One SASS Teflon-Energy Dispersive XRF; ⁴Met One SASS Nylon-Ion Chromatography; ⁵Met One SASS Quartz-STN TOT; ⁶URG 3000N w/Pall Quartz filter and Cyclone Inlet

Table 4. Parameters for EC and OC artifact correction regression

	Detroit		Chicago	
	EC	OC	EC	OC
Outliers Deleted	none	2009/7/24: OC _{MET} = 8.230, OC _{URG} = 2.146 2009/11/9: OC _{MET} = 1.369, OC _{URG} = 6.107	2009/05/1, 7, 10, 13, 25 and 2009/6/6: EC _{MET} = 0.11115 (after blank correction) and EC _{URG} varied by ±0.1.	2009/7/24: OC _{MET} = 10.311, OC _{URG} = 2.04
Y artifact	0.77	1.0333	0.8668	0.8645
R ²	0.13737	0.12625	0.2338877	0.303
	0.578	0.7729	0.6949	0.8518

Table 5. Starting date (month and year) and percent above detection limit (%>DL) of hourly CO, NO, NO₂ and NO_x data at Detroit area monitoring sites.

AQS ID	Site name	Poll	Method*	Start	End	N	DL (ppb)	%>DL (%)
261630001	suburban	CO	IGFC	1/11	12/14	32,841	500	7
		NO	TECO-42S	1/11	12/14	27,962	0.05	98
261630019	school	NO	ICHEM	1/11	12/14	33,820	10	9
		NO ₂	ICHEM	1/11	12/11	8,633	5	77
		NO ₂	ICHEM	1/12	12/14	25,187	1	100
261630093	near-road	NO _x	ICHEM	1/11	12/14	33,820	10	51
		CO	EC9830T	10/11	12/11	2,076	20	100
		CO	INDiI	1/12	12/14	24,838	500	51
		NO	IGpCHEM	10/11	12/13	18,186	10	68
		NO	ICHEM	1/14	12/14	8,584	10	51
		NO ₂	IGpCHEM	10/11	12/13	18,186	5	93
		NO ₂	ICHEM	1/14	12/14	8,584	1	100
		NO _x	IGpCHEM	10/11	12/13	18,186	10	90
261630094	urban	NO _x	ICHEM	1/14	12/14	8,584	10	87
		CO	INDiI	10/11	12/14	27,288	500	26
		NO	IGpCHEM	10/11	12/13	19,304	10	19
		NO	ICHEM	1/14	12/14	8,583	10	16
		NO ₂	IGpCHEM	10/11	12/13	19,304	5	80
		NO ₂	ICHEM	1/14	12/14	8,583	1	100
		NO _x	IGpCHEM	10/11	12/13	19,304	10	63
261631008	industrial	NO _x	ICHEM	1/14	12/14	8,583	10	61
		CO	IGFC	1/12	12/14	25,876	500	10

* Methods: ICHEM = Instrumental Chemiluminescence; IGpCHEM = Instrumental Gas-Phase Chemiluminescence; TECO-42S = Low Level NO_x Instrumental-Teco 42s Chemiluminescence; IGFC = Instrumental Gas Filter Correlation Analyzer; INDiI = Instrumental Non-dispersive Infrared. EC980T = Instrumental Gas Filter Correlation Ecotech EC9830T

Table 6. PM_{2.5} measured at sites in Wayne County, MI

Site#	Parameter Code	POC	Method.Description	FRM Detection Limit	Sample Duration	Sample. Frequency	N	AMDL	Start	End
1	88101	1	R & P	X	2 24 HOUR		262	99.6	4/1/2013	12/31/2013
1	88101	1	R & P	X	2 24 HOUR	EVERY DAY	797	98.9	1/1/2011	3/31/2013
1	88101	1	R & P	X	2 24 HOUR	NA	341	99.7	1/2/2014	12/30/2014
1	88502	3	TEOM30 deg C		0 1 HOUR	NA	15751	100.0	1/1/2011	12/31/2014
1	88502	3	TEOM50 deg C		0 1 HOUR	NA	17622	100.0	4/1/2011	10/29/2014
1	88502	5	Met One SASS Teflon-Gravimetric		0.57 24 HOUR	NA	9	100.0	8/18/2014	9/29/2014
1	88502	5	Met One SASS Teflon-Gravimetric		0.74 24 HOUR	NA	240	99.2	1/3/2011	9/20/2014
1	88502	5	Met One SASS Teflon-Gravimetric		0.75 24 HOUR	NA	7	100.0	4/6/2011	12/14/2012
1	88502	5	Met One SASS Teflon-Gravimetric		0.77 24 HOUR	NA	120	99.2	1/10/2011	8/6/2014
1	88502	5	Met One SASS Teflon-Gravimetric		0.78 24 HOUR	NA	31	100.0	3/13/2011	7/13/2014
1	88502	5	Met One SASS Teflon-Gravimetric		1.1 24 HOUR	NA	40	100.0	4/13/2013	9/26/2014
15	88101	1	R & P	X	2 24 HOUR		91	98.9	4/1/2013	12/30/2013
15	88101	1	R & P	X	2 24 HOUR	EVERY 3RD DAY	270	99.3	1/3/2011	3/29/2013
15	88101	1	R & P	X	2 24 HOUR	NA	115	100.0	1/2/2014	12/31/2014
15	88502	5	Met One SASS Teflon-Gravimetric		0.57 24 HOUR	NA	3	100.0	8/21/2014	9/26/2014
15	88502	5	Met One SASS Teflon-Gravimetric		0.74 24 HOUR	NA	94	98.9	1/15/2011	9/20/2014
15	88502	5	Met One SASS Teflon-Gravimetric		0.75 24 HOUR	NA	15	93.3	1/9/2011	7/22/2014
15	88502	5	Met One SASS Teflon-Gravimetric		0.77 24 HOUR	NA	60	100.0	1/27/2011	9/2/2014
15	88502	5	Met One SASS Teflon-Gravimetric		0.78 24 HOUR	NA	26	100.0	1/3/2011	8/3/2014
15	88502	5	Met One SASS Teflon-Gravimetric		1.1 24 HOUR	NA	22	100.0	4/28/2013	8/9/2014
15	88502	5	Met One SASS Teflon-Gravimetric		1.2 24 HOUR	NA	1	100.0	5/4/2013	5/4/2013
16	88101	1	R & P	X	2 24 HOUR		84	97.6	4/1/2013	12/30/2013
16	88101	1	R & P	X	2 24 HOUR	EVERY 3RD DAY	208	97.1	7/8/2011	3/29/2013
16	88101	1	R & P	X	2 24 HOUR	EVERY DAY	60	100.0	1/3/2011	6/29/2011
16	88101	1	R & P	X	2 24 HOUR	NA	121	99.2	1/2/2014	12/31/2014
19	88101	1	R & P	X	2 24 HOUR		85	97.6	4/1/2013	12/30/2013
19	88101	1	R & P	X	2 24 HOUR	EVERY 3RD DAY	267	98.5	1/3/2011	3/29/2013
19	88101	1	R & P	X	2 24 HOUR	NA	117	100.0	1/2/2014	12/31/2014
25	88101	1	R & P	X	2 24 HOUR		87	97.7	4/1/2013	12/30/2013
25	88101	1	R & P	X	2 24 HOUR	EVERY 3RD DAY	268	97.4	1/3/2011	3/29/2013
25	88101	1	R & P	X	2 24 HOUR	NA	120	99.2	1/2/2014	12/31/2014
33	88101	1	R & P	X	2 24 HOUR		90	98.9	4/1/2013	12/30/2013
33	88101	1	R & P	X	2 24 HOUR	EVERY 3RD DAY	293	99.3	1/3/2011	3/29/2013
33	88101	1	R & P	X	2 24 HOUR	NA	120	100.0	1/2/2014	12/31/2014
33	88101	2	R & P	X	2 24 HOUR		77	98.7	1/3/2011	12/30/2013
33	88101	2	R & P	X	2 24 HOUR	EVERY 3RD DAY	106	99.1	7/2/2011	3/29/2013
33	88101	2	R & P	X	2 24 HOUR	NA	60	100.0	1/5/2014	12/25/2014
33	88502	3	TEOM30 deg C		0 1 HOUR	NA	3447	100.0	1/1/2014	12/31/2014
33	88502	3	TEOM50 deg C		0 1 HOUR	NA	4862	100.0	4/3/2014	10/29/2014
33	88502	5	Met One SASS Teflon-Gravimetric		0.57 24 HOUR	NA	6	100.0	8/3/2014	9/26/2014
33	88502	5	Met One SASS Teflon-Gravimetric		0.74 24 HOUR	NA	118	99.2	1/9/2011	9/8/2014
33	88502	5	Met One SASS Teflon-Gravimetric		0.75 24 HOUR	NA	1	100.0	8/13/2011	8/13/2011
33	88502	5	Met One SASS Teflon-Gravimetric		0.77 24 HOUR	NA	67	100.0	1/3/2011	9/2/2014
33	88502	5	Met One SASS Teflon-Gravimetric		0.78 24 HOUR	NA	9	100.0	2/3/2012	5/11/2014

33	88502	5	Met One SASS Teflon-Gravimetric		1.1	24 HOUR	NA	23	100.0	6/9/2013	8/9/2014
36	88101	1	R & P	X		224 HOUR		86	96.5	4/1/2013	12/30/2013
36	88101	1	R & P	X		224 HOUR	EVERY 3RD DAY	255	97.3	1/3/2011	3/29/2013
36	88101	1	R & P	X		224 HOUR	NA	120	100.0	1/2/2014	12/31/2014
38	88101	1	R & P	X		224 HOUR		57	100.0	1/3/2011	6/29/2011
38	88101	1	R & P	X		224 HOUR	EVERY 3RD DAY	191	96.9	7/2/2011	1/31/2013
39	88101	1	R & P	X		224 HOUR		411	99.5	1/1/2011	12/31/2013
39	88101	1	R & P	X		224 HOUR	EVERY DAY	603	98.5	7/1/2011	3/31/2013
39	88101	1	R & P	X		224 HOUR	NA	346	99.4	1/1/2014	12/31/2014
39	88101	3	Met One BAM-1020 Mass Monitor w/VSCC-Beta Attenuation	X		5 1 HOUR		24594	55.1	1/1/2011	12/31/2013
39	88101	3	Met One BAM-1020 Mass Monitor w/VSCC-Beta Attenuation	X		5 1 HOUR	NA	7351	83.2	1/1/2014	12/31/2014
39	88502	3	TEOM30 deg C			0 1 HOUR	NA	3689	100.0	1/1/2014	12/31/2014
39	88502	3	TEOM50 deg C			0 1 HOUR	NA	4755	100.0	4/3/2014	10/29/2014

Methods: R&P = R & P Model 2025 PM_{2.5} Sequential w/WINS-GRAVIMETRIC; TEOM = PM_{2.5} SCC w/No Correction Factor-TEOM Gravimetric; METONE S = Met One SASS Teflon-Gravimetric

* R&P and Met One BAM are FRM (<https://www3.epa.gov/ttnamti1/files/ambient/criteria/reference-equivalent-methods-list.pdf>)

Table 7. Number of missing met-hours for each NWS data set and hour of the day. There were 1461 hours of data in each hour of the day.

NWS	1	2	3	4	5	6	7	8	9	10	11	12	13	14	15	16	17	18	19	20	21	22	23	24
DET	329	340	345	362	357	350	292	228	193	166	188	177	156	136	107	97	62	67	100	114	184	204	252	301
DTW	283	310	294	297	292	261	230	188	186	177	170	163	163	153	134	93	71	53	66	115	176	223	244	272

Table 8. Annual emissions (tons, rounded to the nearest integer) of modeled and not-modeled point sources of CO, NO_x and PM_{2.5} in Wayne County and the remaining 6 counties.

Pollutant Year	Wayne County		Remaining 6 counties	
	Modeled	Not modeled	Modeled	Not modeled
CO				
2011	31,459	5,037	5,552	1,793
2012	37,884	299	5,061	856
2013	32,970	353	5,127	979
2014	30,992	411	5,299	1,034
NO_x				
2011	17,128	3,099	23,655	929
2012	14,386	275	20,322	705
2013	14,027	335	23,109	748
2014	13,697	348	15,717	823
PM_{2.5}				
2011	1,396	212	1,009	166
2012	1,085	98	886	199
2013	1,337	107	971	233
2014	721	118	2,723	334

Table 9. Hours of traffic count data in each month from 2010 to 2014 separated by NFC class and traffic recorder type (PTR = Permanent Traffic Recorder; SHORT = Short counts).

NFC	TYPE	# of stations	Jan	Feb	Mar	Apr	May	Jun	July	Aug	Sept	Oct	Nov	Dec
11	PTR	1	6,768	6,502	6,734	6,912	7,246	7,104	7,200	7,104	7,048	7,344	7,150	7,200
14	PTR	1	2,784	2,672	2,780	2,784	2,712	3,384	2,846	2,784	2,688	2,928	3,575	3,600
14	SHORT	21					246			192	340	397	563	
16	SHORT	14					96				253	392	561	
17	SHORT	19								96	344	638	454	

Table 10. Allocation of commercial and non-commercial traffic

Traffic type	MC	LDGV	LDGT1	LDGT2	HDGV	LDDV	LDDT	HDDV
Commercial				1	1	0.5	1	1
Non-Commercial	1	1	1			0.5		

Table 11. Aggregated Fleet-mix “reality-check” – vehicle fraction by NFC class.

Vehicle class	11	12	14	16	17	19
LDGV	0.784	0.839	0.840	0.857	0.788	0.809
LDGT1	0.120	0.109	0.109	0.083	0.147	0.151
LDGT2	0.025	0.021	0.020	0.019	0.027	0.014
HDGV	0.003	0.003	0.003	0.005	0.003	0.002
MC	0.005	0.006	0.006	0.007	0.009	0.009
LDDV	0.008	0.008	0.008	0.009	0.007	0.007
LDDT	0.002	0.002	0.002	0.002	0.002	0.001
HDDV	0.053	0.012	0.012	0.019	0.016	0.008

Table 12. Matrix for of percentages used in post-processing MOVES emission rate outputs into aggregated HMPS vehicle classes. Generated using Table 2-4 of Decker 1996 [131], MOVES2014 on-road source types table [151], and SEMCOG Fuel type data.

Source TypeID	sourceTypeName	Fuel Type = Gasoline					Fuel Type = Diesel		
		MC	LDGV	LDGT1	LDGT2	HDGV	LDDV	LDDT	HDDV
11	Motorcycle	100							
21	Passenger Car		100				100		
31	Passenger Truck			66	33			100	
32	Light Commercial Truck			66	33			100	
41	Intercity Bus					100			100
42	Transit Bus					100			100
43	School Bus					100			100
51	Refuse Truck					100			100
52	Single Unit Short-haul Truck					100			100
53	Single Unit Long-haul Truck								100
54	Motor Home					100			100
61	Combination Short-haul Truck								100
62	Combination Long-haul Truck								100

Table 13. Annual modeled emissions (nearest ton) of each pollutant in each year. Major roads have AADT > 10,000.

Emission per road type and year	CO	NO _x
NEI 2011	129,647	29,767
Minor Roads (all years)	48,994	11,695
2010 Major + Minor	86,119	21,280
2011 Major + Minor	85,827	21,205
2012 Major + Minor	86,998	21,507
2013 Major + Minor	87,171	21,552
2014 Major + Minor	87,697	21,688

Table 14. Formulas for various performance metrics [55].

Metric	Symbol	Formula	Eq. #
Mean predicted concentrations	$\overline{C_p}$	$1/N \sum C_{p,i}$	
Mean observed concentrations	$\overline{C_o}$	$1/N \sum C_{o,i}$	
Fractional Bias	FB	$(\overline{C_p} - \overline{C_o}) / [(\overline{C_p} + \overline{C_o}) / 2]$	(1)
Fractional Bias – False positives	FB _{FP}	$[\overline{C_o} - \overline{C_p} + (\overline{C_p} - \overline{C_o})] / (\overline{C_p} + \overline{C_o})$	(21)
Fractional Bias – False negatives	FB _{FN}	$[\overline{C_o} - \overline{C_p} + (\overline{C_o} - \overline{C_p})] / (\overline{C_p} + \overline{C_o})$	(22)
Geometric variance	V _G	$\exp[\overline{(\ln C_o - \ln C_p)^2}]$	(4)
Geometric variance – systematic	Irr.	$\exp(\overline{\ln C_o} - \overline{\ln C_p})^2$	(8)
Geometric variance – random	Red.	$VG = Irr \times Red \rightarrow Red = VG / Irr$	

II.6 Figures

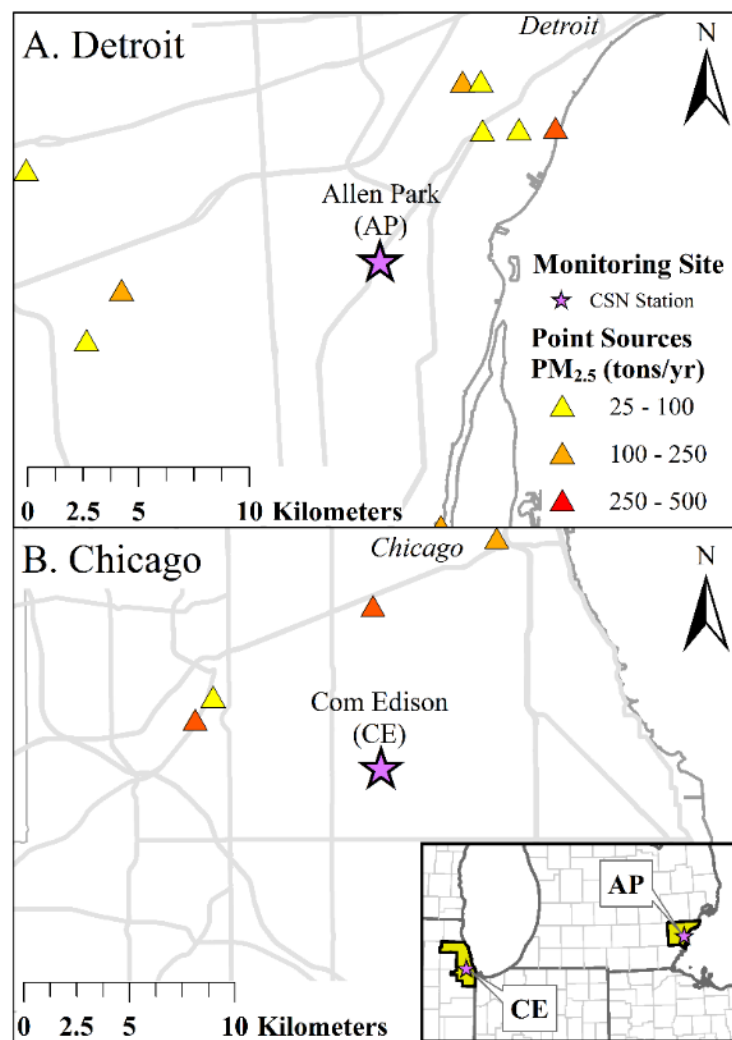


Figure 1. Maps showing Allen Park, Detroit (A) and Com Edison, Chicago (B) monitoring sites and nearby point sources emitting more than 25 tons of PM_{2.5} in 2011

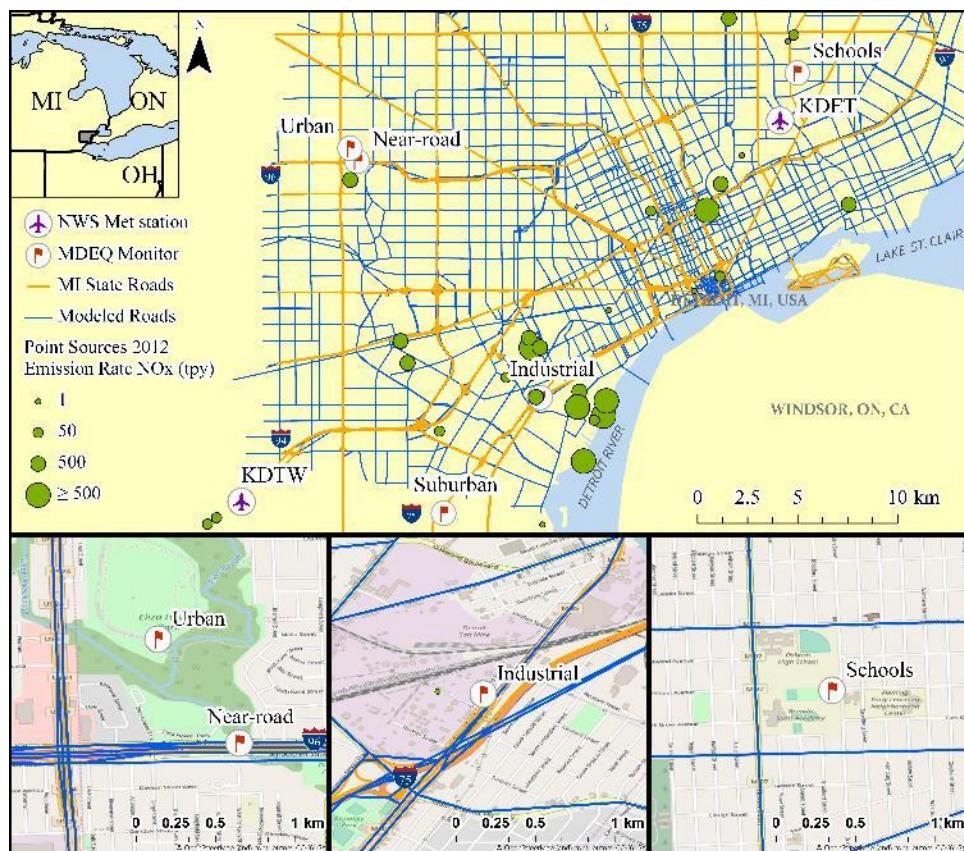


Figure 2. The modeling domain, including Michigan Department of Environmental Quality (MDEQ) monitoring stations, National Weather Service (NWS) meteorological stations, a subset of Michigan State Trunkline Highway System (i.e., ‘major’) and non-Trunkline (‘minor’) roads, all modeled roads, and large point sources of NO_x in 2012 in Wayne County. Areas around the Urban, Near-road, Industrial, and Schools sites are shown (the Suburban site is below the modeled domain).

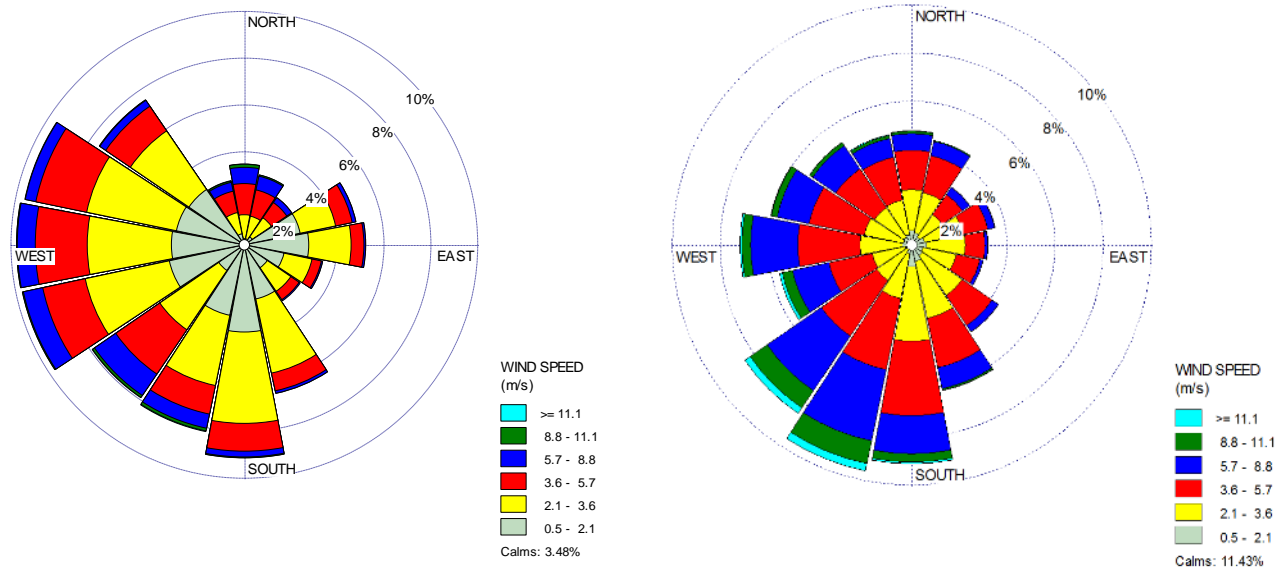


Figure 3. Wind rose for Detroit City Airport (DET) and Detroit Metro Airport (DTW) stations, for 2012.

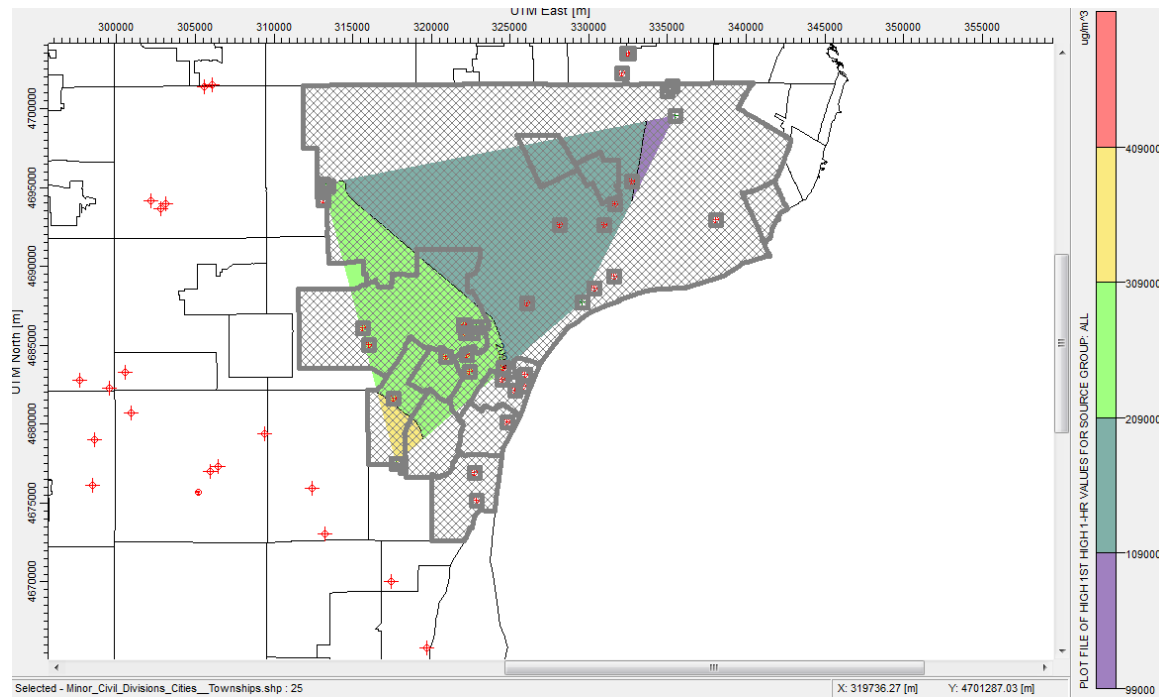


Figure 4. Designation of Urban Sources. Sources in Detroit were classified as “urban” with a reference population of 106 and the default surface roughness [127]. Michigan Department of Environmental Quality (MDEQ) Source IDs are: A6902, A7809, A8638, A8640, A8648, A9831, B1798, B2103, B2132, B2169, B2767, B2810, B2814, B3195, B6230, B6569, K1271, M4008, M4148, M4199, M4456, M4547, M4764, M4803, N1014, N2155, N2999, N6631, N7081, N7238, P0408.

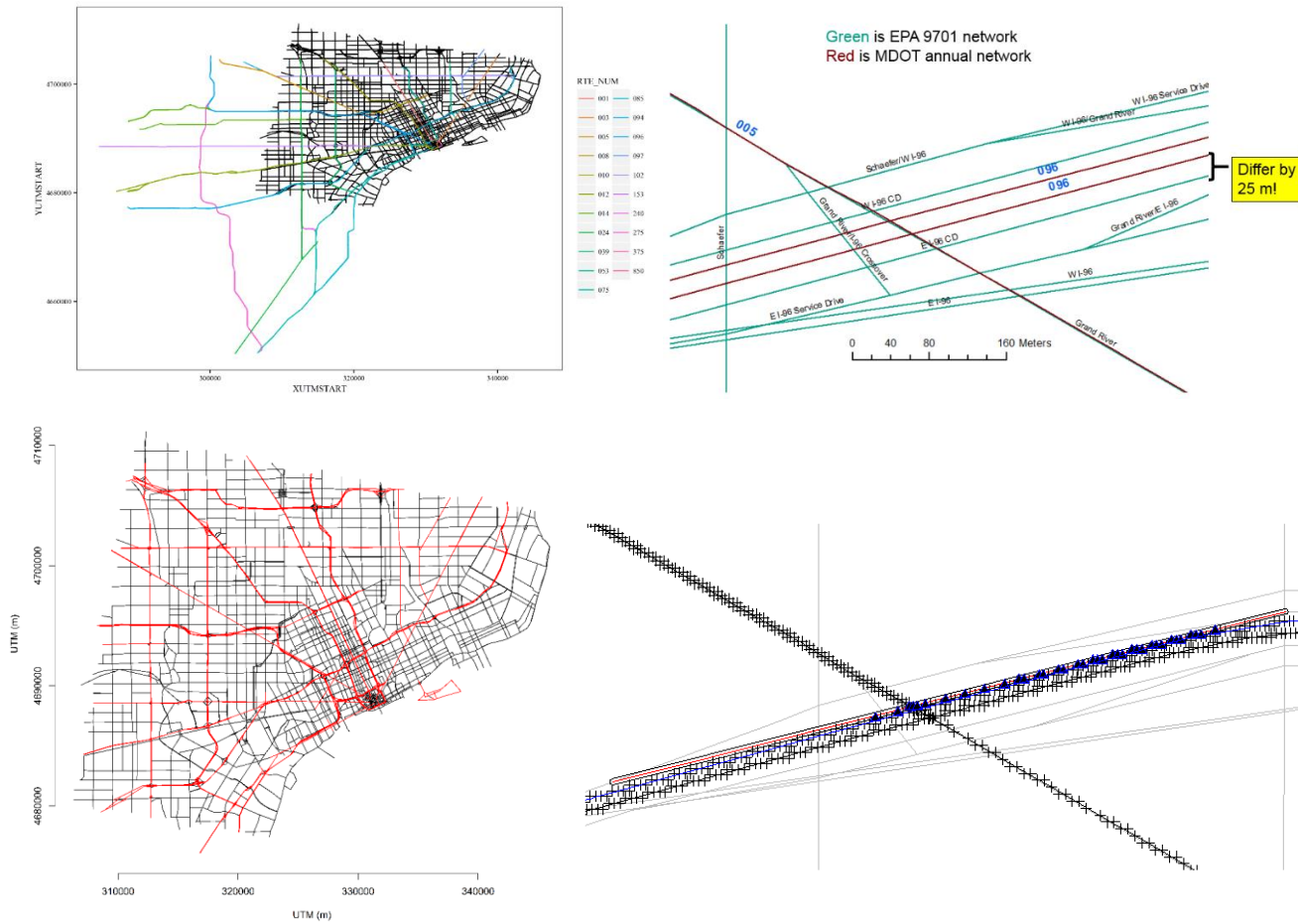


Figure 5. Custom mapping algorithm for aligning state roads with existing link-based inventory. Clockwise from top-left these images depict: 1) the previously modeled road network in black, and the Trunkline system in color; 2) one particular intersection, with modeled segments show in red and Trunkline shown in green; 3) buffers are drawn around previously modeled segments and intersecting MDOT roads (X's) and only roads mostly parallel to previously modeled segments are selected; 4) the final mapping of Trunkline roads (in red) among modeled segments

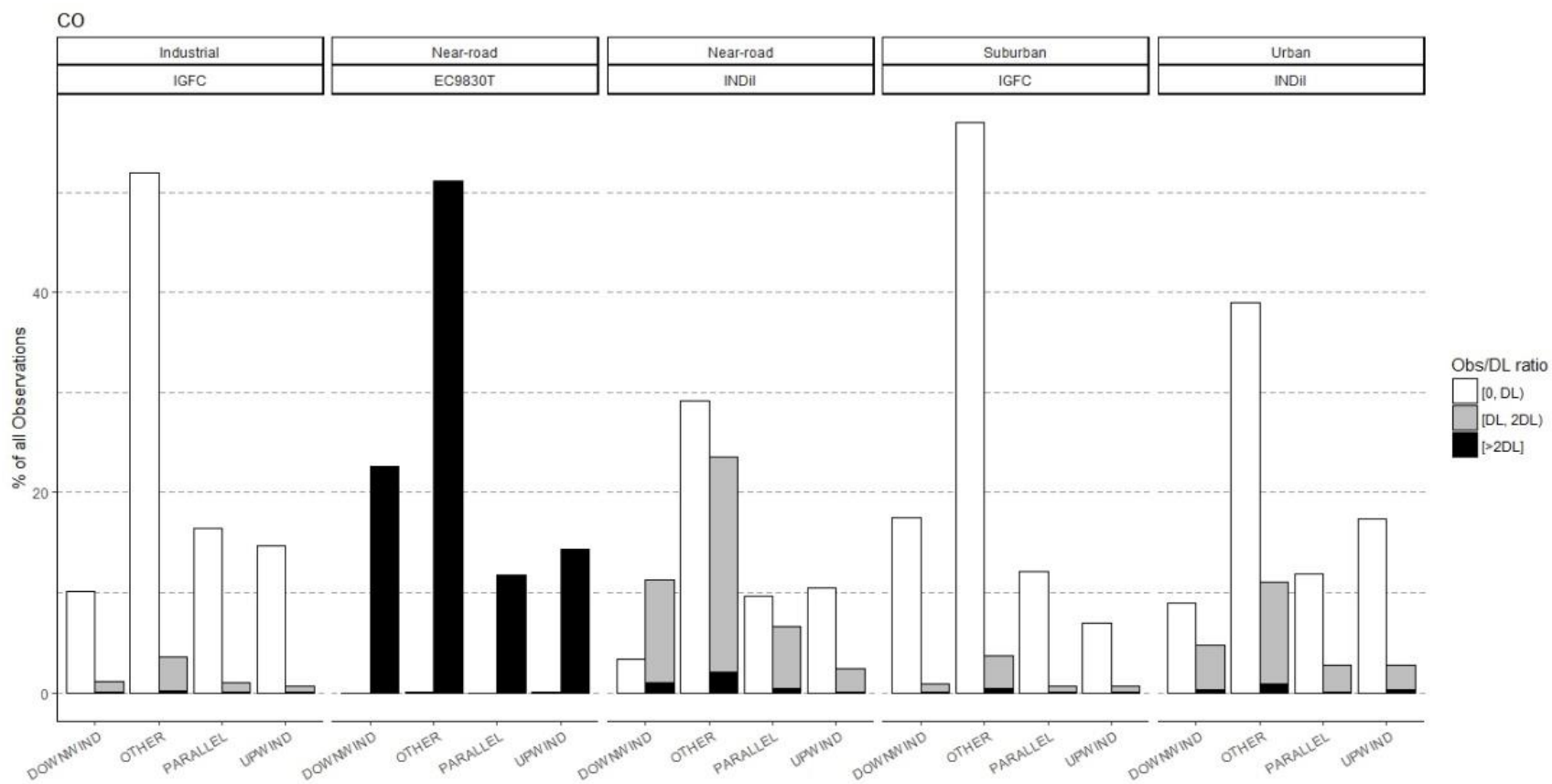


Figure 6. For CO, the % of observations below, within a factor of 1, or greater than the detection limit of each monitoring station and analytical method. For most CO monitors, the % above DL was < 20%, which limited our ability to perform certain analyses and estimate background concentrations using a method to fill in below detection limit values.

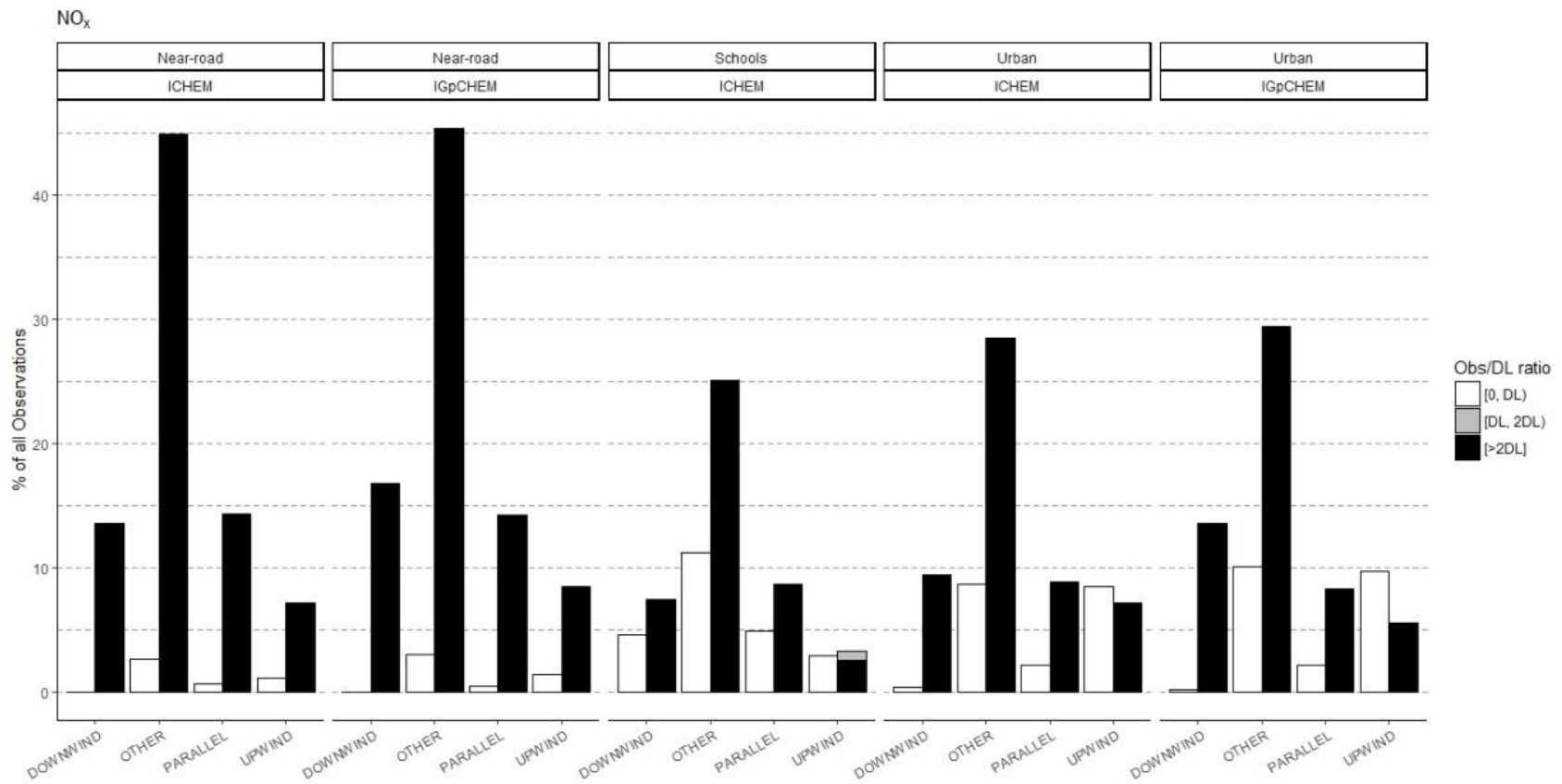


Figure 7. For NO_x, the % of observations below, within a factor of 1, or greater than the detection limit of each monitoring station and analytical method. Censoring of data was not a major consideration in processing of NO_x data.

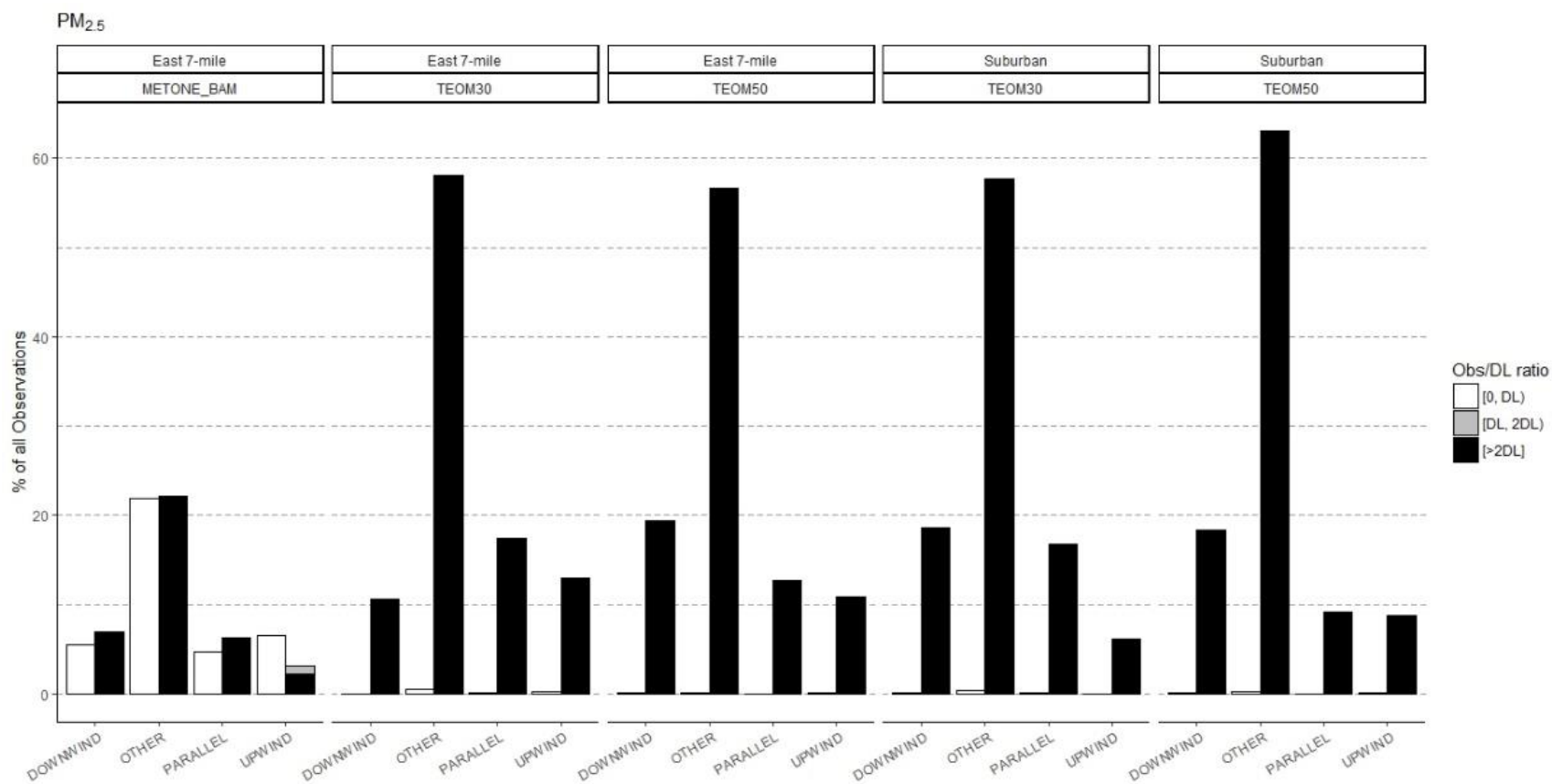


Figure 8. For PM_{2.5}, the % of observations below, within a factor of 1, or greater than the detection limit of each monitoring station and analytical method. Censoring of data was not a major consideration in processing of PM_{2.5} data.

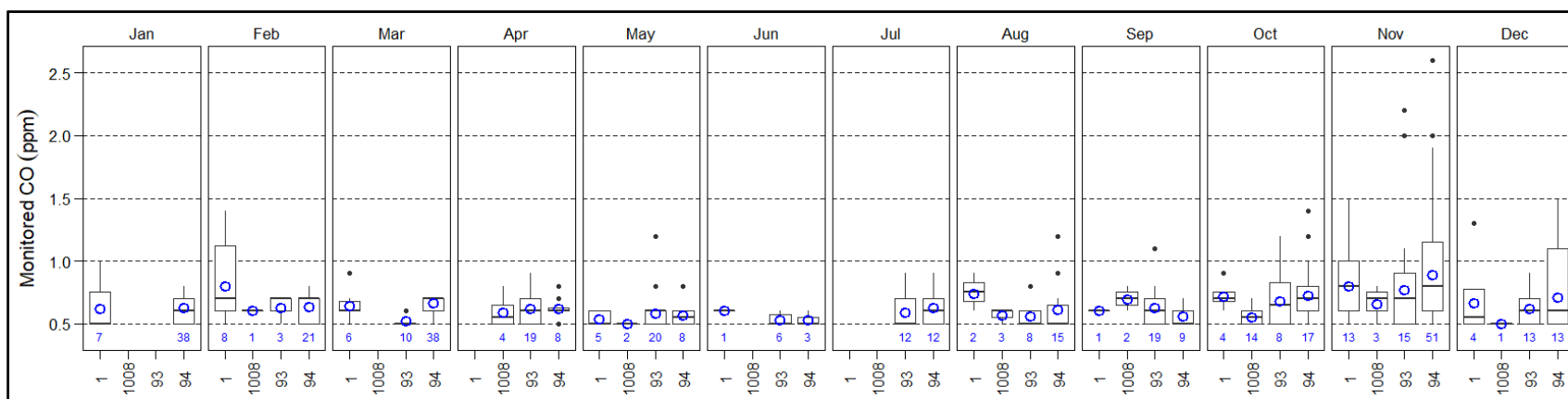


Figure 9. Boxplots of monthly upwind hourly CO measurements at each monitoring stations method for 2012. The x-axis labels are the AQS station ids (see Table 1). The blue circles show the geometric mean at each month, and the numbers below each box are the number of observations in each subset. As seen here, some stations and months have only a few hours of upwind data.

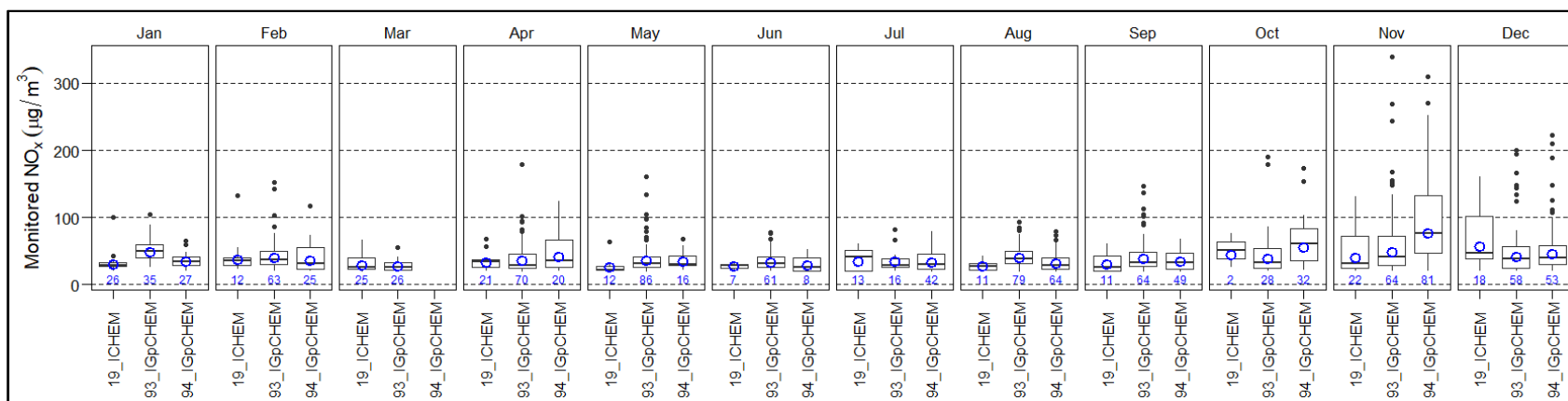


Figure 10. Boxplots of monthly upwind hourly NO_x measurements at each monitoring stations method for 2012. The x-axis labels are the AQS station ids (see Table 1). The blue circles show the geometric mean at each month, and the numbers below each box are the number of observations in each subset. As seen here, some stations and months have only a few hours of upwind data.

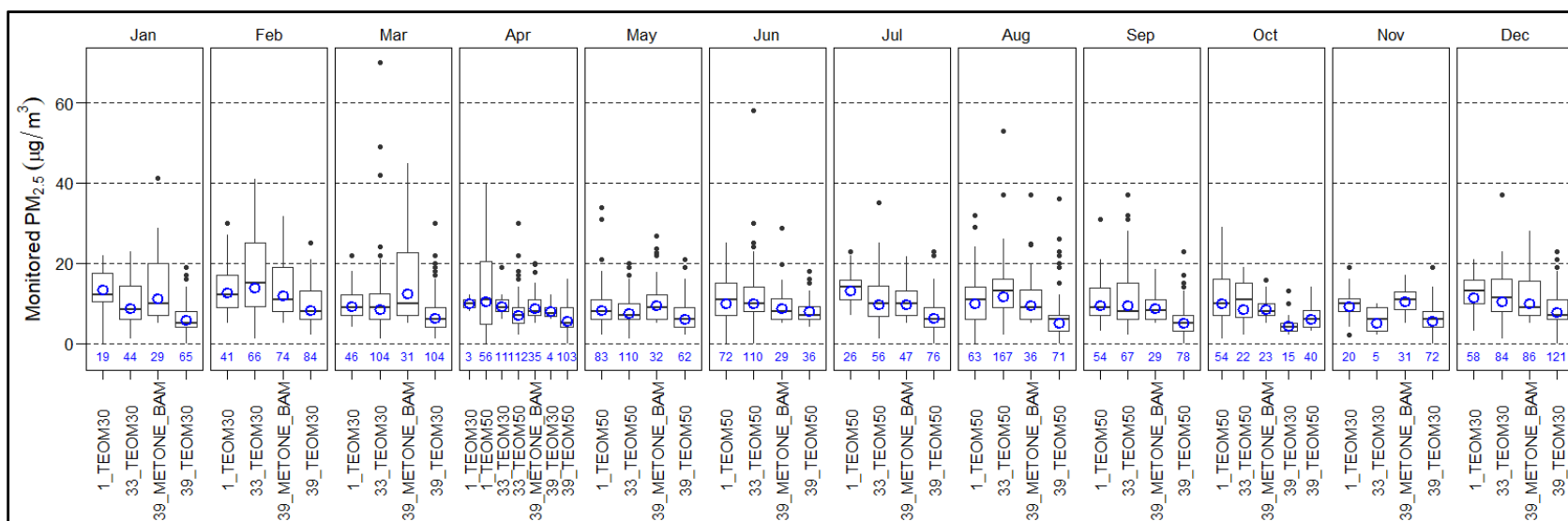


Figure 11. Boxplots of monthly upwind hourly $PM_{2.5}$ measurements at each monitoring stations method for 2012. The x-axis labels are the AQS station ids (see Table 1). The blue circles show the geometric mean at each month, and the numbers below each box are the number of observations in each subset. As seen here, some stations and months have only a few hours of upwind data.

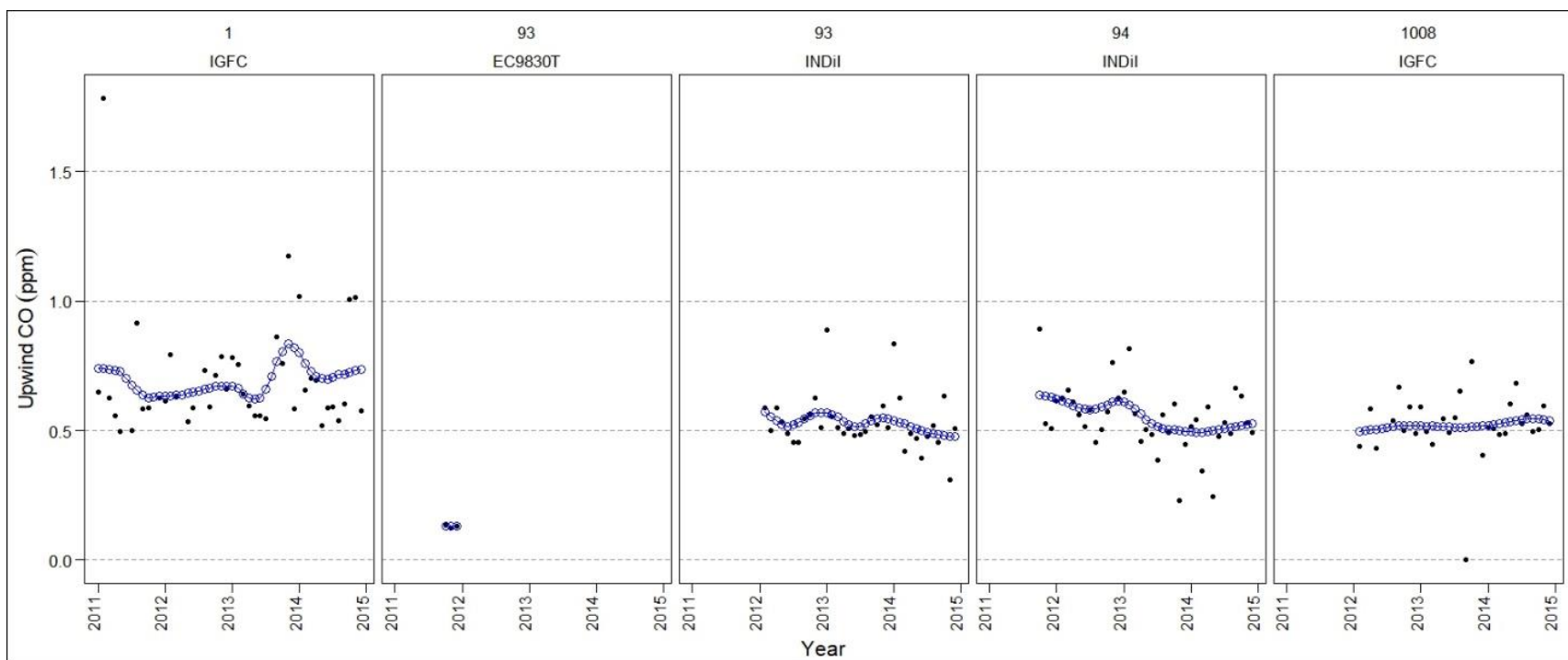


Figure 12. For CO, time-series plots of “leave-one-out” cross validated background values. Each plot is labeled on the top by the AQS Site ID and sampling method (See Table 1). The black points in each plot represent the geometric means shown in blue in Figure R2. As seen in this plot, the upwind values at various monitors vary, but within a relatively tight band (0.5 to 1.0 ppm).

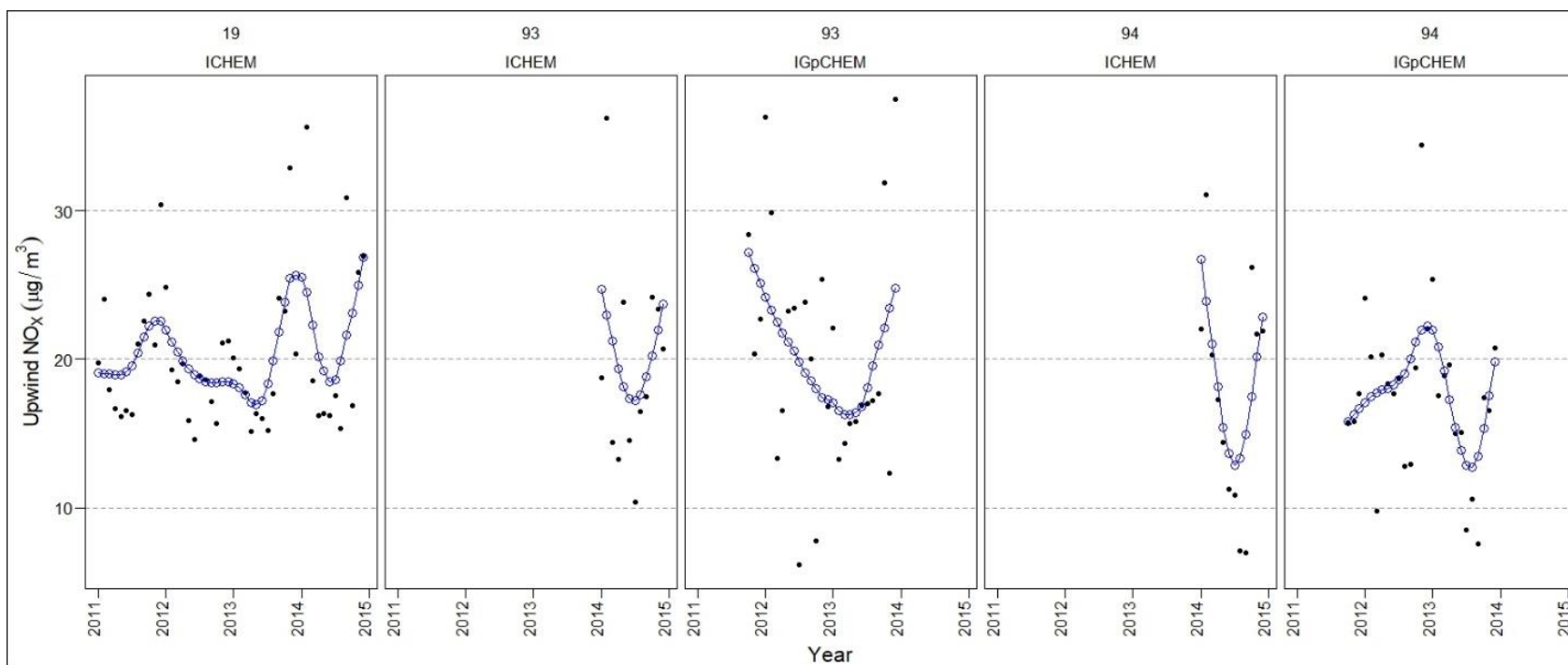


Figure 13. For NO_x, time-series plots of “leave-one-out” cross validated background values. Each plot is labeled on the top by the AQS Site ID and sampling method (See Table 1). The black points in each plot represent the geometric means shown in blue in Figure R2. As seen in this plot, the upwind values at various monitors vary, but within a relatively tight band (12 to 27 µg/m³).

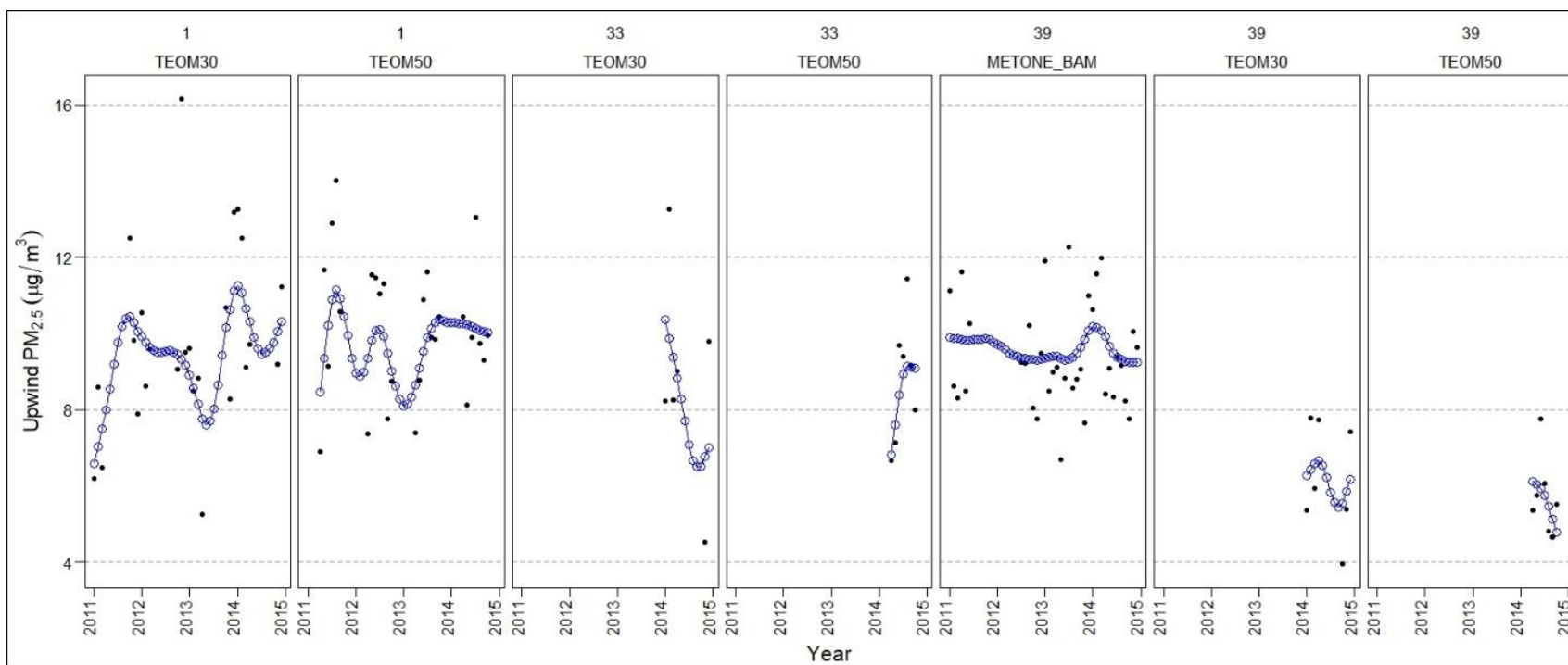


Figure 14. For $PM_{2.5}$, time-series plots of “leave-one-out” cross validated background values. Each plot is labeled on the top by the AQS Site ID and sampling method (See Table 1). The black points in each plot represent the geometric means shown in blue in Figure R2. As seen in this plot, the upwind values at various monitors vary, but within a normal range (5 to 11 $\mu\text{g}/\text{m}^3$)

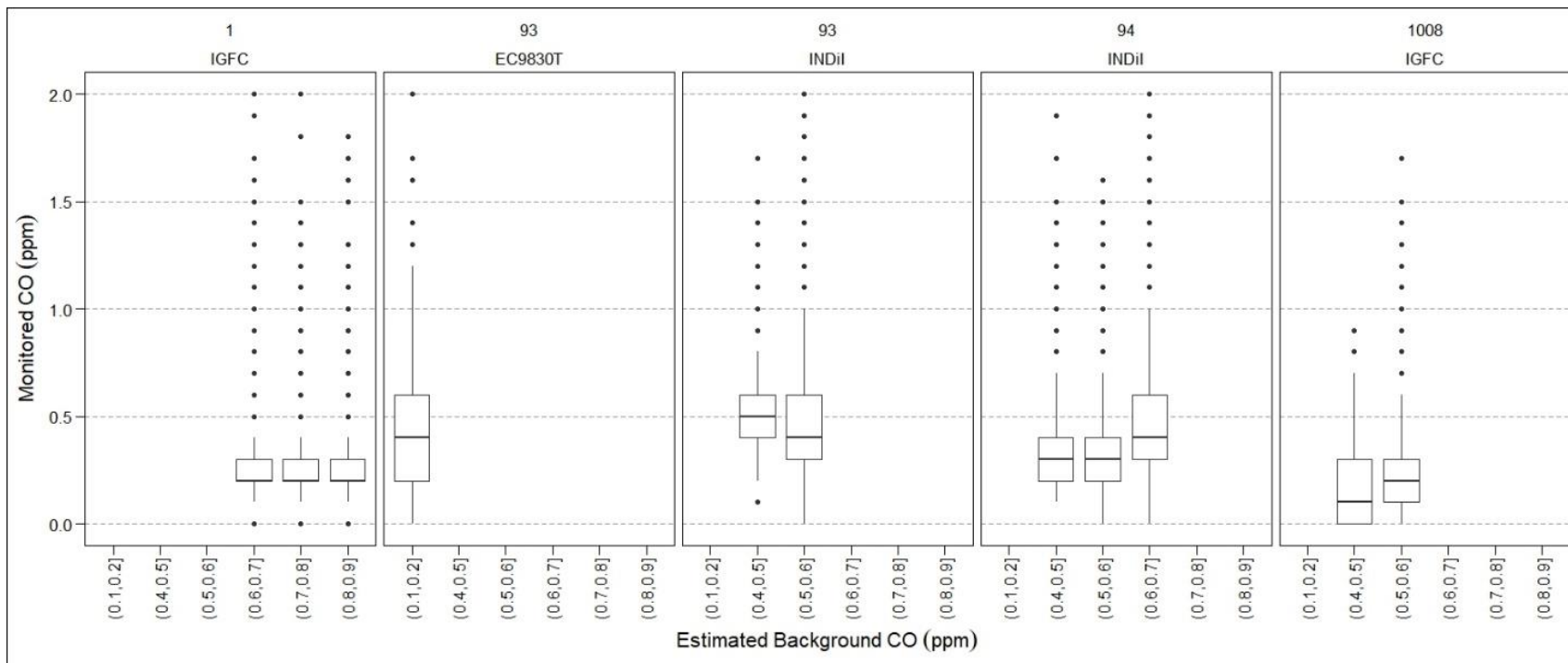


Figure 15. Boxplots of background vs monitored CO levels; across monitoring stations, little correlation is seen. Each plot is labeled on the top by the AQS Site ID and sampling method (See Table 1)

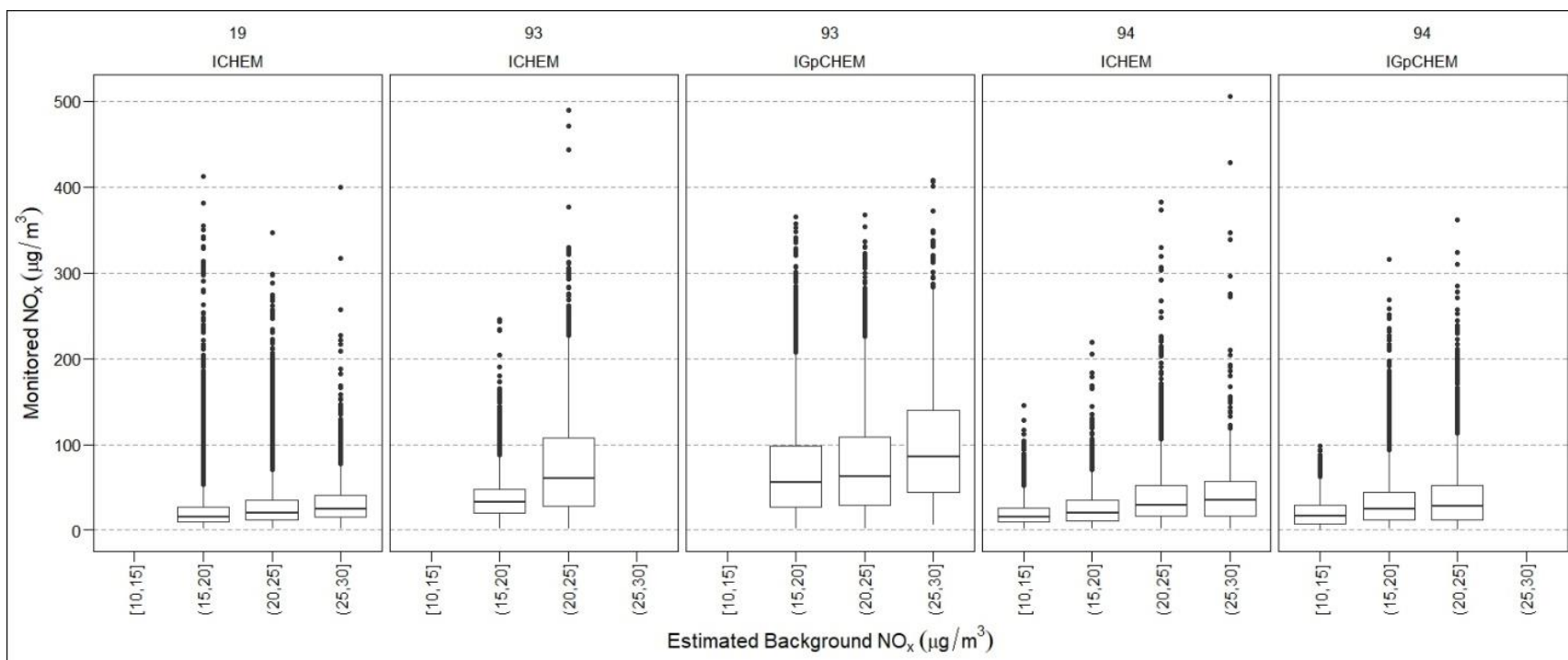


Figure 16. Boxplots of background vs monitored NO_x levels; across monitoring stations, the highest correlation is $R^2 = 0.33$. Each plot is labeled on the top by the AQS Site ID and sampling method (See Table 1)

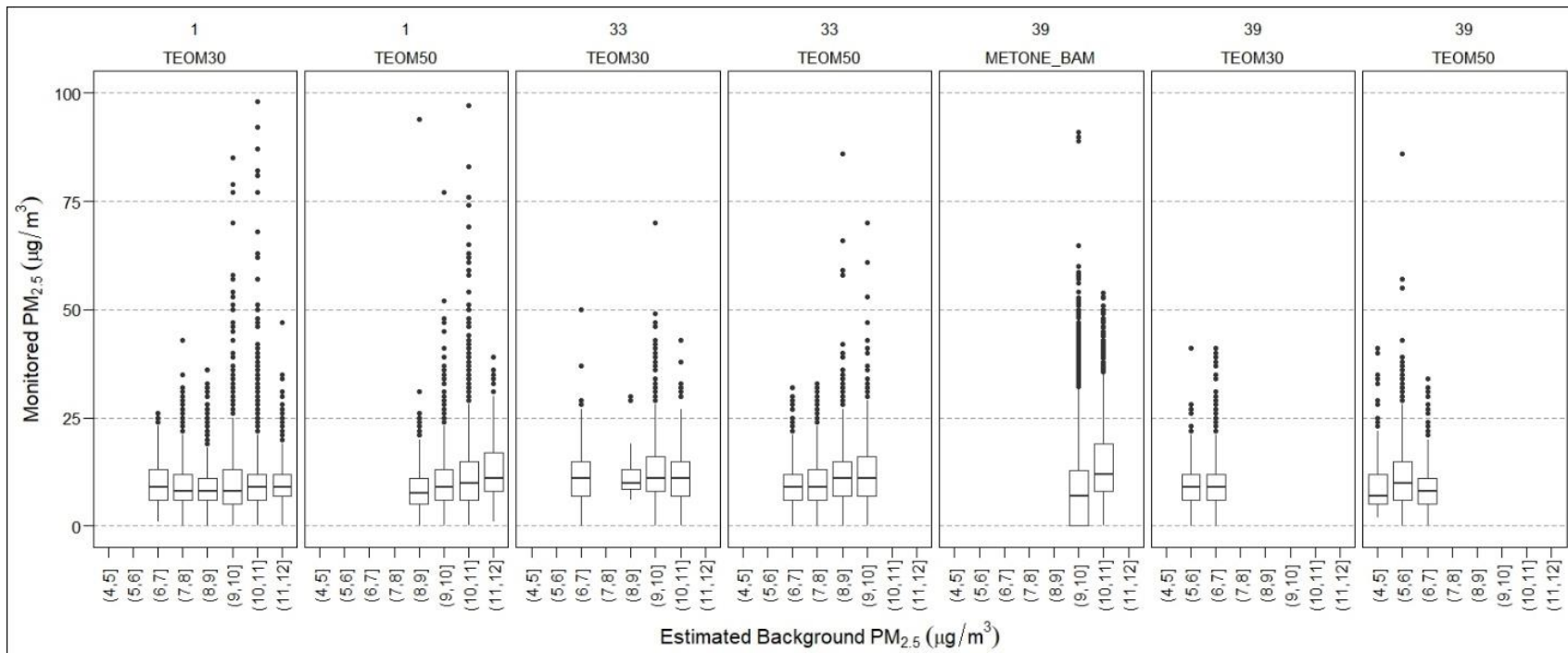


Figure 17. Boxplots of background vs monitored PM_{2.5} levels; across monitoring stations, very little correlation is seen. Each plot is labeled on the top by the AQS Site ID and sampling method (See Table 1)

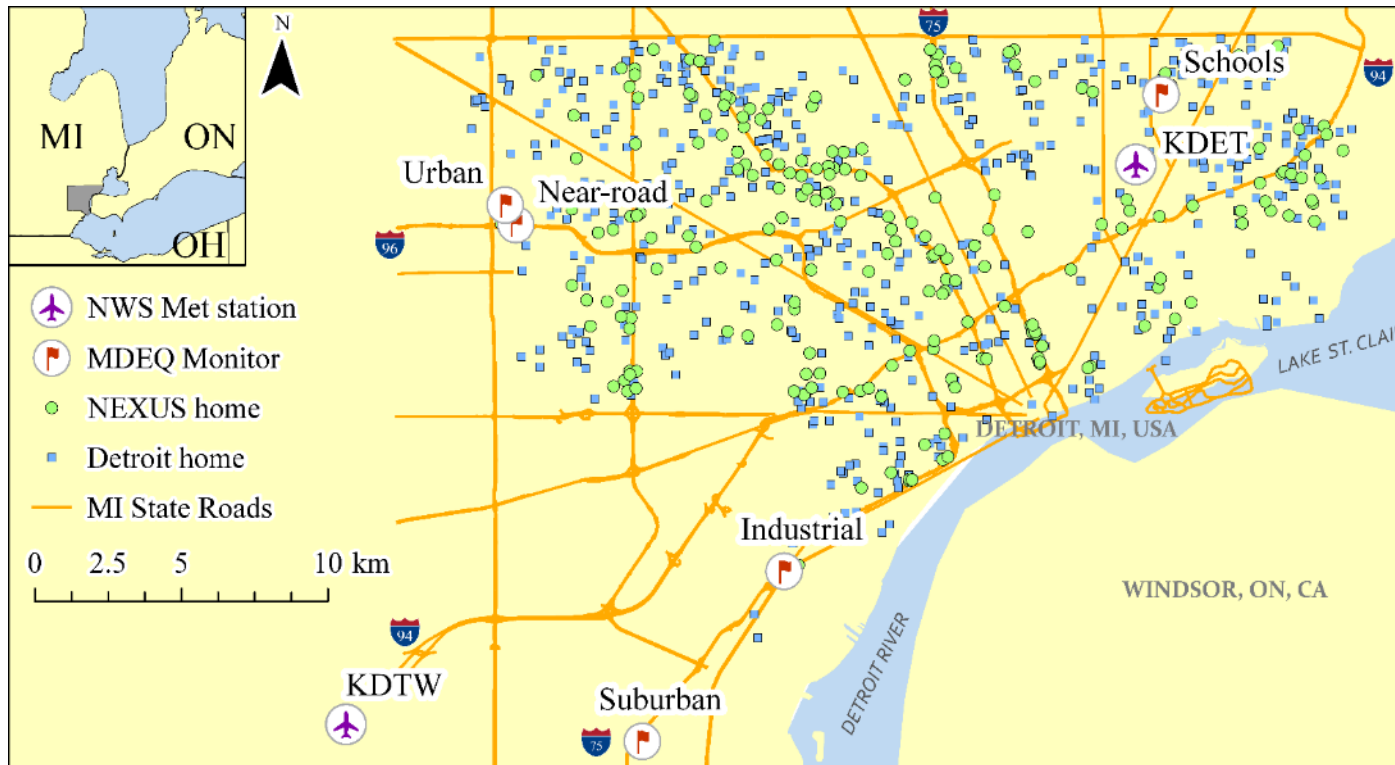


Figure 18. The modeling domain, including National Weather Service (NWS) meteorological stations, Michigan Department of Environmental Quality (MDEQ) air pollution monitors, a subset of Michigan State Trunkline Highway System, locations of NEXUS receptors (representing 206 residences in the NEXUS cohort), location of Detroit receptors (representing a population-weighted sample of residences in Detroit, n = 543).

Chapter III – Trends in PM_{2.5} emissions, concentrations and apportionments in Detroit and Chicago

III.1 Summary

This chapter examines Detroit, MI and Chicago, IL, two U.S. Midwestern cities that have high concentrations of industry, extensive vehicle traffic, historical exceedances of air quality standards, and large low income and minority populations that are susceptible to pollutants. These cities were selected due to the length of the data record available, and to contrast trends in the two cities (in adjacent states) potentially differentially affected by the 2008 recession. This chapter's goal is to understand the trends in the sources contributing to PM_{2.5} concentrations in Detroit and Chicago. In each city, we examine emission inventories, ambient pollutant concentrations, and derive source apportionments using receptor models. Quantile regression is used to analyze trends in concentrations and receptor model apportionments, a novel application of this work. Over the study period, county-wide data suggest emissions from point sources decreased (Detroit) or held constant (Chicago), while emissions from on-road mobile sources were constant (Detroit) or increased (Chicago), however changes in methodology limit the interpretation of inventory trends. Ambient concentration data also suggest source and apportionment trends, e.g., annual median concentrations of PM_{2.5} in the two cities declined by 3.2 to 3.6 %/yr (faster than national trends), and sulfate concentrations (due to coal-fired facilities and other point source emissions) declined even faster; in contrast, organic and elemental carbon (tracers of gasoline and diesel vehicle exhaust) declined more slowly or held constant. The PMF models identified nine sources in Detroit and eight in Chicago, the most important being secondary sulfate, secondary nitrate and vehicle emissions. A minor crustal dust source, metals sources, and a biomass source also were present in both cities. These apportionments showed that the median relative contributions from secondary sulfate sources decreased by 4.2 to 5.5% per year in Detroit and Chicago, while contributions from metals sources, biomass sources, and vehicles increased from 1.3 to 9.2% per year.

III.2 Results and Discussion

III.2.1 Emission inventory trends

Table 15 summarizes PM_{2.5} emissions reported in the 2002 through 2011 NEI data. The NEI source categories, data and emission factors have shifted over the years, resulting in large changes and some difficulty in evaluating trends. The methodological changes can greatly affect results and limit its usefulness for trend analyses, at least for certain source types. For example, fugitive emissions of PM_{2.5} from paved roads, unpaved roads, and construction sources are calculated by applying a factor to modeled PM₁₀ emissions [152], which itself is estimated using emission factors, activity estimates, and other data. These factors have been updated several times since 2002 [153], which partially explains the large changes in construction dust emissions. Uncertainties in the multiplicative factor used to generate PM_{2.5} emissions from PM₁₀ emissions have been discussed at length by Pace [152]. As a second example, on-road emissions were calculated over the study period using several models, i.e., the National Mobile Inventory Model (NMIM) running MOBILE6 in 2002, 2005, and version 1 of the 2008 NEI; and then the Motor Vehicle Emission Simulator (MOVES) in versions 2 and 3 of NEI 2008 and 2011. (For non-road mobile emissions, NMIM is still used [98]) For mobile sources, important uncertainties include the availability and accuracy of the data providing on-road and off-road gasoline and diesel fuel consumption, the age and composition of the fleet, and the emission factors [154]. In addition, not all data in the inventory is updated each period, e.g., the 2005 non-point emissions mostly used the 2002 NEI estimates [155]. Uncertainties in the NEI data also limit many comparisons. With these caveats, we discuss emission trends in the two cities.

Over the study period in Wayne County (encompassing Detroit), NEI point source emissions decreased from 5,364 to 1,610 tons/year, non-road mobile sources decreased from 855 to 493 tons/year, and on-road mobile emissions (mostly diesel exhaust) fluctuated from a low of 916 (2005) to a high of 2,110 tons/year (2008). On-road mobile PM_{2.5} exhaust emissions increased slightly over the study period: both gasoline and diesel vehicle exhaust emissions dropped in 2005, but then nearly doubled in 2008. Non-point source emissions (excluding mobile sources) also fluctuated, from 1,682 tons/year (2002) to 5,782 tons/year (2008), and of the sources in this category, construction dust had the greatest changes, increasing 25-fold from 2005 to 2008 (to 350 tons/year), then decreasing by the same amount in 2011. Other non-point sources, primarily residential wood combustion, commercial cooking and various industrial processes (550, 450 and

586 tons/year in 2011, respectively), collectively represent the largest fraction of PM_{2.5} emissions in the inventory (45% in 2011). These non-point emissions had large changes from 2005 to 2011, e.g., residential wood combustion increased from 69 (2005) to 1,649 tons/year (2008). The large (over 3-fold) increase in non-point source emissions between 2005 and 2008 was due mostly to updated estimates of fugitive dust.

Emission trends for Cook County (including Chicago) reflect those in Wayne County with several exceptions. First, point source emissions stayed fairly constant (2,390 to 2,510 tons/year, excluding much higher emissions in 2005), compared to the large decreases in Wayne County. Second, Cook County had very high emissions of construction dust (up to 6,351 tons/year, 31% of total PM_{2.5} in 2011), possibly resulting from construction activities (including a number of high-rise buildings), high wind speeds that increase entrainment [156], and changes in the calculation methods (noted above). As in Wayne County, non-point sources exhibited an over 3-fold increase from 2005 to 2008, and on-road mobile gasoline and diesel exhaust emissions dropped in 2005 but then approximately doubled in 2008. Non-road mobile sources steadily decreased to 7% of total PM_{2.5} emissions in 2011.

Comparing the two cities, mobile on-road PM_{2.5} emissions were constant in Detroit (1,126 to 1,188 tons/year) and increased in Chicago (1,782 to 2,163 tons/year in Cook County) over the study period. On-road mobile sources represented 10 to 17% of total PM_{2.5} emissions (depending on year and city). On an area basis, however, mobile emissions in the two cities were similar, i.e., 0.75 and 0.88 tons/year/km² in Wayne and Cook Counties, respectively (2011 data). On-road emissions were dominated by heavy-duty diesel vehicle exhaust (comprising 61% of emissions in this category in 2011), followed by light-duty gasoline vehicle exhaust (28%). Non-road mobile source emission rates were also 1.5 to 2 times higher in Cook County, but similar on an areal basis, and the largest source in both cities was exhaust from off-road diesel construction vehicles. Diesel railroad emissions in Wayne County were small (29 tons/year in 2002-5, dropping to 0.5 tons/year in 2008-11), compared to initially much higher levels in Cook County (555 tons/year in 2002-5, but these emissions also plummeted to only 2.8 tons/year in 2008-11). These differences may reflect the higher rail activity in Chicago, effects of controls imposed by the 2004 rules for heavy duty diesel vehicles [157], the 2008 rules for locomotives [158], and other fleet and emission factor changes.

The large uncertainties in nonpoint emissions, the changing methodology in mobile source emissions, and potentially other issues in the emissions inventory data can severely limit trend analyses of the emissions data. Still, several broad trends are apparent. In 2011, on-road emissions exceeded non-road mobile emissions in both cities, and the total mobile emissions matched (Detroit) or exceeded (Chicago) point source emissions. These data suggest several factors that may have affected emissions. In Detroit, the steady decline in point source emissions can be attributed to cleaner fuels (natural gas has replaced considerable coal), updated emission controls on some facilities, and reduced activity in automobile manufacturing and other industries, witnessed by the shuttering of businesses and the continued exodus of a large fraction of the population [102], particularly during the 2008-9 recession. In Chicago, industrial and commercial activity is more diversified (e.g., manufacturing, publishing, finance/insurance, food processing, transport/distribution), the population has been more stable, and the recession's impact on local emitters was likely smaller (e.g., the largest local PM_{2.5} source, a wet corn mill at Corn Products International, likely responds less to economic fluctuations than vehicle manufacturing). Estimates of traffic activity in both cities showed only small changes, e.g., vehicle miles traveled (VMT) in Detroit decreased by 2% since 2004 [159], and Chicago did not have a consistent trend [160]. In both cities, the switch to low-sulfur diesel fuel in combination with introduction of particle traps have reduced diesel exhaust emissions, although this may be offset by the growth in the number of trucks, based on state-level data.

For comparison, we investigated recent regional or national apportionment studies that analyzed NEI data. Using NEI data from 2002 through 2011 and predefined source profiles in a chemical mass balance (CMB) model in the southeast US, point source emissions showed large decreases, while mobile source emissions showed comparable or smaller decreases [161]. The largest sources identified by a Bayesian source apportionment model, which used CSN data in Boston and Phoenix from 2000 onwards, NEI 2002 data, and profiles from the SPECIATE database, were coal and oil combustion, vegetative burning, road dust, and vehicles [162]. A hybrid receptor-chemical transport model (CTM) using projected NEI 2002 data in six major US cities indicated that coal combustion and on-road gasoline emissions were the largest sources of primary and secondary PM_{2.5} [163]. Using fuel-based estimates from on- and non-road mobile sources in California, a range of vehicle types showed decreases in emissions and the growing contribution of non-road mobile sources relative to on-road sources [164]. Although these earlier studies have some

similarities to the present work, they neither compared NEI data with CSN data and PMF results over the same period nor investigated long-term trends from mobile sources in the Midwest, the focus of this work. Lastly, we note that year-to-year emissions of other criteria pollutants (SO_2 , CO, NO_x) tend to be more stable than $\text{PM}_{2.5}$, probably because the underlying data (e.g., emission and activity factors) are more robust and less subject to large methodological changes.

III.2.2 Concentration trends

Table 16 summarizes annual and seasonal ambient concentrations in the two cities, including test results showing differences between year-blocks. Several $\text{PM}_{2.5}$ constituents show considerable seasonal variation, e.g., NO_3^- levels tended to be highest in winter and fall, and S and SO_4^- were highest in summer, thus, seasonal analyses are needed to understand trends.

In Detroit, concentrations of $\text{PM}_{2.5}$, NH_4 , NO_3^- , SO_4^- and many other species changed significantly between year-blocks ($p < 0.05$ for KW and MW tests); in contrast, changes in EC and usually OC concentrations were not statistically significant. Comparing the 2006-2009 and 2013-2015 periods, for example, median SO_4^- concentrations fell 33% (from 2.36 to 1.57 $\mu\text{g}/\text{m}^3$), while median EC (URG sampler) levels were unchanged (0.32 and 0.33 $\mu\text{g}/\text{m}^3$). Most species decreased less rapidly than SO_4^- , e.g., median $\text{PM}_{2.5}$ concentrations decreased only slightly (10.9 to 10.6 $\mu\text{g}/\text{m}^3$), although 90th percentile $\text{PM}_{2.5}$ levels fell from 23.4 to 17.5 $\mu\text{g}/\text{m}^3$. Seasonal statistics are similar. In Chicago, concentrations were more stable, e.g., only NH_4^+ and SO_4^- changed annually and in each season, and $\text{PM}_{2.5}$, NO_3^- and S concentrations varied annually and in winter and fall seasons. Concentrations tended to decrease from 2006-2009 to 2010-2013, however, levels after 2013 sometimes increased. Again, EC and OC showed smaller and fewer significant differences compared to the other species. The instrument switch in spring 2010 likely dampened EC and OC trends.

Across the two cities, QR results showed that 50th and 90th percentile concentrations of $\text{PM}_{2.5}$ and many of the major species significantly decreased over the study period (Figure 19 and Figure 20). In Detroit, median concentrations of $\text{PM}_{2.5}$ fell by 3.6 %/yr, and seasonal decreases from 2.7 (winter) to 4.9 (spring) %/yr. At the 90th percentile, $\text{PM}_{2.5}$ concentrations declined slightly faster with annual levels falling by 4.9 %/yr and seasonal decreases from 3.5 (winter) to 5.6 (summer) %/yr. Annual and seasonal trends of NH_4^+ and NO_3^- (at both percentiles) were nearly identical, e.g., median levels decreased by 7.0 and 5.5 %/yr overall, and declines were fastest in spring (8.6

and 8.2 %/yr) and slowest in winter (5.4 and 3.6 %/yr); 90th percentile concentrations decreased fastest in summer (9.5 and 8.8 %/yr) and slowest in winter (3.4 and 2.1 %/yr). Unsurprisingly, SO₄⁼ and S trends were nearly identical, e.g., median concentrations decreased by 5.8 and 4.9 %/yr overall, and changes were the smallest in winter (4.0 and 2.9 %/yr) and similar in other seasons (4.8 to 5.9 %/yr); 90th percentile levels fell fastest in fall (9.2 and 8.9 %/yr) and slowest in winter (3.6 and 2.8 %/yr). QR results for the two types of EC measurements differed, e.g., EC_{MET} levels did not change at annual and seasonal levels other than a 2.7 %/yr decrease seen in the median summer levels, while EC_{URG} decreased by 5.0 and 5.8 %/yr at median and 90th percentile levels, respectively, largely due to decreases in fall and spring, respectively. OC_{MET} and OC_{URG} also showed differences, e.g., median OC_{MET} levels decreased by 6.5 %/yr on an annual level and from 4.6 (summer) to 8.5 (fall) %/yr on a seasonal basis; OC_{URG} did not show significant changes in any season or percentile. Overall, the seasonal patterns of PM_{2.5}, NH₄⁺ and NO₃⁻ were similar. The shorter time series of EC and OC available for each instrument may have obscured trends. In the following PMF application, a complete record of adjusted EC and OC concentrations is used to derive long-term trends.

Chicago showed fewer trends that were statistically significant, as well as less consistency across related species (Figure 20). Median and 90th percentile levels of PM_{2.5} dropped by 3.2 and 4.1 %/yr, respectively, and summer and fall changes at the 90th percentile were significant (7.6 and 5.3 %/yr). Decreases in median levels of NH₄⁺ (8.6 %/yr) were slightly larger than changes in Detroit, and decreases in summer and fall were particularly rapid (13.5 and 14.2 %/yr). For NO₃⁻, statistically significant decreases were only seen in fall (median and 90th percentile) and winter (90th percentile), and NO₃⁻ and NH₄⁺ changes were not correlated, unlike in Detroit. SO₄⁼ and S trends in Chicago also differed from those in Detroit: the largest decreases occur in summer (10.0 and 7.3 %/yr for medians), and the smallest in both winter and spring. (Detroit's largest changes for SO₄⁼ and S were in fall and the smallest in winter.) EC and OC trends in Chicago were less pronounced and few attained statistical significance, however, there were some similarities in EC trends with patterns observed in Detroit. Median levels of EC_{MET} decreased greatly in summer (15.2 %/yr); and both median and 90th percentile levels of EC_{URG} fell significantly (3.6 and 5.1 %/yr). Seasonal concentrations of OC_{MET} fluctuated (both increased and decreased) across the study period, but changes were not statistically significant. Since only three years of data (2006 to early 2010) were available for the Chicago EC_{MET} and OC_{MET} measurements, trends for these

variables are not reliable. Median and 90th percentile concentrations of OC_{URG} decreased (1.9 and 3.9 %/yr). Overall, PM_{2.5} concentrations in Chicago and Detroit decreased at similar rates, but few of the major constituents in Chicago showed seasonal trends that were significant or consistent with Detroit's.

Many of the major species (e.g., NH₄⁺, NO₃⁻, SO₄⁻ and S) had greater changes across the study period in summer and fall when concentrations were higher, as compared to winter when concentrations were often lower. In Detroit, trends in annual median NO₃⁻ and NH₄⁺ concentrations were driven more by changes in spring and less by changes in winter; peak concentrations were driven more by changes in summer peaks and less (again) by changes in winter peaks. Similarly, changes in annual median SO₄⁻ and S concentrations were driven less by changes in winter; changes in peak SO₄⁻ and S were also highest in summer and fall. Trends in median and peak PM_{2.5} concentrations most resembled patterns for the nitrogen components, which suggests that in Detroit changes in NO₃⁻ exerted a greater influence on PM_{2.5} levels than SO₄⁻. This result is unexpected since NO₃⁻ and NH₄⁺ comprise a smaller PM_{2.5} fraction than OC and SO₄⁻, however, this analysis does not consider a mass balance (e.g., reconstructed mass) or account for correlated species and source contributions (as described in the PMF modeling following). Trends in Chicago have some similarities, but also notable differences: trends in peak PM_{2.5} concentrations resembled patterns for SO₄⁻ rather than NO₃⁻; reductions in SO₄⁻ and S in summer and fall were the highest among seasons, and only peak PM_{2.5} trends in summer and fall were statistically significant. This pattern also conforms to the KW and MW test results, and suggests that PM_{2.5} levels in Chicago aligned more with changes in SO₄⁻ than NO₃⁻.

Both regional and local sources influence concentration trends. Secondary regional pollutants are important constituents of PM_{2.5} in the Midwest, and much of the SO₄⁻ in the region results from long range transport from large coal-fired boilers and power plants. Many of these facilities have reduced emissions of precursor SO₂ in recent decades by the addition of scrubbers and fuel switching. In cases, such changes have not occurred for the generally smaller and often older coal-fired facilities located in cities, a result of space constraints, costs and other issues. NO₃⁻, another secondary pollutant from precursor NO and NO₂ emissions (largely from mobile sources and power plants), often has the highest levels in winter and spring when O₃ concentrations are low [165]. Both SO₄⁻ and NO₃⁻ are present in the Midwest atmosphere as ammonium sulfate and

ammonium nitrate due to ammonia emissions from fertilizers and animal feed [166]. OC is derived from primarily vehicle emissions and biomass burning [35]. The largest contributor to EC is diesel exhaust emissions [167]. Road dust contributions (i.e., Si, Ti, Ca, Al) are normally low in winter due to lower siltation levels [168]. Concentrations of major species in both cities followed expected seasonal trends [169], e.g., NH_4^+ and NO_3^- were highest in the winter, SO_4^- was highest in the summer, and EC and OC were higher in summer than winter.

Overall, median $\text{PM}_{2.5}$ concentrations in the two cities declined by 4.3 to 4.5 %/yr: comparable rates have been shown in several national and regional assessments. Nationally, a 27% drop in average $\text{PM}_{2.5}$ from 2000 to 2010 (2.7 %/yr) has been reported [170, 171]. The Lake Michigan Air Directors Consortium (LADCO) estimate a $0.51 \mu\text{g}/\text{m}^3$ per year decrease in 90th percentile $\text{PM}_{2.5}$ concentrations from 1999 to 2007 across the region [172], which (when converted) is in the range of %/yr decreases in the present work. The monitoring data also reveal the changing composition of $\text{PM}_{2.5}$: the share is growing for EC and OC, but declining for SO_4^- and NO_3^- . While many sources emit EC and OC, local vehicle emissions are one of the larger contributors [168, 173, 174]. In contrast, SO_4^- largely arises from local and regional point sources [28]. The less pronounced trends at Chicago may reflect the shorter study period, as well as smaller changes in the local and regional sources.

Trends in the ambient monitoring data have some consistencies with the emissions inventory data discussed earlier, particularly for the combustion sources (point and mobile exhaust). For example, ambient levels of SO_4^- , NO_3^- , and NH_4^+ in Detroit fell by 5 to 10 %/yr over the 2002 and 2011 study period, while point source emissions decreased by roughly 11 %/yr. In contrast, ambient levels of EC showed few significant changes, consistent with fluctuating trends of on-road diesel exhaust emissions. In Chicago, SO_4^- and NH_4^+ also decreased significantly from 2006 to 2014, and the emissions inventory showed a concurrent drop in point source emissions. As noted earlier, a number of issues in the emissions inventories limits the comparability of trends.

Concentration trends also can be framed in the context of species abundance (i.e., species concentration / $\text{PM}_{2.5}$ concentration on a per-sample basis). However, given issues with EC and OC measurements (key tracers for vehicle emissions), uncertainties in the stoichiometric balance, and the correlation among both major and minor species, trend analyses of PMF factor contributions should be more meaningful; in addition, PMF contributions (by definition) sum to

unity on a per-sample basis. We next extend the trend analyses to examine source contributions apportioned using receptor modeling.

III.2.3 Long term source apportionments

The final PMF model for Detroit had nine factors with 5% additional model uncertainty, and the final model for Chicago had eight factors with 0% additional model uncertainty (Figure 21). This number of factors and the (small) uncertainty additions (in Detroit) yielded factors that were interpretable and comparable to those in the literature, and both models closely matched PM_{2.5} observations (Detroit: $R^2 = 0.96$; Chicago: $R^2 = 0.90$). Sources associated with each factor, which have been identified in previous apportionments [34, 115], included secondary SO₄⁻ (characterized by SO₄⁻ and NH₄⁺), secondary NO₃⁻ (NO₃⁻ and NH₄⁺), vehicle emissions (EC for diesel vehicles and OC for gasoline vehicles), biomass burning (K⁺), industrial metal working (Ni, Cr, Mn, Fe), crustal sources (e.g., entrained soil as noted by Al, Si, Ca, Ti), and a zinc factor (which also can represent industrial emissions) [34]. While not unique tracers, OC and EC have been used to separate vehicle emissions into gasoline and diesel categories, respectively [35]; a factor containing both OC and EC can represent emissions from a mixed fleet. In the final models, a single factor contained moderate to high levels of both EC and OC, and thus the vehicle factor represents contributions from a mixed fleet.

The final PMF models using the full dataset gave nearly identical apportionments in Detroit and Chicago for the largest sources: sulfate formed 32 - 33% of PM_{2.5}; vehicles contributed 21 - 22%; nitrate constituted 21%; and biomass was 7 - 9%. These four sources represent over 80% of PM_{2.5}. Minor sources, e.g., crustal (4 - 8% of PM_{2.5}), several metals (4 - 11%) and Cl/NaCl (2 - 5%) showed greater variation, but accounted for relatively little PM_{2.5} mass. The similarity of the apportionments for the major local sources (e.g., vehicles and biomass) is supported by the emissions inventory, e.g., the similarity of traffic emissions when expressed on an area basis; and the similarity of the secondary contributions (e.g., sulfate and nitrate) may reflect the same regional sources in these nearby cities (e.g., a large number of coal-fired power plants).

III.2.4 Source apportionment trends

The QR analysis of trends for the PM_{2.5} PMF factors in Detroit is displayed in Figure 22. These trends only roughly followed results seen for the major species in each factor (shown earlier in Figure 19). Median concentrations of the secondary sulfate factor declined by 8.3 %/yr, and

seasonal changes were largest in fall and smallest in winter and summer. At the 90th percentile, sulfate factor concentrations declined slightly faster, 9.2 %/yr overall, and declines were greatest in summer and smallest in winter. Changes in SO₄⁼ or NH₄⁺ concentrations (dominant contributions to this factor) did not match the secondary sulfate pattern with the exception of the 90th percentile concentration change of NH₄⁺. For the secondary nitrate factor, overall concentrations declined 7.0 %/yr, and statistically significant decreases of 9.2 to 11.7 %/yr occurred in spring, summer and fall (but not winter). This pattern (as well as the 90th percentile pattern) was not matched by NO₃⁻ and NH₄⁺, this factor's major contributors. For the vehicle factor, decreases in median and 90th percentile factor concentrations were fairly consistent (2.8 to 5.2 %/yr, depending on season) but dissimilar to trends in measured EC and OC. The biomass factor did significantly change over the study period. Trends of factors representing the smaller PM_{2.5} fractions may be less reliable for several reasons, e.g., PMF uncertainties (smaller factors are dominated by species with higher %BDL and thus higher associated uncertainties) and factor splitting (where changing the number of factors causes minor species to group in ways that may affect trends in minor factors). Still, several of the smaller components had statistically significant changes: the metals factor increased by 3.9 and 2.4 %/yr for the median and 90th percentile, respectively; and the crustal factor declined by 5.8 % and 3.3 %/yr for the median and 90th percentile, respectively (the large decrease in winter was particularly notable).

The QR trend analysis for the Chicago PMF factors is depicted in Figure 23. Median concentrations of the secondary sulfate factor decreased by 9.3 and 9.2 %/yr for the median and 90th percentile, respectively; decreases were largest in summer. As in Detroit, these patterns differed from the trends of SO₄⁼ and NH₄⁺ concentrations (Figure 20). For the secondary nitrate factor, the only significant trends were decreases in the median concentrations in overall and in fall. Concentrations attributed to the vehicle factor did not change significantly. Few of the smaller factors at Chicago had statistically significant trends other than the median biomass contribution, which grew by 8.9%/yr due to large increases in spring and fall seasons.

III.2.5 Fractional apportionment trends

A key result of this analysis is to show that PM_{2.5} contributions from different sources have been evolving at different rates. In both cities, secondary sulfate decreased faster than both the total PM_{2.5} concentration and contributions of other factors identified by PMF, thus the relative

significance of non-sulfate source factors increased over time. This is shown for Detroit in Figure 24, which ranks the PMF source factors from left to right by the magnitude of their annual and seasonal trends measured as the annual change (%/yr) over the study period in the fraction (%) of total PM_{2.5} contributed by the factor, i.e., the relative contribution of that factor. (This differs from Figure 22, which shows trends measured as the annual change (%/yr) over the study period in the concentration (µg/m³) contributed by the source factor, i.e., the absolute contribution.) Figure 24 reveals the changing nature of apportionments in Detroit over the 2001 to 2014 period: secondary sulfate contributions decreased in all seasons and at most percentiles (except winter 90th percentile); secondary nitrate decreased except in winter (the 90th percentile summer change was not significant); crustal sources were largely unchanged; vehicle contributions increased significantly in spring and fall; and both biomass and metals factors increased, by over 10 %/yr in several cases. In summary, over the 2001 to 2014 period, the major PM_{2.5} contributors in Detroit have been shifting away from coal-fired facilities producing secondary sulfate and nitrate, while contributions from biomass sources have been increasing in both relative (fraction of PM_{2.5}) and absolute (concentration) terms. In addition, given that vehicle and biomass sources have been constant or just slightly declining while PM_{2.5} levels have been declining faster, these sources also are becoming an increasing fraction of PM_{2.5}. Detroit contains two large steel mills and numerous metals processing facilities, and an examination of PM_{2.5} emissions from the steel facilities shows large decreases over the study period. Trends in biomass sources are difficult to assess given changes in classification (SCC codes are used in 2002 and 2005, while EI sectors are used in 2008 and 2011) and underlying methodology (e.g., residential wood combustion dropped from 1649 tons in 2008 to 551 tons in 2011, while PM_{2.5} from industrial biomass combustion is not listed in 2008 but is 191 tons in 2011).

Changes in the relative contributions of the ranked PMF source factors to the total PM_{2.5} in Chicago are shown in Figure 25. As was the general trend in Detroit, secondary sulfate declined in every season and both percentiles. Few other factors in the PMF model had significant changes: the secondary nitrate factor declined in fall at the median; the vehicle factor slightly increased (median and 90th percentile overall, and 90th percentile in winter and summer); and upward trends for metals and biomass sources occurred overall or in a few seasons (as in Detroit). In summary, over the period from 2006 to 2014, Chicago experienced large decreases in secondary sulfate, while contributions from vehicles, biomass and metal sources increased their share of PM_{2.5}. Biomass-

related PM_{2.5} increased in both absolute ($\mu\text{g}/\text{m}^3$) and relative (fraction of PM_{2.5}) terms. (In Detroit, biomass increased in only relative terms.) This key result of the present work, that impacts of some sources decrease – and in some cases, increase – faster than other sources, is important in targeting sources for further investigation and regulation.

III.2.6 Vehicle apportionments and comparison to previous work

Many of the apportionment results described previously follow trends suggested by the emissions inventory and concentration data, and they also resemble previous apportionments in both cities conducted over the past 35 years. Here we examine those previous studies, focusing on vehicle apportionments given their significance as local emission sources in both cities.

In Detroit, using data from June through August of 1981 and a six source principal components model, vehicles accounted for 20% of the variability of PM_{2.5} [28]. Vehicles accounted for 10 to 25% of PM_{2.5} in a six factor PMF model using summer and early autumn data from 2000 to 2003 [29]. Using 2000 to 2005 data and a nine factor model, 21% of PM_{2.5} in Detroit was attributed to vehicles [175]. Using the same data in an eight factor PMF model, gasoline and diesel vehicle contributions were separated with 15% and 4% apportioned, respectively [34]. That analysis did not include Ni or Cr, which may have affected the EC distribution between factors and changed results for diesel, and a lack of seasonality in the gasoline and vehicle factors was noted, contrary to the present findings (which used some of the same data). A recent analysis of 1999 to 2002 data attributed 22% of PM_{2.5} to OC combustion sources and 15% to EC combustion sources in southwest Detroit, however, NO₃⁻ was not measured, potentially increasing the mass assigned to these factors [36]. Using August 2004 and July and August 2005 data, 29% and 8% of PM_{2.5} was assigned to gasoline and diesel sources, and 31% to a combined gasoline and diesel fleet [30]. A recent Detroit area study, using 2004 to 2006 Allen Park data in a seven factor PMF model, attributed 22% of PM_{2.5} to gasoline and diesel sources [33]. Using 2007 data from nearby Dearborn, Michigan, in an analysis incorporating wind direction, approximately 10% of PM_{2.5} was apportioned to vehicles (diesel plus gasoline) [176]. Other apportionments cited in Michigan's PM_{2.5} 2008 State Implementation Plan [177] showed vehicle apportionments comparable to the present work. Differences in samplers, species selected, length and seasons of the monitoring data used, and choices made in PMF modeling can diminish the comparability of these studies. Still,

vehicle contributions in these earlier studies mostly ranged from 15 to 30% of $PM_{2.5}$, commensurate with the apportionments in the present analysis.

Several source apportionments have been performed in Chicago. Again, we focus on the vehicle component. In Northbrook IL (close to Chicago), using data from January, 2003 to March, 2005, 14% of $PM_{2.5}$ was apportioned to gasoline sources and 13% to diesel [31]. The diesel profile included Al and Pb, elements assigned to other factors in the present study. Using 2001 to 2003 data at two CSN sites (Lawndale and Springfield, IL), 23% of $PM_{2.5}$ was apportioned to a combined vehicle profile [115]. That apportionment included both SO_4^- and SO_2 (26), as well as both ionic and molecular forms of Na, Na^+ , K and K^+ . Despite these and other differences, the fraction of $PM_{2.5}$ attributed to gasoline and diesel vehicles in Chicago studies compare favorably to our estimates.

Vehicle apportionment trends have been studied elsewhere in the U.S. In Los Angeles and Rubidoux, CA, a recent analysis using 2002 to 2013 STN data apportioned 20% of $PM_{2.5}$ to vehicles, and median $PM_{2.5}$ concentrations attributed to vehicles fell 21 to 24% between the first and last 4 year blocks of the study period [37]. Vehicle-related $PM_{2.5}$ decreased while traffic volume was stable, suggesting the success of recent vehicle emissions controls. Like the present work, that study shows the relevance of receptor modeling apportionments for air quality management, as well as the evolution of source contributions to total $PM_{2.5}$. In contrast, we show that the share of $PM_{2.5}$ contributed by vehicles, biomass and other local emissions is stable or growing, and that trends depend on the city, percentile, and sometimes season.

III.2.7 Limitations

Limitations of the analysis are recognized. Emission inventory data at the county level may not reflect the impact at monitoring sites, which can be affected by small but nearby sources, as well as large but distant sources (including sources outside county and country borders). A number of issues with the accuracy and consistency of the emissions inventory data were highlighted, e.g., fugitive dust emissions estimates are highly uncertain. The monitoring record is limited in both the duration and the number of sites available. Only two cities, and a single site in each, were examined. (Previous work has shown spatial trends in several $PM_{2.5}$ species [101]). However, the selected non-source and population-oriented monitoring sites should be reasonably representative. As noted, monitoring data near strong sources would be expected to show different trends for some

PM_{2.5} constituents as well as different apportionments, however, secondary sulfate, secondary nitrate, and potentially the vehicle contribution might not change greatly since these pollutants are widely distributed. The EC and OC instrument switch complicated the investigation of trends, particularly for mobile sources given the importance of these tracers. Still, most results follow national trends, and thus results appear broadly applicable to many U.S. cities.

The PMF analyses have additional limitations. First, results can be sensitive to the number of factors, species selected, and the data subset used. In sensitivity analyses, separate PMF models for individual four year blocks obtained average apportionments that were similar to those using the final model (across all years), but some trends were difficult to compare because factors varied across models. (Still, separate PMF models used for periods before and after the EC/OC instrument switch returned similar vehicle apportionments in models using different number of factors.) For these reasons, the current analysis used a single dataset that encompassing the entire study period. Second, trend analyses of PMF results can be sensitive to the model selected. The stability of PMF results was investigated using 200 bootstrapped runs for each factor. In over 180 of 200 bootstrap runs at each city, the same factors emerged that are presented in these results. (Additional bootstrap results are presented in Table 17 and Table 18) Third, PMF apportionments may not uniquely identify or completely characterize source classes, e.g., many factors might contribute to secondary sulfate trends. Similarly, unspecified minor sources and secondary pollutants can contribute to factors. Fourth, data screening can affect results, particularly for species near the DL. Fifth, PMF trend analyses may incorporate some biases because observations were removed by the reconstructed mass criterion. However, only 7% of sampling days at Detroit, and 6% at Chicago, were removed. Sixth, we did not apply conditional probability functions (CPF), which might provide additional qualitative information regarding the strength of local sources that complements the PMF results [178]. Finally, the QR results do not account for the uncertainty of the PMF results, and thus determinations of statistical significance are approximate.

The chapter's key finding that, in both cities, the mobile source, biomass, and metal source contributions to PM_{2.5} have increased even as overall PM_{2.5} concentrations have declined, has significant implications for air quality management. It emphasizes the need to investigate these sources in policies and regulations aimed at maintaining or decreasing PM_{2.5} concentrations.

III.3 Tables

Table 15. Summary of emissions inventory data in Detroit and Chicago. Expressed as short tons/yr of PM_{2.5} primary (filterable + condensable) and % of total PM_{2.5}. Derived from NEI.

Year	Point	On-Road Mobile			Non-Road Mobile		Non-Point Sources			Total
	Sources	Diesel Ex. ¹	Gas Ex. ²	Other	Diesel Ex. ¹	Other	Construction ³	Paved Road ⁴	Other ⁵	
Detroit										
2002	5364 (59%)	724 (8%)	245 (3%)	156 (2%)	567 (6%)	288 (3%)	14 (0%)	136 (2%)	1532 (17%)	9026
2005	4402 (57%)	589 (8%)	164 (2%)	163 (2%)	547 (7%)	155 (2%)	14 (0%)	136 (2%)	1550 (20%)	7720
2008	2345 (22%)	1380 (13%)	521 (5%)	209 (2%)	378 (4%)	140 (1%)	350 (3%)	627 (6%)	4805 (45%)	10754
2011	1610 (23%)	725 (10%)	335 (5%)	128 (2%)	350 (5%)	143 (2%)	18 (0%)	573 (8%)	3194 (45%)	7076
Chicago										
2002	2394 (21%)	1191 (10%)	305 (3%)	285 (3%)	2277 (20%)	503 (4%)	72 (1%)	176 (2%)	4154 (37%)	11357
2005	3591 (30%)	965 (8%)	254 (2%)	299 (2%)	2125 (17%)	497 (4%)	72 (1%)	176 (1%)	4169 (34%)	12147
2008	2510 (11%)	2025 (9%)	795 (4%)	383 (2%)	1085 (5%)	494 (2%)	5743 (26%)	917 (4%)	8496 (38%)	22448
2011	2451 (12%)	1297 (6%)	565 (3%)	301 (1%)	1006 (5%)	492 (2%)	6351 (31%)	1181 (6%)	6595 (33%)	20239

¹ Diesel Ex. = diesel exhaust; ² Gas Ex. = gasoline exhaust; ³ Construction = construction dust for the county; ⁴ Paved Road = paved road dust for the county ⁵ In NEI 2002 and 2005, mobile emissions are not included in non-point emissions, while in NEI 2008 and 2011, mobile emissions are included in non-point emissions. In this table, “Other” non-point sources do not include mobile emissions.

Table 16. Median and 90th percentile concentrations by year-block and statistical differences between year-block concentrations. Differences based on Kruskal-Wallis (comparing 3+ groups) or Mann-Whitney (comparing 2 groups) tests, and $\alpha = 0.05$, with at least 10 valid observations per group.

Species	All					Winter					Spring					Summer					Fall					
	2001	2002	2006	2010	2013	2001	2002	2006	2010	2013	2001	2002	2006	2010	2013	2001	2002	2006	2010	2013	2001	2002	2006	2010	2013	
	2002	2005	2009	2013	2015	2002	2005	2009	2013	2015	2002	2005	2009	2013	2015	2002	2005	2009	2013	2015	2002	2005	2009	2013	2015	
Detroit																										
PM _{2.5}	50 th	13.0	12.7	10.9	8.9	10.6	20.8	12.9	13.2	9.8	13.1	14.2	11.9	8.5	7.8	8.3	13.2	14.7	11.2	11.2	10.9	10.5	11.1	9.8	7.8	11.4
	90 th	32.4	26.8	23.4	18.2	17.5	38.0	26.8	24.7	19.9	21.6	27.0	24.2	21.1	15.7	13.6	35.4	30.2	22.7	19.3	15.5	25.1	28.2	23.8	16.8	17.4
NH ₄ ⁺	50 th	1.42	1.66	1.29	0.76	0.94	2.22	1.78	2.05	1.15	1.05	1.56	1.76	1.13	0.76	0.98	1.43	1.53	1.08	0.67	0.65	0.74	1.36	1.09	0.54	0.49
	90 th	5.16	4.35	3.70	2.31	2.57	5.84	4.14	3.93	3.12	3.02	3.94	4.33	3.49	1.88	2.19	5.98	4.26	3.06	1.79	1.78	3.81	4.79	3.80	1.77	1.86
NO ₃ ⁻	50 th	1.59	2.01	1.44	1.07	1.69	4.40	3.57	3.65	2.59	3.08	2.29	2.71	1.49	1.09	1.98	1.31	0.91	0.65	0.55	0.59	1.15	1.86	1.27	0.97	0.95
	90 th	8.17	6.67	5.98	4.12	6.35	13.7	9.32	8.08	6.69	7.17	8.40	6.86	5.65	3.32	4.36	3.97	3.19	1.96	1.48	1.53	4.48	5.75	4.49	3.20	3.73
SO ₄ ⁼	50 th	3.02	2.73	2.36	1.56	1.57	3.09	2.16	2.55	1.47	1.52	2.68	2.94	2.19	1.64	1.53	3.33	4.13	2.84	2.22	2.40	2.28	2.43	1.93	1.28	1.42
	90 th	9.82	8.27	5.59	4.02	3.13	8.10	4.44	4.06	3.28	3.07	7.49	6.22	5.24	3.27	3.02	15.6	11.0	7.46	5.52	4.36	7.94	9.87	5.89	3.37	3.02
S	50 th	0.99	0.91	0.78	0.56	0.56	1.04	0.71	0.81	0.50	0.56	0.85	0.95	0.73	0.56	0.54	1.03	1.39	0.96	0.85	0.83	0.85	0.78	0.68	0.45	0.49
	90 th	3.20	2.64	1.83	1.42	1.16	2.49	1.52	1.34	1.19	1.06	2.27	2.11	1.68	1.12	1.14	4.83	3.67	2.47	2.01	1.61	2.69	3.25	2.05	1.24	1.16
EC _{MetOne}	50 th	0.59	0.66	0.65	0.63	—	0.54	0.58	0.56	0.62	—	0.43	0.54	0.48	0.91	—	0.76	0.80	0.72	—	—	0.67	0.77	0.79	0.40	—
	90 th	1.05	1.25	1.26	1.49	—	1.02	1.02	0.90	1.43	—	0.82	0.96	0.99	1.70	—	1.06	1.37	1.24	—	—	1.03	1.46	1.59	0.40	—
EC _{URG3k}	50 th	—	—	0.32	0.38	0.33	—	—	—	0.30	0.32	—	—	0.25	0.33	0.29	—	—	0.37	0.45	0.43	—	—	0.42	0.45	0.38
	90 th	—	—	0.84	0.73	0.67	—	—	—	0.55	0.58	—	—	0.56	0.63	0.51	—	—	0.68	0.81	0.73	—	—	0.94	0.85	0.94
OC _{MetOne}	50 th	2.87	2.81	2.11	1.19	—	3.63	2.48	1.84	1.17	—	2.62	2.55	1.82	2.24	—	3.69	3.76	3.13	—	—	2.63	2.58	1.77	1.17	—
	90 th	5.93	5.63	4.86	3.18	—	7.63	5.19	4.82	2.82	—	4.76	4.30	3.98	4.61	—	6.13	6.71	5.15	—	—	5.73	4.98	4.77	1.17	—
OC _{URG3k}	50 th	—	—	1.76	1.85	1.83	—	—	—	1.62	1.73	—	—	1.41	1.49	1.62	—	—	1.95	2.34	2.23	—	—	1.99	1.79	1.87
	90 th	—	—	3.76	3.42	3.53	—	—	—	3.06	3.48	—	—	2.34	2.89	2.98	—	—	3.21	4.04	3.50	—	—	4.58	3.40	4.52
Chicago																										
PM _{2.5}	50 th	—	—	10.9	9.4	9.7	—	—	12.7	9.8	10.7	—	—	10.2	9.5	8.55	—	—	10.7	10.6	9.85	—	—	10	7.7	9.45
	90 th	—	—	22.3	18	19.3	—	—	21.9	19.9	23.3	—	—	21.3	18.2	18.9	—	—	24.4	16.7	16	—	—	21.9	17.2	14.4
NH ₄ ⁺	50 th	—	—	1.40	0.79	0.95	—	—	2.02	1.11	1.36	—	—	1.27	0.94	1.04	—	—	1.11	0.62	0.57	—	—	1.19	0.55	0.66
	90 th	—	—	3.70	2.39	2.79	—	—	4.15	3.28	3.15	—	—	3.44	2.48	2.86	—	—	3.08	1.59	1.69	—	—	3.53	1.92	1.74
NO ₃ ⁻	50 th	—	—	1.62	1.14	2.00	—	—	4.19	2.75	3.60	—	—	1.82	1.58	2.47	—	—	0.69	0.60	0.68	—	—	1.43	0.81	1.18
	90 th	—	—	6.46	5.14	7.14	—	—	8.60	8.11	8.47	—	—	5.68	4.15	7.33	—	—	2.35	1.37	3.24	—	—	6.18	3.50	3.94
SO ₄ ⁼	50 th	—	—	2.12	1.60	1.48	—	—	2.38	1.44	1.38	—	—	2.02	1.69	1.56	—	—	2.51	1.77	1.76	—	—	1.92	1.25	1.25
	90 th	—	—	5.51	3.72	3.30	—	—	3.85	3.42	2.75	—	—	4.56	3.78	3.30	—	—	7.73	4.82	3.73	—	—	5.97	3.22	3.02
S	50 th	—	—	0.72	0.57	0.51	—	—	0.80	0.50	0.51	—	—	0.67	0.58	0.57	—	—	0.86	0.72	0.67	—	—	0.66	0.47	0.45
	90 th	—	—	1.83	1.35	1.16	—	—	1.33	1.12	0.97	—	—	1.55	1.25	1.16	—	—	2.62	1.64	1.37	—	—	1.96	1.19	1.04
EC _{MetOne}	50 th	—	—	0.62	0.82	—	—	—	0.54	0.71	—	—	—	0.61	0.88	—	—	—	0.66	—	—	—	—	0.66	—	—
	90 th	—	—	1.25	1.36	—	—	—	0.95	1.15	—	—	—	1.30	1.44	—	—	—	1.40	—	—	—	—	1.16	—	—

EC _{URG3k}	50 th	—	—	0.42	0.36	0.34	†	—	—	0.33	0.29	0.33	◦	—	—	0.35	0.36	0.31	—	—	0.45	0.43	0.46	◦	—	—	0.46	0.38	0.36	†	
	90 th	—	—	0.84	0.76	0.66	†	—	—	0.61	0.55	0.53	◦	—	—	0.70	0.77	0.61	◦	—	—	0.88	0.83	0.69	◦	—	—	1.02	0.76	0.80	†
OC _{MetOne}	50 th	—	—	2.65	2.21	—	†	—	—	1.94	1.70	—	◦	—	—	2.59	2.31	—	◦	—	—	3.60	—	—	—	—	—	2.40	—	—	—
	90 th	—	—	4.71	4.21	—	†	—	—	3.74	4.10	—	◦	—	—	4.06	4.40	—	◦	—	—	6.09	—	—	—	—	—	3.98	—	—	—
OC _{URG3k}	50 th	—	—	2.15	1.93	1.94	†	—	—	2.17	1.69	1.70	†	—	—	1.70	1.82	1.73	◦	—	—	2.33	2.40	2.33	◦	—	—	2.19	1.87	2.04	◦
	90 th	—	—	3.89	3.59	3.17	†	—	—	3.26	2.87	2.98	†	—	—	3.64	3.44	2.89	◦	—	—	4.02	3.94	3.89	◦	—	—	4.41	3.64	3.23	◦

† Reject the null hypothesis

◦ Do not reject the null hypothesis

^a The Met One SASS sampler was used until 3/30/10 at Detroit and 4/29/10 at Chicago

^b The URG 3000N sampler was used starting 4/1/09 at Detroit and 5/3/07 at Chicago

Table 17. Bootstrapped % of species mass at Detroit (200 bootstrapped runs, block size = 220, total samples = 1433)

Factor	Species	Base%	Bootstrap Range				
			5th	25th	50th	75th	95th
Sulfate	PM _{2.5}	33.4	29.9	32.3	34.1	36.8	36.8
	NH ₄ ⁺	50.4	46.4	49.5	50.8	54.8	54.8
	SO ₄ ⁼	76.5	69.6	73.6	76.1	80.9	80.9
Cl	PM _{2.5}	2.1	1.3	1.6	1.9	3.6	3.6
	Cl	86.7	65.8	82.1	85.1	92.2	92.2
Cu	PM _{2.5}	3.5	2.1	2.7	3.3	5.6	5.6
	Cu	81.6	78.4	81.3	83.0	93.3	93.3
Vehicles	PM _{2.5}	20.8	8.3	13.2	16.6	24.7	24.7
	EC	79.3	18.0	59.0	68.0	86.4	86.4
	OC	53.2	18.6	31.9	41.1	72.6	72.6
Nitrate	PM _{2.5}	20.8	19.1	20.4	21.2	23.7	23.7
	NH ₄ ⁺	37.9	35.7	37.2	38.5	43.8	43.8
	NO ₃ ⁻	84.2	77.8	80.5	82.1	85.3	85.3
Biomass	PM _{2.5}	7.1	3.8	6.5	10.5	16.1	16.1
	K ⁺	79.3	59.8	79.6	86.9	96.3	96.3
	Na ⁺	59.5	0.0	0.0	34.6	65.3	65.3
Metals	PM _{2.5}	5.4	3.5	4.5	5.6	11.1	11.1
	Cr	86.9	60.8	79.9	87.3	100.0	100.0
	Fe	36.9	25.5	33.3	39.0	52.7	52.7
	Mn	24.6	16.0	20.4	25.5	42.5	42.5
	Ni	67.0	44.6	58.8	66.7	76.7	76.7
Crustal	PM _{2.5}	3.9	2.8	3.6	4.2	7.2	7.2
	Al	53.9	47.3	53.4	56.4	61.6	61.6
	Ca	61.0	36.8	53.2	63.2	70.1	70.1
	Si	71.9	63.9	67.1	70.5	78.4	78.4
	Ti	34.3	27.4	31.2	33.4	44.2	44.2
Zn	PM _{2.5}	2.9	0.7	1.3	2.8	5.0	5.0
	Zn	72.4	66.0	69.9	72.4	76.6	76.6

Table 18. Bootstrapped % of species mass at Chicago (200 bootstrapped runs, block size = 50, total samples = 763)

Factor	Species	Base%	Bootstrap Range				
			5th	25th	50th	75th	95th
Sulfate	PM _{2.5}	31.9	28.7	30.5	32.1	35.2	35.2
	NH ₄ ⁺	47.3	41.5	44.7	46.8	51.4	51.4
	SO ₄ ⁻	77.3	68.5	72.7	75.6	83.0	83.0
NaCl	PM _{2.5}	5.0	2.3	3.2	5.1	9.6	9.6
	Cl	65.1	36.2	65.6	86.1	100.0	100.0
	Na ⁺	76.1	0.0	6.6	17.8	89.0	89.0
Vehicles	PM _{2.5}	22.2	16.7	19.0	21.2	26.0	26.0
	EC	75.7	60.2	68.1	71.3	76.3	76.3
	OC	61.2	47.4	55.7	58.0	62.3	62.3
Nitrate	PM _{2.5}	21.0	16.2	18.6	20.2	24.3	24.3
	NH ₄ ⁺	45.8	35.9	41.6	44.0	52.3	52.3
	NO ₃ ⁻	77.5	73.7	76.1	78.1	84.3	84.3
Biomass	PM _{2.5}	8.9	5.4	7.1	8.6	12.1	12.1
	K ⁺	95.3	61.4	71.1	78.4	99.6	99.6
Metals	PM _{2.5}	2.8	1.4	2.5	3.2	6.2	6.2
	Cr	29.7	10.2	18.5	25.2	50.8	50.8
	Fe	63.8	50.7	54.6	58.4	69.9	69.9
	Mn	48.8	37.7	42.6	45.1	55.1	55.1
	Ni	26.9	5.0	14.3	22.5	50.1	50.1
Crustal	PM _{2.5}	7.5	4.2	5.7	6.8	9.4	9.4
	Al	62.5	18.6	54.9	60.4	71.8	71.8
	Ca	83.6	18.4	72.0	79.2	86.4	86.4
	Si	74.4	18.0	65.9	71.4	79.9	79.9
Zn	PM _{2.5}	0.7	0.2	0.9	1.6	3.9	3.9
	Zn	76.5	65.2	72.3	75.5	82.4	82.4

III.4 Figures

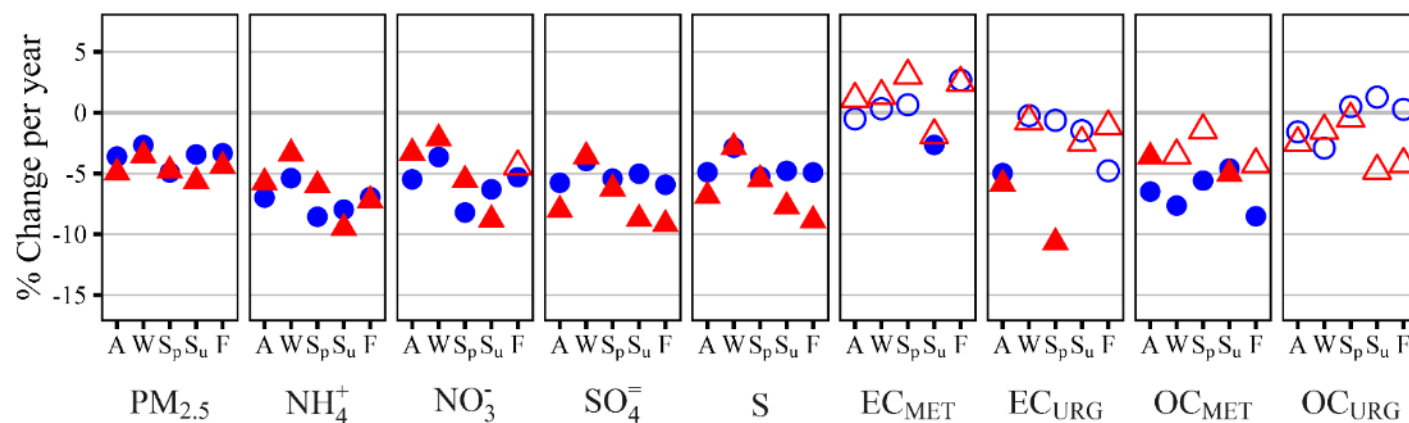


Figure 19. Annual and seasonal concentration trends in Detroit from 2001 to 2015. Shows annual changes in median concentrations as blue circles (●, ○) and in 90th percentile concentrations as red triangles (▲, △) for selected major species, expressed as %/yr for all seasons (A), winter (W), spring (S_p), summer (S_u) and fall (F). Based on quantile regressions of ambient measurements. Filled symbols (e.g., ●) are statistically significant, i.e., trend exceeded 2-times its bootstrapped standard error.

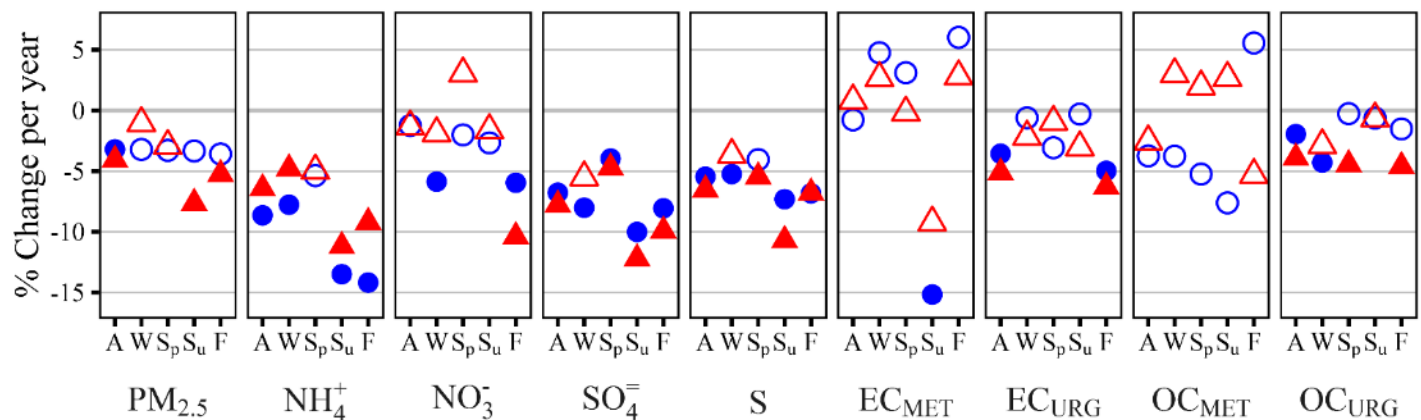


Figure 20. Annual and seasonal concentration trends in Chicago for median and 90th percentile concentrations from 2006 to 2014. Shows annual changes in median concentrations as blue circles (●, ○) and in 90th percentile concentrations as red triangles (▲, △) for selected major species, expressed as %/yr for all seasons (A), winter (W), spring (Sp), summer (Su) and fall (F). Based on quantile regressions of ambient measurements. Filled symbols (e.g., ●) are statistically significant, i.e., trend exceeded 2-times its bootstrapped standard error.

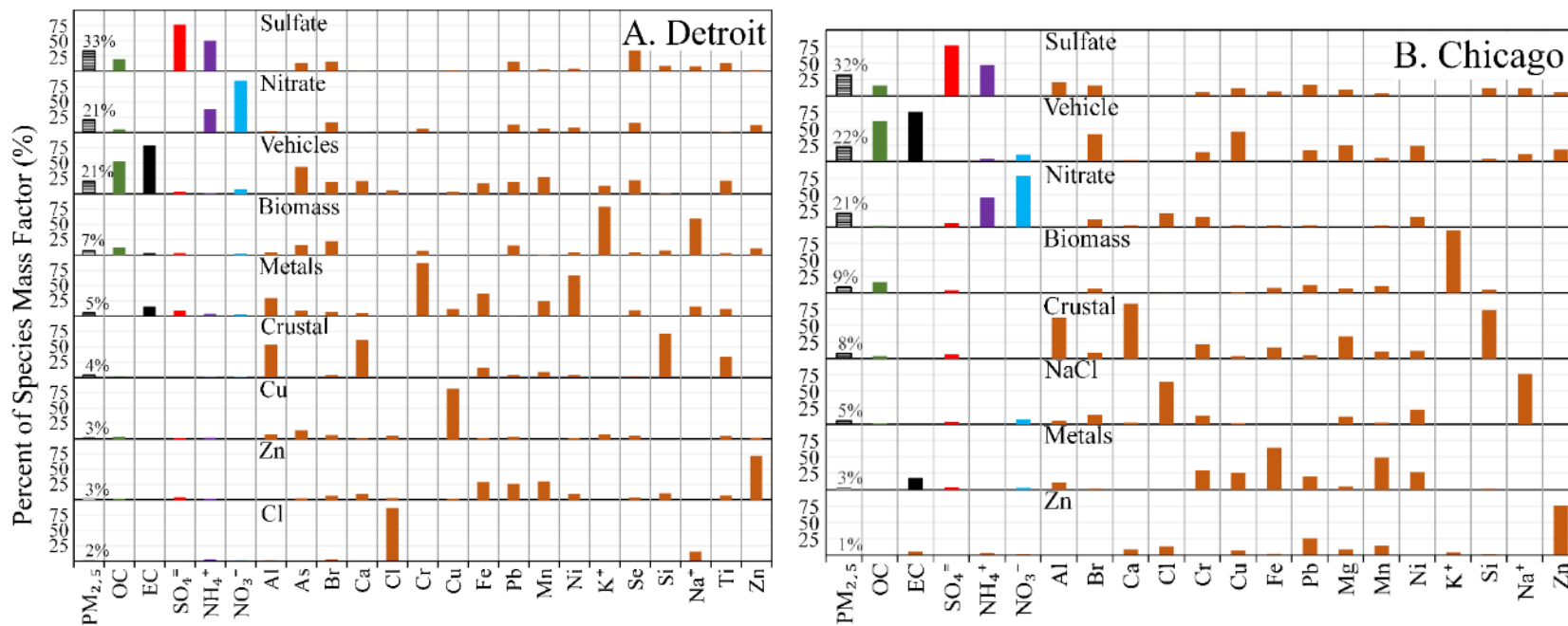


Figure 21. Distribution of species by factor in PMF models for Detroit (A) and Chicago (B). Overall percentage contribution to modeled $PM_{2.5}$ is listed for each factor.

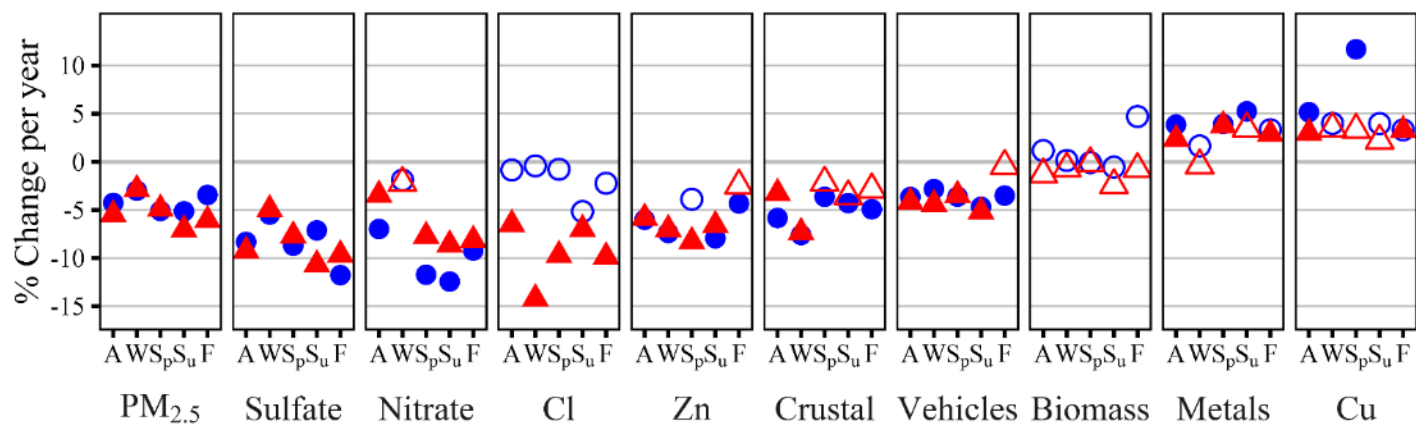


Figure 22. Annual and seasonal trends of PMF apportionments by source category in Detroit from 2001 to 2014. Shows changes in median concentrations as blue circles (●, ○) and 90th percentile concentrations as red triangles (▲, △), expressed as %/yr for all seasons (A), winter (W), spring (S_p), summer (S_u), and fall (F). Based on quantile regressions of estimated concentration apportionments from nine factor PMF model. Filled symbols (e.g., ●) are statistically significant, i.e., trend exceeded 2-times its bootstrapped standard error. Values below 0 not censored.

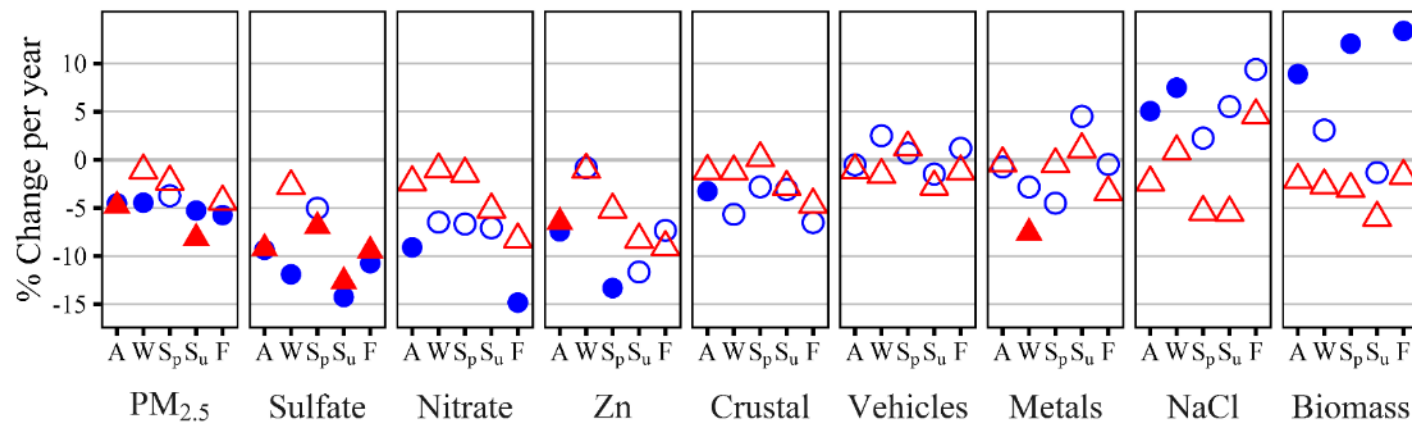


Figure 23. Annual and seasonal trends of PMF apportionments by source category in Chicago from 2006 to 2014 using an 8-factor model. Shows changes in median concentrations as blue circles (●, ○) and 90th percentile concentrations as red triangles (▲, △), expressed as %/yr for all seasons (A), winter (W), spring (S_p), summer (S_u), and fall (F). Based on quantile regressions of estimated concentration apportionments from nine factor PMF model. Filled symbols (e.g., ●) are statistically significant, i.e., trend exceeded 2-times its bootstrapped standard error. Values below 0 not censored.

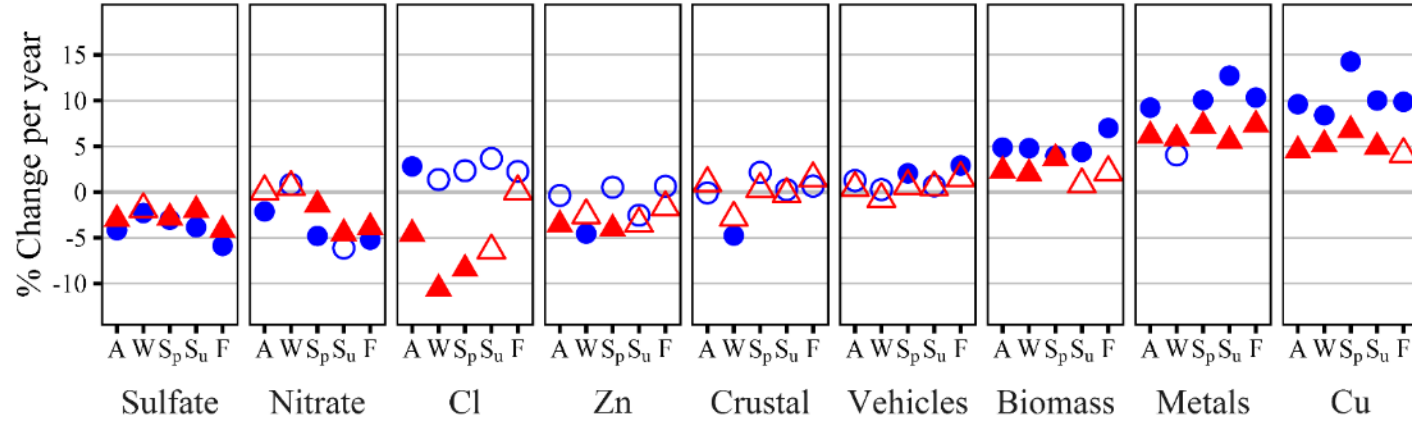


Figure 24. Annual and seasonal trends of fractional PMF apportionments by source category in Detroit from 2001 to 2014. Shows changes in median fractional apportionments as blue circles (●, ○) and 90th percentile fractional apportionments as red triangles (▲, △), expressed as %/yr for all seasons (A), winter (W), spring (S_p), summer (S_u), and fall (F). Based quantile regressions of fractional apportionments (% of total PM_{2.5} mass) from a nine factor PMF model. Filled symbols (e.g., ●) are statistically significant, i.e., trend exceeded 2-times its bootstrapped standard error. Values below 0 not censored.

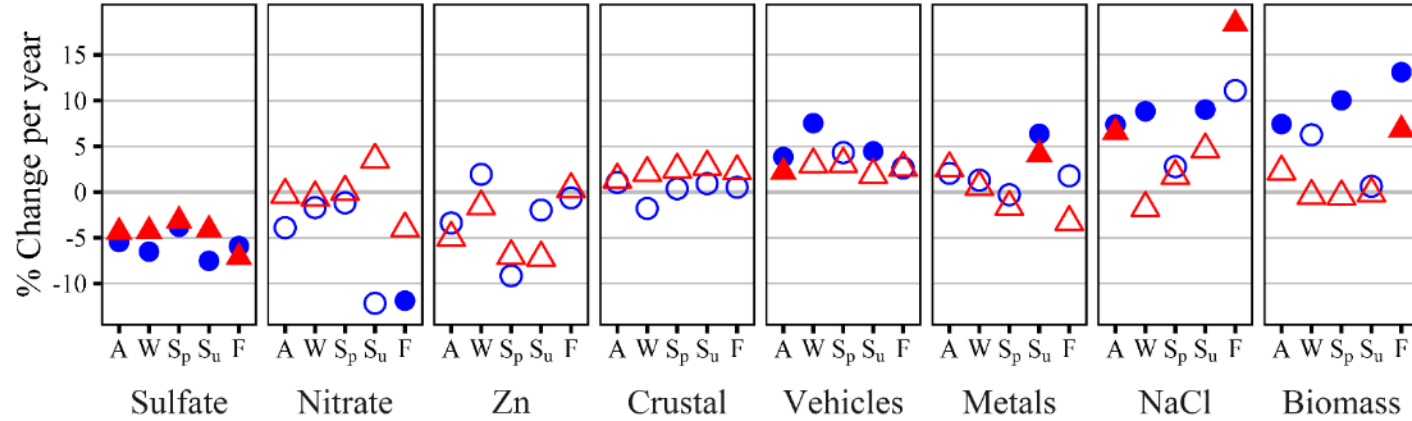


Figure 25. Annual and seasonal trends of fractional PMF apportionments by source category in Chicago from 2006 to 2014 using an 8-factor model. Shows changes in median fractional apportionments as blue circles (\bullet , \circ) and 90th percentile fractional apportionments as red triangles (\blacktriangle , \triangle), expressed as %/yr for all seasons (A), winter (W), spring (S_p), summer (S_u), and fall (F). Based quantile regressions of fractional apportionments (% of total $PM_{2.5}$ mass) from a nine factor PMF model. Filled symbols (e.g., \bullet) are statistically significant, i.e., trend exceeded 2-times its bootstrapped standard error. Values below 0 not censored.

Chapter IV – Operational evaluation of the RLINE dispersion model for studies of traffic-related air pollutants

IV.1 Summary

This chapter describes an operational evaluation of a combined modeling system using RLINE and AERMOD [40] dispersion models and point source emissions models. The evaluation focuses on daily exposure measures and the traffic-related portion modeled by RLINE, in an application relevant to many epidemiologic and health impact studies. We utilize routine observations of pollutant concentrations, emissions, meteorology and other variables with the goal of characterizing prediction uncertainties and limitations of models for particular applications, and include statistical and graphical analyses to determine whether model estimates agree with observations in an overall sense [179]. Here, daily average concentrations of nitrogen oxides (NO_x), carbon monoxide (CO), and fine particulate matter (PM_{2.5}) measured at sites across Detroit, MI for the 2011 to 2014 period are compared to predictions from RLINE and AERMOD dispersion models, for line and point sources respectively. Performance is evaluated by pollutant, site, wind speed, meteorological condition, averaging time and other factors. We discuss implications regarding the use of RLINE in epidemiologic studies. For CO and NO_x, model performance was best at sites close to major roads, during downwind conditions, during weekdays, and during certain seasons. For PM_{2.5}, the ability to discern local and particularly the traffic-related portion was limited, a result of high background levels, the sparseness of the monitoring network, and large uncertainties for certain processes (e.g., formation of secondary aerosols) and non-mobile sources (e.g., area, fugitive). Overall, RLINE's performance in near-road environments suggests its usefulness for estimating spatially- and temporally-resolved exposures.

IV.2 Results

IV.2.1 Background and un-modeled contribution

For NO_x, most hourly measurements exceeded DLs (51 to 100%, depending on site), and background estimates generated fell into a narrow range (15 to 18 ppb; Table 20). For CO,

observations frequently fell below the DL for the less sensitive instruments (IGFC and INDiI), which yielded relatively high background estimates (averaging 519 to 671 ppb); background levels were lower (128 ppb) for the more sensitive instrument (EC9830T). Because the background estimates reflected the instrument's DL, datasets were not pooled across sites or instruments. For PM_{2.5}, background estimates averaged 8.8 $\mu\text{g m}^{-3}$ at the schools and suburban sites, equal to 88 to 92% of observed levels (9.5 and 10 $\mu\text{g m}^{-3}$, respectively; Table 21), and day-to-day variability was significant. Predicted contributions from point and on-road mobile sources were small (averaging from 0.1 to 0.8 $\mu\text{g m}^{-3}$), and including these sources in daily background estimates did not increase the correlation between observed and estimated background levels. Thus, the performance evaluation for PM_{2.5} was not considered informative, a function of the dominance of regional sources and the small signal remaining from local sources, the gaps and uncertainties of the PM_{2.5} emission inventory, the absence of chemical transformations in RLINE, and the paucity of near-road PM_{2.5} monitoring data.

IV.2.2 Performance by site

For NO_x, daily mean predictions (20 to 38 ppb) were similar to observations (23 to 48 ppb; Table 20). Performance tended to decrease with distance from the roadway, e.g., R_{SP} was from 0.58 to 0.74 at the near-road site (10 m from I-96), 0.57 to 0.58 at the urban site (100 m from I-96), and 0.32 at the schools site (350 m from MI-97). The near-road site using the IGpCHEM monitor had the highest R_{SP}, the lowest % reducible V_G, and the highest mean model-to-background ratio. (Figure 26 shows correlations for various subsets of NO_x and CO at the near-road site.) However, this case had the highest FB, mainly because the IGpCHEM measurements (average of 48 ppb) exceeded the ICHEM measurements (37 ppb), while predictions during these periods were similar (38 and 37 ppb, respectively). Performance at other sites varied: the schools site was under-predicted; the suburban, urban and industrial sites were over-predicted; and reducible errors at all four sites exceeded systematic errors, suggesting that improvements in model inputs or parameterization could improve model performance. (Additional results are shown in Appendix A: Table A. 1 and Table A. 2, and graphically in Figure A. 1, Figure A. 2, Figure A. 3, and Figure A. 4.)

For CO, daily predictions (180 to 320 ppb) generally fell below observed levels (479 to 673 ppb). As seen for NO_x, performance tended to decrease with distance from the roadway, e.g., R_{SP} was

0.45 to 0.89 at the near-road site, 0.17 at the urban site, and 0.21 at the suburban site. Despite its proximity to I-75 (150 m), the industrial site had R_{SP} near zero, possibly a result of that monitor's high DL that falsely elevated the background estimates. (The estimated background averaged 91% of measurements.) This site was also adjacent to active rail lines and large industrial emission sources. Ranks of mean predictions followed observations except for the suburban and near-road EC9830T samplers; at the suburban site, predictions fell below observations, probably because this site was far from known CO sources, and lower observations were recorded at the near-road EC9830T sampler (reflecting the lower DL of the EC9830T instrument), which influenced background estimates at this site. As for NO_x , the near-road site (with the EC9830T instrument) had the highest R_{SP} and again, this case had the lowest ratio of reducible to overall V_G , the highest mean model-to-background ratio, but the highest FB. Patterns at the other sites were similar to those seen for NO_x : daily averages at the schools site were under-predicted; suburban, urban and industrial sites were over-predicted; and reducible errors exceeded systematic errors.

IV.2.3 Performance by wind direction

For NO_x , downwind conditions gave higher F2 (except for one case) and higher R_{SP} (0.30 to 0.64) than parallel conditions (Table 22). The exception was the near-road site using the ICHEM monitor, but both downwind and parallel winds had high F2 ($\geq 90\%$) and large and reducible errors ($V_G \geq 1.16$, % reducible $\geq 99\%$), indicating the potential to improve model parameterization. Other performance metrics gave mixed results, e.g., at the urban site during downwind periods, FB was slightly lower, V_G was unchanged, and the % reducible error was lower (mainly with the ICHEM monitor). Despite some inconsistencies, the F2 and R_{SP} metrics results indicated better performance during downwind as compared to parallel wind conditions.

Performance for CO also was generally better during downwind periods, albeit less conclusively than for NO_x . F2 exceeded 92% at all sites. The near-road and urban sites had higher R_{SP} (0.29 to 0.83) during downwind periods compared to parallel winds (-0.07 to 0.60). (Other sites had insufficient data for robust evaluations.) At the near-road site with the EC9830T monitor, which had the highest R_{SP} , downwind conditions increased FB and decreased F2, but the fraction of reducible to overall errors was higher. Similar results were seen at the urban site with the INDiI monitor. While limited by high DLs, the CO dataset again indicates better performance during downwind conditions.

IV.2.4 Performance by day-of-week

For NO_x , performance on weekdays generally was better than on Saturdays and Sundays (Table 23): weekdays gave higher F2 in all but one case (near-road site with the IGpCHEM monitor), although F2 exceeded 95%, and weekdays also had higher R_{SP} (although the urban site with the ICHEM monitor had comparable $R_{SP} = 0.59$ on both weekends and Saturdays, though still higher than on Sunday when $R_{SP} = 0.46$). At the near-road site with the IGpCHEM monitor, R_{SP} was high and comparable on weekdays, Saturdays and Sundays (0.75, 0.73 and 0.72, respectively), and weekdays had more under-predictions. Given that the reducible V_G on weekdays was low at this site, however, the overall conclusion of better performance on weekdays is unchanged.

For CO, the evaluation by day-type was hampered by data limitations, but weekday performance appeared better. F2 exceeded 92% at all sites. The near-road site had the highest R_{SP} on weekends (0.47 and 0.91 for INDiI and EC9830T samplers, respectively). The suburban site had higher R_{SP} for Saturdays than weekdays, but the sample size was small (weekend $n = 7$). At the urban site, weekdays and Saturdays had higher R_{SP} (0.17 and 0.23) than Sundays (0.01), but all correlations were low. The other performance metrics gave mixed results.

IV.2.5 Performance by season

For NO_x , seasonal performance trends varied by site and method, however, slightly better performance was suggested during winter (Table 24). For example, the near-road site in winter had the highest R_{SP} (both instruments), the highest F2 (ICHEM instrument, and nearly so with the IGpCHEM instrument), and the lowest relative reducible error. The urban site had the highest R_{SP} (IGpCHEM) in winter. However, trends differed at other sites, e.g., R_{SP} was highest in summer at the schools site and highest in spring at the urban site (ICHEM monitor), and V_G was not lowest in winter at any site.

Seasonal trends for CO were inconsistent, although some measures showed better performance in winter. R_{SP} was highest during winter at the near-road (both monitors) and industrial sites, however, R_{SP} was highest in spring at the urban site and negative during winter. F2 was uniformly high ($\geq 91\%$ and most values approached 100%). Data limitations restrict the reliability of the CO trends.

IV.3 Discussion

The operational evaluation characterized dispersion modeling performance for daily average concentrations of NO_x and CO at multiple sites in Detroit over a four-year period. The performance metrics often, but not always, gave consistent information, and generally met criteria laid out in evaluation guidelines [55, 56]. Some interpretations can be complex, e.g., if R_{SP} is low, then comparisons of FB and V_G across sites may provide little information. Most downwind NO_x and CO predictions were within a factor of two of observations (F2 > 90%), and correlation coefficients were moderate to high for NO_x (0.32 to 0.74), but variable for CO (0 to 0.89). Agreement between observed and predicted concentrations improved when monitors were downwind of major roads, as shown by high R_{SP}, low FB (-0.19 to 0.34 for NO_x; -0.17 to 0.50 for CO), and somewhat consistent and positive FB at the best-performing sites. We found over-prediction and increased scatter with low NO_x observations and parallel winds, high contributions from on-road sources to CO levels at the near-road monitors, and uniform background levels of NO_x (15 – 18 ppb) across Detroit.

Dispersion models like RLINE are expected to perform best at unobstructed sites that are close to roads since the modeled on-road sources will contribute a larger fraction of observed concentrations and since flows around buildings and other features are not explicitly modeled by Gaussian plume models. (RLINE simulates near-source dispersion using a general surface roughness parameter and dispersion parameters.) For NO_x and CO, two pollutants emitted primarily from traffic-related sources in urban areas, performance improved with proximity to major roads, and the best performance in Detroit was attained at the Eliza Howell near-road site located very close to the busy I-96 freeway.

Performance was generally better during downwind as compared to parallel wind conditions. Both observed and predicted concentrations tended to be higher under downwind conditions, thus, the increased agreement may reflect the greater signal from local (on-road) emission sources. (Plume models can produce the highest concentrations at near-road receptors with winds that are parallel or near-parallel to the road, although this was never observed in the daily averages in Detroit.)

Performance was better on weekdays as compared to weekends, possibly because the more regular traffic volume and fleet mix patterns on weekdays are better represented by temporal allocation factors [132]. In contrast, traffic patterns on weekends, especially on Sundays, are more variable.

The higher traffic volumes and stop-and-go congestion on weekdays might increase emissions, and the lower speeds and greater vehicle density might affect near-road turbulence and dispersion, thus increasing concentrations. The under-prediction on weekdays might result from these factors, and possibly due to a higher diesel fraction in the fleet mix than predicted. Such speculations might be examined using diagnostic (rather than operational) evaluations that focus on rush hour periods.

Model performance appeared slightly better in winter although results varied by site and method. Potentially important seasonal changes in Detroit include: shifts in prevailing wind directions, which alter the likelihood that a monitoring site will be downwind; changes in the frequency of stability regimes; large temperature swings, which alter MOVES emission factors (impacts on NO_x are complex) [180]; changes in temperature and the atmospheric composition (especially OH^\cdot) that can alter pollutant lifetime and fate; and changes in regional pollutants (particularly for $\text{PM}_{2.5}$). Only some of these processes are captured in dispersion models.

While of significant interest, no evaluation for $\text{PM}_{2.5}$ is presented as results were not informative. This largely results from the limited ability to discern $\text{PM}_{2.5}$ from local sources given the strength of background and regional sources of $\text{PM}_{2.5}$, and the lack of spatially- and temporally- resolved emissions data for area and non-road mobile emissions. Area and non-road emissions of $\text{PM}_{2.5}$ can be substantial, e.g., modeled on-road mobile sources constituted 48% of NO_x and 54% of CO emissions, but only 21% of $\text{PM}_{2.5}$ emissions (Table 19). Other studies have noted very high background concentrations of $\text{PM}_{2.5}$ (>70%) in Sacramento and London [181]. Diagnostic evaluations at near-road sites measuring PM-related pollutants that are more specific to TRAPs, e.g., black carbon and ultrafine PM for combustion products, and other markers for tire, road, and brake wear, might help indicate some of the factors affecting model performance.

IV.3.1 Comparison to literature

Many of our findings are consistent with prior applications of RLINE (e.g., in Detroit), and diagnostic evaluations using tracer gases (e.g., SF_6). For Detroit (all-direction) hourly NO_x at the schools site, an earlier study found a mean bias of 30% and F2 was 62% [51]; and for Detroit downwind near-road NO_x and CO, F2 was 100% [46]. For downwind hourly near-road NO data, F2 was 93% and the geometric mean (M_G) was 1.12 [43]. Also similar to previous work, we found positive FB at the near road site, and over-prediction and increased scatter at low NO_x concentrations [43–45]. Our estimate of the ratio of the average on-road to background CO levels

at the near-road site (1.46 at the more sensitive monitor) is similar to an earlier value for Detroit [51]. Finally, similarly uniform background concentrations of NO_x across Detroit have been reported [51]. Compared to studies using tracer gases, results are also comparable. For example, downwind 3-hour averages of SF_6 at near-road sites in Sacramento, California showed $F_2 > 80\%$ and M_G was 1.18 [43]; using this same dataset, another study obtained $F_2 > 78\%$ [45]. For downwind and hourly SF_6 gas data collected in rural Idaho, F_2 was 75 to 100% [44, 45]. Using near-road and downwind SF_6 measurements, FB was 0.05 and $NMSE$ was 0.34 [45].

In contrast to earlier work, we did not show significant over-prediction with parallel winds [43] or downwind peaks [44], and our normalized mean square error estimates were smaller than those in a recent RLINE evaluation [45]. We estimated that background sources were responsible for 70 to 90% of NO_x at the schools site, compared to approximately 50% estimated using hourly data [51]. These differences likely arose from our inclusion of background and point sources (also in [51]), the use of daily averages, and differences in the estimated background.

Operational evaluations should be distinguished from diagnostic, dynamic and probabilistic evaluations. Comparisons to the previous RLINE evaluations, which were mostly diagnostic in nature, are limited by several factors. First, we examined daily concentrations, which are relevant to many health-related applications. Second, we did not evaluate performance as a function of meteorological conditions. Lower performance and over-prediction has been reported during stable periods [43–45]. Third, performance during upwind periods was not evaluated (measurements during these periods were used to estimate background); prior work shows over-prediction and increased scatter at upwind receptors [43, 45]. Fourth, our large scale and multiyear urban application used data from a sparse (though typical) air quality monitoring network, and the ability to assess spatial performance was limited. In comparison, most other studies used tracer gases, a higher density of monitoring sites, few sources, a small study domain ($<1 \text{ km}^2$), and short study periods.

IV.3.2 Implications of varying performance

Dispersion models can be useful in developing exposure estimates of TRAP in health-related studies owing to their ability (given requisite data) to provide estimates with high spatial and temporal resolution. However, it is important to account for model performance and exposure measurement errors, that is, differences between the measured (or predicted) exposure compared

to the underlying true exposure, or exposure misclassification, the analogous term for a categorical exposure variable. These errors may vary spatially or temporally, and they may differentially affect different groups of study participants. Exposure measurement error can lead to incorrect inferences in health impact and epidemiologic studies, specifically, biased and/or imprecisely estimated effect coefficients that may be serious enough to invalidate inferences regarding the effect of pollution on health [182].

The operational evaluation suggested that model performance is best at near-road sites (e.g., within 10 to 100 m from the road) and that uncertainty increases with distance from roadways. RLINE represented much of the day-to-day variation observed in daily average concentrations, suggesting that dispersion modeling can provide near-road (and potentially on-road exposures) predictions with good fidelity: this is important since many people live or work near roads where TRAP concentrations are highest [2]. While these results may be driven by the ability to discern contributions from local emission sources, dispersion model performance is likely to degrade with distances in urban settings for several reasons [20], e.g., shifts in wind fields, the presence of unknown or unmodeled sources (including other local roads), and atmospheric transformation and other unmodeled processes. Thus, at farther distances, daily fluctuations in concentrations may be less accurately estimated. This may increase the likelihood of errors from dispersion model-based exposure estimates if study participants are exposed over a range of distances from major roads. Such studies might benefit from weighting exposure estimates by their uncertainties.

A second concern is the effect of wind direction relative to the orientation of (major) roads and locations of study participants. Dispersion models perform best at downwind receptors, i.e., when winds are approximately perpendicular to the road's orientation. Correlation between the prevailing wind direction(s), road alignment(s) and study participant locations might yield differential errors. For example, in Detroit, prevailing winds come from the west and southwest. (Figure 3 shows wind roses at two local airports.) Thus, model performance will be best for roads with north-south and northwest-southeast alignments with study participants on the downwind side, and poorer for roads that are aligned with the prevailing wind directions or with participants in upwind locations. These errors were investigated in Detroit by identifying the nearest (within 150 m) major road (AADT > 10,000) for a random sample of residences (n = 4,000). Most roads are aligned on a north-south or east-west axis, thus directions from a residence to the nearest major

road are mainly north and south (Figure 27). Based on prevailing winds and the largest roads, individuals living downwind are east of north-south roads (e.g., M-10, M-39, I-75), “upwind” individuals live on west of the same roads, and individuals living south or north of east-west roads (e.g., I-96, I-94) will often experience parallel winds. Even if all individuals in a study lived at similar distances and/or had similar TRAP exposure, upwind and parallel groups have an increased likelihood of exposure measurement errors. In general, population patterns and the importance of directional effects will depend on many factors, e.g., demographic clustering (e.g., of residences, schools, workplaces) [183, 184], geographic boundaries (mountains, coastlines), economic (real estate) and administrative (municipal boundaries) factors. Some concerns might be addressed by selecting appropriate areas or, again, by using weights to account for prediction uncertainty.

Other implications for health or epidemiologic studies arise from the day-of-week variation in model performance and the reliability of time-activity data needed to assign exposures. Consider a statistical model associating health outcomes with the prior day’s exposure, e.g., outcomes on Sundays and Mondays require exposure estimates for Saturdays and Sundays. Many models use 3- to 5-day lags. With a 3-day lag, Sunday’s through Wednesday’s outcomes require weekend exposure data. Given lower performance of the dispersion model and greater uncertainty (as well as variability) of weekend time-activity information, exposure measurement errors may increase from Saturday through Wednesday. Thus, a study incorporating 3-day exposure lags might emphasize, weight or separately test the health data for Thursdays, Fridays and possibly Saturdays when exposure uncertainty is smaller to control for these effects. A related concern is RLINE’s tendency to under-predict on weekdays, which could bias concentration-outcome relationships if the (estimated) exposure variability is compressed, increase uncertainty since health models typically include both weekday and weekend periods, and falsely attribute variation to day-of-week or weekend/weekend covariates, if used. Such effects are hypothetical. Calibrating the dispersion model (i.e., mobile source inventory, TAFs) and the exposure assumptions might help to resolve this issue.

Lastly, seasonal variation in dispersion model performance, while less consistent than the day-of-week effects, raises additional concerns in epidemiologic applications. This variation can be coupled to seasonal time-activity information that affects exposure, e.g., the summer school holiday period for children, which can increase uncertainty since the home-school-home pattern is

absent or less consistent and because of increased time spent outdoors. In addition, July, August and sometimes early September traffic patterns can have greater variability, a result of summer vacation, holiday travel and decreased commuting.

IV.3.3 Uncertainty and limitations

Comparisons between observed and predicted pollutant concentrations are affected by many factors. Our results show the importance of selecting pollutants, sites and instrumentation that together produce concentration trends that are markedly influenced by local traffic-related emissions. The ability to discern traffic-related contributions of PM_{2.5} was limited, a result of high background concentrations, the lack of spatial and temporal detail for area, non-road and fugitive emissions, the omission of pollutant transformations in RLINE, and the sparseness of the monitoring network. The use of monitoring parameters more specific to TRAP, e.g., black carbon or ultrafine PM, would be valuable.

Modeling results can be affected by many factors. While detailed, the mobile source inventory used estimates of traffic volumes, time allocation factors derived from mostly larger roads, and MOVES emission factors for the greater Detroit area that may not have fully reflected local traffic volume, vehicle mix and emissions. Point sources were aggregated to the facility level, used average emission rates, and temporal variability was not modeled. Background estimates only partly accounted for regional sources and may not have fully represented short-term fluctuations and gradients. (Other studies have used complex regional chemical models to estimate background [136].) The classification of downwind and parallel periods refers to only the nearest major road. We assumed that the meteorological datasets driving the model were representative and appropriate. Hours when measured concentrations were low ($< DL$) were omitted from the evaluation, which may artificially increase correlations by limiting analyses to those observations when local source impacts are seen. This was tested by setting values below the DL to $\frac{1}{2} DL$ and repeating all analyses. This dampened some trends, e.g., the wind direction analysis of NO_x, and R_{SP} and other metrics changed noticeably. However, removing low values has the advantage of largely eliminating (meaningless) comparisons between modeled and measured background, which can be important if roadway impacts are small or if monitoring methods have low detection frequencies. Finally, the relatively few observations available on weekends may have influenced results.

Overall, results highlight the sensitivity of evaluation results to monitor placement, instrument sensitivity (e.g., DL), and the ability to observe contributions from local sources. Results for NO_x appear most meaningful given the NO_x instrumentation's greater sensitivity and ability to detect traffic-related emissions. In contrast, the CO evaluation was limited by low detection frequencies at some sites, which resulted in a small number of valid observations, especially when analyses were stratified by wind direction, day-of-week and season.

IV.4 Tables

Table 19. Summary of 2011 Wayne County CO, NO_x and PM_{2.5} emissions from the National Emission Inventory [124] in short tons (rounded to the nearest ton), percent of total emissions (bolded), and of each category (not bolded).

Emission category	CO	%	NO _x	%	PM _{2.5}	%
Non-point	7,316	3	6,307	10	1,930	38
Industrial processes	194	3	4	0	489	25
Miscellaneous area sources	< 1	0	7	0	27	1
Mobile sources†	107	1	872	14	689	36
Natural sources	642	9	167	3	-	-
Stationary source fuel combustion	6,347	87	5,087	81	725	38
Waste disposal, treatment and recovery	27	0	170	3	-	-
Non-road mobile sources	65,491	27	6,847	11	493	10
On-road mobile sources	129,647	54	29,767	48	1,098	21
Highway - Compressed Natural Gas	54	0	42	0	0	0
Highway - Diesel	6,260	5	15,740	53	748	68
Highway - Gasoline	123,332	95	13,985	47	349	32
Point	36,335	15	19,489	31	1,610	31
External combustion	67	0	211	1	18	1
External combustion boilers	7,422	20	10,516	54	246	15
Industrial processes	20,230	56	3,082	16	904	56
Internal combustion engines	3,193	9	1,363	7	260	16
Mobile sources*	4,702	13	2,326	12	85	5
Petroleum and solvent evaporation	13	0	20	0	52	3
Waste disposal	708	2	1,972	10	46	3
Grand Total	238,788		62,411		5,131	

† Railroad equipment and marine vessels; * Aircraft and airport support vehicles

Table 20. Model performance for daily average NO_x and CO.

Poll	Site	Method	Days	Means (ppb)						FB			V _G		
				Obs	Back	Model	Ncom	Com	Point	F2	R _{SP}	FP	FN	Irr	Red
NO _x															
	school	ICHEM	918	23	17	3	1.2	0	1	95	0.32	0.07	0.22	1.01	1.12
	near-road	ICHEM	334	37	16	21	18.6	2	1	92	0.58	0.17	0.17	1.01	1.18
		IGpCHEM	705	48	15	23	18.5	4	1	95	0.74	0.05	0.28	1.03	1.11
	urban	ICHEM	238	25	18	11	8.5	1	1	93	0.57	0.22	0.09	1.03	1.12
		IGpCHEM	565	26	16	12	8.5	2	1	97	0.58	0.15	0.09	1.01	1.09
CO															
	suburban	IGFC	40	673	671	27	19	3	5	100	0.21	0.11	0.07	1.00	1.04
	near-road	EC9830T	82	479	128	192	180	9	4	94	0.89	0.00	0.40	1.14	1.05
		INDiI	655	667	519	291	277	9	5	99	0.45	0.21	0.01	1.04	1.03
	urban	INDiI	284	639	545	126	115	5	6	99	0.17	0.12	0.07	1.00	1.05
	industrial	IGFC	63	585	535	115	100	10	5	100	0.00	0.14	0.03	1.01	1.03

Abbreviations: Back = Modeled background contribution; Com. = Modeled contribution from commercial traffic; F2 = % of model + background within a factor of 2 of observed; FB = Fractional bias; fp = false positive; fn = false negative; ICHEM = Instrumental Chemiluminescence; IGpCHEM = Instrumental Gas-Phase Chemiluminescence; Irr = Irreducible or systematic component of VG; Model = Modeled contribution from commercial, non-commercial and point sources; Ncom. = Modeled contribution from non-commercial traffic; NMSE = Normalized mean squared error; Obs. = Observed concentrations; Point = Modeled contribution from point sources; R_{SP} = Spearman's correlation coefficient; Red = reducible or random component of VG; VG = geometric variance.

Table 21. Daily average observed and modeled PM_{2.5} concentrations at the suburban and schools sites (µg/m³).

Site	Subset	Days	Hours	Obs.	Back	Model
Suburban		1,379	27,504	10.0	8.8	0.6
	Weekday	984	19,684	9.9	8.8	0.6
	Saturday	197	3,907	10.8	8.8	0.5
	Sunday	198	3,913	10.2	8.8	0.4
	Winter	330	7,113	11.4	9.7	0.7
	Spring	357	7,316	8.6	7.9	0.5
	Summer	356	6,593	11.1	9.2	0.5
	Fall	336	6,482	9.1	8.4	0.6
Schools		462	9,686	9.5	8.8	0.3
	Weekday	330	6,958	9.4	8.8	0.3
	Saturday	67	1,408	10.0	8.7	0.3
	Sunday	65	1,320	9.6	8.8	0.3
	Winter	120	2,640	10.9	9.7	0.4
	Spring	119	2,517	7.5	7.9	0.3
	Summer	116	2,342	10.7	9.2	0.3
	Fall	107	2,187	9.0	8.4	0.4

Acronyms: Back = Modeled background contribution; Model = Modeled contribution from commercial, non-commercial and point sources; Obs. = Observed concentrations

Table 22. Model performance for daily average NO_x and CO by wind direction type.

Poll	Site	Method	Wind Dir	Days	Means (ppb)						FB		V _G			
					Obs	Back	Model	Ncom	Com	Point	F2	R _{SP}	FP	FN	Irr	Red
NO_x																
schools	ICHEM	Downwind	134	22	17	3	1	1	1	96	0.30	0.09	0.21	1.00	1.13	
			138	28	17	2	1	0	0	80	0.16	0.04	0.44	1.08	1.25	
near-road	ICHEM	Downwind	76	44	16	25	21	2	2	91	0.37	0.16	0.23	1.00	1.22	
			71	35	16	18	16	2	1	90	0.52	0.16	0.17	1.00	1.19	
	IGpCHEM	Downwind	186	61	15	28	22	4	2	90	0.60	0.02	0.36	1.10	1.09	
			150	40	15	19	15	3	0	95	0.51	0.08	0.25	1.02	1.14	
urban	ICHEM	Downwind	51	25	19	12	9	1	3	96	0.64	0.23	0.04	1.05	1.08	
			39	25	22	8	6	1	1	92	0.23	0.26	0.10	1.05	1.15	
	IGpCHEM	Downwind	170	29	16	14	10	2	3	97	0.57	0.15	0.09	1.01	1.10	
			74	23	17	9	7	2	1	92	0.31	0.20	0.07	1.02	1.11	
CO																
suburban	IGFC	Downwind	1	-	-	-	-	-	-	-	-	-	-	-	-	
			4	-	-	-	-	-	-	-	-	-	-	-	-	
near-road	EC9830T	Downwind	26	557	128	205	192	9	5	92	0.83	0.00	0.50	1.28	1.04	
			11	326	128	146	136	7	2	100	0.60	0.04	0.21	1.02	1.05	
	INDiI	Downwind	182	685	519	297	280	9	7	100	0.44	0.18	0.01	1.03	1.03	
			53	623	518	271	260	9	2	96	0.15	0.24	0.01	1.06	1.04	
urban	INDiI	Downwind	62	651	552	138	125	5	8	98	0.29	0.13	0.07	1.01	1.05	
			19	615	561	61	56	3	2	100	-0.07	0.08	0.07	1.00	1.03	
industrial	IGFC	Downwind	1	-	-	-	-	-	-	-	-	-	-	-	-	
			2	-	-	-	-	-	-	-	-	-	-	-	-	

Abbreviations: Back = Modeled background contribution; Com. = Modeled contribution from commercial traffic; F2 = % of model + background within a factor of 2 of observed; FB = Fractional bias; fp = false positive; fn = false negative; ICHEM = Instrumental Chemiluminescence; IGpCHEM = Instrumental Gas-Phase Chemiluminescence; Irr = Irreducible or systematic component of VG; Model = Modeled contribution from commercial, non-commercial and point sources; Ncom. = Modeled contribution from non-commercial traffic; NMSE = Normalized mean squared error; Obs. = Observed concentrations; Point = Modeled contribution from point sources; R_{SP} = Spearman's correlation coefficient; Red = reducible or random component of VG; VG = geometric variance.

Table 23. Model performance for daily average NO_x and CO by day type.

Poll	Site	Method	Wind Dir	Days	Means (ppb)						FB		V _G			
					Obs	Back	Model	Ncom	Com	Point	F2	R _{SP}	FP	FN	Irr	Red
NO _x																
	schools	ICHEM	Weekday	701	23	17	3	1	0	1	96	0.38	0.07	0.22	1.01	1.11
			Saturday	120	23	17	3	1	0	1	94	0.17	0.07	0.22	1.01	1.12
			Sunday	97	22	17	3	1	0	2	91	0.02	0.12	0.22	1.00	1.17
	near-road	ICHEM	Weekday	247	40	16	22	19	2	1	96	0.65	0.13	0.19	1.00	1.16
			Saturday	43	30	16	19	17	1	1	81	0.30	0.25	0.12	1.02	1.20
			Sunday	44	25	16	19	17	1	1	82	0.33	0.37	0.04	1.14	1.14
		IGpCHEM	Weekday	506	54	15	25	19	4	1	95	0.75	0.03	0.33	1.07	1.09
			Saturday	99	39	15	22	19	2	1	99	0.73	0.09	0.14	1.00	1.09
			Sunday	100	31	15	17	15	2	1	95	0.72	0.14	0.10	1.00	1.09
urban	ICHEM	Weekday	183	26	18	11	8	1	1	96	0.65	0.18	0.10	1.02	1.10	
		Saturday	32	22	17	10	8	1	1	91	0.59	0.31	0.08	1.06	1.13	
		Sunday	23	21	19	12	10	1	2	74	-0.15	0.42	0.01	1.21	1.12	
	IGpCHEM	Weekday	422	28	16	12	9	2	1	98	0.59	0.12	0.10	1.00	1.08	
		Saturday	77	24	16	11	9	1	2	91	0.59	0.23	0.07	1.05	1.09	
		Sunday	66	21	17	9	7	1	2	97	0.46	0.27	0.06	1.06	1.10	
CO																
	suburban	IGFC	Weekday	27	675	671	30	21	3	5	100	0.26	0.12	0.08	1.00	1.05
			Saturday	7	668	672	22	16	2	5	100	0.57	0.09	0.06	1.00	1.03
			Sunday	6	669	672	16	14	1	1	100	-0.32	0.08	0.05	1.00	1.02
	near-road	EC9830T	Weekday	58	495	128	199	185	10	4	93	0.91	0.00	0.41	1.16	1.04
			Saturday	12	492	128	225	211	7	7	100	0.85	0.00	0.33	1.11	1.03
			Sunday	12	386	128	129	122	4	3	92	0.90	0.02	0.42	1.09	1.13
		INDiI	Weekday	496	680	519	299	283	11	5	99	0.47	0.20	0.01	1.04	1.03

		Saturday	88	646	516	278	267	6	5	100	0.36	0.23	0.02	1.04	1.04
		Sunday	71	602	515	254	244	6	4	99	0.33	0.25	0.00	1.06	1.03
urban	INDiI	Weekday	223	639	543	132	120	5	6	99	0.17	0.12	0.06	1.00	1.04
		Saturday	36	625	551	109	98	3	8	100	0.23	0.13	0.07	1.01	1.05
		Sunday	25	665	549	106	97	3	6	96	0.01	0.09	0.11	1.00	1.07
industrial	IGFC	Weekday	51	582	536	113	98	10	5	100	-0.06	0.14	0.03	1.01	1.03
		Saturday	4	-	-	-	-	-	-	-	-	-	-	-	-
		Sunday	8	596	540	141	128	8	5	100	-0.47	0.17	0.04	1.02	1.04

Abbreviations: Back = Modeled background contribution; Com. = Modeled contribution from commercial traffic; F2 = % of model + background within a factor of 2 of observed; FB = Fractional bias; fp = false positive; fn = false negative; ICHEM = Instrumental Chemiluminescence; IGpCHEM = Instrumental Gas-Phase Chemiluminescence; Irr = Irreducible or systematic component of VG; Model = Modeled contribution from commercial, non-commercial and point sources; Ncom. = Modeled contribution from non-commercial traffic; NMSE = Normalized mean squared error; Obs. = Observed concentrations; Point = Modeled contribution from point sources; R_{SP} = Spearman's correlation coefficient; Red = reducible or random component of VG; VG = geometric variance.

Table 24. Model performance for daily average NO_x and CO by season.

Poll	Site	Method	Wind Dir	Days	Means (ppb)						F2	R _{SP}	FB		V _G	
					Obs	Back	Model	Ncom	Com	Point			FP	FN	Irr	Red
NO _x	schools	ICHEM	Winter	311	25	17	3	1	0	1	94	0.29	0.05	0.28	1.03	1.13
			Spring	195	23	16	2	1	0	1	91	0.21	0.06	0.25	1.02	1.13
			Summer	165	19	16	3	1	0	2	99	0.44	0.10	0.08	1.00	1.05
			Fall	247	23	17	3	1	0	2	98	0.33	0.09	0.20	1.00	1.12
	near-road	ICHEM	Winter	84	51	20	21	19	2	1	99	0.79	0.05	0.27	1.03	1.12
			Spring	85	34	15	17	15	1	1	88	0.52	0.17	0.20	1.00	1.19
			Summer	87	22	12	22	19	2	1	85	0.59	0.43	0.00	1.21	1.06
			Fall	78	41	15	25	22	2	1	96	0.58	0.13	0.14	1.00	1.12
		IGpCHEM	Winter	184	55	16	21	16	3	1	91	0.84	0.01	0.41	1.14	1.08
			Spring	168	42	15	19	15	3	1	98	0.79	0.03	0.25	1.04	1.07
			Summer	142	39	14	25	20	4	1	97	0.69	0.11	0.12	1.00	1.10
			Fall	211	53	16	28	22	4	1	96	0.71	0.06	0.27	1.03	1.12
	urban	ICHEM	Winter	69	32	27	10	8	1	1	84	0.47	0.29	0.13	1.08	1.19
			Spring	59	25	17	9	7	1	1	98	0.60	0.12	0.08	1.01	1.07
			Summer	49	17	10	11	9	1	2	94	-0.02	0.24	0.05	1.03	1.09
			Fall	61	25	16	13	10	1	2	97	0.51	0.19	0.05	1.03	1.07
IGpCHEM		Winter	168	31	19	11	8	2	1	97	0.63	0.10	0.14	1.00	1.09	
		Spring	130	24	16	10	7	1	1	100	0.56	0.13	0.07	1.01	1.06	
		Summer	97	19	13	12	9	2	2	93	0.40	0.29	0.01	1.08	1.05	
		Fall	170	28	16	14	10	2	2	97	0.59	0.15	0.09	1.01	1.09	
CO	suburban	IGFC	Winter	24	651	666	31	24	3	3	100	0.51	0.12	0.05	1.01	1.04
			Spring	2	-	-	-	-	-	-	-	-	-	-	-	-
			Summer	3	-	-	-	-	-	-	-	-	-	-	-	-
			Fall	11	738	684	19	10	1	7	100	-0.18	0.07	0.12	1.00	1.04
	near-road	EC9830T	Winter	25	484	128	196	183	9	4	100	0.91	0.00	0.40	1.15	1.02
			Spring	-	-	-	-	-	-	-	-	-	-	-	-	-
			Summer	-	-	-	-	-	-	-	-	-	-	-	-	-
			Fall	57	476	128	191	178	8	4	91	0.88	0.00	0.40	1.14	1.07

	INDiI	Winter	133	677	540	262	247	10	5	100	0.57	0.19	0.02	1.03	1.02
		Spring	152	651	523	229	216	8	5	99	0.34	0.17	0.02	1.02	1.03
		Summer	188	650	502	338	324	10	5	100	0.39	0.26	0.00	1.07	1.03
		Fall	182	690	517	315	300	10	5	100	0.54	0.20	0.01	1.04	1.03
urban	INDiI	Winter	97	665	564	101	92	4	5	98	-0.05	0.09	0.09	1.00	1.05
		Spring	61	677	570	98	87	4	7	100	0.45	0.07	0.08	1.00	1.03
		Summer	55	549	506	155	143	5	7	100	0.20	0.19	0.01	1.03	1.02
		Fall	71	643	526	164	150	5	8	99	0.21	0.14	0.07	1.01	1.06
industrial	IGFC	Winter	13	565	514	114	97	12	5	100	0.15	0.14	0.03	1.01	1.03
		Spring	15	602	536	77	64	7	6	100	-0.57	0.07	0.06	1.00	1.02
		Summer	24	583	544	121	106	9	6	100	0.26	0.15	0.02	1.02	1.02
		Fall	11	587	541	157	142	12	3	100	0.01	0.20	0.02	1.03	1.04

Abbreviations: Back = Modeled background contribution; Com. = Modeled contribution from commercial traffic; F2 = % of model + background within a factor of 2 of observed; FB = Fractional bias; fp = false positive; fn = false negative; ICHEM = Instrumental Chemiluminescence; IGpCHEM = Instrumental Gas-Phase Chemiluminescence; Irr = Irreducible or systematic component of VG; Model = Modeled contribution from commercial, non-commercial and point sources; Ncom. = Modeled contribution from non-commercial traffic; NMSE = Normalized mean squared error; Obs. = Observed concentrations; Point = Modeled contribution from point sources; R_{SP} = Spearman's correlation coefficient; Red = reducible or random component of VG; VG = geometric variance.

IV.5 Figures

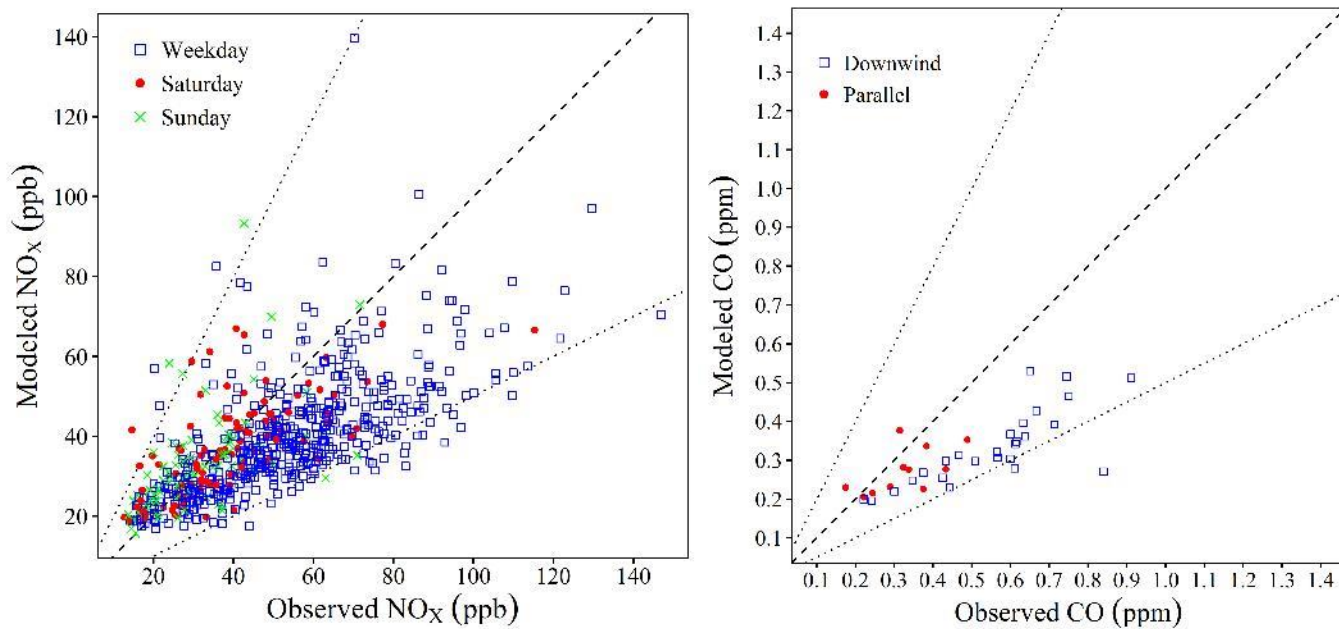


Figure 26. Observed versus modeled NO_x and CO at the near-road site using the EC9830T and IGpCHEM monitors. Figures show 1:1 and factor of 2 lines. For NO_x and CO respectively, day-of-week and prevailing wind-direction comparisons are differentiated by point color and shape.

Appendix A - Expanded tables of Model Performance

Table A. 1. Model performance metrics for daily average NO_x and various daily subsets.

Site	Subset	Days	Hours	Mean (µg/m ³)						R _{SP}	FAC2 (%)	FB			MG	NMSE			V _G		
				Obs.	Back	Model	Ncom.	Com.	Point			fp	fn	Δ		Irr	Red	Σ	Irr	Red	Π
School	ICHEM	918	11,541	41.8	30.7	5.2	2.1	0.7	2.4	0.32	95	0.07	0.22	0.15	1.09	0.02	0.20	0.23	1.01	1.12	1.13
	Downwind	134	1,159	40.7	31.2	5.1	2.6	1.0	1.4	0.30	96	0.09	0.21	0.12	1.05	0.01	0.20	0.21	1.00	1.13	1.13
	Parallel	138	1,211	50.7	30.8	3.1	1.7	0.5	0.9	0.16	80	0.04	0.44	0.40	1.32	0.17	0.55	0.72	1.08	1.25	1.35
	Other	577	5,821	42.5	30.8	5.7	2.0	0.7	3.1	0.37	96	0.06	0.21	0.15	1.10	0.02	0.18	0.20	1.01	1.10	1.11
	Weekday	701	8,920	42.1	30.7	5.4	2.2	0.9	2.3	0.38	96	0.07	0.22	0.15	1.10	0.02	0.19	0.21	1.01	1.11	1.12
	Saturday	120	1,485	41.3	30.8	4.7	2.0	0.4	2.4	0.17	94	0.07	0.22	0.15	1.09	0.02	0.22	0.24	1.01	1.12	1.13
	Sunday	97	1,136	39.6	31.0	4.9	1.7	0.3	2.9	0.02	91	0.12	0.22	0.10	1.02	0.01	0.28	0.29	1.00	1.17	1.17
	Winter	311	4,827	45.8	31.4	5.0	2.1	0.7	2.2	0.29	94	0.05	0.28	0.23	1.17	0.05	0.23	0.28	1.03	1.13	1.16
	Spring	195	2,091	41.2	29.9	4.0	1.7	0.6	1.7	0.21	91	0.06	0.25	0.19	1.13	0.04	0.21	0.25	1.02	1.13	1.15
	Summer	165	1,477	34.7	29.6	5.8	2.3	0.8	2.7	0.44	99	0.10	0.08	-0.02	0.95	0.00	0.05	0.05	1.00	1.05	1.05
Fall	247	3,146	41.9	31.3	6.1	2.5	0.9	2.8	0.33	98	0.09	0.20	0.11	1.05	0.01	0.21	0.22	1.00	1.12	1.12	
Near-road	ICHEM	334	5,524	66.6	28.4	38.7	33.9	2.9	1.8	0.58	92	0.17	0.17	-0.01	0.92	0.00	0.20	0.20	1.01	1.18	1.19
	Downwind	76	765	80.1	28.8	45.3	38.6	3.2	3.6	0.37	91	0.16	0.23	0.08	0.98	0.01	0.23	0.24	1.00	1.22	1.22
	Parallel	71	627	63.4	29.7	32.8	29.1	2.8	0.9	0.52	90	0.16	0.17	0.01	0.95	0.00	0.22	0.22	1.00	1.19	1.19
	Other	288	3,192	66.7	28.6	36.8	32.3	2.8	1.7	0.60	93	0.15	0.17	0.02	0.95	0.00	0.19	0.19	1.00	1.17	1.17
	Weekday	247	4,095	72.4	28.4	40.1	34.9	3.4	1.8	0.65	96	0.13	0.19	0.06	0.97	0.00	0.19	0.19	1.00	1.16	1.16
	Saturday	43	733	54.5	28.4	33.7	30.7	1.6	1.4	0.30	81	0.25	0.12	-0.13	0.86	0.02	0.26	0.28	1.02	1.20	1.22
	Sunday	44	696	45.7	28.3	35.4	31.8	1.4	2.2	0.33	82	0.37	0.04	-0.33	0.69	0.11	0.13	0.25	1.14	1.14	1.31
	Winter	84	1,511	92.3	35.5	38.5	33.7	2.9	1.9	0.79	99	0.05	0.27	0.22	1.19	0.05	0.14	0.19	1.03	1.12	1.15
	Spring	85	1,367	61.4	28.1	31.5	27.4	2.4	1.7	0.52	88	0.17	0.20	0.03	0.95	0.00	0.26	0.26	1.00	1.19	1.19
	Summer	87	1,284	40.4	22.7	39.7	35.1	2.9	1.8	0.59	85	0.43	0.00	-0.43	0.65	0.19	0.08	0.27	1.21	1.06	1.28
Fall	78	1,362	73.7	27.3	45.4	40.0	3.4	2.0	0.58	96	0.13	0.14	0.01	0.98	0.00	0.12	0.12	1.00	1.12	1.12	
IGpCHEM	ICHEM	705	11,845	87.9	27.7	42.2	33.6	6.5	2.1	0.74	95	0.05	0.28	0.23	1.20	0.05	0.14	0.19	1.03	1.11	1.15
	Downwind	186	2,014	110.9	27.9	51.2	39.5	7.3	4.4	0.60	90	0.02	0.36	0.34	1.36	0.12	0.12	0.24	1.10	1.09	1.20
	Parallel	150	1,293	73.4	27.6	34.4	27.8	5.8	0.9	0.51	95	0.08	0.25	0.17	1.15	0.03	0.17	0.20	1.02	1.14	1.16

Other	594	6,566	85.9	27.6	37.9	30.1	6.0	1.8	0.76	94	0.04	0.31	0.27	1.24	0.07	0.15	0.22	1.05	1.11	1.16
Weekday	506	8,551	97.4	27.7	44.8	34.9	7.8	2.1	0.75	95	0.03	0.33	0.29	1.30	0.09	0.12	0.21	1.07	1.09	1.17
Saturday	99	1,670	70.4	27.6	39.8	33.8	3.7	2.3	0.73	99	0.09	0.14	0.04	1.01	0.00	0.10	0.10	1.00	1.09	1.09
Sunday	100	1,624	56.9	27.6	31.7	26.8	2.9	2.1	0.72	95	0.14	0.10	-0.04	0.94	0.00	0.12	0.12	1.00	1.09	1.09
Winter	184	3,290	100.7	29.4	37.4	29.4	6.1	1.9	0.84	91	0.01	0.41	0.40	1.43	0.17	0.13	0.30	1.14	1.08	1.22
Spring	168	2,759	77.0	27.0	34.4	27.1	5.4	1.9	0.79	98	0.03	0.25	0.23	1.21	0.05	0.09	0.14	1.04	1.07	1.11
Summer	142	2,213	70.3	25.0	44.7	36.1	6.6	2.0	0.69	97	0.11	0.12	0.01	0.97	0.00	0.09	0.09	1.00	1.10	1.10
Fall	211	3,583	97.2	28.4	50.9	40.7	7.6	2.6	0.71	96	0.06	0.27	0.20	1.18	0.04	0.14	0.18	1.03	1.12	1.15
Urban IChem	238	3,404	46.0	32.9	19.6	15.4	1.6	2.5	0.57	93	0.22	0.09	-0.13	0.84	0.02	0.21	0.23	1.03	1.12	1.15
Downwind	51	488	45.9	33.7	21.6	15.6	1.4	4.6	0.64	96	0.23	0.04	-0.19	0.81	0.04	0.09	0.13	1.05	1.08	1.13
Parallel	39	329	45.5	39.5	13.8	10.8	2.0	1.0	0.23	92	0.26	0.10	-0.16	0.80	0.03	0.19	0.21	1.05	1.15	1.20
Other	167	1,789	47.0	34.4	18.5	14.7	1.5	2.2	0.56	93	0.21	0.09	-0.12	0.86	0.01	0.24	0.25	1.02	1.11	1.14
Weekday	183	2,712	48.2	32.9	19.4	15.1	1.8	2.5	0.65	96	0.18	0.10	-0.08	0.88	0.01	0.21	0.22	1.02	1.10	1.12
Saturday	32	409	39.7	31.3	18.3	15.0	1.0	2.2	0.59	91	0.31	0.08	-0.22	0.79	0.05	0.18	0.24	1.06	1.13	1.20
Sunday	23	283	37.6	34.6	22.7	18.3	1.1	3.3	-0.15	74	0.42	0.01	-0.41	0.65	0.18	0.12	0.30	1.21	1.12	1.36
Winter	69	1,153	57.8	49.6	18.3	14.4	1.6	2.3	0.47	84	0.29	0.13	-0.16	0.76	0.03	0.33	0.36	1.08	1.19	1.29
Spring	59	802	45.3	30.6	16.5	13.0	1.3	2.1	0.60	98	0.12	0.08	-0.04	0.93	0.00	0.08	0.08	1.01	1.07	1.07
Summer	49	557	31.4	17.5	20.4	16.0	1.6	2.8	-0.02	94	0.24	0.05	-0.19	0.84	0.04	0.11	0.14	1.03	1.09	1.13
Fall	61	892	45.1	28.5	23.4	18.4	2.0	3.0	0.51	97	0.19	0.05	-0.14	0.85	0.02	0.08	0.10	1.03	1.07	1.10
IGpChem	565	8,433	48.1	29.8	21.2	15.5	3.1	2.6	0.58	97	0.15	0.09	-0.06	0.90	0.00	0.11	0.11	1.01	1.09	1.10
Downwind	170	1,771	51.9	29.4	25.6	17.5	3.3	4.8	0.57	97	0.15	0.09	-0.06	0.90	0.00	0.10	0.10	1.01	1.10	1.11
Parallel	74	591	41.5	30.5	16.9	13.0	2.9	1.1	0.31	92	0.20	0.07	-0.13	0.86	0.02	0.14	0.16	1.02	1.11	1.13
Other	387	4,129	49.9	30.3	20.1	14.9	3.1	2.2	0.60	97	0.13	0.12	-0.01	0.94	0.00	0.13	0.13	1.00	1.09	1.10
Weekday	422	6,435	50.5	29.7	21.9	15.8	3.6	2.5	0.59	98	0.12	0.10	-0.02	0.95	0.00	0.10	0.10	1.00	1.08	1.08
Saturday	77	1,100	43.1	30.0	20.8	15.9	1.9	2.9	0.59	91	0.23	0.07	-0.16	0.80	0.03	0.13	0.16	1.05	1.09	1.14
Sunday	66	898	38.6	30.3	17.2	12.9	1.5	2.8	0.46	97	0.27	0.06	-0.21	0.78	0.04	0.13	0.17	1.06	1.10	1.17
Winter	168	2,809	55.7	33.9	19.5	14.4	3.0	2.1	0.63	97	0.10	0.14	0.04	0.99	0.00	0.13	0.13	1.00	1.09	1.10
Spring	130	1,823	44.3	29.6	17.4	12.4	2.6	2.4	0.56	100	0.13	0.07	-0.06	0.92	0.00	0.06	0.06	1.01	1.06	1.07
Summer	97	1,215	34.9	24.2	22.2	15.9	3.1	3.1	0.40	93	0.29	0.01	-0.28	0.75	0.08	0.06	0.14	1.08	1.05	1.14
Fall	170	2,586	51.0	29.0	25.2	18.6	3.6	3.1	0.59	97	0.15	0.09	-0.06	0.91	0.00	0.11	0.12	1.01	1.09	1.10

Acronyms: Back = Modeled background contribution; Com. = Modeled contribution from commercial traffic; F2 = % of model + background within a factor of 2 of observed; FB = Fractional bias; fp = false positive; fn = false negative; IChem = Instrumental Chemiluminescence; IGpChem = Instrumental Gas-Phase Chemiluminescence; Irr = Irreducible or systematic component of VG; Model = Modeled contribution from commercial, non-commercial and point sources; Ncom. = Modeled contribution from non-commercial traffic; NMSE = Normalized mean squared error; Obs. = Observed concentrations; Point = Modeled contribution from point sources; R_{SP} = Spearman's correlation coefficient; Red = reducible or random component of VG; VG = geometric variance. Δ = Total FB; Σ = Sum of Irr. and Red. NMSE; ∏ = Product of Irr. and Red. VG.

Table A. 2. Model performance metrics for daily average CO and various daily subsets.

Site	Subset	Days	Hours	Mean (ppm)						R _{SP}	FAC2 (%)	FB			MG	NMSE			V _G		
				Obs.	Back	Model	Ncom.	Com.	Point			fp	fn	Δ		Irr	Red	Σ	Irr	Red	Π
Suburban	IGFC	40	346	0.67	0.67	0.03	0.02	0.00	0.00	0.21	100	0.11	0.07	-0.04	0.94	0.00	0.05	0.05	1.00	1.04	1.05
	Downwind	1	12	-	-	-	-	-	-	-	-	-	-	-	-	-	-	-	-	-	-
	Parallel	4	26	-	-	-	-	-	-	-	-	-	-	-	-	-	-	-	-	-	-
	Other	19	164	0.74	0.67	0.02	0.01	0.00	0.00	0.27	100	0.06	0.13	0.07	1.04	0.00	0.06	0.07	1.00	1.05	1.06
	Weekday	27	250	0.67	0.67	0.03	0.02	0.00	0.01	0.26	100	0.12	0.08	-0.04	0.94	0.00	0.06	0.06	1.00	1.05	1.05
	Saturday	7	59	0.67	0.67	0.02	0.02	0.00	0.01	0.57	100	0.09	0.06	-0.04	0.95	0.00	0.03	0.03	1.00	1.03	1.03
	Sunday	6	37	0.67	0.67	0.02	0.01	0.00	0.00	-0.32	100	0.08	0.05	-0.03	0.97	0.00	0.02	0.03	1.00	1.02	1.03
	Winter	24	236	0.65	0.67	0.03	0.02	0.00	0.00	0.51	100	0.12	0.05	-0.07	0.91	0.00	0.05	0.06	1.01	1.04	1.05
	Spring	2	12	0.70	0.64	0.01	0.01	0.00	0.00	1.00	100	0.04	0.10	0.07	1.06	0.00	0.02	0.02	1.00	1.02	1.02
	Summer	3	18	0.59	0.68	0.03	0.02	0.00	0.01	0.50	100	0.19	0.00	-0.19	0.82	0.04	0.00	0.04	1.04	1.00	1.04
	Fall	11	80	0.74	0.68	0.02	0.01	0.00	0.01	-0.18	100	0.07	0.12	0.05	1.03	0.00	0.04	0.05	1.00	1.04	1.04
Near-road	EC9830T	82	1,526	0.48	0.13	0.19	0.18	0.01	0.00	0.89	94	0.00	0.40	0.40	1.44	0.16	0.11	0.27	1.14	1.05	1.20
	Downwind	26	328	0.56	0.13	0.21	0.19	0.01	0.00	0.83	92	0.00	0.50	0.50	1.64	0.27	0.07	0.34	1.28	1.04	1.33
	Parallel	11	108	0.33	0.13	0.15	0.14	0.01	0.00	0.60	100	0.04	0.21	0.17	1.17	0.03	0.06	0.09	1.02	1.05	1.08
	Other	66	842	0.47	0.13	0.18	0.17	0.01	0.00	0.90	94	0.00	0.40	0.39	1.43	0.16	0.14	0.30	1.14	1.06	1.21
	Weekday	58	1,071	0.50	0.13	0.20	0.19	0.01	0.00	0.91	93	0.00	0.41	0.41	1.47	0.17	0.11	0.28	1.16	1.04	1.21
	Saturday	12	239	0.49	0.13	0.23	0.21	0.01	0.01	0.85	100	0.00	0.33	0.33	1.38	0.11	0.04	0.15	1.11	1.03	1.14
	Sunday	12	216	0.39	0.13	0.13	0.12	0.00	0.00	0.90	92	0.02	0.42	0.40	1.35	0.17	0.20	0.37	1.09	1.13	1.23
	Winter	25	504	0.48	0.13	0.20	0.18	0.01	0.00	0.91	100	0.00	0.40	0.40	1.46	0.16	0.07	0.23	1.15	1.02	1.18
	Spring	-	-	-	-	-	-	-	-	-	-	-	-	-	-	-	-	-	-	-	-
	Summer	-	-	-	-	-	-	-	-	-	-	-	-	-	-	-	-	-	-	-	-
	Fall	57	1,022	0.48	0.13	0.19	0.18	0.01	0.00	0.88	91	0.00	0.40	0.40	1.43	0.16	0.13	0.29	1.14	1.07	1.21
INDiI	655	8,552	0.67	0.52	0.29	0.28	0.01	0.00	0.45	99	0.21	0.01	-0.19	0.82	0.04	0.03	0.07	1.04	1.03	1.07	
	Downwind	182	1,789	0.69	0.52	0.30	0.28	0.01	0.01	0.44	100	0.18	0.01	-0.17	0.84	0.03	0.03	0.06	1.03	1.03	1.06
	Parallel	53	373	0.62	0.52	0.27	0.26	0.01	0.00	0.15	96	0.24	0.01	-0.24	0.79	0.06	0.05	0.11	1.06	1.04	1.10
	Other	426	3,988	0.68	0.52	0.29	0.27	0.01	0.00	0.52	100	0.18	0.02	-0.16	0.85	0.03	0.03	0.06	1.03	1.03	1.06
	Weekday	496	6,518	0.68	0.52	0.30	0.28	0.01	0.00	0.47	99	0.20	0.01	-0.18	0.83	0.03	0.03	0.07	1.04	1.03	1.06
	Saturday	88	1,184	0.65	0.52	0.28	0.27	0.01	0.01	0.36	100	0.23	0.02	-0.21	0.81	0.04	0.05	0.10	1.04	1.04	1.09
	Sunday	71	850	0.60	0.52	0.25	0.24	0.01	0.00	0.33	99	0.25	0.00	-0.25	0.78	0.06	0.03	0.10	1.06	1.03	1.09
	Winter	133	1,651	0.68	0.54	0.26	0.25	0.01	0.00	0.57	100	0.19	0.02	-0.17	0.84	0.03	0.03	0.06	1.03	1.02	1.06
	Spring	152	1,874	0.65	0.52	0.23	0.22	0.01	0.01	0.34	99	0.17	0.02	-0.14	0.86	0.02	0.04	0.06	1.02	1.03	1.06
	Summer	188	2,611	0.65	0.50	0.34	0.32	0.01	0.00	0.39	100	0.26	0.00	-0.26	0.77	0.07	0.03	0.10	1.07	1.03	1.10
	Fall	182	2,416	0.69	0.52	0.32	0.30	0.01	0.01	0.54	100	0.20	0.01	-0.19	0.83	0.03	0.03	0.07	1.04	1.03	1.07

Urban	INDiI	284	3,519	0.64	0.54	0.13	0.12	0.00	0.01	0.17	99	0.12	0.07	-0.05	0.94	0.00	0.06	0.06	1.00	1.05	1.05
	Downwind	62	610	0.65	0.55	0.14	0.12	0.01	0.01	0.29	98	0.13	0.07	-0.06	0.93	0.00	0.06	0.07	1.01	1.05	1.05
	Parallel	19	153	0.62	0.56	0.06	0.06	0.00	0.00	-0.07	100	0.08	0.07	-0.01	0.98	0.00	0.03	0.03	1.00	1.03	1.03
	Other	160	1,630	0.66	0.55	0.11	0.10	0.00	0.01	0.18	99	0.09	0.08	-0.01	0.98	0.00	0.05	0.05	1.00	1.04	1.04
	Weekday	223	2,811	0.64	0.54	0.13	0.12	0.01	0.01	0.17	99	0.12	0.06	-0.06	0.93	0.00	0.06	0.06	1.00	1.04	1.05
	Saturday	36	412	0.63	0.55	0.11	0.10	0.00	0.01	0.23	100	0.13	0.07	-0.05	0.93	0.00	0.07	0.07	1.01	1.05	1.05
	Sunday	25	296	0.67	0.55	0.11	0.10	0.00	0.01	0.01	96	0.09	0.11	0.02	0.99	0.00	0.10	0.10	1.00	1.07	1.07
	Winter	97	1,440	0.66	0.56	0.10	0.09	0.00	0.01	-0.05	98	0.09	0.09	0.00	0.98	0.00	0.07	0.07	1.00	1.05	1.05
	Spring	61	826	0.68	0.57	0.10	0.09	0.00	0.01	0.45	100	0.07	0.08	0.01	1.00	0.00	0.03	0.03	1.00	1.03	1.03
	Summer	55	539	0.55	0.51	0.15	0.14	0.00	0.01	0.20	100	0.19	0.01	-0.19	0.83	0.03	0.02	0.05	1.03	1.02	1.05
	Fall	71	714	0.64	0.53	0.16	0.15	0.01	0.01	0.21	99	0.14	0.07	-0.07	0.92	0.00	0.08	0.09	1.01	1.06	1.06
Industrial	IGFC	63	533	0.58	0.54	0.12	0.10	0.01	0.01	0.00	100	0.14	0.03	-0.11	0.90	0.01	0.03	0.05	1.01	1.03	1.04
	Downwind 1	9	-	-	-	-	-	-	-	-	-	-	-	-	-	-	-	-	-	-	-
	Parallel 2	13	-	-	-	-	-	-	-	-	-	-	-	-	-	-	-	-	-	-	-
	Other	29	224	0.61	0.53	0.13	0.11	0.01	0.01	0.00	100	0.13	0.05	-0.09	0.92	0.01	0.05	0.06	1.01	1.04	1.05
	Weekday	51	448	0.58	0.54	0.11	0.10	0.01	0.01	-0.06	100	0.14	0.03	-0.11	0.90	0.01	0.03	0.05	1.01	1.03	1.04
	Saturday	4	28	-	-	-	-	-	-	-	-	-	-	-	-	-	-	-	-	-	-
	Sunday	8	57	0.60	0.54	0.14	0.13	0.01	0.00	-0.47	100	0.17	0.04	-0.13	0.87	0.02	0.04	0.06	1.02	1.04	1.06
	Winter	13	138	0.56	0.51	0.11	0.10	0.01	0.01	0.15	100	0.14	0.03	-0.11	0.90	0.01	0.03	0.04	1.01	1.03	1.04
	Spring	15	119	0.60	0.54	0.08	0.06	0.01	0.01	-0.57	100	0.07	0.06	-0.02	0.98	0.00	0.03	0.03	1.00	1.02	1.03
	Summer	24	191	0.58	0.54	0.12	0.11	0.01	0.01	0.26	100	0.15	0.02	-0.13	0.88	0.02	0.03	0.05	1.02	1.02	1.04
	Fall	11	85	0.59	0.54	0.16	0.14	0.01	0.00	0.01	100	0.20	0.02	-0.17	0.85	0.03	0.04	0.07	1.03	1.04	1.07

Acronyms: Back = Modeled background contribution; Com. = Modeled contribution from commercial traffic; F2 = % of model + background within a factor of 2 of observed; FB = Fractional bias; fp = false positive; fn = false negative; ICHEM = Instrumental Chemiluminescence; IGpCHEM = Instrumental Gas-Phase Chemiluminescence; Irr = Irreducible or systematic component of VG; Model = Modeled contribution from commercial, non-commercial and point sources; Ncom. = Modeled contribution from non-commercial traffic; NMSE = Normalized mean squared error; Obs. = Observed concentrations; Point = Modeled contribution from point sources; R_{SP} = Spearman's correlation coefficient; Red = reducible or random component of VG; VG = geometric variance. Δ = Total FB; Σ = Sum of Irr. and Red. NMSE; \prod = Product of Irr. and Red. VG.

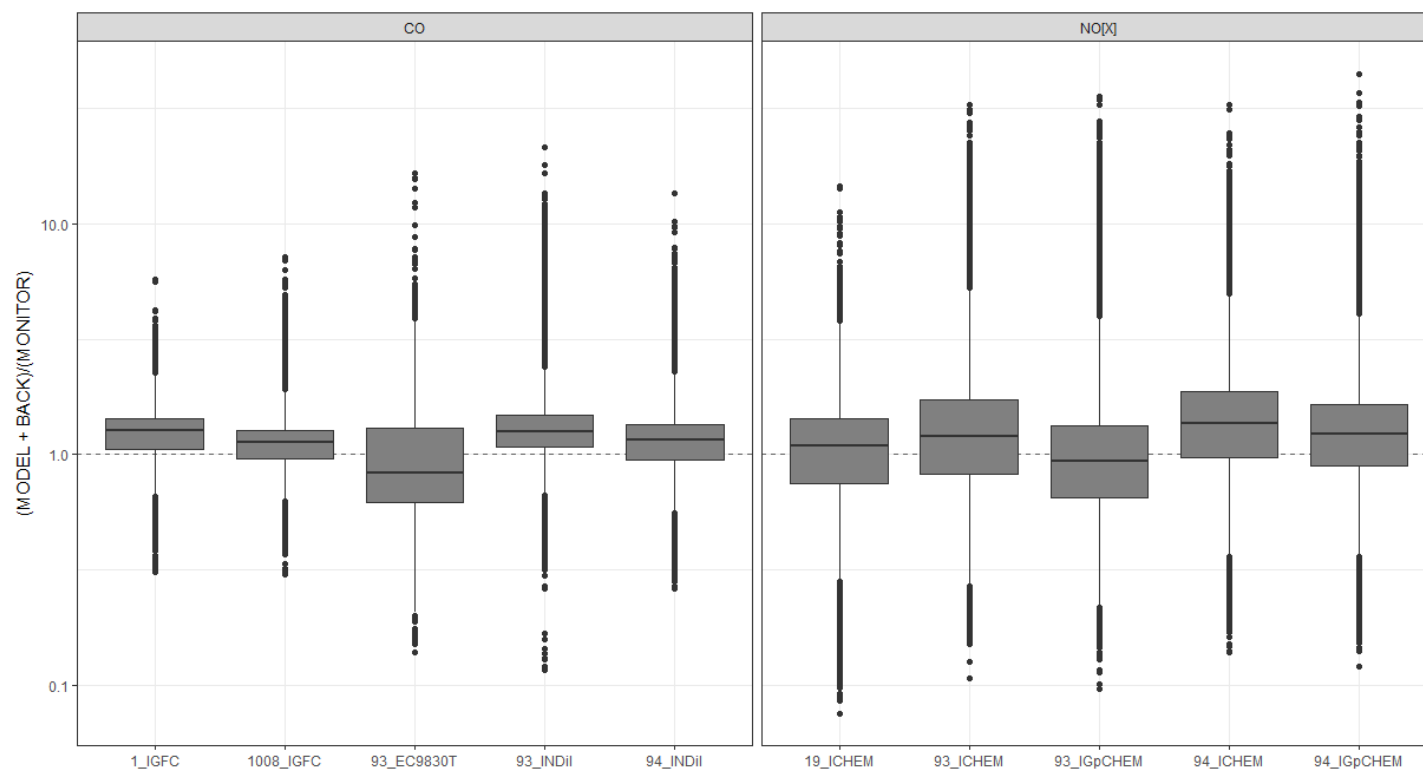


Figure A. 1. Comparison of the ratio between predicted and observed concentrations of CO and NO_x at each monitoring site. The x-axis labels describe the AQS Site and the sampling device used.

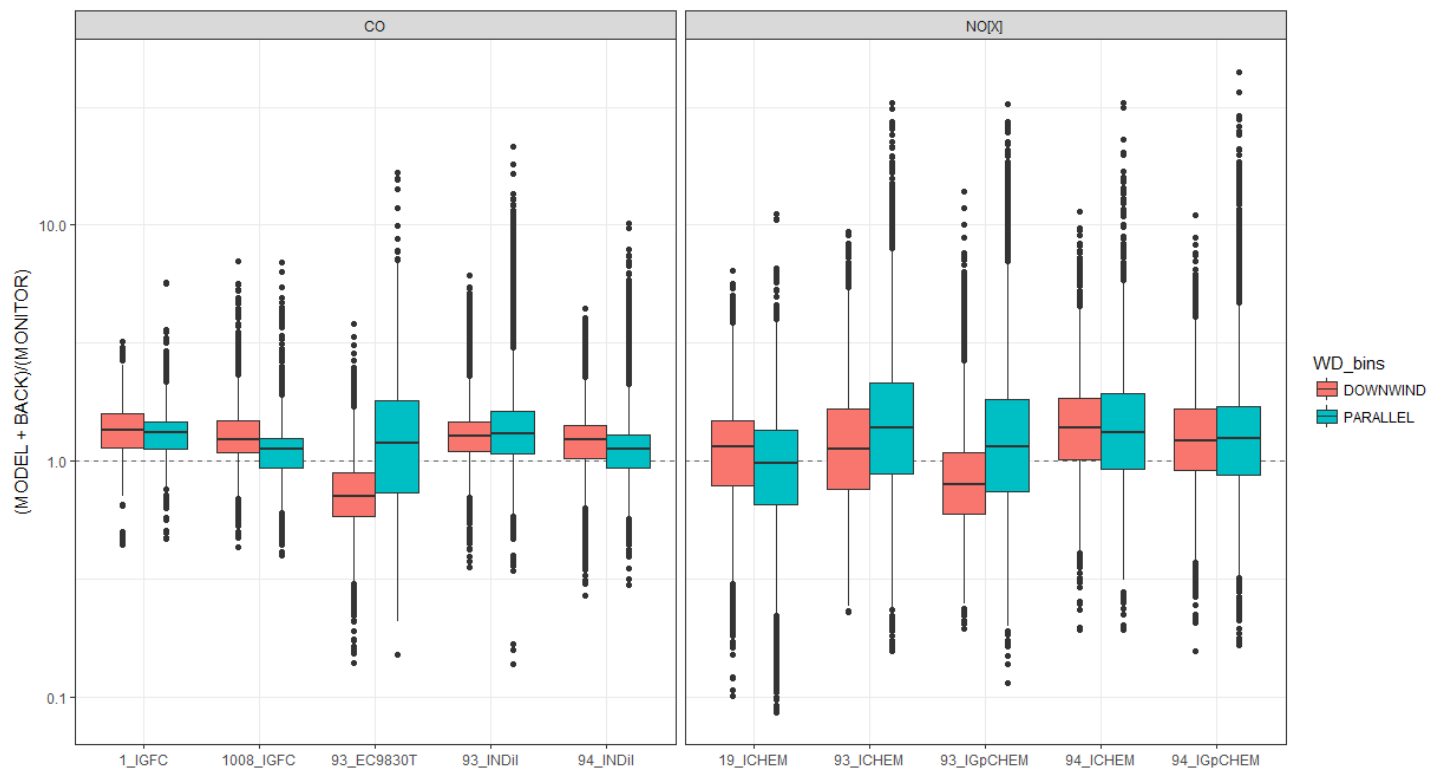


Figure A. 2. Comparison of the ratio between predicted and observed concentrations of CO and NO_x at each monitoring site, differentiated by prevailing wind direction (either downwind or parallel winds). The x-axis labels describe the AQS Site and the sampling device used.

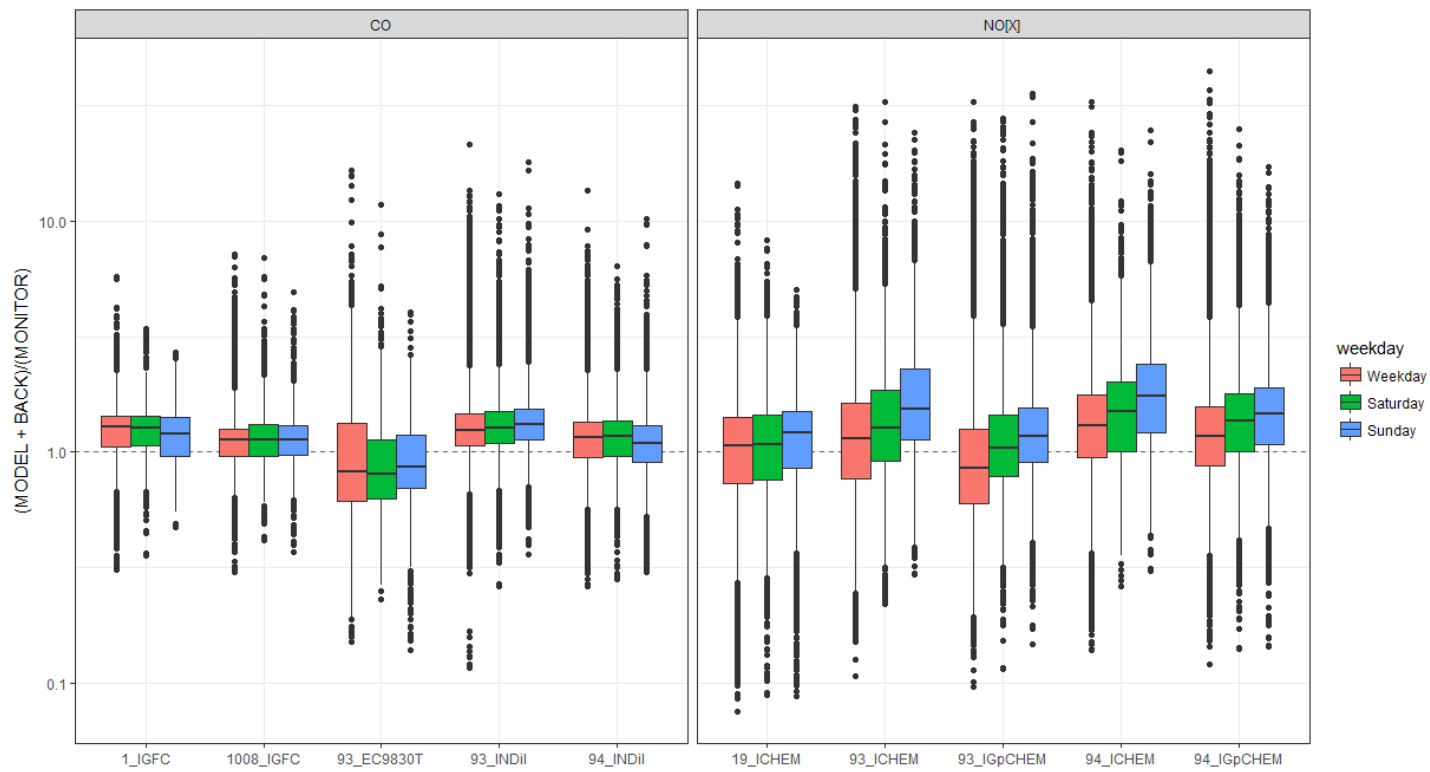


Figure A. 3. Comparison of the ratio between predicted and observed concentrations of CO and NO_x at each monitoring site, differentiated by day-of-week. The x-axis labels describe the AQS Site and the sampling device used.

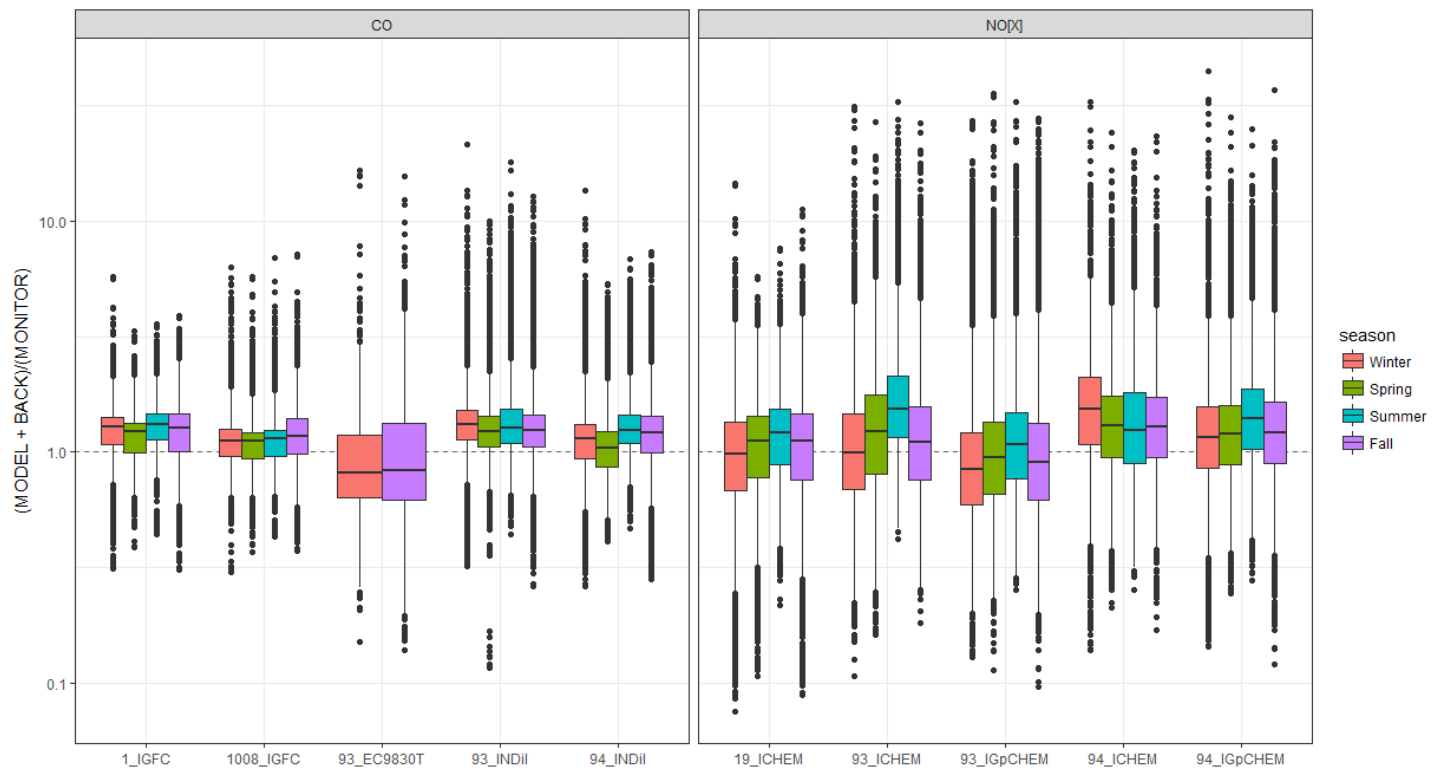


Figure A. 4. Comparison of the ratio between predicted and observed concentrations of CO and NO_x at each monitoring site, differentiated by season. The x-axis labels describe the AQS Site and the sampling device used.

Chapter V – Sensitivity analysis of the near-road dispersion model RLINE - an evaluation at Detroit, Michigan

V.1 Summary

This chapter examines the sensitivity of exposure estimates for health applications produced by dispersion models to meteorological, emission and traffic allocation inputs. The analysis used the Research Line source model (RLINE), a research-grade dispersion model specifically designed for near-road applications [43], to predict daily average concentrations of two common TRAP, oxides of nitrogen (NO_x) and carbon monoxide (CO). These concentrations were compared to measurements at near-road monitoring sites in Detroit, MI, and were used to assess the potential for exposure measurement error in cohort and population-based studies. $\text{PM}_{2.5}$ was also measured at near-road monitoring stations in Detroit; however, previous analyses [92] showed that background levels of $\text{PM}_{2.5}$ were high ($> 85\%$ of total), thus the sensitivity to changes in mobile source modeling were not examined. The analysis shows considerable sensitivity to meteorological inputs; generally, the best performance was obtained using data specific to each monitoring site. An updated emission factor database provided some improvement, particularly at near-road sites, while the use of site-specific diurnal traffic allocations did not improve performance compared to simpler default profiles.

V.2 Results

At four of the monitoring sites (all but the industrial site), both NO_x and CO predictions met recommended performance criteria [55, 56], specifically, $F2 \geq 50\%$, $V_G \leq 1.6$, and mean bias $\leq 30\%$ (not considered in this work). These criteria were not met at the industrial site, where performance was poor (e.g., $R_{SP} < 0.1$). While close to I-75 (150 m), CO levels at this site may be affected by many factors that are incompletely known and/or modeled, including emissions from three adjacent and active rail lines and nearby industry (e.g., refining, cement, salt, steel, coke, sludge incineration). In addition, both I-75 and a major arterial (Fort St.) at the site become

elevated to cross the rail lines and the River Rouge. For these reasons, this site was excluded from further analysis.

V.2.1 Sensitivity to meteorological inputs

Comparisons of RLINE predictions were sensitive to the selection of the meteorological inputs (metrics shown in Table 25, indicators shown in Table 26). Generally, the best match to monitored data was obtained using on-site/KDET meteorology. For example, for NO_x at the near-road and urban sites, on-site/KDET meteorology gave the highest R_{SP} (0.57 to 0.74), among the lowest bias, and the lowest V_G . The best performing case (NO_x monitored at the near-road site using the IGpCHEM instrument) also had the lowest % Red with the on-site/KDET data. While the schools site performed better with the NWS data, R_{SP} was low (0.40 to 0.43 with KDTW data, compared to 0.32 for KDET data). Comparing the NWS data both with and without the on-site data, KDET obtained better performance in most cases. CO results were similar, e.g., on-site/KDET data attained among the highest R_{SP} at near-road and urban sites, the best performing case (near-road site, EC9830T method) had the only improvement seen in % Red (although higher bias), and V_G was generally lowered. At sites more distant from roads, performance trends for CO were less clear and often comparable for the four meteorological datasets due to the variation and overlap of R_{SP} and FB across the sites, while V_G and % Red were very similar at most sites.

Analyses by wind direction, weekday and season, while not definitive, again suggested that best performance was attained using on-site/KDET meteorology (Appendix B Tables B. 1 to B. 6). For NO_x , weekday results largely mirrored results discussed earlier, but Saturday and Sunday results were improved (e.g., higher R_{SP}) at only the near-road site (IGpCHEM instrument). By season, only the near-road site followed the overall trend. Interestingly, results by wind direction show better performance using KDTW rather than KDET meteorology at the near-road site. This site is at the western part of the study area and, unlike the other monitoring sites, is about the same distance to KDTW (20 km) and to KDET (22 km). Nevertheless, both NWS datasets gave relatively high R_{SP} at this site (0.57 – 0.70; IGpCHEM monitor). For CO, missing data hampered analyses, but on-site/KDET sometimes improved performance, e.g., this dataset obtained the highest R_{SP} at the near-road (EC9308T method) and urban sites during weekdays and during downwind conditions, and during winter at the near-road site (EC9830T) other site had lower bias and V_G using on-site/KDET. However, the other CO results were inconsistent, e.g., on-site/KDET

meteorology increased bias and V_G during downwind conditions at the near-road and urban sites, and parallel winds lowered R_{SP} at the urban site. Changes at the suburban mostly fell below the significance threshold (e.g., 0.05 for R_{SP}).

V.2.2 Emission factors

The updated (2015) emission factors mostly did not change R_{SP} for NO_x , though FB and V_G were lowered (i.e., improved) in three cases (at the near-road/ICHEM and urban sites; Table 27). CO showed similar but less consistent effects. Results for downwind and parallel winds suggested improvements for NO_x using the updated emission factors, e.g., R_{SP} increased and bias decreased at the near-road/ICHEM and urban sites, V_G increased at the same sites, and % Red decreased at the near-road/IGpCHEM site. For CO, the updated dataset did not change R_{SP} for downwind and parallel winds, but % Red was lowered at the near-road/EC9830T site, and bias and V_G were lowered at the other sites.

Day-of-week analyses for NO_x showed that the updated emission factors improved R_{SP} , bias and V_G on weekdays (all sites) and Saturdays and Sundays (most sites) (Appendix B Tables B.7 to B.12). Day-of-week analysis for CO gave similar trends, e.g., the updated emission factors lowered bias and V_G at the near-road/INDiI site across all day types. Seasonal trends were less consistent. For NO_x , the updated emission factors improved R_{SP} at the near-road and urban/IGpCHEM sites, and lowered bias and V_G at the urban site in winter; effects in other seasons were less consistent. For CO, investigations were hampered by missing data, but results with the updated inventory showed some improvements, e.g., in winter and fall, % Red decreased at the near-road site, and bias and V_G were lowered in most cases, and in spring and summer, bias and V_G were lowered at the near-road/INDiI and industrial sites.

V.2.3 Temporal Allocation Factors

The three sets of TAFs yielded few differences above significance thresholds in either NO_x and CO predictions. Thus, the Detroit-specific TAFs that separated commercial and non-commercial traffic did not perform better than the simpler and default TAFs. Given the large changes in the hourly profiles, this lack of sensitivity to the TAFs is surprising. It might result from the use of daily averages in the evaluation, which could mask hourly changes, or other compensating errors.

V.2.4 Exposure estimates

Predictions of daily average NO_x concentrations using the KDET and KDTW meteorology respectively at the NEXUS receptors averaged 12.5 and 15.6 µg m⁻³, higher than those at the Detroit receptors (8.3 and 11.1 µg m⁻³), reflecting locational differences between the receptor sets, and in particular, the proximity of many NEXUS participants to major roads (Table 29).

Scatterplots of daily NO_x predictions comparing predictions using KDET and KDTW meteorology for receptor sets 2 (NEXUS) and 3 (Detroit receptors) show high correlation ($R_{SP} > 0.85$) on most days (Figure 28). Somewhat lower correlations on a few days (e.g., for 8/28/2011, NEXUS $R_{SP} = 0.81$ and Detroit $R_{SP} = 0.79$) were due to relatively large changes at a subset of receptors located across the area; otherwise no systematic spatial or other pattern was observed on these days. The most striking observation, however, of this comparison are the large day-to-day shifts in the bias between predictions using KDET and KDTW meteorology. Of the 30 days modeled, predictions using KDTW meteorology were biased upwards on 16 days, downwards on 3 days (4/6/2011, 5/12/2011, 9/21/2011), and similar on the remaining 11 days. These results, which include weekdays and weekends, are attributable solely to the meteorological inputs. (Stratification by season, day type and other factors was not attempted due to the limited sample size.) These changes appear to be driven by wind speed and stability effects, and receptors clustered within about 100m of M-10 and I-94 were especially affected (Figure 29). These large changes were unexpected since daily averages and meteorological parameters at the two NWS sites were highly correlated (Table 28).

The positive prediction bias at the NEXUS and Detroit receptors was reflected in predicted health outcomes. The average attributable health impact differed significantly between KDET and KDTW on all but one of the 30 days modeled, and KDTW meteorology increased the frequency of adverse outcomes on most days, especially for the NEXUS cohort (Table 30). Similarly, when outcomes were pooled across receptors and days, differences in average attributable cases at NEXUS receptors exceeded those for the Detroit receptors (Table 31).

V.3 Discussion

V.3.1 Meteorology

The sensitivity of RLINE results to meteorological inputs highlights the importance of appropriate input data. Some results tended to differ by site. For the sites nearest roads, on-site/KDET followed

by KDET performed best, e.g., attaining the highest R_{SP} . At the suburban and urban sites, performance with KDET data also was better than with KDTW, but NWS data performed better than on-site. These sites are farther from major roads, and monitored concentrations likely result from multiple emission sources and not just traffic on the nearby road. In these cases, on-site meteorological measurements may be less representative for dispersion modeling than airport data, at least under some source and meteorological conditions, e.g., ground level emissions during calms, and NWS data may better represent the conditions affecting dispersion from roadways. Prior dispersion modeling in Detroit has judged both NWS sites to be representative, e.g., modeling of SO_2 emitted from mostly elevated point sources used KDTW [127], while TRAP modeling used KDET [185]. As noted, individual meteorological parameters, e.g., wind speed or direction, typically are highly correlated between the nominal and alternative inputs, although some differences were identified, especially at the suburban site (Table 28). However, the combined effect of different meteorological datasets is best determined by sensitivity analyses examining pollutant predictions.

Application to the NEXUS and Detroit receptors receptor sets showed that meteorological datasets obtained at NWS stations 18 km or more apart can make large differences in daily concentration predictions on some days, which supports findings from comparisons at the monitoring sites. Both NWS are at airports, and the surrounding terrain is flat and mostly urban, commercial, wooded, or agricultural. The differences in predicted concentrations likely result from changes in atmospheric stability that alters near-road concentration gradients, possibly due to very stable conditions which can cause the highest concentrations [43]. This suggests the possibility of significant exposure measurement error if the meteorological data are not representative, e.g., measured at a distant site. Moreover, errors may be higher for more vulnerable populations, as portrayed by the NEXUS receptors for children who lived close to major roads.

Due to siting and instrumentation limitations, relatively few air quality monitoring sites, including the near-road sites, measure all of the meteorological parameters required for research or regulatory-grade dispersion modeling. Thus, local measurements were blended together with NWS (or other) observations. While this approach is workable, incorporated in the AERMET processor, and generally obtained the best performance in the Detroit application, a full set of local measurements may be preferable for obtaining wind fields that are the most representative of near-

road environments. This option, which could not be fully tested in Detroit, leads to a recommendation to collect a full set of local meteorological measurements for dispersion modeling when practicable (including factors such as ground cover, surface roughness, and other factors that affect the spatial variation in wind fields). This reinforces long standing model guidance that recognizes the increased heat flux and surface roughness in urban areas and the general need for multiple monitoring sites in large urban areas [60, 186]. However, no specific guidance is yet provided for near-road modeling. For larger roads in urban settings, such modeling involves winds, emissions and pollutant dispersion transitioning from the road “microenvironment,” defined by large paved areas (e.g., portions of the right-of-way for I-96 in Detroit exceeds 150 m in width as each traffic direction includes three local and three express lanes, a two lane service road, multiple shoulders, and some vegetated buffers), to the adjacent populated “microenvironment,” which can be mostly suburban in nature, dominated by buildings and trees and with relatively fewer flat paved surfaces. Guidance defining the most representative meteorological data for traffic-related emissions in such settings, which differs from the general urban environment, would improve near-road predictions.

V.3.2 Emission factors

The performance analysis suggested that RLINE performed slightly better using the alternative emission factors as compared to nominal ones. The alternative inputs substantially changed emission factors for several vehicle classes, e.g., overall emissions from light duty gas vehicle (LDGV) and heavy duty diesel vehicle (HDDV) classes decreased by 48 and 30% for NO_x , and by 30 and 23% respectively for CO (Table 32 and Table 33); changes at certain speeds and temperatures could be larger. To help interpret these changes as well as traffic activity estimates, which are frequently reduced to vehicle counts (see next section), emission factor differences among vehicle classes can be expressed as passenger car equivalents (PCEs) [132, 187]. As examples, using LDGV emissions as a base: NO_x emissions from a single HDDV represent 12 to 63 PCEs; CO emissions represent only 0.2 to 1.3 PCEs; and both NO_x and CO PCEs increase at lower speeds and colder temperatures (Table 34). The large changes in NO_x emission factors suggest that emission estimates can be very sensitive to the estimated traffic activity (e.g., commercial traffic counts), especially during cold weather and congestion when speeds are lower and the PCEs are high. The temperature and pressure dependence of MOVES-generated emission factors might partially mask modeled differences in predicted concentrations obtained using

different emission factor sets, although the post-processing steps taken (e.g., creating temperature-specific emission factors) may mitigate this effect. Alternatively, changes in fleet mix could also have a large impact on emission. factor changes also depend on the fleet mix. Our fleet mix estimates for commercial vehicles (which are mostly diesel) in Detroit range from 3 to 5% on most roads to 9% on portions of major roads, e.g., I-75 and I-94 (Table 35). Considering a NO_x PCE of 20 and 5% HDDVs, emissions from HDDVs and LDVs are equivalent, which shows the need to obtain accurate traffic activity data.

Uncertainty in mobile source emission inventories can arise from many sources, e.g., the representation of the road network geometry, uncertainty in traffic activity (e.g., vehicle-kilometers traveled or VKT, volume, vehicle type and age, speed, acceleration, and the number of cold starts), uncertainty in emission factors estimates for engine exhaust noted above [188–190]. These factors can vary temporally and spatially. Other notable factors include a lack of traffic counts and on-road emission measurements, and discrepancies between fleet classifications and VKT needed by models and the available statistical summaries [128, 191]. Because fleet mix and VKT data usually are collected and aggregated at the county level, data may not be representative of the city or the roads of interest. As noted above, even modest changes in the commercial fraction of traffic may significantly affect emissions since, for NO_x, one HDDV can emit the equivalent of many passenger cars. This may be especially important in Detroit given the considerable through-traffic of commercial vehicles (mostly HDDVs) crossing the Ambassador Bridge to or from Canada via along I-75 and I-94, which may have the effect of increasing the HDDV fraction among these roads and boosting NO_x emissions. NO_x also may have been underestimated since the simplified emission factors averaged out higher emissions from cold starts. While these issues may be less important for mobile source inventories when aggregated to the annual average and city-wide level, these issues may be important for estimating spatially- and temporally resolved exposures.

V.3.3 Temporal allocation factors

The three sets of TAFs yielded few differences above significance thresholds in either NO_x and CO predictions. Thus, the alternative Detroit-specific TAFs that separated commercial and non-commercial traffic did not perform better than the nominal TAFs. This result was unanticipated, especially for NO_x, given the differences between commercial and non-commercial vehicles, and

the differences seen in the simplified analyses (discussed previously). The fairly large hour-to-hour differences in TAFs at the hourly level may be “washed out” at the daily level or just not observable given other errors and uncertainties. In addition, the local TAFs were based on only the larger Detroit area roads equipped with permanent traffic monitoring recorders. Smaller roads can account for a sizable fraction of TRAP emissions, e.g., based on the Detroit link-based inventory [128], the smaller (non-trunkline) roads accounted for 60% of total VKT in 2010. Our calculations show VKT for all vehicles and commercial vehicles increasing by 1 and 2 % per year, similar to a recent SEMCOG report [192]. The use of local TAFs might improve modeling at the hourly level, which was beyond the present scope, as has been suggested elsewhere [193].

V.3.4 Application

The large differences in predictions that occurred on a few days (see Figure 28 and Figure 29), while uncommon, can result from changes in atmospheric stability that alters the near-road concentration gradient. Thus, while KDTW and KDET obtain mostly similar measurements, the hours or days that differ can cause potentially large impacts on the estimated health impacts. This possibility may increase when meteorological data are obtained at a distant site or is not representative of local conditions. For this simple application, predicted exposures differed significantly using the two NWS datasets, and the effect was magnified for the vulnerable population. Thus, effects due to exposure measurement errors may be magnified among sensitive populations, as seen by the greater difference in the NEXUS sample.

The spatial nature of NEXUS homes likely places a role in the above effect. Distances to the nearest “major” road, i.e., AADT > 10,000 (a conservative cut-point for distinguishing high trafficked roads), were calculated for receptors in sets 2 and 3 (Figure 30). For the NEXUS receptors, 61% were within 200 m, 20% within 200 – 400 m, and 19% beyond 400 m; for the Detroit receptors, these three groups contained 57, 29 and 13% of the population-weighted receptors, respectively. The differences between receptor sets 2 and 3 reflect the design of the NEXUS study which selected households that were near major roads (<200 m) as well as comparison households that were further away (>350 m), however, differences are somewhat diminished since many NEXUS children moved during the study period. We also calculated the number of major roads within 500 m of each receptor. For the NEXUS receptors, 10% of receptors had no major roads within 500 m, 66% had between 1 and 10 major roads within 500 m, and 23%

had more than 10 major roads within 500 m; for Detroit receptors, the corresponding percentages are 7, 74 and 17%, respectively. Thus, not only are NEXUS receptors closer to major roads, they are also closer to more major roads than the general Detroit population.

V.3.5 Comparison to Literature

The sensitivity of dispersion model results and model-based exposure estimates to input data has been explored, however in scenarios with limited generalizability. A city-scale study (189 km²) that used the Atmospheric Dispersion Modelling System (ADMS) to simulate industrial mercury emissions in northwestern England showed that varying meteorological inputs (e.g., meteorological station, release point temperature) changed population-weighted exposures by up to 16% [62]. Meteorological inputs also produced the largest variability (compared to other inputs) in exposures in a study using ADMS to simulate traffic-related emissions of PM₁₀ [194]. A local-scale study (8 km²) that used AERMOD and the Industrial Source Complex Short Term model (ISCT3) to simulate hexavalent chromium emissions from a shipbuilding facility in California showed similar dependence (25% variation) on meteorological inputs [63]. The variations owing to meteorological data in these studies on non-TRAP pollutants were similar to results found in this work. As well, an assessment of airport and local meteorological data used in urban canyon models found that use of local data improved results [57]. However, with reference to the present application, these applications have not studied traffic-related pollutants, which are of concern in urban areas, used recent roadway dispersion models, or commented on the potential influence on sensitive near-road communities.

V.3.6 Limitations and Uncertainty

Several limitations and uncertainties are noted. Predictions did not include chemical transformations and cold start emissions. The summary comparisons of modeled and monitored concentrations used a chosen threshold (0.05) to denote differences in the performance measures, which does not imply statistical significance. The computational burden limited the number of days that could be simulated, and thus seasonal and day-of-week analyses were not attempted. Exposures and health outcomes were based on point estimates of the concentration-response coefficient, and consideration of the confidence intervals may dampen observed results. We did not consider statistical power, or how results might vary given different samples of Detroit receptors (e.g., a population-weighted sample). There was an issue with identifying the sampling

instrument at certain sites, which was not resolved – however, the sampling method and detection limit for all were identified. Some sources of potential errors pertaining to near-road modeling may be important, but were not examined, e.g., geospatial errors in the road network linearization. The exposure results did not account for indoor/outdoor relationships or time-activity information, e.g., the time children spent at school. We had insufficient data to distinguish results by season.

V.4 Tables

Table 25. Data for Summary of sensitivity analysis for meteorology inputs, showing results of performance evaluation for NO_x and CO for three comparisons.

Metric	NWS	w/ onsite	NO _x						CO				
			Schools ICHEM	Near-road ICHEM	Near-road IGpCHEM	Urban ICHEM	Urban IGpCHEM	Suburban IGFC	Near-road EC9830T	Near-road INDil	Urban INDil	Suburban IGFC	
Rsp	DET	x	0.32	0.58	0.74	0.57	0.58	0.21	0.89	0.45	0.17	0.00	
			0.43	0.56	0.67	0.57	0.54	0.41	0.86	0.44	0.18	-0.04	
	DTW	x	0.32	0.41	0.65	0.50	0.54	0.13	0.76	0.41	0.07	0.02	
			0.40	0.36	0.57	0.48	0.52	0.22	0.75	0.39	0.10	-0.10	
FB_total	DET	x	0.15	-0.01	0.23	-0.13	-0.06	-0.04	0.40	-0.19	-0.05	-0.11	
			-0.01	-0.29	-0.05	-0.35	-0.29	-0.23	0.12	-0.35	-0.20	-0.14	
	DTW	x	0.20	-0.13	0.09	-0.21	-0.12	-0.03	0.21	-0.25	-0.11	-0.10	
			0.04	-0.40	-0.14	-0.43	-0.32	-0.20	0.01	-0.39	-0.24	-0.18	
FB_fn	DET	x	0.22	0.17	0.28	0.09	0.09	0.07	0.40	0.01	0.07	0.03	
			0.12	0.06	0.12	0.02	0.03	0.00	0.17	0.00	0.03	0.02	
	DTW	x	0.26	0.13	0.20	0.07	0.07	0.09	0.26	0.01	0.05	0.04	
			0.16	0.06	0.09	0.02	0.03	0.02	0.14	0.00	0.02	0.03	
VG	DET	x	1.13	1.19	1.15	1.15	1.10	1.05	1.20	1.07	1.05	1.04	
			1.09	1.35	1.15	1.27	1.21	1.07	1.09	1.17	1.10	1.05	
	DTW	x	1.15	1.28	1.15	1.20	1.12	1.06	1.14	1.10	1.06	1.05	
			1.11	1.56	1.22	1.39	1.25	1.08	1.11	1.22	1.12	1.08	
VG_red	DET	x	1.12	1.18	1.11	1.12	1.09	1.04	1.05	1.03	1.05	1.03	
			1.09	1.19	1.15	1.12	1.11	1.01	1.07	1.04	1.06	1.03	
	DTW	x	1.13	1.23	1.15	1.12	1.09	1.05	1.10	1.04	1.04	1.04	
			1.11	1.27	1.18	1.14	1.11	1.04	1.11	1.05	1.06	1.05	

Table 26. Summary of sensitivity analysis for meteorology inputs, showing results of performance evaluation for NO_x and CO for three comparisons. Symbols: ● = improved/supporting, ○ = diminished/contrary, ~ = comparable, ‘ ’ indeterminate (sets overlap by more than the minimum of 0.05 and 50% of the smaller within-set range). (See Table 25 for underlying data.)

Metric	Supporting argument	NO _x						CO			
		Schools ICHEM	Near-road ICHEM	Near-road IGpCHEM	Urban ICHEM	Urban IGpCHEM	Suburban IGFC	Near-road EC9830T	Near-road INDii	Urban INDii	
R _{SP}	On-site/KDET highest?	○	~	●	~	~	○	~	~	~	
	KDET > KDTW?		●	●	●	●	●	●	●	●	
	On-site > NWS?	○		●		●	○				
FB	On-site/KDET lowest?	○	●	○	●	●	~	○	●	●	
	KDET < KDTW ?										
	On-site < NWS ?	○		○				○			
V _G	On-site/KDET lowest?	~	●	~	~	~	~	○	~	~	
	KDET < KDTW?						●				
	On-site < NWS?	○	●	●	●	●	●	○	●	●	
% Red	On-site/KDET lowest?	○	○	●	○	○	○	●	○	○	
	KDET < KDTW?							●			
	On-site < NWS?	●	○		○	○	○	●	○	○	

Table 27. Summary of sensitivity analysis for emission factor inputs, comparing results of performance evaluation for nominal (2010) and alternative (2015) emission inventory. Symbols: ● = improved/supporting, ○ = diminished/contrary, ~ = comparable).

Metric	Supporting argument	NO _x						CO			
		Schools ICHEM	Near-road ICHEM	Near-road IGpCHEM	Urban ICHEM	Urban IGpCHEM	Suburban IGFC	Near-road EC9830T	Near-road INDiI	Urban INDiI	
R _{SP}	2015 inventory highest?	~	~	~	~	~	~	~	~	○	
FB	2015 inventory lowest?	~	●	○	●	●	~	○	●	~	
V _G	2015 inventory lowest?	~	●	~	●	●	~	○	●	~	
% Red	2015 inventory lowest?	~	○	●	○	○	~	●	○	○	

Table 28. Matrix of circulation correlation coefficient for wind direction (upper right values) and Pearson correlation coefficients of wind speeds (lower left values) across sites. Heat map shows sites that have different (red) to similar (green) wind speeds and wind directions.

		Circular correlation of wind directions												
		KDET						KDTW						
		NWS only	Suburban	Industrial	Schools	Near-road	Urban	NWS only	Suburban	Industrial	Schools	Near-road	Urban	
Pearson correlation of wind speeds	KDET	NWS only		0.76	1.00	0.94	0.97	0.90	0.88	0.73	0.88	0.85	0.87	0.84
		Suburban	0.58		0.76	0.81	0.76	0.68	0.72	0.95	0.72	0.74	0.74	0.71
		Industrial	1.00	0.58		0.94	0.97	0.90	0.88	0.73	0.88	0.85	0.87	0.84
		Schools	0.87	0.63	0.87		0.90	0.81	0.86	0.77	0.86	0.89	0.83	0.80
		Near-road	0.89	0.52	0.89	0.75		0.91	0.84	0.73	0.84	0.81	0.90	0.84
		Urban	0.89	0.50	0.89	0.76	0.86		0.76	0.67	0.76	0.74	0.80	0.88
	KDTW	NWS only	0.79	0.51	0.79	0.71	0.70	0.74		0.75	1.00	0.95	0.95	0.91
		Suburban	0.51	0.93	0.51	0.57	0.46	0.45	0.57		0.75	0.77	0.77	0.74
		Industrial	0.79	0.51	0.79	0.71	0.70	0.74	1.00	0.57		0.95	0.95	0.91
		Schools	0.70	0.56	0.70	0.84	0.60	0.64	0.88	0.62	0.88		0.90	0.87
		Near-road	0.71	0.46	0.71	0.61	0.83	0.73	0.89	0.51	0.89	0.76		0.92
		Urban	0.73	0.46	0.73	0.64	0.71	0.85	0.92	0.49	0.92	0.79	0.88	

Table 29. Annual (2011) average NO_x concentrations (µg m⁻³) predicted at NEXUS and Detroit receptors using KDET and KDTW meteorology.

NWS station	NEXUS	Detroit
KDET	12.5	8.3
KDTW	15.6	11.1

Table 30. Difference in average attributable cases (per 10⁻⁴) of various health outcomes predicted using KDET and KDTW meteorology; difference < 0 indicates outcomes predicted using KDTW were greater than those for KDET. Only 1 day (3/25/2011) did not show significant ($\alpha = 0.05$) differences.

	Asthma ED visit		Asthma exacerbation		Hospitalization due to asthma		Hospitalization due to COPD	
	NEXUS	Detroit	NEXUS	Detroit	NEXUS	Detroit	NEXUS	Detroit
1/12/2011	-0.055	-0.045	-89.8	-77.9	-1.39E-03	-1.10E-03	-0.046	-0.044
1/24/2011	-0.108	-0.081	-210.4	-156.5	-2.87E-03	-2.15E-03	-0.072	-0.066
2/5/2011	-0.054	-0.043	-90.7	-75.4	-1.30E-03	-1.06E-03	-0.047	-0.042
2/17/2011	-0.011	-0.008	-19.2	-13.9	-2.62E-04	-1.88E-04	-0.010	-0.008
3/1/2011	-0.070	-0.051	-116.5	-89.4	-1.84E-03	-1.30E-03	-0.053	-0.047
3/13/2011	-0.010	-0.009	-16.5	-14.3	-2.50E-04	-1.99E-04	-0.010	-0.009
3/25/2011								
4/6/2011	0.062	0.040	113.2	74.5	1.55E-03	1.01E-03	0.050	0.038
4/18/2011	-0.007	-0.009	-13.4	-17.7	-1.87E-04	-2.26E-04	-0.007	-0.010
4/30/2011	-0.019	-0.013	-32.7	-22.9	-4.65E-04	-3.22E-04	-0.018	-0.014
5/12/2011	0.070	0.048	125.9	87.7	1.76E-03	1.21E-03	0.060	0.049
5/24/2011	-0.007	-0.005	-11.6	-9.5	-1.61E-04	-1.27E-04	-0.007	-0.006
6/5/2011	-0.042	-0.033	-77.5	-58.9	-1.12E-03	-8.13E-04	-0.039	-0.034
6/17/2011	-0.045	-0.032	-77.1	-55.5	-1.11E-03	-7.52E-04	-0.039	-0.032
6/29/2011	-0.058	-0.043	-98.7	-74.5	-1.39E-03	-1.03E-03	-0.053	-0.045
7/11/2011	-0.004	-0.004	-5.9	-7.5	-6.62E-05	-1.09E-04	-0.004	-0.005
7/23/2011	-0.041	-0.026	-70.6	-47.2	-9.68E-04	-6.47E-04	-0.034	-0.027
8/4/2011	-0.033	-0.024	-53.2	-41.9	-8.09E-04	-5.91E-04	-0.031	-0.026
8/16/2011	-0.119	-0.087	-214.4	-160.0	-3.03E-03	-2.19E-03	-0.091	-0.082
8/28/2011	-0.030	-0.023	-46.8	-39.5	-7.19E-04	-5.44E-04	-0.026	-0.023
9/9/2011	-0.041	-0.033	-66.3	-55.1	-1.04E-03	-7.72E-04	-0.032	-0.030
9/21/2011	0.051	0.033	94.4	62.6	1.25E-03	8.32E-04	0.040	0.032
10/3/2011	-0.032	-0.026	-52.8	-45.6	-7.73E-04	-6.30E-04	-0.027	-0.026
10/15/2011	-0.004	-0.003	-7.9	-5.9	-9.87E-05	-7.43E-05	-0.005	-0.004
10/27/2011	0.056	0.038	107.0	68.3	1.53E-03	9.94E-04	0.044	0.036
11/8/2011	-0.037	-0.031	-72.4	-60.4	-1.03E-03	-8.13E-04	-0.030	-0.030
11/20/2011	-0.006	-0.005	-7.9	-8.4	-1.32E-04	-1.20E-04	-0.005	-0.005
12/2/2011	0.038	0.030	71.8	57.0	1.03E-03	7.90E-04	0.029	0.027
12/14/2011	-0.019	-0.018	-35.3	-32.9	-5.47E-04	-4.70E-04	-0.017	-0.018
12/26/2011	-0.028	-0.019	-47.5	-34.7	-6.55E-04	-4.77E-04	-0.025	-0.020

Table 31. Average attributable cases made using KDET and KDTW meteorology at NEXUS and Detroit receptors for various NO_x related health outcomes. All differences were significant (Wilcoxon signed rank test CI of 95%).

Health outcome	Units	Age group	NEXUS		Detroit	
			KDET mean cases	KDTW mean cases	KDET mean cases	KDTW mean cases
Asthma ED visit	per 10,000	0-17	0.81×10^{-1}	1.01×10^{-1}	4.96×10^{-2}	6.56×10^{-2}
Hospitalization due to asthma	per 10,000	0-64	2.00×10^{-3}	2.50×10^{-3}	1.21×10^{-3}	1.61×10^{-3}
Asthma exacerbation	per 10,000	6-14	1.40×10^2	1.73×10^2	0.87×10^2	1.15×10^2

Table 32. Percent difference in emission factors between average 2010 and 2015 EF for the 8 Highway Performance Monitoring System (HMPS) classes. Blue-filled cells indicate 2015 emission factors which are greater than 2010 emission factors.

Pollutant	HMPS Vehicle Class							
	LDGV	LDGT1	LDGT2	HDGV	MC	LDDV	LDDT	HDDV
CO	30	52	75	67	11	832	13	23
NO _x	48	62	80	49	15	73	57	30

Table 33. Checking the impact of the large change in LDDV EF indicated above.

Vehicle class	NFC 11				
	Fleet Mix	2010 EF (g/VMT)	2010 EF (g /1000VMT)	2015 EF (g/VMT)	2015g / 1000VMT
LDGV	0.784	6.29	4929	4.23	3320
LDGT1	0.12	8.90	1068	4.17	500
LDGT2	0.025	8.90	222	2.15	54
HDGV	0.003	21.26	64	33.99	102
MC	0.005	18.36	92	19.47	97
LDDV	0.008	0.70	6	4.93	39
LDDT	0.002	4.27	9	3.88	8
HDDV	0.053	4.35	231	3.35	177

So in 2010, LDDV contributed 0.1% of the total mass, so even though this increases to 1% in 2015, the significance in a 7-factor increase in LDDV EF is diminished because of the low volume of LDDV in Detroit and because of the overall trend of decreasing mass from vehicles.

Table 34. Ratio between MOVES 2015 emission factors for HDDV to LDGV averaged across months by speed and temperature.

Speed (mph)	Temperature (°F)											Temperature (°F)										
	0	10	20	30	40	50	60	70	80	90	100	0	10	20	30	40	50	60	70	80	90	100
	CO											NO_x										
2.5	1.3	1.3	1.3	1.3	1.3	1.3	1.3	1.3	1.0	0.8	0.7	63	63	63	63	63	64	64	58	42	34	30
5	1.2	1.2	1.2	1.2	1.2	1.2	1.2	1.2	0.9	0.8	0.7	41	41	41	41	41	42	42	39	31	26	24
10	1.1	1.1	1.1	1.1	1.1	1.1	1.1	1.0	0.8	0.6	0.6	29	29	29	29	29	29	30	29	24	22	20
15	1.0	1.0	1.0	1.0	1.0	1.0	1.0	0.9	0.7	0.6	0.5	26	26	26	26	26	26	26	26	23	21	20
20	0.9	0.9	0.9	0.9	0.9	0.9	0.9	0.9	0.7	0.5	0.5	24	24	24	24	24	24	24	24	22	20	19
25	1.0	1.0	1.0	1.0	1.0	1.0	1.0	0.9	0.7	0.6	0.5	22	22	22	22	22	22	22	22	20	19	18
30	0.9	0.9	0.9	0.9	0.9	0.9	0.9	0.8	0.6	0.5	0.5	22	22	22	22	22	22	22	22	20	19	18
35	0.8	0.8	0.8	0.8	0.8	0.8	0.8	0.8	0.6	0.5	0.4	19	19	19	19	19	19	19	19	18	17	16
40	0.8	0.8	0.8	0.8	0.8	0.8	0.8	0.7	0.5	0.4	0.4	18	18	18	18	18	18	18	18	17	16	15
45	0.7	0.7	0.7	0.7	0.7	0.7	0.7	0.7	0.5	0.4	0.4	17	17	17	17	17	17	17	17	16	15	14
50	0.7	0.7	0.7	0.7	0.7	0.7	0.7	0.7	0.5	0.4	0.4	16	16	16	16	16	16	16	16	15	14	13
55	0.7	0.7	0.7	0.7	0.7	0.7	0.7	0.6	0.5	0.4	0.3	15	15	15	15	15	15	15	15	14	13	13
60	0.7	0.7	0.7	0.7	0.7	0.7	0.7	0.6	0.5	0.4	0.3	14	14	14	14	14	15	15	15	13	13	12
65	0.6	0.6	0.6	0.6	0.6	0.6	0.6	0.6	0.4	0.4	0.3	15	15	15	15	15	15	15	15	14	13	13
70	0.5	0.5	0.5	0.5	0.5	0.5	0.5	0.5	0.4	0.3	0.3	15	15	15	15	15	15	15	15	14	13	12
75	0.4	0.4	0.4	0.4	0.4	0.4	0.4	0.4	0.3	0.2	0.2	14	14	14	14	14	14	15	14	13	13	12

Table 35. Aggregated vehicle class fraction by NFC class (i.e., “fleet-mix”).

Vehicle Classifier	Commercial/ Non-commercial	11	12	14	16	17	19
LDGV	Non-commercial	0.784	0.839	0.840	0.857	0.788	0.809
LDGT1	Non-commercial	0.120	0.109	0.109	0.083	0.147	0.151
LDGT2	Commercial	0.025	0.021	0.020	0.019	0.027	0.014
HDGV	Commercial	0.003	0.003	0.003	0.005	0.003	0.002
MC	Non-commercial	0.005	0.006	0.006	0.007	0.009	0.009
LDDV	Both (50-50)	0.008	0.008	0.008	0.009	0.007	0.007
LDDT	Commercial	0.002	0.002	0.002	0.002	0.002	0.001
HDDV	Commercial	0.053	0.012	0.012	0.019	0.016	0.008

V.5 Figures

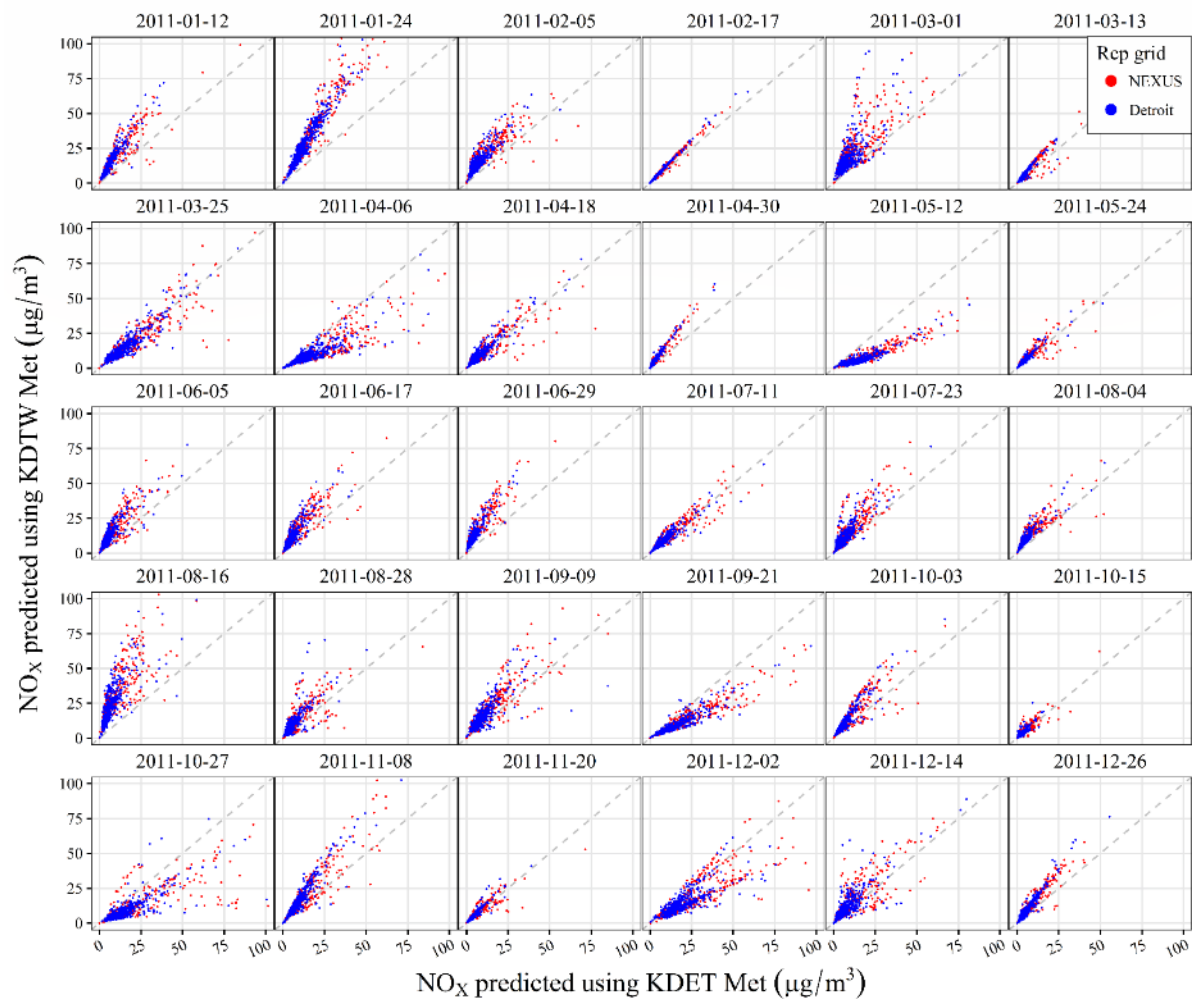


Figure 28. Scatterplots of NO_x predicted using KDET or KDTW meteorology at NEXUS (n=206) and Detroit receptors (n=543) by days. Each plot shows the 1:1 line and is truncated at 100 µg m⁻³.

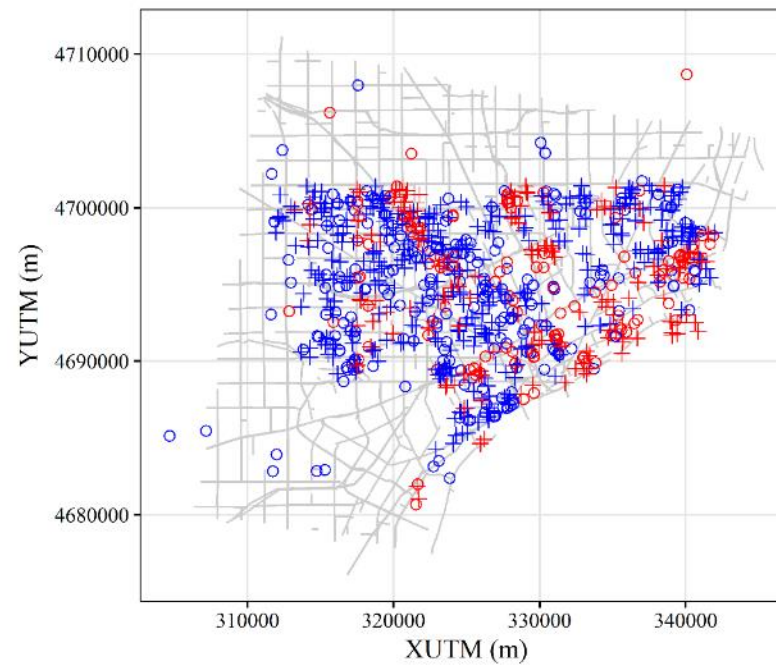
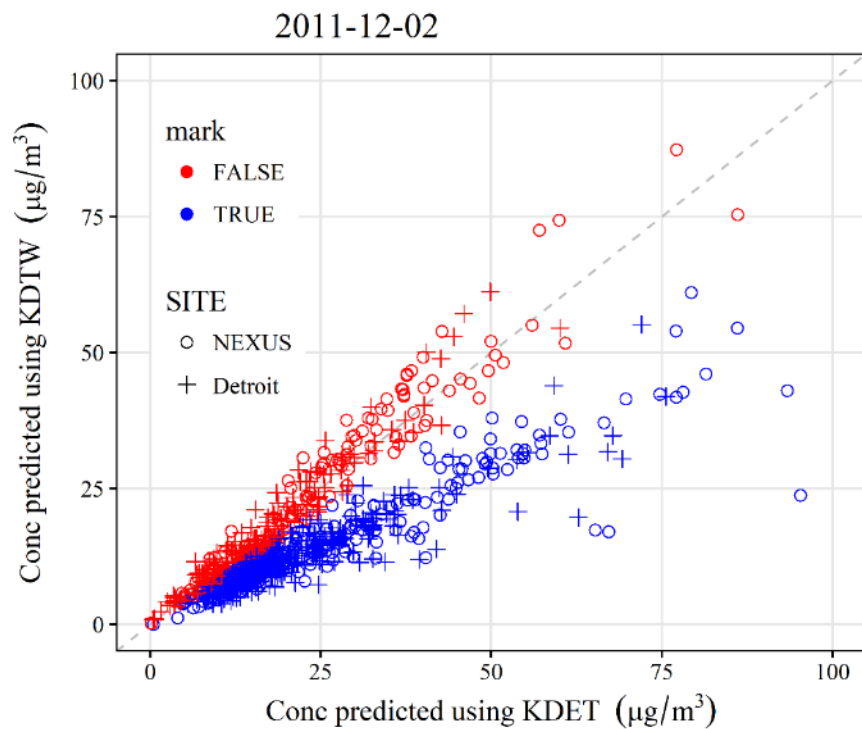


Figure 29. Investigation of spatial relationship of points on 12/2/11 with large discrepancies in the relationship between KDET and KDTW (i.e., ratio of KDTW / KDET > 1.2, depicted as 'mark = T').

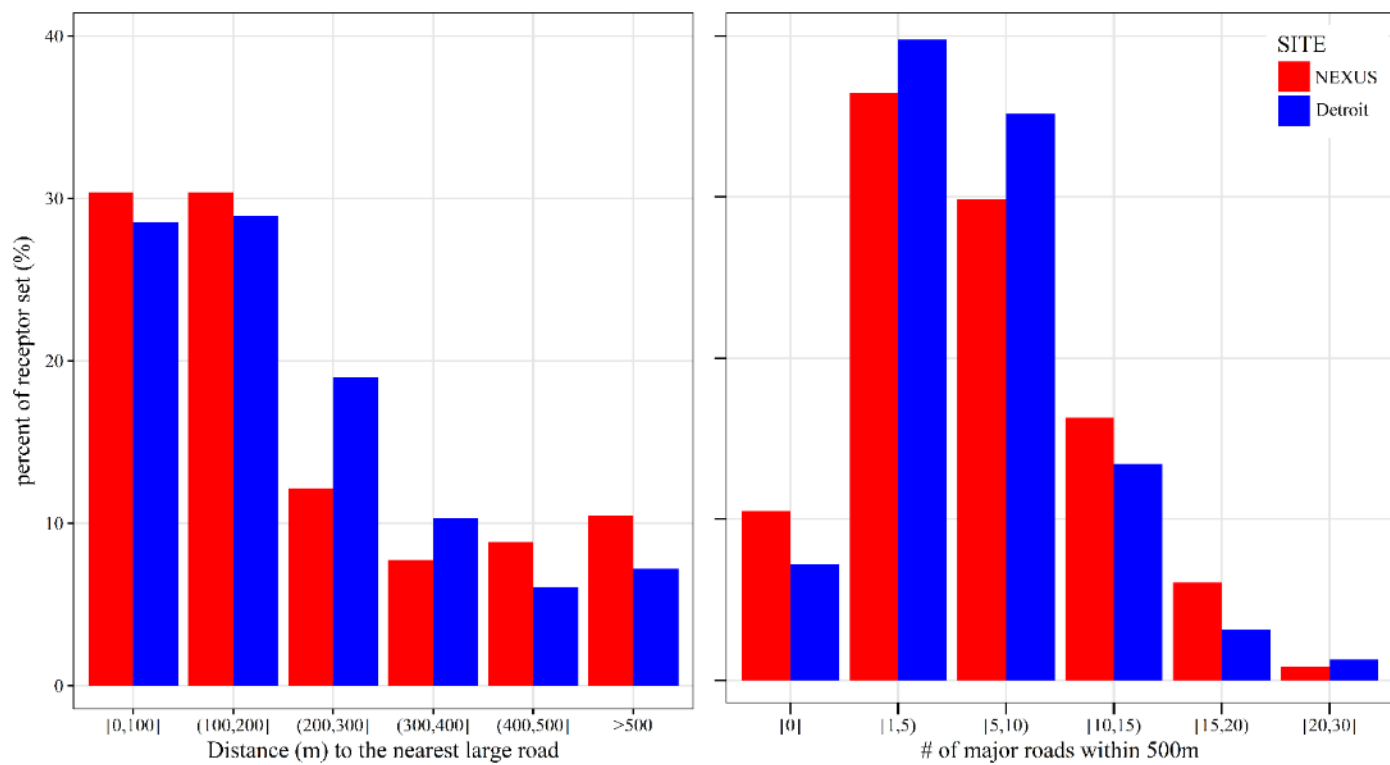


Figure 30. Histograms of distance between receptors to the nearest major (AADT > 10,000) roads, and the number of nearby large roads. Results for both NEXUS and Detroit receptors are shown.

Appendix B – Expanded tables of Model Sensitivity

Table B. 1. Summary of sensitivity analysis for meteorology inputs, showing results of performance evaluation for NO_x, separated by prevailing wind direction (downwind or parallel). Symbols: ● = improved/supporting, ○ = diminished/contrary, ~ = comparable, ‘ ’ indeterminate (sets overlap by more than the minimum of 0.05 and 50% of the smaller within-set range).

		19-ICHEM93-ICHEM93-IGpCHEM94-ICHEM94-IGpCHEM					19-CHEM93-ICHEM93-IGpCHEM94-ICHEM94-IGpCHEM				
		Downwind	Downwind	Downwind	Downwind	Downwind	Parallel	Parallel	Parallel	Parallel	Parallel
RSP	DET ONSITE highest?	○	○	○	●	○	○	○	~	○	○
	DET > DTW?	○	○	○		○		●	●	●	●
	ONSITE > BASE?		●		●	●	○				
BIAS	DET ONSITE lowest?	○	~	○	~	~	○	●	~	~	~
	DET < DTW ?	○									
	ONSITE < BASE ?			○			○				
VG	DET ONSITE lowest?	~	~	○	~	~	○	●	~	●	●
	DET < DTW?	○						●	●	●	●
	ONSITE < BASE?	●	●	○	●	●	○			●	
% RED	DET ONSITE lowest?	~	○	~	○	○	○	○	○	○	○
	DET < DTW?						○		○	●	●
	ONSITE < BASE?		○	●	○	○		○		○	

Table B. 2. Summary of sensitivity analysis for meteorology inputs, showing results of performance evaluation for NO_x, separated by day of week. Symbols: ● = improved/supporting, ○ = diminished/contrary, ~ = comparable, ‘ ’ indeterminate (sets overlap by more than the minimum of 0.05 and 50% of the smaller within-set range), LOW RSP = the spearman R was too low to evaluate trends.

		19-CHEM93-ICHEM93-IGpCHEM94-ICHEM94-IGpCHEM					19-CHEM93-ICHEM93-IGpCHEM94-ICHEM94-IGpCHEM					19-CHEM93-ICHEM93-IGpCHEM94-ICHEM94-IGpCHEM				
		Weekday	Weekday	Weekday	Weekday	Weekday	Saturday	Saturday	Saturday	Saturday	Saturday	Sunday	Sunday	Sunday	Sunday	Sunday
RSP	DET ONSITE highest?	○	~	●	~	●	○	○	●	○	~	○	~	●	○	○
	DET > DTW?		●	●	●	●		●	●	●			●	●		
	ONSITE > BASE?	○		●		●	○	○	●		●	○		●	○	○
BIAS	DET ONSITE lowest?	○	~	○	●	●	○	●	●	●	○	●	●	●	●	~
	DET < DTW ?						○					○				
	ONSITE < BASE ?	○		○			○					○				
VG	DET ONSITE lowest?	~	●	~	~	~	~	●	●	~	~	○	●	●	●	~
	DET < DTW?		●						●							
	ONSITE < BASE?	○	●		●	●	○	●	●	●	●	○	●	●	●	●
% RED	DET ONSITE lowest?	○	○	●	○	○	○	○	○	○	○	○	○	○	○	○
	DET < DTW?															
	ONSITE < BASE?	●	○	●	○	○	●	○	○	○	○	○	○	○	○	○

Table B. 3. Summary of sensitivity analysis for meteorology inputs, showing results of performance evaluation for NO_x, separated by season. Symbols: ● = improved/supporting, ○ = diminished/contrary, ~ = comparable, ‘ ’ indeterminate (sets overlap by more than the minimum of 0.05 and 50% of the smaller within-set range), LOW RSP = the spearman R was too low to evaluate trends.

		19- CHEM Winter	93- ICHEM Winter	93- IGpCHEM Winter	94- ICHEM Winter	94- IGpCHEM Winter	19- CHEM Spring	93- ICHEM Spring	93- IGpCHEM Spring	94- ICHEM Spring	94- IGpCHEM Spring	19- CHEM Summer	93- ICHEM Summer	93- IGpCHEM Summer	94- ICHEM Summer	94- IGpCHEM Summer	19- CHEM Fall	93- ICHEM Fall	93- IGpCHEM Fall	94- ICHEM Fall	94- IGpCHEM Fall
RSP	DET ONSITE highest?	○	~	~	○	○	○	~	●	~	~	~	●	●	LOW RSP	●	○	●	~	~	~
	DET > DTW?	●	●	●	●	●		●	●	●	●	●	●		LOW RSP			●	●	●	○
	ONSITE > BASE?	○			○		○			●			●	●	LOW RSP	●	○		●		●
BIAS	DET ONSITE lowest?	○	○	○	●	~	○	~	○	●	~	~	●	●	LOW RSP	~	○	●	○	●	●
	DET < DTW ?														LOW RSP						
	ONSITE < BASE ?	○	○	○			○		○						LOW RSP		○				
VG	DET ONSITE lowest?	○	~	○	~	~	○	●	~	~	~	~	●	~	LOW RSP	~	~	●	~	~	~
	DET < DTW?				●	●			●						LOW RSP						
	ONSITE < BASE?	○	●	○	●	●	○	●		●	●	●	●	●	LOW RSP	●	○	●	●	●	●
% RED	DET ONSITE lowest?	~	~	●	○	○	○	○	●	○	○	○	○	○	LOW RSP	○	○	○	●	○	○
	DET < DTW?														LOW RSP						
	ONSITE < BASE?	●		●	○	○	●	○	●	○	○	○	○	○	LOW RSP	○		○		○	○

Table B. 4. Summary of sensitivity analysis for meteorology inputs, showing results of performance evaluation for CO, separated by prevailing wind direction (downwind or parallel). Symbols: ● = improved/supporting, ○ = diminished/contrary, ~ = comparable, ‘ ’ indeterminate (sets overlap by more than the minimum of 0.05 and 50% of the smaller within-set range), LOW RSP = the spearman R was too low to evaluate trends.

		1 - IGFC	93 - EC9830T	93 - INDil	94 - INDil	1008 - IGFC	1 - IGFC	93 - EC9830T	93 - INDil	94 - INDil	1008 - IGFC	
		Downwind	Downwind	Downwind	Downwind	Downwind	Parallel	Parallel	Parallel	Parallel	Parallel	
RSP	DET ONSITE highest?		~	○	●			~	○			LOW RSP
	DET > DTW?			○	●			●	●			LOW RSP
	ONSITE > BASE?		●						○			LOW RSP
BIAS	DET ONSITE lowest?		○	~	~			○	~			LOW RSP
	DET < DTW ?		○									LOW RSP
	ONSITE < BASE ?		○									LOW RSP
VG	DET ONSITE lowest?		○	~	~			~	●			LOW RSP
	DET < DTW?		○					●				LOW RSP
	ONSITE < BASE?		○	●	●					●		LOW RSP
% RED	DET ONSITE lowest?		●	○	○			○	○			LOW RSP
	DET < DTW?			○	○			○	●			LOW RSP
	ONSITE < BASE?		●	○	○				○			LOW RSP

Table B. 5. Summary of sensitivity analysis for meteorology inputs, showing results of performance evaluation for CO, separated day of week. Symbols: ● = improved/supporting, ○ = diminished/contrary, ~ = comparable, ‘ ’ indeterminate (sets overlap by more than the minimum of 0.05 and 50% of the smaller within-set range), LOW RSP = the spearman R was too low to evaluate trends.

		1 - IGFC 93 - EC9830T 93 - INDii 94 - INDii 1008 - IGFC					1 - IGFC 93 - EC9830T 93 - INDii 94 - INDii 1008 - IGFC					1 - IGFC 93 - EC9830T 93 - INDii 94 - INDii 1008 - IGFC				
		Weekday	Weekday	Weekday	Weekday	Weekday	Saturday	Saturday	Saturday	Saturday	Saturday	Sunday	Sunday	Sunday	Sunday	Sunday
RSP	DET ONSITE highest?	○	~	~	~	LOW RSP		~	○	○		~	○	○	LOW RSP	
	DET > DTW?	●	●	●	●	LOW RSP		○	●	●		○		○	LOW RSP	
	ONSITE > BASE?					LOW RSP				○			○	●	LOW RSP	
BIAS	DET ONSITE lowest?	~	○	●	●	LOW RSP		○	●	●		○	~	~	LOW RSP	
	DET < DTW ?					LOW RSP						○			LOW RSP	
	ONSITE < BASE ?		○			LOW RSP		○				○			LOW RSP	
VG	DET ONSITE lowest?	~	○	~	~	LOW RSP		○	~	~		○	~	~	LOW RSP	
	DET < DTW?	●				LOW RSP						○			LOW RSP	
	ONSITE < BASE?	●	○	●	●	LOW RSP		○	●	●		○	●	●	LOW RSP	
% RED	DET ONSITE lowest?	○	●	○	○	LOW RSP		●	○	○		●	○	○	LOW RSP	
	DET < DTW?		●			LOW RSP				○			○		LOW RSP	
	ONSITE < BASE?	○	●	○	○	LOW RSP		●	○	○		●	○	○	LOW RSP	

Table B. 6. Summary of sensitivity analysis for meteorology inputs, showing results of performance evaluation for NO_x, separated by season. Symbols: ● = improved/supporting, ○ = diminished/contrary, ~ = comparable, ‘ ’ indeterminate (sets overlap by more than the minimum of 0.05 and 50% of the smaller within-set range), LOW RSP = the spearman R was too low to evaluate trends.

		1 -	93 -	93 -	94 -	1008 -	1 -	93 -	93 -	94 -	1008 -	1 -	93 -	93 -	94 -	1008 -	1 -	93 -	93 -	94 -	1008 -
		IGFC	EC9830T	INDii	INDii	IGFC	IGFC	EC9830T	INDii	INDii	IGFC	IGFC	EC9830T	INDii	INDii	IGFC	IGFC	EC9830T	INDii	INDii	IGFC
		Winter	Winter	Winter	Winter	Winter	Spring	Spring	Spring	Spring	Spring	Summer	Summer	Summer	Summer	Summer	Fall	Fall	Fall	Fall	Fall
RSP	DET ONSITE highest?	○	~	○	○	○			~	●	LOW RSP			●	●	○	LOW RSP	~	~	○	○
	DET > DTW?	●	●					●	●		LOW RSP			●	●	●	LOW RSP	●		●	○
	ONSITE > BASE?			○	○	●			●		LOW RSP			●	●		LOW RSP		●		
BIAS	DET ONSITE lowest?	~	○	●	●	~			~	~	LOW RSP			●	●	~	LOW RSP	○	●	●	~
	DET < DTW ?		○								LOW RSP						LOW RSP				
	ONSITE < BASE ?		○								LOW RSP						LOW RSP	○			
VG	DET ONSITE lowest?	~	○	~	~	~			~	~	LOW RSP			~	~	~	LOW RSP	○	~	~	~
	DET < DTW?					●					LOW RSP						LOW RSP				●
	ONSITE < BASE?	●	○	●	●			●	●		LOW RSP			●	●	●	LOW RSP	○	●	●	
% RED	DET ONSITE lowest?	○	●	○	○	○			○	○	LOW RSP			○	○	○	LOW RSP	●	○	○	○
	DET < DTW?		●			○					LOW RSP			○	○		LOW RSP				●
	ONSITE < BASE?	○		○	○	○			○	○	LOW RSP			○		○	LOW RSP	●	○	○	○

Table B. 7. Summary of sensitivity analysis for emission factor inputs, showing results of performance evaluation for NO_x, separated by prevailing wind direction (downwind or parallel). Symbols: ● = improved/supporting, ○ = diminished/contrary, ~ = comparable, LOW RSP = the spearman R was too low to evaluate trends.

		19 - ICHEM Downwind	93 - ICHEM Downwind	93 - IGpCHEM Downwind	94 - ICHEM Downwind	94 - IGpCHEM Downwind	19 - ICHEM Parallel	93 - ICHEM Parallel	93 - IGpCHEM Parallel	94 - ICHEM Parallel	94 - IGpCHEM Parallel
RSP	2015 highest ?	○	●	~	~	~	~	●	~	~	●
FB	2015 lowest ?	~	●	○	●	●	~	●	○	●	●
VG	2015 lowest ?	~	●	○	●	●	~	●	●	●	●
% Red	2015 lowest ?	~	○	●	○	○	~	○	●	○	~

Table B. 8. Summary of sensitivity analysis for emission factor inputs, showing results of performance evaluation for NO_x, separated by weekday. Symbols: ● = improved/supporting, ○ = diminished/contrary, ~ = comparable, LOW RSP = the spearman R was too low to evaluate trends.

		19 - ICHEM Weekday	93 - ICHEM Weekday	93 - IGpCHEM Weekday	94 - ICHEM Weekday	94 - IGpCHEM Weekday	19 - ICHEM Saturday	93 - ICHEM Saturday	93 - IGpCHEM Saturday	94 - ICHEM Saturday	94 - IGpCHEM Saturday	19 - ICHEM Sunday	93 - ICHEM Sunday	93 - IGpCHEM Sunday	94 - ICHEM Sunday	94 - IGpCHEM Sunday
RSP	2015 highest ?	~	~	~	~	~	○	●	~	~	●	○	●	~	LOW RSP	●
FB	2015 lowest ?	~	●	○	●	●	~	●	●	●	●	~	●	●	LOW RSP	●
VG	2015 lowest ?	~	●	○	●	●	~	●	●	●	●	~	●	●	LOW RSP	●
% Red	2015 lowest ?	~	○	●	○	○	~	○	○	~	○	~	○	○	LOW RSP	●

Table B. 9. Summary of sensitivity analysis for emission factor inputs, showing results of performance evaluation for NO_x, separated by season. Symbols: ● = improved/supporting, ○ = diminished/contrary, ~ = comparable, LOW RSP = the spearman R was too low to evaluate trends.

		19 - ICHE M	93 - ICHE M	93 - IGpCHE M	94 - ICHE M	94 - IGpCHE M	19 - ICHE M	93 - ICHE M	93 - IGpCHE M	94 - ICHE M	94 - IGpCHE M	19 - ICHEM	93 - ICHEM	93 - IGpCHE M	94 - ICHEM	94 - IGpCHE M	19 - ICHE M	93 - ICHE M	93 - IGpCHE M	94 - ICHE M	94 - IGpCHE M
		Winter	Winter	Winter	Winter	Winter	Spring	Spring	Spring	Spring	Spring	Summe r	Summe r	Summer	Summe r	Summer	Fall	Fall	Fall	Fall	Fall
RSP	2015 highest ?	○	~	~	○	~	~	~	~	~	~	~	~	~	LOW RSP	~	~	~	~	~	~
FB	2015 lowest ?	~	○	○	●	~	~	●	○	●	●	~	●	●	LOW RSP	●	~	●	○	●	●
VG	2015 lowest ?	~	~	○	●	●	~	●	~	~	●	~	●	●	LOW RSP	●	~	●	~	●	●
% Red	2015 lowest ?	~	●	●	○	○	~	○	●	○	○	○	○	○	LOW RSP	~	~	○	●	○	○

Table B. 10. Summary of sensitivity analysis for emission factor inputs, showing results of performance evaluation for CO, separated by weekday. Symbols: ● = improved/supporting, ○ = diminished/contrary, ~ = comparable, LOW RSP = the spearman R was too low to evaluate trends.

		1 - IGFC Downwind	93 - EC9830T Downwind	93 - INDil Downwind	94 - INDil Downwind	1008 - IGFC Downwind	1 - IGFC Parallel	93 - EC9830T Parallel	93 - INDil Parallel	94 - INDil Parallel	1008 - IGFC Parallel
RSP	2015 highest ?		~	~	○		~	~	LOW RSP		
FB	2015 lowest ?		○	●	●		○	●	LOW RSP		
VG	2015 lowest ?		○	~	~		~	●	LOW RSP		
% Red	2015 lowest ?		●	○	○		●	~	LOW RSP		

Table B. 11. Summary of sensitivity analysis for emission factor inputs, showing results of performance evaluation for CO, separated by weekday. Symbols: ● = improved/supporting, ○ = diminished/contrary, ~ = comparable, LOW RSP = the spearman R was too low to evaluate trends.

		1 - IGFC 93 - EC9830T 93 - INDil 94 - INDil 1008 - IGFC					1 - IGFC 93 - EC9830T 93 - INDil 94 - INDil 1008 - IGFC					1 - IGFC 93 - EC9830T 93 - INDil 94 - INDil 1008 - IGFC				
		Weekday	Weekday	Weekday	Weekday	Weekday	Saturday	Saturday	Saturday	Saturday	Saturday	Sunday	Sunday	Sunday	Sunday	Sunday
RSP	2015 highest ?	~	~	~	○	LOW RSP	●	~	~	○	LOW RSP	~	●	○	LOW RSP	
FB	2015 lowest ?	~	○	●	~	LOW RSP	~	○	●	~	LOW RSP	○	●	~	LOW RSP	
VG	2015 lowest ?	~	○	●	~	LOW RSP	~	○	●	~	LOW RSP	○	●	~	LOW RSP	
% Red	2015 lowest ?	~	●	○	○	LOW RSP	~	●	○	○	LOW RSP	●	~	~	LOW RSP	

Table B. 12. Summary of sensitivity analysis for emission factor inputs, showing results of performance evaluation for CO, separated by weekday. Symbols: ● = improved/supporting, ○ = diminished/contrary, ~ = comparable, LOW RSP = the spearman R was too low to evaluate trends.

		1 - IGFC	93 - EC9830T	93 - INDil	94 - INDil	1008 - IGFC	1 - IGFC	93 - EC9830T	93 - INDil	94 - INDil	1008 - IGFC	1 - IGFC	93 - EC9830T	93 - INDil	94 - INDil	1008 - IGFC	1 - IGFC	93 - EC9830T	93 - INDil	94 - INDil	1008 - IGFC
		Winter	Winter	Winter	Winter	Spring	Spring	Spring	Spring	Spring	Summer	Summer	Summer	Summer	Summer	Fall	Fall	Fall	Fall	Fall	
RSP	2015 highest ?	~	~	~	LOW RSP	~	~	○	LOW RSP	~	~	~	~	~	●	LOW RSP	~	~	○	LOW RSP	
FB	2015 lowest ?	~	○	●	LOW RSP	●	~	~	LOW RSP	~	~	~	~	~	~	LOW RSP	○	●	●	LOW RSP	
VG	2015 lowest ?	~	○	●	LOW RSP	~	~	~	LOW RSP	~	~	~	~	~	~	LOW RSP	○	●	~	LOW RSP	
% Red	2015 lowest ?	○	●	○	LOW RSP	○	~	~	LOW RSP	~	~	~	~	~	~	LOW RSP	●	○	○	LOW RSP	

Chapter VI – Air pollution exposure apportionment among vulnerable residents of Detroit, MI

VI.1 Summary

This chapter presents a framework to apportion exposures of ambient air pollutants. In this chapter, “exposure apportionment” refers to the quantification of contributions from various emissions sources to the exposure received by individuals in specific micro-environments, specifically, “indoor-at-home,” “other indoor,” “outdoors,” “vehicle cabin,” and “near-road” compartments. Exposure apportionment identifies the source-compartment pairs that provide important contributions to the total air pollution dose for individuals and groups of interest, allowing targeted interventions that reduce exposure. Using the modeling framework developed in the second aim, point and mobile source contributions and background levels of NO_x are estimated, and a probabilistic human exposure model (the Air Pollution EXposures model, APEX) is used to estimate concentrations of pollutants in various urban micro-environments (ME) and population time-activity in each ME for children, adults, and the elderly. Estimated exposures were derived from “background” levels and during the evening and morning commute in the indoor-at-home compartment, largely due to non-commercial traffic. This examination complements results of Aims 2 (Chapter III) and 3 (Chapter IV) pertaining to emissions and concentrations. The focus of this chapter, however, focuses on understanding the contribution of on-road mobile sources, specifically the non-commercial fleet, to cumulative exposures in Detroit.

VI.2 Results

Overall, exposures mostly occurred in the indoor MEs (i.e., indoor-at-home and other indoor), and exposures were dominated by background sources and non-commercial traffic (Figure 31). For adults, background sources contributed an average of 8.28 ppb (standard deviation or sd = 5.96 ppb), representing 52% of the total NO_x exposures derived from modeled NO_x (Figure 32). Exposure to background sources primarily occurred in the other indoor micro-environment (i.e., workplace, school) during day time hours (9 am to 6 pm) (Table 36), and exposures were highest during the winter (Table 37) and on weekdays (

Table 38). Non-commercial traffic contributed the second most to overall exposure, contributing an average of 4.60 ppb (sd = 9.34 ppb), representing 30% of total exposure among adults. The influence from non-commercial traffic sources occurred mostly during evening and early morning hours (7 pm to 8 am) in the indoor-at-home micro-environments. Contributions from commercial traffic and point sources were less than those for non-commercial traffic, and exposures occurred during the evening and early morning (i.e., in the indoor-at-home ME). Exposure to commercial traffic among adults was similar across seasons, but almost twice as high during the week as on the weekends.

Exposures of children (age < 20 years) were similar to those of adults, and exposures among elderly (age > 65) were mostly lower than both adults or children. Exposures of children were similar to those of adults from all source groups for all seasons and by day of week type. Interestingly, exposure to non-commercial and commercial traffic was similar for children and adults, despite adults spending more time in vehicle cabins (Table 39); however, both adults and children spent more time (an order of magnitude) in indoor MEs than in vehicle cabins or near-road. Elderly populations experienced lower exposures to background levels, non-commercial traffic, and commercial traffic in each season and day of week, and the differences between the three groups were significant (KW $p < 0.01$) for these sources. The only non-significant difference in exposure came for exposures to point sources: exposures for adults, children, and elderly were similar in all seasons and by day-type.

VI.3 Discussion

Exposure apportionment identifies the sources and micro-environments that contribute large fractions of cumulative exposure or have high concentrations. In this work, exposures from on-road mobile sources amounted to an average of 37 to 40% of an individual's cumulative exposure to NO_x, with most of the exposure happening while indoors. This is a surprising finding given the relative portions of each day time that adults spent indoors (an average of 88% on weekdays) versus in vehicle cabins or the near-road environments (a combined total of 8% for the same period), as well as the higher concentrations predicted in the near-road environment (Table 20). This finding highlights the importance of accounting for time-activity when predicting exposures to air pollutants, and underscores the utility of this methodology for exposure apportionment; the

insights above are made available through the detailed inventory and modeling framework generated in earlier work.

No significant differences in exposure between children and adults were found, however, elderly individuals had lower exposure, especially from background and non-commercial traffic. This highlights how potential differences in exposures could inform policies and actions aimed at reducing exposures; legislation could specifically aim to reduce exposures to children from non-commercial traffic. Exposure apportionment can provide a link between modeling of the impact of sources on pollutant levels (“source apportionment” as was accomplished in Chapter III) and estimating health effects associated with specific sources (“effects apportionment”). Effects apportionment might provide additional insight into the impact of local sources, but also may miss or under-estimate health effects among community members. Such exposure apportionment efforts should consider sources of uncertainty and potential sources of exposure estimate error.

Another interesting result are the differences between “apportionments” based on emissions (Chapter III), concentrations (Chapter IV) and exposures. Considering the NO_x emissions data in the National Emission Inventory (NEI) in 2011 (Table 19), emissions from diesel and gasoline vehicles in Wayne county (roughly corresponding to commercial and non-commercial traffic, respectively) are similar: each contributes approximately half of the total on-road mobile emissions, which in turn composes around half of the total NO_x emissions in 2011. By volume, commercial traffic comprised only 9% of total on-road vehicles on major surface roads, and much less on smaller roads (Table 35). Dispersion modeling showed that background levels dominated, with non-commercial traffic playing a secondary role, especially within 10 m of a major roadway (Table 20). Trends in exposures largely follow those of the concentration data. This comparison could be extended by considering health impacts (e.g., Disability-Adjusted Life-Years, or DALYs) using non-linear health impact functions [146–149], which would add consideration of population demographics and health status, and apportioning the sources of attributable environmental disease. Profiles based on emissions, concentrations, exposures and impacts place increasingly heavy demands on data and modeling. To some extent, these concepts have been implemented in the life-cycle literature, using intake fraction and characterization factors [195, 196], although the this approach allows neither spatial resolution nor characterization of vulnerable groups.

VI.3.1 Comparison to literature

A number of studies have estimated the fraction of cumulative exposure to derive from mobile and other sources, and several studies have obtained similar results. A study of PM_{2.5} exposures in Los Angeles, CA, showed that intake fractions attributed to light duty traffic (i.e., gasoline vehicles, called “non-commercial” in this aim) were 1.1 to 1.4 times higher than those for heavy duty traffic (i.e., diesel or “commercial” vehicles) [197]. During a 2-week pollution episode in Philadelphia, PA, outdoor sources of PM_{2.5} were shown to contribute slightly more than indoor sources to the 24-hr average dose (a metric that adjusts exposures estimates by an individual’s inhalation rate and other physiological parameters) [86]. An exposure apportionment of coarsely modeled NO₂ and time-activity in Paris, France, stated that the highest of the 4-yr exposures occurred in the “downtown” area with the highest traffic volumes and congestion [87]. An apportionment of traffic related emissions in Hillsborough County, Florida [198] showed similar indoor-at-home concentrations (12.1 ppb as compared to 12.6 in this work) as well as similar percent contributions to total exposure from exposures in-cabin (6% as compared to 8% in this work). However, as stated previously, results from different urban areas may not be comparable to the Detroit findings given differences in emission levels, meteorology, topography, time-activity patterns, and possibly other factors.

VI.3.2 Limitations and uncertainty

We considered only NO_x for the exposure apportionment given the availability of monitoring data and output from previous modeling efforts. Apportionments using PM_{2.5} would be more health-relevant as this pollutant is believed to drive most health impacts. Unfortunately, modeling PM_{2.5} is very complex, involving both primary and secondary pollutants, very high background levels, modeling is largely not validated, and the need for many parameters to account for outdoor-to-indoor penetration and fate of PM_{2.5}. In addition, recent analyses using data from the near-road monitoring stations in the U.S. showed little relationship between (annual average) PM_{2.5} levels and traffic volumes [199].

This work used largely national databases for commuting and time-activity, and the results may not be representative. In Detroit, several factors might act to increase travel times for commuters, especially for certain groups, e.g., the poor regional transit, a declining population, and commuting patterns from suburbs to the certain portions of the city. As a result, in-vehicle and near-road

exposures may be under-estimated. CHAD contains data from several time-activity studies in Wayne County, however, only the Detroit Exposure and Aerosol Research Study (DEARS) [32] contains personal diary data of Detroit residents (the other studies – the Population Study of Income Dynamics and the National Human Activity Pattern Study – were performed via phone interviews). There are large differences in population demographic makeup between these studies (Figure 33 (a)), thus the majority of CHAD data for Wayne County may not adequately represent actual time-activity patterns in Detroit. The age distribution of Detroit participants (Figure 33 (b)) shows little data from some key age-groups, namely young adults who might be more likely to hold several (part-time) jobs, thus increasing commuting time and in-cabin exposures. Further investigation of the underlying time-activity of the simulated population showed an average of less than 10 min/day is spent on childcare among adults, thus pregnant or new mothers (i.e., a “sentinel” population) are likely not well represented in the CHAD data (Table 40). These limitations have been recognized in the literature. For example, time-activity databases can miss key exposure times for vulnerable populations, including travel time, in-vehicle exposure for urban commuters, [72–74] and behavior related to aging, e.g., increased time indoors or in-vehicle cabins. These omissions can cause large errors [75, 76]. In addition, available time-activity data for minority or low income populations living in urban areas with pollution “hotspots” can be limited [77] or not representative [78].

Dispersion and exposure modeling involves a number of uncertainties. Emission inventory uncertainties have been explained in previous work [128]. For NO_x , NEI data indicates that emissions from commercial traffic are similar to that from non-commercial traffic, but dispersion model results show larger impacts from non-commercial traffic. This discrepancy may result from several factors: highways that were outside the domain and were not modeled; the traffic demand model used to generate link-based emissions was run for 2010, not 2014; traffic patterns or relative levels may have changed; and the concentration of commercial traffic along a relatively small number of highways compared to the much more dispersed pattern of non-commercial traffic. Under-prediction of on-road NO_x levels, a trend of the dispersion model used, may have contributed to lower-than-expected in-cabin exposures. In the exposure modeling effort, the spatial resolution of modeling efforts is somewhat simplified, which could limit identification of individual sources as key contributors. However, the source-group method employed was

computationally efficient, and roadway contributions were estimated using validated modeled data at a near-road monitor.

An important limitation of exposure apportionment is its general inability to be validated. Even when personal exposures are measured, direct associations between exposures and specific sources are difficult or impossible to identify without source-specific chemical tracers, a result of the many sources of pollutants like $PM_{2.5}$ and NO_x in urban areas. In part, validation can be addressed by characterizing the quality of the input data for each model component, and by establishing and confirming the performance of each modeling component in simplified settings. This will help evaluate key drivers, and perhaps could be called “credibility analysis.”

VI.4 Tables

Table 36. Mean hourly exposures (ppb) contributed by source groups in each micro-environment (ME). Exposures < 0.05 ppb have been removed from this table. Higher mean exposures are shaded darker.

Source	ME	Hour of day																							
		0	1	2	3	4	5	6	7	8	9	10	11	12	13	14	15	16	17	18	19	20	21	22	23
Background	Indoor-at-home	4.2	4.3	4.3	4.3	4.3	4.3	4.3	4.1	3.3	2.6	2.2	1.9	1.7	1.8	1.7	1.8	2.0	2.3	2.8	3.1	3.2	3.5	3.8	4.0
	Other indoor	0.5	0.5	0.4	0.3	0.2	0.2	0.3	0.5	2.0	4.7	6.1	6.9	7.0	6.4	6.8	6.3	5.2	4.0	2.6	2.0	2.1	1.8	1.2	0.8
	Outdoors	0.2	0.1	0.1	0.1	0.1	0.1	0.1	0.3	0.5	0.7	0.9	1.1	1.3	1.4	1.4	1.7	1.5	1.5	1.3	1.0	0.8	0.6	0.4	0.3
	Near-road	0.1							0.1	0.3	0.4	0.5	0.6	0.7	0.7	0.6	0.6	0.7	0.7	0.7	0.5	0.5	0.3	0.2	0.1
	Vehicle cabin	0.3	0.2	0.1	0.1	0.1	0.1	0.2	0.6	1.4	1.2	1.1	1.1	1.3	1.6	1.5	1.6	1.9	2.0	1.9	1.4	1.1	0.9	0.7	0.5
Non-commercial traffic	Indoor-at-home	7.2	7.0	6.4	5.6	4.8	4.4	4.4	4.8	4.4	3.2	2.0	1.3	0.9	0.8	0.7	0.7	0.9	1.3	2.1	3.0	3.5	4.4	5.9	6.9
	Other indoor	0.3	0.3	0.2	0.1	0.1	0.1	0.1	0.2	0.7	1.6	1.4	1.1	0.9	0.7	0.7	0.6	0.6	0.6	0.5	0.4	0.5	0.6	0.5	0.4
	Outdoors	0.1	0.1	0.1					0.1	0.2	0.1	0.1	0.1	0.1	0.1	0.1	0.1	0.1	0.1	0.2	0.2	0.3	0.3	0.3	0.2
	Near-road									0.1	0.1	0.1							0.1	0.1	0.1	0.1	0.1	0.1	0.1
	Vehicle cabin	0.2	0.1	0.1					0.2	0.4	0.3	0.1	0.1	0.1	0.1	0.1	0.1	0.1	0.2	0.3	0.3	0.3	0.3	0.3	0.2
Commercial traffic	Indoor-at-home	1.8	1.8	1.7	1.5	1.3	1.3	1.5	1.7	1.5	1.1	0.7	0.4	0.3	0.2	0.2	0.2	0.2	0.4	0.5	0.7	0.9	1.2	1.6	1.8
	Other indoor	0.1	0.1						0.1	0.3	0.6	0.5	0.4	0.3	0.2	0.2	0.2	0.2	0.2	0.1	0.1	0.1	0.2	0.1	0.1
	Outdoors									0.1									0.1	0.1	0.1	0.1	0.1	0.1	0.1
	Near-road																								
	Vehicle cabin								0.1	0.2	0.1								0.1	0.1	0.1	0.1	0.1	0.1	0.1
Point sources	Indoor-at-home	1.3	1.4	1.5	1.5	1.5	1.5	1.5	1.4	1.1	0.9	0.7	0.6	0.5	0.5	0.4	0.4	0.4	0.5	0.6	0.6	0.7	0.9	1.1	1.2
	Other indoor	0.1	0.1						0.1	0.2	0.4	0.5	0.5	0.5	0.4	0.4	0.4	0.3	0.2	0.1	0.1	0.1	0.1	0.1	0.1
	Outdoors									0.1	0.1	0.1	0.1	0.1	0.1	0.1	0.1	0.1	0.1	0.1	0.1	0.1	0.1	0.1	0.1
	Near-road																								
	Vehicle cabin								0.1	0.1	0.1	0.1	0.1	0.1	0.1	0.1	0.1	0.1	0.1	0.1	0.1	0.1	0.1	0.1	0.1

Table 37. Mean exposure by source and during different seasons; differences between exposures for adults, children and the elderly compared by the KW test.

Source	season	Mean exposure (ppb)			p
		Adult	Child	Elderly	
Background	Winter	10.4	10.9	9.0	< 0.01
	Spring	8.2	8.2	6.7	< 0.01
	Summer	6.7	5.9	5.0	< 0.01
	Fall	7.8	7.6	6.2	< 0.01
Non-commercial traffic	Winter	5.1	5.3	4.1	< 0.01
	Spring	4.0	4.1	3.2	< 0.01
	Summer	4.3	4.4	3.4	< 0.01
	Fall	5.1	5.3	4.1	< 0.01
Commercial traffic	Winter	1.5	1.5	1.1	< 0.01
	Spring	1.1	1.1	0.8	< 0.01
	Summer	1.2	1.3	0.9	< 0.01
	Fall	1.5	1.5	1.2	< 0.01
Point sources	Winter	1.3	1.3	1.2	>0.50
	Spring	1.2	1.2	1.2	>0.50
	Summer	1.3	1.3	1.3	>0.50
	Fall	1.4	1.4	1.4	>0.50

Table 38. Mean exposure by source and during weekday vs weekend; differences between exposures for adults, children and the elderly compared by the KW test.

Source	Day of week	Mean exposure (ppb)			p
		Adult	Child	Elderly	
Background	Weekday	8.7	8.5	6.7	< 0.01
	Weekend	7.4	7.1	6.5	< 0.01
Commercial traffic	Weekday	1.5	1.5	1.2	< 0.01
	Weekend	0.8	0.9	0.7	< 0.01
Non-commercial traffic	Weekday	4.5	4.6	3.5	< 0.01
	Weekend	4.9	5.2	4.2	< 0.01
Point sources	Weekday	1.3	1.2	1.3	>0.50
	Weekend	1.3	1.3	1.3	>0.50

Table 39. Average min/day spent in various micro-environments (ME) for simulated persons in Detroit in 2014.

ME	Adult (n = 68)		Child (n = 19)		Elderly (n = 13)	
	Weekday	Weekend	Weekday	Weekend	Weekday	Weekend
Indoor-at-home	958	1,100	923	1,061	1,180	1,219
Other indoor	307	152	310	136	135	80
Outdoors	55	75	99	126	45	45
Near-road	29	24	53	34	21	34
Vehicle cabin	91	88	56	83	57	62

Table 40. Average min/day spent doing various activities for simulated persons in Detroit in 2014.

Activity	Adult (n = 68)		Child (n = 19)		Elderly (n = 13)	
	Weekday	Weekend	Weekday	Weekend	Weekday	Weekend
Work	256	74	67	28	38	9
Household	122	139	30	59	124	123
Childcare	7	6	2	1	3	11
Obtain goods	26	33	14	32	47	19
Personal needs	628	675	724	730	691	693
Education / training	5	1	211	9	2	0
Entertainment / social	50	119	36	98	186	198
Leisure	341	391	356	482	344	383
Travel	4	3	1	1	3	4

VI.5 Figures

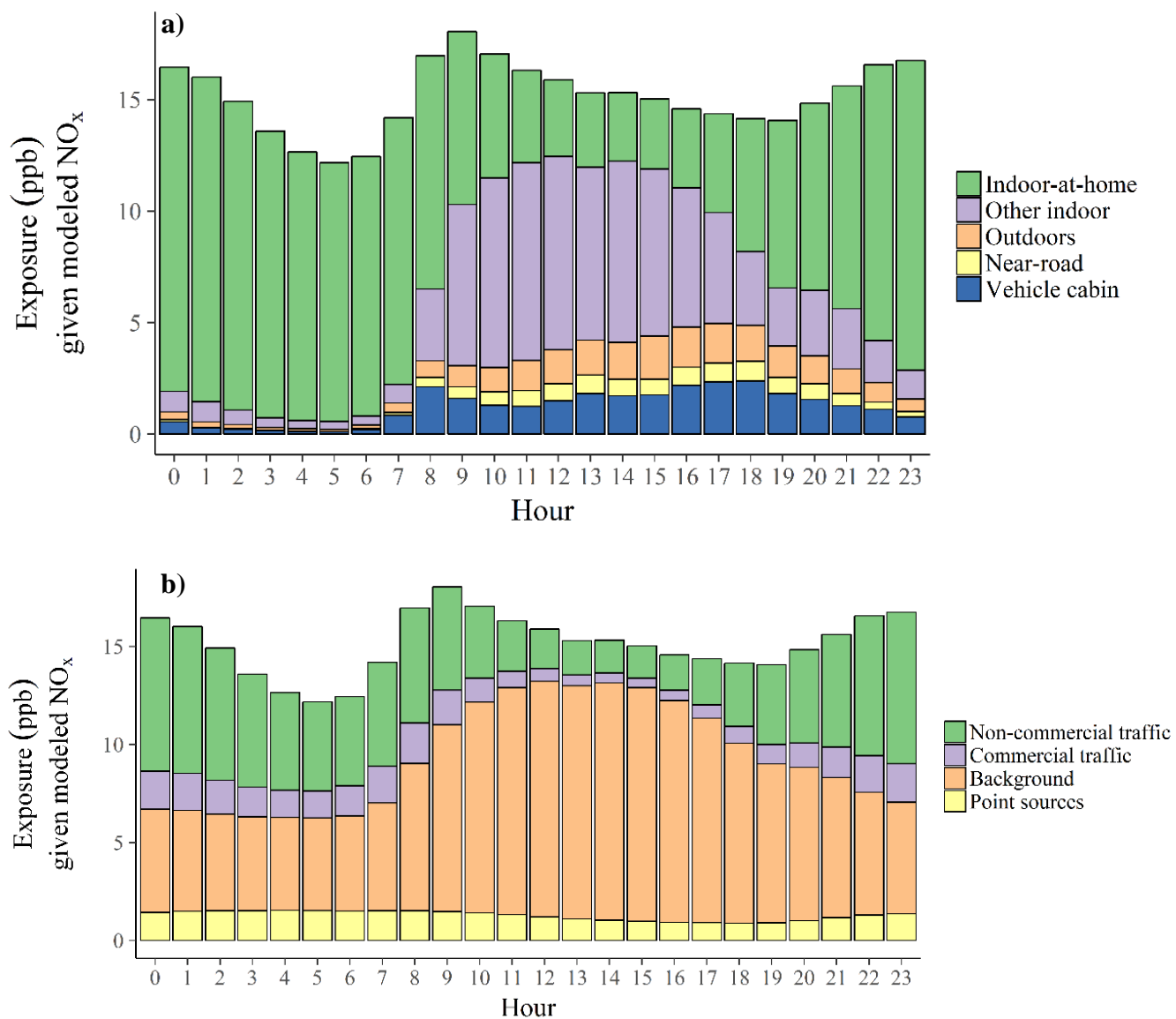
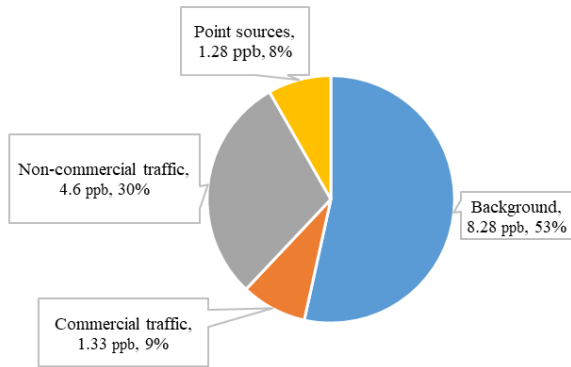
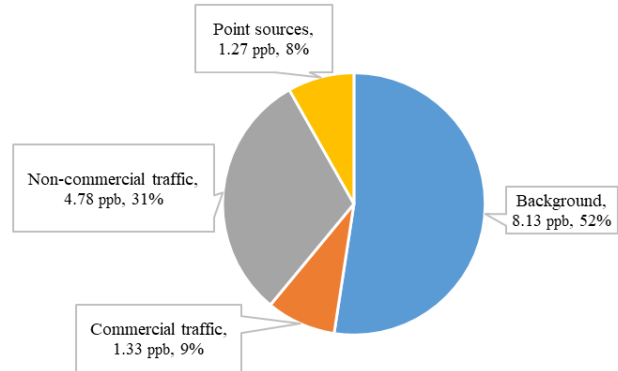


Figure 31. Hour-of-day average exposures, separated by a) micro-environment and b) source, for 100 simulated individuals in Detroit for 2014, calculated using monitored NO_x

A) Average exposure contributions from source groups to adults



B) Average exposure contributions from source groups to children



C) Average exposure contributions from source groups to the elderly

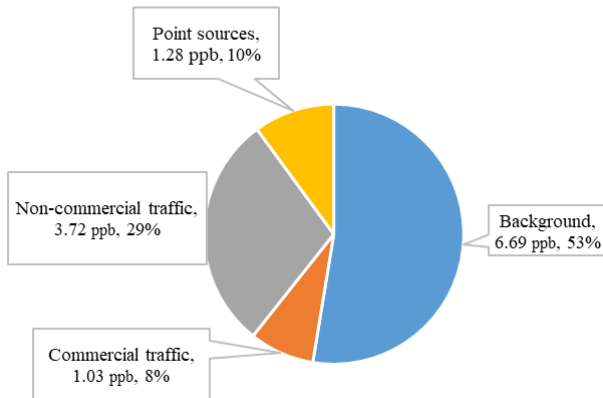


Figure 32. Average exposure contributions from background, point sources, non-commercial traffic, and commercial traffic to populations of A) adults (n = 68), B) children (n=19), and C) the elderly (n=13).

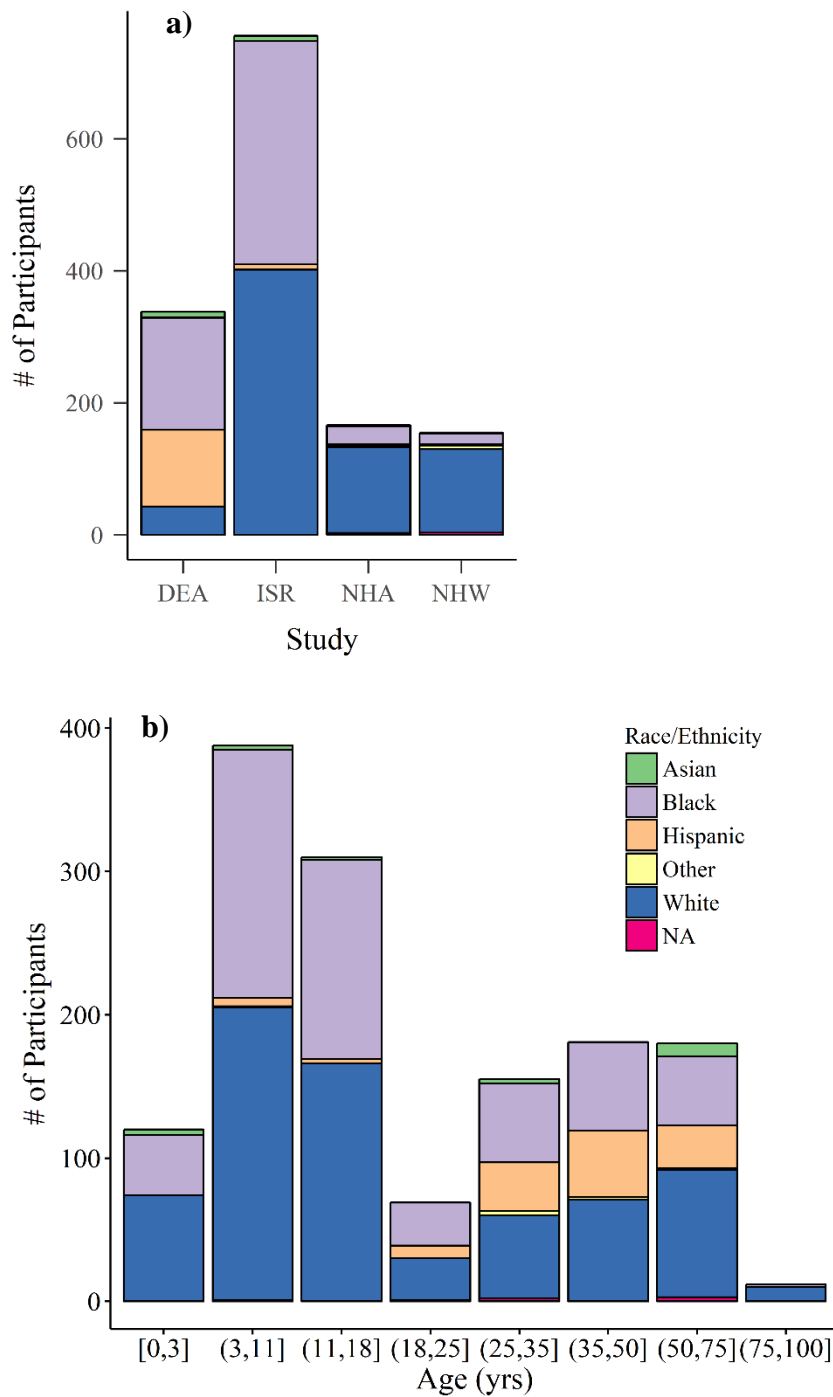


Figure 33. Bar plots showing the demographic breakdown of participants in time-activity studies in Consolidated Human Activity Database data from Wayne County, MI (which contains Detroit) by a) study and b) age. Study abbreviations: DEA = DEARS; ISR = Population Study of Income Dynamics PSID III; NHA = National Human Activity Pattern Study: Air; NHW = National Human Activity Pattern Study: Water

Chapter VII – Conclusions and Recommendations

This dissertation examined current methods used to estimate exposure to traffic-related air pollutants (TRAP) at high spatial or temporal resolutions. Each dissertation aim explored and applied different methods of modeling TRAP: Aim 1 analyzed long-term trends in PM_{2.5} emissions, concentrations and apportionments created using positive matrix factorization, and focused on the mobile source component; Aim 2 performed an operational evaluation of RLINE, a research-level line-source dispersion model developed by EPA for the near-road environment, and obtained results pertinent to model application in health studies; Aim 3 provided a sensitivity analysis of RLINE, and highlighted the impact of the model's meteorological, emission and traffic allocation inputs on exposure predictions; Aim 4 demonstrated a method for apportioning exposures to various contributing source-groups, and examined the contribution of on-road mobile sources to cumulative exposures of a sample population in Detroit, MI.

The analyses emphasized techniques for mobile source models which can inform policies and regulations intended to decrease pollutant concentrations in urban areas. Models for mobile emission sources, which are growing in their contribution to air pollution in some cities, require different input data than models for large industrial point sources, which dominated exposures in the past; evaluation of mobile source pollution at high temporal and spatial resolution, as was done in this dissertation, reflects one of these differences. In addition, researchers and practitioners should endeavor to collect regulatory-quality meteorological data near the study domain. Modeling mobile sources at high spatial and temporal resolutions can be complemented with the collection of time-activity data for individuals in vulnerable groups, compared to the use of national-level databases, especially if exposure reduction interventions are being evaluated. The increases in traffic and human proximity to large roadways suggest that exposure to traffic-related emissions will be a continuing source of human health impacts. Thus far, efforts to control traffic-related air pollutants have occurred mostly in developed countries, while the highest exposures are mostly

experienced in megacities in developing countries. The approaches and considerations described in this dissertation can help address this need and provide guidance for characterizing exposures to mobile sources and helping to evaluate the efficacy of proposed exposure control scenarios.

The remainder of this chapter summarizes and synthesizes results from the four aims, and presents recommendations for future research.

VII.1 Aim 1

Work on this aim analyzed trends and apportionments over a long record of emissions and ambient monitoring data obtained for Chicago and Detroit. Analyses were constructed that provided consistent results, combined emissions and ambient data, and focused on contributions from both regional and local sources. While several differences between the two cities were noted, many or most trends were consistent and supported by both emissions and ambient data, as well as the source apportionments generated using positive matrix factorization. In both cities, PM_{2.5} levels have been declining, primarily due to reductions in secondary sulfate and, to a more limited extent, in nitrate sources, while the importance of emissions due to vehicles, biomass, and metals sources is increasing. This is supported by examining three data sources: county emission data, which show constant or declining emissions from point sources and slightly increasing or constant emissions from on-road mobile sources; ambient monitoring data, which show rapid declines in SO₄²⁻ and NO₃⁻ concentrations, but steady or increasing abundances of OC and EC, tracers for gasoline and diesel vehicle exhaust; and receptor model results, which show increasing relative (percentage) contributions from these sources.

An understanding of long term trends can inform air quality regulation and policy, including the formulation and implementation of emission and ambient standards, which in turn can lead to emission controls, new technologies, and promotion of cleaner fuels, among other options. These responses are most effective when emission sources can be clearly defined and apportioned. However, this approach may not adequately protect vulnerable populations given recent trends, including decreasing concentrations of regional and national pollutants [170], increasingly indistinct profiles and identifications of local emission sources, the significance of secondary pollutants, and the still nascent understanding of health impacts associated with low concentration exposures and pollutant mixtures. A better understanding of emissions, ambient concentrations and source apportionments is required to reduce pollutant exposure and health impacts. The

integration of source- and receptor-oriented apportionments, utilized in the present analysis, can enhance the ability to tease out contributions of sources for targeted interventions.

Future analyses may be strengthened in several ways. First, analyses might be stratified by climatic or meteorological variables to better account for seasonal factors than calendar-based periods, and to better separate trends in primary and secondary components [178]. Second, weekday/weekend groupings may reveal additional trends and better discriminate sources, particularly since truck traffic decreases significantly on Sundays [132]. Similarly, there may be opportunities to stratify by wind direction and other meteorological factors, although the duration (24 hr) and frequency (every third day) of the CSN measurements may prove limiting. Third, hourly speciation measurements and stratification of PMF results by wind direction may improve the ability to identify sources [175]. Fourth, comparisons of factor contribution on high and low pollution days might help distinguish contributions of local sources, e.g., traffic-related air pollutants [172]. Fifth, while emissions trends can be tracked for some sources, greater consistency in methods and source grouping across years would improve long-term studies. In particular, emissions data for crustal, fugitive, metals and biomass sources are highly uncertain. Sixth, regional emission inventories might be examined to help confirm changes in regional contributors of secondary sulfate and nitrate. Finally, applications of long term trend analyses to other cities would help confirm trends.

VII.2 Aim 2

Aim 2, an operation evaluation of dispersion model performance, characterized the agreement between daily average predictions and observations of traffic-related air pollutants (TRAP) in an urban scale application in Detroit, Michigan that used a detailed link-based mobile source inventory and the RLINE model. Model performance was best for locations downwind of major roads, for winds perpendicular to roads, for sites near major roads, on weekdays, and during winter and spring seasons. On a pollutant-specific basis, model performance was best for NO_x and CO; the evaluation was not informative for PM_{2.5} mainly due to the scarcity of monitors near major roads and the presence of high background levels. These findings were consistent across most sites and for the two pollutants. Performance evaluations should test a wide range of environments, utilize sampling methods that are sufficiently sensitive and ideally selective for TRAP, and use an ensemble of evaluations to provide robust and representative results. The results are consistent

with the literature, and they demonstrate factors that affect model performance for the 24-hour averages commonly used in epidemiologic studies.

RLINE's performance in near-road environments suggests its usefulness for estimating spatially- and temporally-resolved exposure estimates. However, the use of dispersion models in epidemiologic studies should address factors that can influence model performance and result in exposure measurement errors, including distance and direction from the road, day-of-week and seasonal effects. Appropriate study designs and analytical techniques can help avoid exposure measurement errors and improve the exposure estimates used in health and epidemiologic studies.

VII.3 Aim 3

The goal of Aim 3 was to examine the sensitivity of dispersion model predictions of TRAP exposure to key model inputs. While data and computationally intensive, dispersion models and especially high fidelity models can provide great flexibility and theoretical strength, and can represent the spatial variability of TRAP concentrations at locations not measured by conventional and spatially sparse air quality monitoring networks. However, model estimates were sensitive to input data, and our applications highlighted the need for representative meteorological data to predict near-road exposures. In particular, several systematic biases can cause exposure measurement errors that could affect results and subsequent calculations, e.g., estimated health impacts.

Several recommendations follow from the work completed for this aim. These include: the need to develop guidance that defines appropriate meteorological data for dispersion modeling of the complex near-road environment (e.g., robust wind fields created by computational fluid dynamics models); the use of on-site (local) meteorological inputs in near-road dispersion modeling; and that air quality monitoring sites be equipped with meteorological instrumentation sufficient to obtain parameters needed by the AERMET meteorological pre-processor for generating the input files necessary to run RLINE and other dispersion models. Finally, to confirm and extend our results, other operational performance evaluations and sensitivity analysis should be conducted across a range of urban settings.

VII.4 Aim 4

The goal of Aim 4 was to demonstrate a method to apportion exposures using an application in Detroit, MI. The method used modeled concentrations at receptors in Detroit as inputs to a

probabilistic human exposure model (the Air Pollution EXposures model, APEX) that estimated exposures of a simulated population of children, adults, and the elderly in various urban micro-environments. The majority of exposure derived from background levels and non-commercial traffic, especially during evening and early morning in the “indoor-at-home” micro-environment. The apportioned exposures were sensitive to the pollutant selected (NO_x rather than PM_{2.5}), and the time-activity and other databases used (e.g., national rather than local). While the method did not account for uncertainty in modeling pollutant data, the probabilistic sampling of time-activity data may account for some variation in exposures among individuals in various groups. The method may be especially useful in determining the relative (rather than absolute) magnitude of exposures attributed to various sources and pollutants.

Recommendations for future research on exposure apportionment are warranted. First, a small case studying using personal exposure measurements in a less complex environment could provide a way to “field test” the exposure apportionment methodology and compare measured and modeled source contributions in various micro-environments. Location (GPS) data with corroborating personal time-lapse photography could be used to develop time-activity data. This may be especially relevant for individuals in vulnerable groups whose time-activity may not be covered in traditional or national databases. As a second example, a multi-model comparison between APEX and an epidemiological regression model could allow some verification (“reality checking”) of exposure apportionment results. Model-to-model comparisons might be especially fruitful across major cities in the US with known differences in their emission, concentration and exposure profiles. Such comparisons could identify similarities and differences in estimated exposures, especially for vulnerable groups. One output might demonstrate the impact of additional commuting or the effect of different transport modes on a person’s daily roadway-related exposure. Other studies might examine how missing or alternative time-activity data might affect exposure estimates, and how exposures vary for different pollutants and populations, and the impact of exposure measurement errors on epidemiological and health impact study results.

REFERENCES

1. Transportation Research Board (2002) The Congestion Mitigation and Air Quality Improvement Program. Assessing 10 Years of Experience
2. Health Effects Institute (HEI) (2010) Traffic-related air pollution: a critical review of the literature on emissions, exposure, and health effects. 1–386
3. Boehmer TK, Foster SL, Henry JR, Woghiren-Akinnifesi EL, FY Y, Boehmer TK, Foster SL, Henry JR, Woghiren-Akinnifesi EL, Yip FY, Centers for Disease C, Prevention (2013) Residential Proximity to Major Highways – United States, 2010. *MMWR Surveill Summ* 62:46
4. Caiazzo F, Ashok A, Waitz IA, Yim SHL, Barrett SRH (2013) Air pollution and early deaths in the United States. Part I: Quantifying the impact of major sectors in 2005. *Atmos Environ* 79:198–208 . doi: 10.1016/J.ATMOSENV.2013.05.081
5. US Department of Transportation (US DOT) (2012) Fatality Analysis Reporting System Database
6. Landrigan PJ, Fuller R, Acosta NJR, Adeyi O, Arnold R, Basu N (Nil), Baldé AB, Bertollini R, Bose-O'Reilly S, Boufford JI, Breyse PN, Chiles T, Mahidol C, Coll-Seck AM, Cropper ML, Fobil J, Fuster V, Greenstone M, Haines A, Hanrahan D, Hunter D, Khare M, Krupnick A, Lanphear B, Lohani B, Martin K, Mathiasen K V, McTeer MA, Murray CJL, Ndahimananjara JD, Perera F, Potočnik J, Preker AS, Ramesh J, Rockström J, Salinas C, Samson LD, Sandilya K, Sly PD, Smith KR, Steiner A, Stewart RB, Suk WA, van Schayck OCP, Yadama GN, Yumkella K, Zhong M (2018) The Lancet Commission on pollution and health. *Lancet* 391:462–512 . doi: 10.1016/S0140-6736(17)32345-0
7. Krzyżanowski M, Kuna-Dibbert B, Schneider J (2005) Health effects of transport-related air pollution
8. Benbrahim-Tallaa L, Baan RA, Grosse Y, Lauby-Secretan B, El Ghissassi F, Bouvard V, Guha N, Loomis D, Straif K (2012) Carcinogenicity of diesel-engine and gasoline-engine exhausts and some nitroarenes. *Lancet Oncol* 13:663–664 . doi: 10.1016/S1470-2045(12)70280-2
9. Bert B, Nicole AHJ, Jeroen de H, Hendrik H, Mirjam K, Patricia van V, Brunekreef B, Janssen NAH, Hartog J de, Harssema H, Knappe M, Vliet P van (1997) Air Pollution from Truck Traffic and Lung Function in Children Living near Motorways. *Epidemiology* 8:298 . doi: 10.2307/3702257
10. Stieb DM, Chen L, Hystad P, Beckerman BS, Jerrett M, Tjepkema M, Crouse DL, Omariba

- DW, Peters PA, van Donkelaar A, Martin R V, Burnett RT, Liu S, Smith-Doiron M, Dugandzic RM (2016) A national study of the association between traffic-related air pollution and adverse pregnancy outcomes in Canada, 1999–2008. *Env Res* 148:513
11. Fang SC, Schwartz J, Yang M, Yaggi HK, Bliwise DL, Araujo AB (2015) Traffic-related air pollution and sleep in the Boston Area Community Health Survey. *J Expo Sci Environ Epidemiol* 25:451–456 . doi: 10.1038/jes.2014.47
 12. Adar SD, Gold DR, Coull BA, Schwartz J, Stone PH, Suh H (2007) Focused exposures to airborne traffic particles and heart rate variability in the elderly. *Epidemiology* 18:95–103 . doi: 10.1097/01.ede.0000249409.81050.46
 13. Jennifer W, Joel DK, Adam AS, Cynthia C, Robin CP, Todd B, Denis AE, Carlos FM de L (2016) Exposure to Traffic-Related Air Pollution in Relation to Progression in Physical Disability among Older Adults. *Environ Health Perspect* 124:1000
 14. Hoffmann B, Moebus S, Möhlenkamp S, Stang A, Lehmann N, Dragano N, Schmermund A, Memmesheimer M, Mann K, Erbel R, Jöckel KH (2007) Residential exposure to traffic is associated with coronary atherosclerosis. *Circulation* 116:489–496 . doi: 10.1161/CIRCULATIONAHA.107.693622
 15. Davis LW (2008) The Effect of Driving Restrictions on Air Quality in Mexico City. *J Polit Econ* 116:38–81 . doi: 10.1086/529398
 16. US Environmental Protection Agency (US EPA) (1999) Nitrogen oxides (NO_x), why and how they are controlled. *Epa-456/F-99-006R* 48 . doi: EPA 456/F-99-006R
 17. Jones AM, Harrison RM, Barratt B, Fuller G (2012) A large reduction in airborne particle number concentrations at the time of the introduction of “ sulphur free” diesel and the London Low Emission Zone. *Atmos Environ* 50:129–138 . doi: 10.1016/j.atmosenv.2011.12.050
 18. Kelly FJ, Kelly J, Consortium HEIL (2009) London air quality: a real world experiment in progress. *Biomarkers* 14 Suppl 1:5–11 . doi: 10.1080/13547500902965252
 19. Morfeld P, Groneberg DA, Spallek MF (2014) Effectiveness of low emission zones: large scale analysis of changes in environmental NO₂, NO and NO_x concentrations in 17 German cities. *PLoS One* 9:e102999 . doi: 10.1371/journal.pone.0102999
 20. Jerrett M, Arain A, Kanaroglou P, Beckerman B, Potoglou D, Sahsuvaroglu T, Morrison J, Giovis C (2005) A review and evaluation of intraurban air pollution exposure models. *J Expo Anal Environ Epidemiol* 15:185–204 . doi: 10.1038/sj.jea.7500388
 21. Hand JL, Schichtel BA, Malm WC, Frank NH (2013) Spatial and temporal trends in PM_{2.5} organic and elemental carbon across the United States. *Adv Meteorol* 2013:1–13 . doi: 10.1155/2013/367674
 22. US Environmental Protection Agency (US EPA) (2014) Chemical Speciation Network Database
 23. Peng RD, Bell ML, Geyh AS, McDermott A, Zeger SL, Samet JM, Dominici F (2009) Emergency admissions for cardiovascular and respiratory diseases and the chemical

- composition of fine particle air pollution. *Environ Health Perspect* 117:957–63 . doi: 10.1289/ehp.0800185
24. Haupt SE (2005) A demonstration of coupled receptor/dispersion modeling with a genetic algorithm. *Atmos Environ* 39:7181–7189 . doi: 10.1016/j.atmosenv.2005.08.027
 25. Park SK, Auchincloss AH, O'Neill MS, Prineas R, Correa JC, Keeler J, Graham Barr R, Kaufman JD, Diez Roux A V. (2010) Particulate air pollution, metabolic syndrome, and heart rate variability: The multi-ethnic study of atherosclerosis (MESA). *Environ Health Perspect* 118:1406–1411 . doi: 10.1289/ehp.0901778
 26. Zhang K, Batterman S (2013) Air pollution and health risks due to vehicle traffic. *Sci Total Environ* 450–451:307–316 . doi: 10.1016/j.scitotenv.2013.01.074
 27. Paatero P, Tapper U (1994) Positive Matrix Factorization: A Non-Negative Factor Model with Optimal Utilization of Error Estimates of Data Values. *Environmetrics* 5:111–126
 28. Wolff GT, Korsog PE, Kelly NA, Ferman MA (1985) Relationships between fine particulate species, gaseous pollutants, and meteorological parameters in Detroit. *Atmos Environ* 19:1341–1349
 29. Morishita M, Keeler GJ, Wagner JG, Harkema JR (2006) Source identification of ambient PM_{2.5} during summer inhalation exposure studies in Detroit, MI. *Atmos Environ* 40:3823–3834 . doi: 10.1016/j.atmosenv.2006.03.005
 30. Morishita M, Keeler GJ, Kamal AS, Wagner JG, Harkema JR, Rohr AC (2011) Identification of ambient PM_{2.5} sources and analysis of pollution episodes in Detroit, Michigan using highly time-resolved measurements. *Atmos Environ* 45:1627–1637 . doi: 10.1016/j.atmosenv.2010.09.062
 31. Buzcu-Guven B, Brown SG, Frankel A, Hafner HR, Roberts PT (2007) Analysis and apportionment of organic carbon and fine particulate matter sources at multiple sites in the Midwestern United States. *J Air Waste Manag Assoc* 57:606–619 . doi: 10.3155/1047-3289.57.5.606
 32. Williams R, Rea A, Vette A, Croghan C, Whitaker D, Stevens C, McDow S, Fortmann R, Sheldon L, Wilson H, Thornburg J, Phillips M, Lawless P, Rodes C, Daughtrey H (2009) The design and field implementation of the detroit exposure and aerosol research study. *J Expo Sci Environ Epidemiol* 19:643–659 . doi: 10.1038/jes.2008.61
 33. Duvall RM, Norris GA, Burke JM, Olson DA, Vedantham R, Williams R (2012) Determining spatial variability in PM_{2.5} source impacts across Detroit, MI. *Atmos Environ* 47:491–498 . doi: 10.1016/j.atmosenv.2011.09.071
 34. Gildemeister AE, Hopke PK, Kim E (2007) Sources of fine urban particulate matter in Detroit, MI. *Chemosphere* 69:1064–1074 . doi: 10.1016/j.chemosphere.2007.04.027
 35. Kundu S, Stone EA (2014) Composition and sources of fine particulate matter across urban and rural sites in the Midwestern United States. *Environ Sci Process Impacts* 16:1360–1370 . doi: 10.1039/C3EM00719G
 36. Hammond DM, Dvonch JT, Keeler GJ, Parker EA, Kamal AS, Barres JA, Yip FY,

- Brakefield-Caldwell W (2008) Sources of ambient fine particulate matter at two community sites in Detroit, Michigan. *Atmos Environ* 42:720–732 . doi: 10.1016/j.atmosenv.2007.09.065
37. Hasheminassab S, Daher N, Ostro BD, Sioutas C (2014) Long-term source apportionment of ambient fine particulate matter (PM_{2.5}) in the Los Angeles Basin: A focus on emissions reduction from vehicular sources. *Environ Pollut* 193:54–64 . doi: 10.1016/j.envpol.2014.06.012
 38. Dionisio KL, Baxter LK, Burke J, Özkaynak H (2015) The importance of the exposure metric in air pollution epidemiology studies: When does it matter, and why? *Air Qual Atmos Heal* 9:495 . doi: 10.1007/s11869-015-0356-1
 39. Batterman S, Burke J, Isakov V, Lewis T, Mukherjee B, Robins T (2014) A comparison of exposure metrics for traffic-related air pollutants: Application to epidemiology studies in Detroit, Michigan. *Int J Environ Res Public Health* 11:9553–9577 . doi: 10.3390/ijerph110909553
 40. Cimorelli AJ, Perry SG, Venkatram A, Weil JC, Paine RJJ, Wilson RB, Lee RF, Peters WD, Brode RW (2005) AERMOD: A dispersion model for industrial source applications. Part I: General model formulation and boundary layer characterization. *J Appl Meteorol* 44:682–693 . doi: 10.1175/jam2227.1
 41. Benson P (1989) CALINE4 - A Dispersion Model For Predicting Air Pollutant Concentrations Near Roadways. *Calif Dep Transp FHWA/CA/TL:1–247* . doi: www.dot.ca.gov/hq/env/air/index.html
 42. USEPA (2015) Technical Support Document (TSD) for Replacement of CALINE3 with AERMOD for Transportation Related Air Quality Analyses
 43. Snyder MG, Venkatram A, Heist DK, Perry SG, Petersen WB, Isakov V (2013) RLINE: A line source dispersion model for near-surface releases. *Atmos Environ* 77:748–756 . doi: 10.1016/j.atmosenv.2013.05.074
 44. Venkatram A, Snyder MG, Heist DK, Perry SG, Petersen WB, Isakov V (2013) Re-formulation of plume spread for near-surface dispersion. *Atmos Environ* 77:846–855 . doi: 10.1016/j.atmosenv.2013.05.073
 45. Heist D, Isakov V, Perry S, Snyder M, Venkatram A, Hood C, Stocker J, Carruthers D, Arunachalam S, Owen RC (2013) Estimating near-road pollutant dispersion: A model inter-comparison. *Transp Res Part D Transp Environ* 25:93–105 . doi: 10.1016/j.trd.2013.09.003
 46. Chang SY, Vizuete W, Valencia A, Naess B, Isakov V, Palma T, Breen M, Arunachalam S (2015) A modeling framework for characterizing near-road air pollutant concentration at community scales. *Sci Total Environ* 538:905–921 . doi: 10.1016/j.scitotenv.2015.06.139
 47. Rao ST, Sistla G, Keenan MT, Wilson JS (1980) An Evaluation of Some Commonly Used Highway Dispersion Models. *J Air Pollut Control Assoc* 30:239–246 . doi: 10.1080/00022470.1980.10465941
 48. Oetl D, Kukkonen J, Almbauer RA, Sturm PJ, Pohjola M, Härkönen J (2001) Evaluation of a Gaussian and a Lagrangian model against a roadside data set, with emphasis on low

- wind speed conditions. *Atmos Environ* 35:2123–2132 . doi: 10.1016/S1352-2310(00)00492-1
49. Levitin J, Härkönen J, Kukkonen J, Nikmo J (2005) Evaluation of the CALINE4 and CAR-FMI models against measurements near a major road. *Atmos Environ* 39:4439–4452 . doi: 10.1016/j.atmosenv.2005.03.046
 50. Ganguly R, Broderick BM (2008) Performance evaluation and sensitivity analysis of the general finite line source model for CO concentrations adjacent to motorways: A note. *Transp Res Part D Transp Environ* 13:198–205 . doi: 10.1016/j.trd.2008.01.006
 51. Isakov V, Arunachalam S, Batterman S, Bereznicki S, Burke J, Dionisio K, Garcia V, Heist D, Perry S, Snyder MG, Vette A (2014) Air Quality Modeling in Support of the Near-Road Exposures and Effects of Urban Air Pollutants Study (NEXUS). *Int J Environ Res Public Health* 11:8777–8793
 52. Patton AP, Milando C, Durant JL, Kumar P (2016) Assessing the Suitability of Multiple Dispersion and Land Use Regression Models for Urban Traffic-Related Ultrafine Particles. *Environ Sci Technol* 51:384–392 . doi: 10.1021/acs.est.6b04633
 53. Zhai X, Russell AG, Sampath P, Mulholland JA, Kim BU, Kim Y, D’Onofrio D (2016) Calibrating R-LINE model results with observational data to develop annual mobile source air pollutant fields at fine spatial resolution: Application in Atlanta. *Atmos Environ* 147:446–457 . doi: 10.1016/j.atmosenv.2016.10.015
 54. Pachón JE, Saavedra C, Pérez MP, Galvis BR, Arunachalam S (2016) Exposure Assessment to High-Traffic Corridors in Bogota Using a Near-Road Air Quality Model. 403–407 . doi: 10.1007/978-3-319-24478-5_66
 55. Chang JC, Hanna SR (2004) Air quality model performance evaluation. *Meteorol Atmos Phys* 87:167–196 . doi: 10.1007/s00703-003-0070-7
 56. Hanna S, Chang J (2012) Acceptance criteria for urban dispersion model evaluation. *Meteorol Atmos Phys* 116:133–146 . doi: 10.1007/s00703-011-0177-1
 57. Vardoulakis S, Fisher BEA, Gonzalez-Flesca N, Pericleous K (2002) Model sensitivity and uncertainty analysis using roadside air quality measurements. *Atmos Environ* 36:2121–2134
 58. Dhyani R, Sharma N (2017) Sensitivity analysis of CALINE4 model under mix traffic conditions. *Aerosol Air Qual Res* 17:314–329 . doi: 10.4209/aaqr.2016.01.0012
 59. Gulia S, Nagendra S, Khare M (2015) Comparative Evaluation of Air Quality Dispersion Models for PM_{2.5} at Air Quality Control Regions in Indian and UK Cities. *MAPAN* 30:249
 60. Salizzoni P, Soulhac L, Corti A, Giambini P, Salizzoni P, Soulhac L, Corti A (2012) Influence of Meteorological Input Parameters on Urban Dispersion Modelling for Traffic Scenario Analysis. In: Steyn DG, Trini Castelli S (eds) *Air Pollution Modeling and its Application XXI*. Springer Netherlands, Dordrecht, pp 453–457
 61. US Environmental Protection Agency (US EPA) (2015) Near-road Monitoring Network Metadata

62. Hodgson S, Nieuwenhuijsen MJ, Colvile R, Jarup L (2007) Assessment of exposure to mercury from industrial emissions: Comparing “distance as a proxy” and dispersion modelling approaches. *Occup Environ Med* 64:380–388 . doi: 10.1136/oem.2006.026781
63. Sax T, Isakov V (2003) A case study for assessing uncertainty in local-scale regulatory air quality modeling applications. *Atmos Environ* 37:3481–3489 . doi: 10.1016/S1352-2310(03)00411-4
64. Batterman S (2015) Temporal and spatial variation in allocating annual traffic activity across an urban region and implications for air quality assessments. *Transp Res Part D Transp Environ* 41:401–415 . doi: 10.1016/j.trd.2015.10.009
65. Rao KS (2005) Uncertainty analysis in atmospheric dispersion modeling. *Pure Appl Geophys* 162:1893–1917 . doi: 10.1007/s00024-005-2697-4
66. Duan N (1981) Micro-environment types: a model for human exposure to air pollution
67. Letz R, Ryan PB, Spengler JD ESTIMATED DISTRIBUTIONS OF PERSONAL EXPOSURE TO RESPIRABLE PARTICLES
68. Fugas M (1975) Assessment of total exposure to an air pollutant. In: *proceedings of the International Conference on Environmental Sensing and Assessment*. p #75-CH 1004{1 ICESA
69. US Environmental Protection Agency (US EPA) (2015) Air Pollutants Exposure Model Documentation APEX Version 4. Volume I: User’s Guide
70. McCURDY THOMAS, GLEN GRAHAM, SMITH LUTHER, LAKKADI YESHPAL (2000) The National Exposure Research Laboratory’s Consolidated Human Activity Database. *J Expo Anal Environ Epidemiol* 10:566–578 . doi: 10.1038/sj.jea.7500114
71. Jones RR, Özkaynak H, Nayak SG, Garcia V, Hwang S-AA, Lin S (2013) Associations between summertime ambient pollutants and respiratory morbidity in New York City: Comparison of results using ambient concentrations versus predicted exposures. *J Expo Sci Environ Epidemiol* 23:616–626 . doi: 10.1038/jes.2013.44
72. Wang C, Xi J-Y, Hu H-Y, Xi J-Y, Hu H-Y, Arhami M, Polidori A, Polidori A, Delfino R, Tjoa T, Tjoa T, Sioutas C, Wang C, Xi J-Y, Hu H-Y, Xi J-Y, Hu H-Y, Pacheco A, Freitas M, Pratt G, Dymond M, Dymond M, Krzyzanowski J, Luo H-L, Chang W-C, Lin D-F, Pennell K, Bozkurt O, Suuberg E, Bozkurt O, Suuberg E, Isakov V, Touma J, Burke J, Touma J, Burke J, Lobdell D, Palma T, Rosenbaum A, zkaynak H, Lipfert F, Wyzga R, Baty J, Miller J, Miller J, Mohan R, Leonardi G, Robins A, Jefferis S, Jefferis S, Coy J, Wight J, Wight J, Murray V (2009) Combining Regional- and Local-Scale Air Quality Models with Exposure Models for Use in Environmental Health Studies. *J Air Waste Manage Assoc* 59:461–472 . doi: 10.3155/1047-3289.59.4.461
73. Liu X, Frey HC (2011) Modeling of in-vehicle human exposure to ambient fine particulate matter. *Atmos Environ* 45:4745–4752 . doi: 10.1016/j.atmosenv.2011.04.019
74. George BJ, McCurdy T (2011) Investigating the American Time Use Survey from an exposure modeling perspective. *J Expo Sci Environ Epidemiol* 21:92–105 . doi: 10.1038/jes.2009.60

75. Tuttle L, Meng Q, Moya J, Johns DO (2013) Consideration of Age-Related Changes in Behavior Trends in Older Adults in Assessing Risks of Environmental Exposures. *J Aging Health* 25:243–273
76. Breen MMS, Long TC, Schultz BD, Williams RW, Richmond-Bryant J, Breen MMS, Langstaff JE, Devlin RB, Schneider A, Burke JM, Batterman SA, Meng QY (2015) Air Pollution Exposure Model for Individuals (EMI) in Health Studies: Evaluation for Ambient PM_{2.5} in Central North Carolina. *Environ Sci Technol* 49:14184–14194 . doi: 10.1021/acs.est.5b02765
77. Wu XM, Fan ZT, Ohman-Strickland P (2010) Time-location patterns of a population living in an air pollution hotspot. *J Environ Public Health* 2010:
78. Spalt EW, Curl CL, Allen RW, Cohen M, Adar SD, Stukovsky KH, Avol E, Castro-Diehl C, Nunn C, Mancera-Cuevas K, Kaufman JD (2015) Time–location patterns of a diverse population of older adults: the Multi-Ethnic Study of Atherosclerosis and Air Pollution (MESA Air). *J Expo Sci Environ Epidemiol* 26:349–355 . doi: 10.1038/jes.2015.29
79. Baxter LK, Dionisio KL, Burke J, Sarnat SE, Sarnat JA, Hodas N, Rich DQ, Turpin BJ, Jones RR, Mannshardt E, Kumar N, Beevers SD, Ozkaynak H, Ebelt Sarnat S, Sarnat JA, Hodas N, Rich DQ, Turpin BJ, Jones RR, Mannshardt E, Kumar N, Beevers SD, Ozkaynak H (2013) Exposure prediction approaches used in air pollution epidemiology studies: key findings and future recommendations. *J Expo Sci Env Epidemiol* 23:654–659 . doi: 10.1038/jes.2013.62
80. Breen MMS, Long TC, Schultz BD, Crooks J, Breen MMS, Langstaff JE, Isaacs KK, Tan Y-MM, Williams RW, Cao Y, Geller AM, Devlin RB, Batterman SA, Buckley TJ (2014) GPS-based microenvironment tracker (MicroTrac) model to estimate time–location of individuals for air pollution exposure assessments: Model evaluation in central North Carolina. *J Expo Sci Environ Epidemiol* 24:412–420 . doi: 10.1038/jes.2014.13
81. Liroy PJ (2010) Exposure science: A view of the past and milestones for the future. *Environ Health Perspect* 118:1081–1090 . doi: 10.1289/ehp.0901634
82. Wang S-WW, Tang X, Fan Z-HH, Wu X, Liroy PJ, Georgopoulos PG (2009) Modeling of Personal Exposures to Ambient Air Toxics in Camden, New Jersey: An Evaluation Study. *J Air Waste Manage Assoc* 59:733–746 . doi: 10.3155/1047-3289.59.6.733
83. Gokhale S, Kohajda T, environment US-S of the total, 2008 undefined Source apportionment of human personal exposure to volatile organic compounds in homes, offices and outdoors by chemical mass balance and genetic. Elsevier
84. Miller SL, Anderson MJ, Daly EP, Milford JB (2002) Source apportionment of exposures to volatile organic compounds. I. Evaluation of receptor models using simulated exposure data. *Atmos Environ* 36:3629–3641 . doi: 10.1016/S1352-2310(02)00279-0
85. Zhao W, Hopke PK, Norris G, Williams R, Paatero P (2006) Source apportionment and analysis on ambient and personal exposure samples with a combined receptor model and an adaptive blank estimation strategy. *Atmos Environ* 40:3788–3801 . doi: 10.1016/J.ATMOSENV.2006.02.027

86. Georgopoulos PG, Wang S-WW, Vyas VM, Sun Q, Burke J, Vedantham R, McCurdy T, Özkaynak H (2005) A source-to-dose assessment of population exposures to fine PM and ozone in Philadelphia, PA, during a summer 1999 episode. *J Expo Sci Environ Epidemiol* 15:439–457 . doi: 10.1038/sj.jea.7500422
87. Valari M, Menut L, Chatignoux E (2011) Using a Chemistry Transport Model to Account for the Spatial Variability of Exposure Concentrations in Epidemiologic Air Pollution Studies. *J Air Waste Manage Assoc* 61:164–179 . doi: 10.3155/1047-3289.61.2.164
88. Oreskes N, Shrader-Frechette K, Belitz K (1994) Verification, Validation, and Confirmation of Numerical Models in the Earth Sciences. *Science* (80-) 263:641–646 . doi: 10.1126/science.263.5147.641
89. DAISEY J (1999) RECENT RESEARCH ON INDOOR AIR QUALITY: A COMPILATION IN MEMORY OF
90. Koenker R, Basset G (1978) Regression Quantiles. *Econometrica* 46:33–50
91. Milando C, Huang L, Batterman S (2016) Trends in PM_{2.5} emissions, concentrations and apportionments in Detroit and Chicago. *Atmos Environ* 129:197–209 . doi: 10.1016/j.atmosenv.2016.01.012
92. Milando CWCW, Batterman SASA (2018) Operational evaluation of the RLINE dispersion model for studies of traffic-related air pollutants. *Atmos Environ* 182:213–224 . doi: 10.1016/j.atmosenv.2018.03.030
93. Milando CWCW, Batterman SASA (2018) Sensitivity analysis of the near-road dispersion model RLINE - An evaluation at Detroit, Michigan. *Atmos Environ* 181:135–144 . doi: 10.1016/j.atmosenv.2018.03.009
94. Finn D, Clawson KL, Carter RG, Rich JD, Eckman RM, Perry SG, Isakov V, Heist DK (2010) Tracer studies to characterize the effects of roadside noise barriers on near-road pollutant dispersion under varying atmospheric stability conditions. *Atmos Environ* 44:204–214 . doi: 10.1016/j.atmosenv.2009.10.012
95. Baldauf R, Thoma E, Hays M, Shores R, Kinsey J, Gullett B, Kimbrough S, Isakov V, Long T, Snow R, Khlystov A, Weinstein J, Chen FL, Seila R, Olson D, Gilmour I, Cho SH, Watkins N, Rowley P, Bang J (2008) Traffic and meteorological impacts on near-road air quality: Summary of methods and trends from the Raleigh near-road study. *J Air Waste Manag Assoc* 58:865–878 . doi: 10.3155/1047-3289.58.7.865
96. Barad ML (1958) Project Prairie Grass: a field program in diffusion vol II. *Geophys. Res. Pap. Vol II:1–218*
97. Isaacs K, McCurdy T, Glen G, Nysewander M, Errickson A, Forbes S, Graham S, McCurdy L, Smith L, Tulve N, Vallero D (2013) Statistical properties of longitudinal time-activity data for use in human exposure modeling. *J Expo Sci Environ Epidemiol* 23:328–336 . doi: 10.1038/jes.2012.94
98. US Environmental Protection Agency (US EPA) (2014) National Emission Inventories (NEI) and Technical Support Documents

99. US Environmental Protection Agency (US EPA) (2011) Integrated Science Assessment for Particulate Matter; Report No. EPA/600/R-08/139. National Center for Environmental Assessment–RTP Office, Research Triangle Park, NC
100. Zhang K, Batterman S (2010) Near-road air pollutant concentrations of CO and PM_{2.5}: A comparison of MOBILE6.2/CALINE4 and generalized additive models. *Atmos Environ* 44:1740–1748 . doi: 10.1016/j.atmosenv.2010.02.008
101. Simon C, Sills R, Depa M, Sadoff M, Kim A, Heindorf MA (2005) Detroit Air Toxics Initiative: Risk Assessment Report.
102. No Title. In: US Census Bur. State Cty. Quickfacts Detroit, M.I. 2012. <http://quickfacts.census.gov>
103. MDEQ (Michigan Dept. of Environmental Quality) (2014) Michigan’s 2015 Ambient Air Monitoring Network Review
104. (2013) Illinois Ambient Air Monitoring Network Plan - 2014. Bur. Air Monit. Sect.
105. Dillner AM, Green M, Schichtel B, Malm WC, Rice J, Frank NH, Chow JC, Watson JG, White W, Pitchford M (2012) Rationale and Recommendations for Sampling Artifact Correction for PM_{2.5} Organic Carbon. US EPA, Research Triangle Park, NC
106. Kotchenruther R (2011) PM_{2.5} Carbon Measurements in Region 10 [PowerPoint slides]. NW-AIRQUEST
107. Solomon P, Cumpler D, Flanagan JB, Jayanty RKM, Rickman JEE, Dade C (2014) United States National PM_{2.5} Chemical Speciation Monitoring Networks - CSN and IMPROVE: Description of Networks. *J Air Waste Manag Assoc* 64:1410–1438 . doi: 10.1080/10962247.2014.956904
108. Dutton SJ, Vedal S, Piedrahita R, Milford JB, Miller SL, Hannigan MP (2010) Source apportionment using positive matrix factorization on daily measurements of inorganic and organic speciated PM_{2.5}. *Atmos Environ* 44:2731–2741 . doi: 10.1016/j.atmosenv.2010.04.038
109. Kotchenruther R (2009) EPA Region 10 Guidance for the Use of Receptor Models to Support Policy and Regulatory Decisions. US EPA Region 10
110. Brown SG, Eberly S, Paatero P, Norris G (2015) Methods for estimating uncertainty in PMF solutions: Examples with ambient air and water quality data and guidance on reporting PMF results. *Sci Total Environ* 518–519:626–635
111. Chow JC, Watson JG, Chen LWA, Rice J, Frank NH (2010) Quantification of PM_{2.5} organic carbon sampling artifacts in US networks. *Atmos Chem Phys* 10:5223–5239 . doi: 10.5194/acp-10-5223-2010
112. US Environmental Protection Agency (US EPA) (2014) EPA Positive Matrix Factorization (PMF) 5.0 User Guide
113. Kim E, Hopke P (2005) Identification of PM_{2.5} sources in mid-atlantic US Area. *Waste, Air, Soil Pollut* 168:391–421

114. Frank NH (2014) Calculation of Urban Increments to Support the Air Quality Designations for the 2012 PM_{2.5} Standards National Ambient Air Quality Standards (NAAQS) (SAN 5706) [Memorandum]. Docket No. EPA-HQ-OAR-2012-0918
115. Rizzo MJ, Scheff PA (2007) Fine particulate source apportionment using data from the USEPA speciation trends network in Chicago, Illinois: Comparison of two source apportionment models. *Atmos Environ* 41:6276–6288 . doi: 10.1016/j.atmosenv.2007.03.055
116. Anttila P, Paatero P, Tapper U, Järvinen O (1995) Source identification of bulk wet deposition in Finland by positive matrix factorization. *Atmos Environ* 29:1705–1718 . doi: 10.1016/1352-2310(94)00367-T
117. Koenker R (2012) Quantile Regression in R: A Vignette
118. Dunn OJ (1964) American Society for Quality Multiple Comparisons Using Rank Sums Multiple Comparisons Using Rank Sums. *Source: Technometrics* 6:241–252
119. Michigan Department of Transportation (MDOT) (2014) Annual Average Daily Traffic (AADT) Map
120. US Environmental Protection Agency (US EPA) (2016) Air Quality System Data Mart
121. US Environmental Protection Agency (US EPA) (2017) Sampling Methods for All Parameters
122. National Weather Service (NWS) (2016) Integrated Surface Hourly Data (ISHD) directory
123. National Oceanic and Atmospheric Administration (NOAA) (2016) Earth System Research Laboratory (ESRL) Radiosonde Database
124. US Environmental Protection Agency (US EPA) (2014) 2011 National Emissions Inventory, version 1 Technical Support Document
125. Michigan Department of Environmental Quality (MDEQ) (2014) Michigan Air Emissions Reporting System (MAERS) Annual Pollutant Totals Query
126. Dorn JG, Cooley DM, Huntley R (2013) EPA’s Particulate Matter Augmentation Tool: Automating quality assurance and PM speciation to generate a model-ready inventory. In: 12th Annual CMAS Conference. Chapel Hill, NC
127. Michigan Department of Environmental Quality (MDEQ) (2015) Proposed Sulfur Dioxide One-Hour National Ambient Air Quality Standard State Implementation Plan
128. Snyder M, Arunachalam S, Isakov V, Talgo K, Naess B, Valencia A, Omary M, Davis N, Cook R, Hanna A (2014) Creating locally-resolved mobile-source emissions inputs for air quality modeling in support of an exposure study in Detroit, Michigan, USA. *Int J Environ Res Public Health* 11:12739–12766 . doi: 10.3390/ijerph111212739
129. Michigan Department of Transportation (MDOT) Annual Traffic Volumes
130. Michigan Department of Transportation (MDOT) (2016) Traffic Monitoring Information System (TMIS)

131. Decker S, Suhrbier J, Rhoades K, Weinblat H, Brooks G, Dickson E (1996) Use of Locality-Specific Transportation Data for the Development of Mobile Source Emission Inventories. Emiss Invent Improv Progr Tech Rep Ser Mob Sources (Volume IV, Chapter 2); Cambridge Syst Inc Oakland, CA, USA
132. Batterman S, Cook R, Justin T (2015) Temporal variation of traffic on highways and the development of accurate temporal allocation factors for air pollution analyses. *Atmos Environ* 107:351–363 . doi: 10.1016/j.atmosenv.2015.02.047
133. US Environmental Protection Agency (US EPA) (2015) MOVES 2014a User Guide
134. Southeast Michigan Council of Governments (SEMCOG) (2011) On-Road Mobile Source Emissions Inventory for Southeast Michigan PM_{2.5} Redesignation Request
135. US Environmental Protection Agency (US EPA) (2014) Motor Vehicle Emission Simulator (MOVES): User Guide for MOVES2014
136. Arunachalam S, Valencia A, Akita Y, Serre ML, Omary M, Garcia V, Isakov V (2014) A method for estimating urban background concentrations in support of hybrid air pollution modeling for environmental health studies. *Int J Env Res Public Heal* 11:10518–10536
137. Malby AR, Whyatt JD, Timmis RJ (2013) Conditional extraction of air-pollutant source signals from air-quality monitoring. *Atmos Environ* 74:112–122 . doi: 10.1016/j.atmosenv.2013.03.028
138. Croghan CW, Egeghy PP (2003) Methods of Dealing With Values Below the Limit of Detection Using Sas. *South SAS User Gr* 5
139. Vette A, Burke J, Norris G, Landis M, Batterman S, Breen M, Isakov V, Lewis T, Gilmour MI, Kamal A, Hammond D, Vedantham R, Bereznicki S, Tian N, Croghan C (2013) The Near-Road Exposures and Effects of Urban Air Pollutants Study (NEXUS): Study design and methods. *Sci Total Environ* 448:38–47 . doi: 10.1016/j.scitotenv.2012.10.072
140. Urban N (2014) Motor City Mapping, Winter 2013-14 Certified Results
141. US Census Bureau (2015) TIGER/Line® with Selected Demographic and Economic Data. <https://www.census.gov/geo/maps-data/data/tiger-data.html>
142. DeGuire P, Cao B, Wisnieski L, Strane D, Wahl R, Lyon-Callo S, Garcia E (2016) Detroit: The Current Status of the Asthma Burden. Michigan Department of Health and Human Services: Bureau of Disease Control, Prevention and Epidemiology
143. Batterman S, Lewis T, Robins T, Mentz G, Milano C, Mukherjee B Effects of SO₂ exposures below the National Ambient Standard in a Cohort of Children with Asthma in Detroit, Michigan [Manuscript in preparation]
144. Asthma Initiative of Michigan (AIM) (2014) Current Michigan Asthma Statistics by County, Wayne County
145. US Census Bureau (2015) Detroit QuickFacts. <http://quickfacts.census.gov/qfd/states/26/2622000.html>
146. Linn WS, Szlachcic Y, Gong H, Kinney PL, Berhane KT (2000) Air pollution and daily

- hospital admissions in metropolitan Los Angeles. *Environ Health Perspect* 108:427–434
147. Ito K, Thurston GD, Silverman RA (2007) Characterization of PM_{2.5}, gaseous pollutants, and meteorological interactions in the context of time-series health effects models. *J Expo Sci Env Epidemiol* 17 Suppl 2:S45-60 . doi: 10.1038/sj.jes.7500627
 148. Yang Q, Chen Y, Krewski D, Burnett RT, Shi Y, McGrail KM (2005) Effect of short-term exposure to low levels of gaseous pollutants on chronic obstructive pulmonary disease hospitalizations. *Env Res* 99:99–105 . doi: 10.1016/j.envres.2004.09.014
 149. Schildcrout JS, Sheppard L, Lumley T, Slaughter JC, Koenig JQ, Shapiro GG (2006) Ambient air pollution and asthma exacerbations in children: An eight-city analysis. *Am J Epidemiol* 164:505–517 . doi: 10.1093/aje/kwj225
 150. US Environmental Protection Agency (US EPA) (2012) Total Risk Integrated Methodology (TRIM) Air Pollutants Exposure Model Documentation (TRIM.Expo / APEX, Version 4). Volume II: Technical Support Document. U.S. Environmental Protection Agency, Office of Air Quality Planning and Standards, Health and Environmental Impacts Division, Research Triangle Park, North Carolina
 151. US Environmental Protection Agency (US EPA) (2016) Population and Activity of On-road Vehicles in MOVES2014, EPA-420-R-16-003a
 152. US Environmental Protection Agency (US EPA) (2005) Examination of the Multiplier Used to Estimate PM_{2.5} Fugitive Dust Emissions from PM₁₀. In: 14th International Emission Inventory Conference “Transforming Emission Inventories - Meeting Future Challenges Today.” Las Vegas, Nevada, USA, pp 1–8
 153. (2014) AP 42 Update 2001 to Present - Summary of Changes to Sections
 154. Dallmann TR, Harley RA (2010) Evaluation of mobile source emission trends in the United States. *J Geophys Res Atmos* 115: . doi: 10.1029/2010JD013862
 155. US Environmental Protection Agency (US EPA) (2016) National Emission Inventory for 2005
 156. Schmeling M (2003) Seasonal variations in diurnal concentrations of trace elements in atmospheric aerosols in Chicago. *Anal Chim Acta* 496:315–323 . doi: 10.1016/j.aca.2002.11.001
 157. US Environmental Protection Agency (US EPA) (2004) Clean Air Nonroad Diesel Rule. Epa 1–5
 158. (2014) Nonroad Engines, Equipment, and Vehicles: Locomotives
 159. (2013) Michigan Highway Performance Monitoring System (HPMS)-NFC
 160. Rodriguez J (2011) Vehicle Miles Traveled on Expressways in the Chicago Region Recent Trends - 2011 Update. Chicago Metropolitan Agency for Planning
 161. Blanchard CL, Tanenbaum S, Hidy GM (2013) Source attribution of air pollutant concentrations and trends in the southeastern aerosol research and characterization (SEARCH) network. *Environ Sci Technol* 47:13536–13545 . doi: 10.1021/es402876s

162. Hackstadt AJ, Peng RD (2014) A bayesian multivariate receptor model for estimating source contributions to particulate matter pollution using national databases. *Environmetrics* 25:513–527 . doi: 10.1002/env.2296
163. Hu Y, Balachandran S, Pachon JE, Baek J, Ivey C, Holmes H, Odman MT, Mulholland JA, Russell AG (2014) Fine particulate matter source apportionment using a hybrid chemical transport and receptor model approach. *Atmos Chem Phys* 14:5415–5431 . doi: 10.5194/acp-14-5415-2014
164. McDonald BC, Goldstein AH, Harley RA (2015) Long-term trends in california mobile source emissions and ambient concentrations of black carbon and organic aerosol. *Environ Sci Technol* 49:5178–5188 . doi: 10.1021/es505912b
165. Parrish DD, Trainer M, Buhr MP, Watkins BA, Fehsenfeld FC (1991) Carbon monoxide concentrations and their relation to concentrations of total reactive oxidized nitrogen at two rural US sites. *J Geophys Res* 96:9309–9320 . doi: 10.1029/91JD00047
166. US Environmental Protection Agency (US EPA) (2008) National Air Quality Status and Trends Through 2007. 27711b:1–48
167. Reff A, Bhawe P V., Simon H, Pace TG, Pouliot GA, Mobley JD, Houyoux M (2009) Emissions inventory of PM_{2.5} trace elements across the United States. *Environ Sci Technol* 43:5790–5796 . doi: 10.1021/es802930x
168. Fraser MP, Yue ZW, Buzcu B (2003) Source apportionment of fine particulate matter in Houston, TX, using organic molecular markers. *Atmos Environ* 37:2117–2123 . doi: 10.1016/S1352-2310(03)00075-X
169. Bell ML, Dominici F, Ebisu K, Zeger SL, Samet JM (2007) Spatial and temporal variation in PM_{2.5} chemical composition in the United States for health effects studies. *Environ Health Perspect* 115:989–995 . doi: 10.1289/ehp.9621
170. US Environmental Protection Agency (US EPA) (2015) National Trends in Particulate Matter Levels
171. Rao V, Frank NH, Rice J (2012) Speciation Measurements to Track Changes in PM_{2.5} Composition and Health Outcomes [Draft White Paper]. US EPA
172. Adamski B, Boner M, Callahan B, Compher M, Haywood J, Hodges C, Kenski D, Rubens S, Akron, Sponseller B (2009) Conceptual Model of PM_{2.5} Episodes in the Midwest. Lake Michigan Air Directors Consortium
173. Schauer JJ, Rogge WF, Hildemann LM, Mazurek MA, Cass GR (1996) Source apportionment of airborne particulate matter using organic compounds as tracers. *Atmos Environ* 22:3837–3856
174. Subramanian R, Donahue NM, Bernardo-Bricker A, Rogge WF, Robinson AL (2006) Contribution of motor vehicle emissions to organic carbon and fine particle mass in Pittsburgh, Pennsylvania: Effects of varying source profiles and seasonal trends in ambient marker concentrations. *Atmos Environ* 40:8002–8019 . doi: 10.1016/j.atmosenv.2006.06.055

175. Rubin JI, Brown SG, Wade KS, Hafner HR (2006) Apportionment of PM_{2.5} and Air Toxics in Detroit, Michigan. Prepared for the US EPA by Sonoma Technology, Inc. (STI), Research Triangle Park, NC
176. Pancras JP, Landis MS, Norris GA, Vedantham R, Dvonch JT (2013) Source apportionment of ambient fine particulate matter in Dearborn, Michigan, using hourly resolved PM chemical composition data. *Sci Total Environ* 448:2–13 . doi: 10.1016/j.scitotenv.2012.11.083
177. Division AQ (2008) State Implementation Plan Submittal for Fine Particulate Matter (PM_{2.5}) - Appendix G: Overview of Recent Detroit PM Source Apportionment Studies
178. Ashbaugh L, Malm W, Sadeh W (1985) A residence time probability analysis of sulfur concentrations at Grand Canyon National Park. *Atmos Environ* 19:1263–1270
179. Dennis R, Fox T, Fuentes M, Gilliland A, Hanna S, Hogrefe C, Irwin J, Rao ST, Scheffe R, Schere K, Steyn D, Venkatram A (2010) A Framework for Evaluating Regional-Scale Numerical Photochemical Modeling Systems. *Env Fluid Mech* 10:471–489 . doi: 10.1007/s10652-009-9163-2
180. Chan TW, Meloche E, Kubsh J, Brezny R, Rosenblatt D, Rideout G (2013) Impact of Ambient Temperature on Gaseous and Particle Emissions from a Direct Injection Gasoline Vehicle and its Implications on Particle Filtration. *SAE Int J Fuels Lubr* 6:2013-01–0527 . doi: 10.4271/2013-01-0527
181. Chen H, Bai S, Eisinger D, Niemeier D, Claggett M (2009) Predicting Near-Road PM_{2.5} Concentrations. *Transp Res Rec J Transp Res Board* 2123:26–37 . doi: 10.3141/2123-04
182. Sheppard L, Burnett RT, Szpiro AA, Kim S-Y, Jerrett M, Pope Iii CA, Brunekreef B (2012) Confounding and exposure measurement error in air pollution epidemiology. *Air Qual Atmos Heal* 5:203
183. Fessenden F, Roberts S (2011) Then as Now — New York’s Shifting Ethnic Mosaic. *New York Times*
184. Cable D (2013) 2010 Racial Dot Map. Weldon Cooper Cent. Public Serv.
185. Batterman S, Ganguly R, Isakov V, Burke J, Arunachalam S, Snyder M, Robins T, Lewis T (2014) Dispersion Modeling of Traffic-Related Air Pollutant Exposures and Health Effects Among Children with Asthma in Detroit, Michigan. *Transp Res Rec J Transp Res Board* 2452:105–113 . doi: 10.3141/2452-13
186. US Environmental Protection Agency (US EPA) (2000) Meteorological monitoring guidance for regulatory modeling applications EPA-454/R-99-005
187. Watkins N, Baldauf R (2012) Near-road NO₂ monitoring technical assistance document. 135p
188. Fujita EM, Campbell DE, Zielinska B, Chow JC, Lindhjem CE, DenBleyker A, Bishop GA, Schuchmann BG, Stedman DH, Lawson DR (2012) Comparison of the MOVES2010a, MOBILE6.2, and EMFAC2007 mobile source emission models with on-road traffic tunnel and remote sensing measurements. *J Air Waste Manag Assoc* 62:1134–1149 . doi:

10.1080/10962247.2012.699016

189. Wang H, Chen C, Huang C, Fu L (2008) On-road vehicle emission inventory and its uncertainty analysis for Shanghai, China. *Sci Total Environ* 398:60–67 . doi: 10.1016/j.scitotenv.2008.01.038
190. Li H-L, Gao H, Zhu C, Li G-G, Yang F, Gong Z-Y, Lian J (2009) Spatial and temporal distribution of polycyclic aromatic hydrocarbons (PAHs) in sediments of the Nansi Lake, China. *Environ Monit Assess* 154:469–478 . doi: 10.1007/s10661-009-0752-9
191. Zheng J, Zhang L, Che W, Zheng Z, Yin S (2009) A highly resolved temporal and spatial air pollutant emission inventory for the Pearl River Delta region, China and its uncertainty assessment. *Atmos Environ* 43:5112–5122 . doi: 10.1016/j.atmosenv.2009.04.060
192. Southeast Michigan Council of Governments (SEMCOG) (2015) 2014-2015 Annual Work Program Completion Report
193. Lindhjem CE, Pollack AK, DenBleyker A, Shaw SL (2012) Effects of improved spatial and temporal modeling of on-road vehicle emissions. *J Air Waste Manage Assoc* 62:471–484 . doi: 10.1080/10962247.2012.658955
194. Gulliver J, Briggs DJ (2005) Time-space modeling of journey-time exposure to traffic-related air pollution using GIS. *Environ Res* 97:10–25 . doi: 10.1016/j.envres.2004.05.002
195. Bennett DH, McKone TE, Evans JS, Nazaroff WW, Margni MD, Jolliet O, Smith KR (2002) Peer Reviewed: Defining Intake Fraction. *Environ Sci Technol* 36:206A–211A . doi: 10.1021/es0222770
196. Gronlund CJ, Humbert S, Shaked S, O’Neill MS, Jolliet O (2015) Characterizing the burden of disease of particulate matter for life cycle impact assessment. *Air Qual Atmos Heal* 8:29–46 . doi: 10.1007/s11869-014-0283-6
197. Wu J, Houston D, Lurmann F, Ong P, Winer A (2009) Exposure of PM_{2.5} and EC from diesel and gasoline vehicles in communities near the Ports of Los Angeles and Long Beach, California. *Atmos Environ* 43:1962–1971 . doi: 10.1016/J.ATMOSENV.2009.01.009
198. Gurram S, Stuart AL, Pinjari AR (2015) Impacts of travel activity and urbanicity on exposures to ambient oxides of nitrogen and on exposure disparities. *Air Qual Atmos Heal* 8:97 . doi: 10.1007/s11869-014-0275-6
199. DeWinter JL, Brown SG, Seagram AF, Landsberg K, Eisinger DS (2018) A national-scale review of air pollutant concentrations measured in the U.S. near-road monitoring network during 2014 and 2015. *Atmos Environ*. doi: 10.1016/j.atmosenv.2018.04.003
200. Kottow MH (2003) The Vulnerable and the Susceptible. *Bioethics* 17:460–471 . doi: 10.1111/1467-8519.00361